CHEMICAL ENERGY STORAGE FOR SOLAR THERMAL CONVERSION

FINAL REPORT

RRC-80-R-678

Prepared For:

Sandia Laboratories

Livermore, California

ROCKET RESEARCH COMPANY

A DIVISION OF ROCKCOR

Redmond, Washington

CHEMICAL ENERGY STORAGE
FOR SOLAR THERMAL CONVERSION

Final Report

Prepared For:

Sandia Laboratories
Livermore, California

Under Contract No. 18-2563

Principal Investigator: Richard D. Smith

Contributors: D. R. Poole
                 C. H. Li
                 D. K. Carlson
                 D. R. Peterson

Prepared By:

Rocket Research Company
A Division of ROCKCOR, Inc.
Redmond, Washington 98052

April 27, 1979

ABSTRACT

The technical and economic aspects of using reversible chemical reactions to store energy in Solar Thermal Electric Conversion (STEC) facilities have been studied. The study included identification of nine promising chemical reactions from a list of over 550 candidates, preliminary process designs of energy storage subsystems based on these nine reactions, and extensive systems studies of autonomous (100% solar) and hybrid (requiring alternate energy backup) STEC plants with energy storage subsystems based on the reversible oxidation of SO_2. Storage round-trip thermal efficiencies for the reactions studied ranged from 20 to 50 percent; power-related unit costs varied between 0.5×10^5 and 10×10^5 $/MW$_t$ maximum storage charging rate; and energy-related unit costs varied between 0.5×10^3 and 24×10^3 $/MW$_t$-hr storage capacity. Process designs based on the two reactions, $SO_2 + 1/2\ O_2 = SO_3$, and $CaO + H_2O = Ca(OH)_2$, are discussed in detail. The systems studies used a detailed simulation, based on a year-long, hour-by-hour energy balance, of a central-receiver STEC facility. Over a range of alternate energy cost and geographic location, the optimum busbar energy costs from autonomous STEC plants were 15 to 90 percent higher than those from hybrid plants. Optimum storage requirements of autonomous STEC plants were in the range of 200 to 400 hours, while those for hybrid plants were in the range of 15 to 30 hours.

ACKNOWLEDGEMENTS

TABLE OF CONTENTS

TABLE OF CONTENTS (Concluded)

LIST OF FIGURES

LIST OF FIGURES (Concluded)

LIST OF TABLES

LIST OF TABLES (Concluded)

EXECUTIVE SUMMARY

Introduction

Due to the intermittent nature of solar radiation at the earth's surface, energy storage must play a key role in the effective utilization of solar energy for electric power generation. The general term "energy storage" includes concepts such as batteries, flywheels, superconductors, pumped hydro, compressed air, sensible heat, phase change, and thermochemical energy storage. The last concept, thermochemical energy storage, or simply chemical energy storage, is the subject of this report. In the chemical energy storage (CES) scheme, a large quantity of thermal energy is stored as reactive chemicals formed through an endothermic chemical reaction. This stored energy can be released upon demand by reversing the process in an exothermic chemical reaction which simultaneously regenerates the starting material. In general, the storage or endothermic mode of a chemical energy storage process involves breaking chemical bonds and forming more energetic species which are stored. The energy is thus not stored in a chemical bond, but by the potential to form a chemical bond in an exothermic process.

The development of Solar Thermal Electric Conversion (STEC) power plants has been intrinsically tied to short-term (nominally 6 hours) energy storage. This design constraint results in an intermediate load power plant, i.e., energy is available when nature provides adequate insolation and not necessarily at the time of demand by the customer. The specification of short-term storage capacity in current STEC programs was determined on the basis of economic considerations using sensible and/or latent heat storage systems.

Because the reaction constituents of a chemical energy storage system are stored at a near-ambient temperature, energy can be stored for long periods of time, disregarding scheduled down time. If the storage material is relatively inexpensive, significantly larger quantities of energy may be economically stored than with sensible and latent heat systems. The long-term storage capacity of chemical energy storage systems offers the prospect of solar thermal electric conversion (STEC) plants which can meet up to 100 percent of load requirements.* Such baseload, or autonomous STEC power plants, could conceivably supply a continuous output, 24 hours a day, 365 days a year. Heat storage could level the demand fluctuations during weekends and distribute unused energy from the weekend throughout the week. Moreover, chemical heat storage systems have opened up the possibility of leveling seasonal discrepancies between insolation demand by running off of the storage system on longer winter nights and cloudy days. On the other hand, the advantages of such long storage times must be traded off against the additional cost of the oversized collector fields, receivers, storage system components, and turbomachinery required to provide them.

---

*The STEC plants studied here are intended to be relatively large (100 MW_e) central power plants operated by a utility. The collector-receiver (or "front-end") portion of the STEC facility can be either a central-receiver type or a distributed collection (e.g., parabolic trough) type.

1

While much work had been done previously on various individual reactions believed suitable for CES applications, Rocket Research Company (RRC) believed that a general survey of the chemical literature for promising chemical energy storage reactions was needed, and part of the present study was directed toward that end. Moreover, RRC believed that in addition to a study of the technical aspects of CES systems (suitable reactions, thermodynamic efficiencies, process design problems, etc.), an objective economic evaluation of CES, based on systems studies of STEC facilities with chemical energy storage systems, was needed. In the present work, particular attention has been paid to the potential economic benefits to STEC operation of long-term (e.g. seasonal) chemical energy storage.

Program Objectives

In summary, the overall objective of the present study is the evaluation, on a total system basis, of the concept of chemical energy storage for STEC applications. Included in this overall objective are:

1. Determination of performance and cost requirements for chemical energy storage subsystems used in STEC power plants.

2. Examination of the technical and economic feasibility of extending STEC operation to baseload power generation by use of long-term chemical energy storage.

3. Identification of promising chemical reactions for such storage applications, and preliminary design and evaluation of storage subsystems based on these reactions.

Program Description

The program approach taken to meet the objectives defined above may be divided into three parts:

Systems Analysis – In keeping with the total system approach described above, a simulation of a STEC facility with CES was developed. This simulation, adaptable to a wide range of STEC system types and locations, CES subsystems, and operating conditions, was the basis for a computer code which was used to study the overall economic feasibility of STEC facilities with CES. These systems studies also helped determine the range of performance and cost requirements which CES subsystems would have to meet, thereby defining design criteria for the CES process design effort to follow.

Chemical Reaction Survey – Starting with the periodic table of the elements, an extensive survey and screening process produced a list of 12 promising chemical reactions for the CES process design studies.

Preliminary Process Designs for CES Subsystems – Preliminary process designs were developed for CES subsystems based on the most promising chemical reactions, and the designs were evaluated and compared with respect to cost and performance.

Each of these efforts is discussed in a separate section below.

2

Systems Analysis

The very long storage times achievable with CES systems cause technical limitations to storage duration to become less important than economic limitations. With CES, it appears to be technically feasible to build a STEC plant with enough storage to satisfy a continuous demand. Is such an autonomous, or 100% solar plant, the most economical choice, or would a STEC facility with less storage (and thus satisfying less than 100 percent of the load from solar energy) produce electric power at a lower busbar energy cost? The systems studies described in this section were undertaken to answer this question.

As part of a general inquiry into the overall economics of STEC plants with long-term storage, the variation with location of the cost of STEC-produced electricity was studied. The effects on STEC performance and cost of insolation profiles from four disparate U. S. locations were examined in order to determine the relative value of long-term CES at these locations.

In addition to providing an overall look at the economics of long-term energy storage, these systems studies also helped establish the performance requirements for CES systems in STEC applications. Design requirements such as storage charging and discharging rates and storage capacity, determined with this system-oriented approach, ultimately led to more realistic preliminary process designs of CES systems. Cost and efficiency estimates made from these designs are more realistic as well.

Computer Simulation

For the purposes of computer simulation, the STEC facilities have been modeled as a collection of subsystems — collector field, receiver, turbogenerator, and energy storage (Figure 1). Each of these subsystems is characterized by an operating thermal efficiency and a relation describing subsystem cost as a function of energy or power requirements. In general, the entire power production facility is modeled as a combination of a solar power plant and an alternate energy backup. This alternate energy backup could be an on-site combustion turbine or power purchased from a utility grid whenever necessary.

The central feature of the simulation is an hour-by-hour energy balance on the entire STEC facility, taken over the course of an entire year. From this energy balance and the hour-by-hour system performance map which results from it, the size, and thus cost, of each subsystem is computed.

The STEC simulation can treat both central receiver and distributed collection systems; it can handle any location for which acceptable insolation data are available and can model STEC operation with any CES subsystem which is sufficiently characterized so that charging and discharging thermal efficiencies, as well as power and energy related unit costs, have been defined.

Cases Examined

Although the simulation code is quite general, the STEC systems analysis was limited by the scope of the present study to a few representative cases. Table 1 summarizes the STEC systems considered in the analysis.

Figure 1

SOLAR THERMAL ELECTRIC CONVERSION PLANT MODEL
(WITH ALTERNATE ENERGY BACKUP)
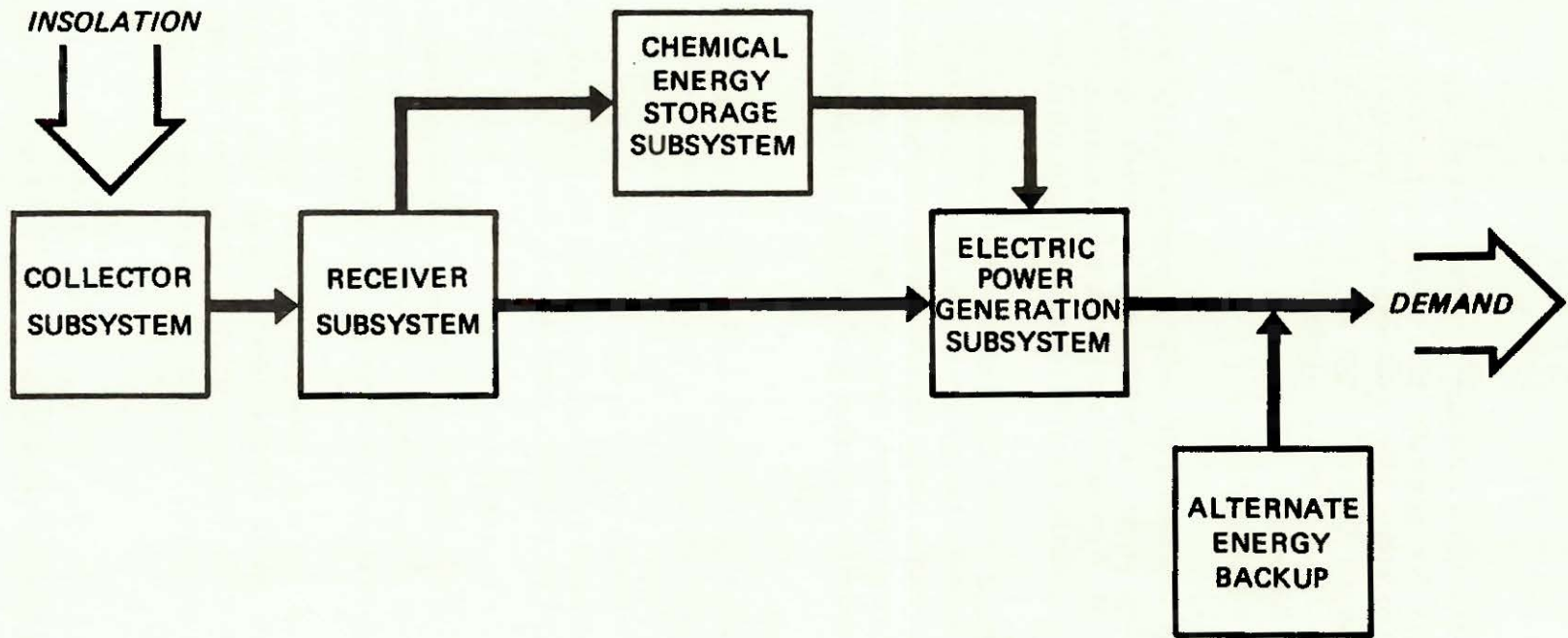
Table 1
CASES ANALYZED WITH STEC SIMULATION CODE

System type:	Central receiver, Open-Brayton power cycle
Locations:	Miami, Florida (SE) Madison, Wisconsin (NC) Albuquerque, New Mexico (SW)
Chemical energy storage reaction:	$SO_2 + 1/2\ O_2 = SO_3$
Plant nameplate power rating:	100 MWe
Demand profile:	Continuous, constant
Solar contribution:	Autonomous (100% solar) Hybrid (<100% solar, with alternate energy backup)

The energy storage subsystem model used in the present systems studies was based on the reversible oxidation of sulfur trioxide: $SO_2 + 1/2\ O_2 = SO_3$. The cost and performance parameters for this model were extracted from a substantially modified version of a SO_2/SO_3 energy storage system design developed by RRC under a previous contract. Although the results of systems studies based on only one energy storage reaction might seem of limited applicability, comparison of this early storage system model with later process designs based on other reactions showed that the efficiency and cost of the earlier model were remarkably true to the later designs. The results of these systems studies are therefore believed to be applicable to CES in general.

Hourly direct normal insolation data for the year 1960 were used for each of the locations listed in Table 1. These data were derived from measured, total-horizontal insolation data and therefore provided a sufficiently accurate rendition of the true insolation profile at these locations.

Electric power demand was assumed to be a continuous, constant 100 MW_e, 24 hours a day. Results of test runs with actual hourly load profiles of electric power grids at the locations of interest were not substantially different from those with the constant loads.

Autonomous and Hybrid STEC Facilities

The time-independent nature of chemical energy storage allowed considerable flexibility in the degree of participation of the solar portion of the solar/alternate hybrid power plant considered here. The solar fraction is defined here as that fraction of the total energy output of the plant which is solar-derived. Thus a STEC plant with a solar fraction of 0.75 would produce 75% of its energy output from the sun (either directly from the receiver or through the storage subsystem), and 25% would be supplied by an alternate energy source.

STEC plants which can supply 100% of the demand load from solar energy are termed autonomous plants in the discussion which follows; those which require some alternate energy backup (solar fractions less than 1.0) are termed hybrid plants.

5

The General STEC Optimization Problem

At the level of detail of the STEC simulation presented here, the most important and useful independent variables are the storage capacity, Q, and the collector or heliostat area, A. The dependent variable of interest for economic evaluation is the busbar energy cost, BBEC. The systems studies reported here, then, were primarily concerned with finding the particular storage capacity and collector area which minimized the BBEC for a given case (plant location, alternate energy cost, etc.). This is true for both autonomous and hybrid STEC plants.

Figure 2 is a schematic representation of the important regions of A-Q space. For a given insolation profile, demand profile, and STEC plant specification, a minimum (or critical) collector area, A*, may be determined. Associated with the critical area, A*, is a critical storage capacity, Q*, and together they define the critical point shown in Figure 2. At all collector areas to the left of A*, it is theoretically impossible to meet 100 percent of the demand from solar energy, regardless of the storage capacity available; therefore, hybrid operation is mandatory.

At all collector areas to the right of A*, it is possible to meet 100 percent of the demand from solar energy, if enough storage is available. The curve in Figure 2 represents (for any A) the minimum storage capacity required to maximize the solar fraction at a given collector area. Points above the curve represent STEC plants with too much storage for their collector area. Points below the curve describe STEC plants which, due to storage limitations, can provide less than the maximum solar fraction which their collectors would allow. Points to the right of A*, but below the curve, can therefore not meet 100 percent of the demand from solar energy due to storage limitations, even though they have enough collector area to do so. Autonomous solutions, then, are confined to the region to the right of A* and on the curve CD. Theoretically, points in the region above the curve CD also represent solutions (albeit unlikely ones) for autonomous operation; the present analysis, however, does not consider solutions with more storage than is necessary for autonomous operation.

From an economic point of view, the general problem addressed by the systems studies described here is an optimization problem in two-space: to find the point in the A-Q plane at which the BBEC is a minimum. It proved convenient, conceptually, to divide this general problem into separate problems for the autonomous and hybrid cases. The domain for the autonomous cases was the curve CD, while the domain for the hybrid cases was the entire area under the curve BCD.

Results for Autonomous Operation

Autonomous STEC plants at all locations studied obeyed autonomous operation curves similar in shape to curve CD in Figure 2, with different absolute values for the A and Q coordinates. The critical point, by definition corresponding to the minimum collector area for which 100 percent solar operation is possible, also corresponded to the greatest storage capacity requirement in all cases. As collector area increased above the critical value, the storage requirement decreased continuously until it eventually reached a constant minimum which corresponded to the length of the longest solar occultation (night, storm, etc.) of the year.

SCHEMATIC OF RELATIONSHIP BETWEEN STORAGE CAPACITY AND COLLECTOR AREA

Solar involvement has been maximized. Pure solar designs must lie to the right of the critical collector area and above the minimum storage size for pure solar applications.

*THE POINT B REPRESENTS THE MINIMUM COLLECTOR AREA FOR WHICH THE PLANT NAMEPLATE OUTPUT CAN STILL BE PROVIDED FROM DIRECT SOLAR ENERGY, AT NOON ON THE BEST SOLAR DAY OF THE YEAR. "SOLAR MULTIPLES" ARE COMMONLY DEFINED IN TERMS OF THIS AREA, WHICH IS GIVEN A SOLAR MULTIPLE EQUAL TO 1.0.

Figure 2-6
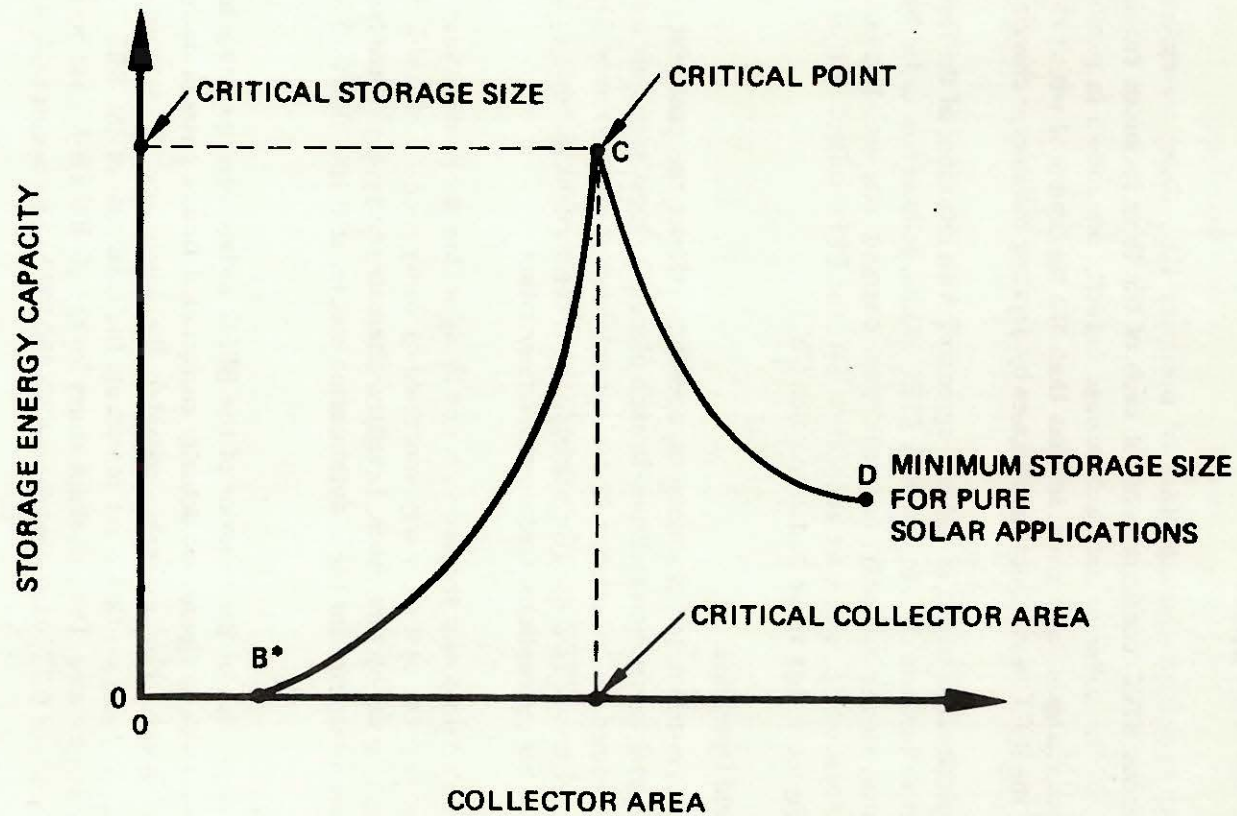
An autonomous STEC facility with area A = A* represents a very poor (expensive) design solution because storage requirements (~1,380 hours† in the case of location NC) and resulting storage costs are extremely high for the $SO_3/SO_2/O_2$ system. These high storage costs are reflected in a relatively high BBEC at A = A*. As the collector area increases above the critical value and the storage requirements decrease, the trade-off in capital cost requirements between the two subsystems produces a minimum in the BBEC.

Table 2 presents important characteristics of optimum (i.e., those corresponding to minimum BBEC), autonomous STEC configurations, at each of the three locations considered. Normalized optimum values of the collector area and storage capacity are shown in parentheses. The yearly maximum storage charging rates given are less than the maximum of which the collector field is capable because the BBEC was reduced in all cases by derating the storage charging capability.

The optimum solutions described in Table 2 agree well with intuition; of the three, Albuquerque is the most attractive location for autonomous STEC plants, followed in order by locations SE and NC. Heliostat area, storage capacity, and maximum charging rate are all greatest at location NC, intermediate at location SE, and least at location SW; the BBEC reflects this ordering, with that at location NC being more than twice that at location SW.

Results for Hybrid Operation

Removal of the constraint for autonomous operation admits the possibility of solar-fossil (or nuclear) hybrid power generation facilities. In such plants, the most economic solar-alternate energy mix will be determined by the relative cost of energy from the two sources. The alternate energy might be produced on a STEC site (for example, by a combustion turbine) or simply provided to the grid from another conventional electric generating station.

Large-scale solar electric power generation is not likely within the next 20 years or so; and while it is safe to assume that the cost of energy generated by conventional means will increase during that time, it is difficult to say by how much. Levelized alternate energy costs were therefore treated as a parameter and set arbitrarily for these optimization studies at 0.100, 0.200, 0.300, 0.400 $/kW-hr in 1978 dollars.

Figure 3 gives some idea of the behavior of the BBEC surface corresponding to the A-Q domain. The curves shown in these figures are actually constructed from a series of optima for the range of collector areas shown. For example, consider the curve for an alternate energy cost of $0.400/kW-hr. Each point on that curve represents the minimum of the BBEC versus storage time curve for that collector area. The global minimum for the $0.400 kW-hr case occurs at a normalized collector area, A/A*, of 0.77, while that for the $0.300 kW-hr case occurs at A/A* = 0.55.

---

†One hour of storage time is the equivalent amount of stored energy which, upon discharge from storage, could produce the nameplate capacity of the plant for one hour.

Table 2
OPTIMUM SOLUTIONS FOR AUTONOMOUS STEC POWER PLANTS
WITH STORAGE CLIPPING

System B, 100 MW_e Continuous Demand

Location	Heliostat* Area (km^2)	Storage* Capacity (hrs)	BBEC[†] ($/Kw-hr)	Maximum Charging Rate** (MW_t)	Capital Equipment Cost Breakdown (%)			
					Heliostats & Receiver	Turb-Gen	Storage	
							Power	Energy
Madison (NC)	9.2 (1.92)	362 (0.27)	0.616	3,874 (0.70)	55	14	8	23
Miami (SE)	5.2 (1.22)	200 (0.35)	0.350	1,908 (0.62)	55	14	8	23
Albuquerque (SW)	3.4 (1.42)	134 (0.16)	0.252	1,769 (0.82)	50	18	11	21

*In parenthesis — Normalized with respect to critical values

**In parenthesis — Normalized with respect to maximum receiver input power.

[†] 1978 Dollars

6

Figure 3

OPTIMUM BBEC AS FUNCTION OF NORMALIZED COLLECTOR AREA
HYBRID STEC PLANT AT LOCATION NC

NOTE: THESE RESULTS CORRESPOND TO THE ESTIMATED INSOLATION DATA DESCRIBED IN SECTION 2.2.5
AND ARE GIVEN HERE FOR ILLUSTRATIVE PURPOSES ONLY. SEE TEXT FOR EXPLANATION.

The constant BBEC curves in Figure 3 indicate the effect which alternate energy cost has on the optimum solution. As alternate energy becomes more expensive, the optimum solution calls for larger collector areas, larger storage capacities, and generally larger solar fractions. In the extreme case of infinite alternate energy cost, the optimum choice is an autonomous STEC plant, located at the minimum of the 100 percent solar curve.

Table 3 presents optimum solutions for hybrid STEC systems at locations NC and SE for an alternate energy cost of $0.400/kW-hr. Optimum solutions for alternate energy costs of 0.100, 0.200, and 0.300 $/kW-hr had extremely low solar fractions, indicating that the optimizer chose primarily to buy alternate energy rather than build a sizeable solar portion of the plant, i.e. at these alternate energy costs, for the subsystem unit costs used in this study, the STEC system modeled here would not be economically competitive. Due to time constraints, hybrid operation at location SW was not studied.

Perhaps the most surprising result of these hybrid studies (especially in the case of location SE) was that such high solar fractions could be achieved with less than 30 hours of storage. The hybrid STEC systems are not very sensitive to the occasional extended storm or cloudy period. Such extended occultations occur relatively infrequently, while nighttime occultation occurs 365 times a year. Overnight storage requirements thus exert far more influence on the optimum storage time. Since the system is not constrained to a 100 percent solar solution, the most economical solution is to increase storage only slightly and purchase alternate energy to satisfy demand during a long cloudy period. Autonomous operation, on the other hand, requires storage capacities large enough to carry the system through the longest period of occultation of the year, and stand-alone plants are therefore more sensitive to changes in the insolation profile.

Conclusions of STEC Systems Analysis

The most important conclusions of the systems studies described above include:

1. The autonomous solar thermal electric conversion plant which uses the (SO_2/SO_3) reaction for seasonal storage does not economically compete with a hybrid plant which has an alternate energy source available to it, based solely on BBEC. Supplying all of the demand with solar energy was found to be 20 to 80 percent more expensive than supplying the demand partly from the sun and partly from alternate energy sources. This is due to the fact that it is cheaper to purchase backup energy, even at fairly high unit costs, than to build solar components which are used at full capacity only infrequently. A storage system with much lower energy-related unit cost would make such competition much closer.

2. Optimum storage requirements for *autonomous* STEC power plants which satisfy continuous baseloads are in the range of 100 to 400 hours.

3. Optimum storage requirements for *hybrid* STEC power plants which satisfy continuous baseloads are in the range of 20 to 30 hours, for a levelized alternate energy cost of $0.400/kW-hr.

11

Table 3
OPTIMUM SOLUTIONS FOR HYBRID STEC POWER PLANTS
ALTERNATE ENERGY COST = $0.400/Kw-hr

System B, 100 MW_e Continuous Demand

Location	Heliostat* Area (km^2)	Storage* Capacity (hrs)	BBEC[†] ($/Kw-hr)	Solar Fraction	Maximum Charging Rate (MW_t)	Capital Equipment Cost Breakdown (%)			
						Heliostats & Receiver	Turb-Gen	Storage	
								Power	Energy
Madison (NC)	2.4 (0.50)	22 (0.02)	0.332	0.57	1,326	56	23	15	6
Miami (SE)	3.2 (0.75)	29 (0.05)	0.298	0.75	1,746	58	22	14	6

*In parenthesis — Normalized with respect to critical values

[†] 1978 Dollars

12

4. In all autonomous and most hybrid cases of interest, the yearly maximum storage charging rates are greater than the maximum discharging rates, with the ratio of these quantities varying between approximately six for the best hybrid case and eighteen for the worst autonomous case. The maximum storage charging rate is, therefore, size determining for power-related storage process equipment used in both the endothermic and exothermic modes.

5. As could be expected under consistent assumptions for the Florida and Wisconsin simulations, the solar plant is more economically attractive in Florida. The Wisconsin system requires much more storage for both hybrid and autonomous operation than does the plant in Florida.

6. The concept of energy discard is important to the optimal design of any solar plant, hybrid or autonomous. The results presented in the body of this report underscore the desirability of oversizing or undersizing subsystems to obtain better utilization factors for the plant as a whole. This approach leads to lower busbar energy costs than designs which utilize all the energy collected. Use of discard energy and/or reject process heat from the storage subsystem, in a "total energy" application, may therefore be an attractive option. option.

The general applicability of these conclusions is of course limited by the many assumptions of efficiency and cost of various subsystems and components on which the model is based. Two key limitations of the systems studies described above bear mentioning:

1. The use throughout the study of heliostat and receiver unit costs of $90/m^2$ and $50/m^2$, respectively.

2. The use of only one storage subsystem model (SO_2/SO_3).

In view of the capital equipment cost breakdown of Tables 2 and 3, it is apparent that large increases or decreases in the front-end unit cost parameters would undoubtedly change the optimum busbar energy costs, collector areas, and storage capacities for both autonomous and hybrid STEC plants, and might substantially alter the solar/alternate mix of the optimum hybrid solutions. Similarly, a storage subsystem model based on a different reversible chemical reaction, with different charging and discharging efficiencies and different power and energy-related unit costs, might substantially alter the character of both the autonomous and hybrid solutions.

Chemical Reaction Survey

The ultimate goal of this screening process was the reduction of the candidate reactions to a manageable number of the most promising reactions for more careful examination and preliminary process design studies. The result was that a list of over 550 candidate reactions was reduced to one containing 12 promising reactions for further study.

The periodic table of the elements served as the starting point for the process of generating and selecting chemical reactions for energy storage applications. After eliminating numerous elements due to their high cost, toxicity, or lack of availability, all known chemical compounds of the

13

remaining elements were considered. In this way, a list of approximately 750 compounds was generated. Methane and methanol were the only organic compounds which were retained, since the reactions of most larger organic molecules suffer, to a greater or lesser extent, from irreversible side reactions.*

Chemical reactions were then listed using the selected elements and compounds, resulting in a list of approximately 550 reactions. Based on the following criteria, 85 candidate reactions were identified.

1. Reaction appears to be reversible.
2. $\Delta H_R \geqslant 110$ kcal/kg
3. $|\Delta G_{298K}|$ or $|\Delta G_{800K}|$ or $|\Delta G_{1200K}| \leqslant 10$ kcal/mole
4. Approximate equilibrium temperature $T = \Delta H^O / \Delta S^O$ in the range of 400K to 1500K.

The temperature range 400 to 1500K was chosen to include, with a comfortable margin for safety, the entire range of output temperatures of receivers likely to be used in STEC applications.

This field of 85 reactions was then rated by four RRC scientists according to a simple scheme which considered such characteristics of each reaction as energy storage density, reversibility, toxicity, corrosivity, and ease of product separation. It was found that nearly all of the reactions could logically be classified into 14 categories based on the reaction or chemical type. The field of 85 reactions was narrowed to 24 by selecting the most highly rated reactions from each of the 14 categories and the 24 reduced to 12 (with the main criterion being reaction kinetic data availability) for further process design studies. The final 12 reactions are listed in Table 4.

Preliminary Process Designs for Chemical Energy Storage Subsystems

The objectives of the preliminary process design work described here include:

1. Evaluation of cost and performance of energy storage subsystems based on the most promising reactions identified by the reaction screening process.
2. Identification of important technical problems, advantages, and trade-offs of chemical energy storage processes, including those which are specific to particular reactions and those which apply to a larger group of reactions or to CES processes in general.

Table 5 presents a summary of the disposition of the reactions originally considered for design studies. Preliminary process designs and cost estimates for nine storage subsystems were developed, with the cost and efficiency estimate for the NH_4HSO_4 system pending publication of the results of workers at the Solar Energy Laboratory of the University of Houston. The $MgO/Mg(OH)_2$ system was eliminated on the basis of poor exothermic reaction kinetics observed by other workers, as was the mono-ammoniated ferrous chloride system. The mono-ammoniated $MgCl_2$ system was eliminated due to the occurrence of irreversible side reactions in the endothermic mode, the products of which are apparently highly corrosive. In place of the mono-ammoniated $MgCl_2$ system, the di-ammoniated $MgCl_2$ system was inserted. While undesirable side reactions apparently occur for this reaction as well, the problem is less severe.

---

*The reversible hydrogenation of benzene to cyclohexane and of ethylene to ethane were added to the final list of 24 reactions described below since they are being studied by other workers at the time of this work.

Table 4
CHEMICAL REACTIONS CHOSEN FOR PRELIMINARY PROCESS DESIGN STUDY

1) $NH_3 + SO_3 + H_2O = NH_4 HSO_4$

2) $CaO + H_2O = Ca(OH)_2$

3) $MgO + H_2O = Mg(OH)_2$

4) $ZnO + SO_3 = ZnSO_4$

5) $CS_2 = C + 2S$

6) $MgCl_2 + NH_3 = MgCl_2 \cdot NH_3$

7) $CaO + CO_2 = Ca CO_3$

8) $MgO + CO_2 = MgCO_3$

9) $2SO_2 + O_2 = 2SO_3$

10) $FeCl_2 \cdot NH_3 + NH_3 = FeCl_2 \cdot 2NH_3$

11) $C_2H_4 + H_2 = C_2H_6$

12) $C_6H_6 + 3H_2 = C_6H_{12}$

Table 5
CHEMICAL REACTIONS CHOSEN FOR PRELIMINARY PROCESS DESIGN STUDIES

$CaO + H_2O = Ca(OH)_2$
$CaO + CO_2 = CaCO_3$
$MgO + CO_2 = M_gCO_3$
$ZnO + SO_3 = ZnSO_4$ — Solid-gas noncatalytic
$CS_2 = C + 2S$
$*MgCl_2 \cdot NH_3 + NH_3 = MgCl_2 \cdot 2NH_3$

Preliminary process designs complete

$2SO_2 + O_2 = 2SO_3$
$C_2H_4 + H_2 = C_2H_6$ — Solid-gas catalytic
$C_6H_6 + 3H_2 = C_6H_{12}$

$NH_3 + SO_3 + H_2O = NH_4 HSO_4$ — Design pending results of other workers

$MgO + H_2O = Mg(OH)_2$
$FeCl_2 \cdot NH_3 + NH_3 = FeCl_2 \cdot 2NH_3$ — Discarded based on experimental results of other workers
$MgCl_2 + NH_3 = MgCl_2 \cdot NH_3$

*Substituted for discarded mono-ammoniate of $MgCl_2$

Each of the nine remaining reactions fall into one of two basic reaction types:

1. Solid-gas, noncatalytic, in which one or more of the reaction constituents is a solid (e.g. CaO, Ca(OH)$_2$), while the remaining constituents are gaseous at reaction temperatures

2. Solid-gas, catalytic, in which all reaction constituents are gaseous at reaction temperatures (e.g. SO$_2$, SO$_3$), but a solid catalyst (or at lease a solid catalyst support) is required for the reactions to proceed efficiently and selectively.

The reactor designs for the catalytic reactions in group 2., while of course complicated by many technical considerations, are fairly standard. Reactants are generally passed through a packed catalyst bed at the appropriate temperature and pressure, where the reaction takes place. Products leaving the reactor are cooled, separated, and recycled or stored as needed. Catalyst poisoning, degeneration, or coking may cause the catalyst activity to decrease to such an extent that replacement or regeneration is necessary.

The solid/gas reactions in group 1., apparently promising based on the thermodynamic analyses, present a challenging reactor design problem, one for which there is not much precedent in the literature. An apparently workable, moving bed reactor design was developed for these group 1 reactions.

Each of the nine preliminary process designs is discussed in the body of the report, and the designs based on the SO$_2$/SO$_3$ and CaO/Ca(OH)$_2$ reactions are treated in some detail. These two reactions were chosen for extended discussion in part because, overall, they are the two most likely reactions for the CES applications considered in this study; in addition, these two reactions are representative of the two different reaction types mentioned above.

Important CES Process Design Assumptions

Any process design work, even the preliminary design work described here, is a series of design decisions based on the experience and judgment of the designer, so it is impossible to list all the design criteria on which the preliminary process designs described here are based. The more important ones have been summarized below.

1. The only source of process heat in the charging mode was the receiver. No lower grade process heat was available from other STEC subsystems or from outside the STEC plant.

2. The only source of process heat in the discharging mode was the exothermic chemical reaction itself. As in 1., no lower grade process heat was available from other sources.

3. No energy credit was taken for storage system reject heat, even though it might be useful to some other process, or in some "total energy" application.

4. All shaft work required by the storage subsystem was supplied by electric motors; the electricity to run these motors was produced at the efficiency of the STEC turbogenerator for the appropriate storage operating mode. Thus, electricity to supply charging mode shaft work was produced by the turbogenerator with energy directly from the receiver, while electricity for discharge parasitic power was produced by the turbogenerator at an efficiency associated with the storage subsystem discharge temperature.

16

5. Endothermic and exothermic reactions were assumed to take place at their approximately optimum temperatures. No attempt was made to force the storage subsystem design to produce energy from storage at the same temperature as the storage input, if the efficiency or cost penalties to do so were prohibitive.

6. Process equipment was designed to be used in both the charging and discharging modes whenever possible.

7. All the CES processes were designed to handle a 2500 MW_t maximum charging rate, defined at storage input, and a maximum discharging rate which was the thermal equivalent of 100 MWe, at the appropriate turbogenerator efficiency.

8. All the CES processes were designed to provide 2.5×10^4 MW_e-hr* storage capacity.

9. Cooling water was assumed to be available to all processes in any quantity needed, and at no charge, at 305 K.

Summary of CES Performance and Cost Estimates

Table 6 summarizes the capital cost and efficiency estimates based on the preliminary process designs of CES subsystems. The round-trip efficiencies in column 3 are thermal-to-thermal efficiencies and represent the useful energy output from storage per unit of energy input to storage. The round-trip efficiency is defined as the product of the charging and discharging efficiencies. The values of round-trip efficiency given in column 4 have been corrected for availability changes due to different storage input and output temperatures. The reader is referred to the body of the report for a more detailed definition of these efficiencies.

Capital cost estimates for each process are divided into power-related and energy-related unit costs. The energy-related cost includes the costs of all storage vessels and reactants, and the power-related cost accounts for all other process equipment. The energy-related unit costs were calculated by dividing the total energy-related capital cost by the total storage capacity, in MW_t-hr at the storage system outlet. The power-related unit costs were calculated by dividing the total power-related capital cost by the maximum charging rate, in MW_t at the storage system inlet.

Conclusions of Preliminary Process Design Studies:

The composite results presented in Table 6, together with the design studies themselves, lead to the following general conclusions:

1. Round-trip efficiencies of chemical energy storage systems designed according to the assumptions listed above will most likely be less than 0.5 with the most likely candidate systems (SO_2/SO_3 and $CaO/Ca(OH)_2$) having efficiencies of approximately 0.35. Efforts to improve these efficiencies should concentrate on integration of the CES subsystems with other processes which could act as heat sources or sinks; such processes might include the turbogenerators of the STEC plant itself, adjoining chemical processes, or district heating systems.

2. Power-related unit costs of these chemical energy storage systems will most likely be greater than $\$1 \times 10^5$/$MW_t$ charging capacity. Energy-related unit costs of such systems

---

*250 hours of storage at 100 MW_e continuous STEC output when running solely on energy from storage.

Table 6

ESTIMATED CAPITAL COSTS AND EFFICIENCIES OF ENERGY STORAGE SUBSYSTEMS

(1978 Dollars)

	Charging Efficiency	Discharging Efficiency	Round-Trip Efficiency	Corrected Round-Trip Efficiency	Power-Related Unit Cost (10^5 \$/MW_t)	Energy-Related Unit Cost (10^3 \$/MW_t-hr)
$CaO + H_2O = Ca(OH)_2$	0.64	0.55	0.35	0.30	2.0	1.0
$CaO + CO_2 = CaCO_3$	0.31	0.88	0.27	0.27	1.0	4.7
$MgO + CO_2 = MgCO_3$	0.48	0.83	0.40	0.29	9.8	9.7
$ZnO + SO_3 = ZnSO_4$	0.39	0.75	0.30	0.30	1.4	3.3
$CS_2 = C + 2S$	0.78	0.80	0.62	0.52	0.5	0.5
$MgCl_2 \cdot NH_3 + NH_3 = MgCl_2 \cdot 2NH_3$	0.43	0.65	0.28	0.23	1.0–1.4	3.2
$2SO_2 + O_2 = 2SO_3$	0.41	0.80	0.33	0.33	1.0	24.0
$C_2H_4 + H_2 = C_2H_6$	0.49	0.78	0.38	0.34	1.0	12.4
$C_6H_6 + 3H_2 = C_6H_{12}$	0.55	0.88	0.48	0.48	0.8	11.1

will most likely be greater than $1 \times 10^3/MW_t$-hr storage capacity. The one exception to these statements, the C/CS_2 system, is discussed in 7. below. Storage systems based on reactions involving noncondensible constituents (e.g., H_2, O_2, CO_2) have energy-related unit costs which are very much higher than those of the other reactions. These high costs are due, of course, to the high capital investment required for high pressure storage vessels.

3. A major design difficulty in all the energy storage systems studied was efficient heat transfer into and out of the reactor, and efficient heat transfer between reactant and product streams. This problem is severe in the systems which use solid reactants and causes such systems to have very high gas circulation rates through the reactors, large and expensive gas-gas heat exchangers for recuperation, and high compressor costs and compression work requirements.

4. The heat transfer problems, mentioned in 3., associated with solid-gas noncatalytic reactions result in an uncommon reactor design; the suggested reactor design for such reactions is a moving-bed type, with direct heat transfer, and radial flow in the gas phase.

5. For the reasons mentioned in 3., energy storage systems based on solid-gas noncatalytic reactions generally exhibit lower round-trip efficiencies than those based on the catalytic reactions considered.

6. Required storage input temperatures for all the process designs considered were higher than expected; and in several cases, storage output temperatures required for most efficient storage system operation were substantially lower than the input temperatures. These temperature differences were due primarily to heat transfer limitations within the storage system. Earlier estimates of storage input and output temperatures were based solely on equilibrium thermodynamics. While all CES systems can be designed to discharge energy at the same temperature at which it was charged, such designs are in many cases far less efficient, far more costly, or both, than designs in which the output temperature is substantially lower than the input temperature.

7. The C/CS_2 system is apparently a promising one according to the preliminary process design, but it must be remembered that its design was based on the key assumptions that CS_2 dissociation kinetics (at present unknown) would offer no insurmountable technical or economic obstacles. Any further study of the C/CS_2 reaction for energy storage applications should attempt first to verify or reject that assumption. In all likelihood, reliable kinetic information, even if it indicates that the reaction will proceed as modeled here, will cause the estimated round-trip efficiency to decrease substantially, causing the unit costs to increase as well.

CHAPTER 1
INTRODUCTION

Due to the intermittent nature of solar radiation at the earth's surface, energy storage must play a key role in the effective utilization of solar energy for electric power generation. The general term "energy storage" includes concepts such as batteries, flywheels, superconductors, pumped hydro, compressed air, sensible heat, phase change, and thermochemical energy storage. The last concept, thermochemical energy storage, or simply chemical energy storage, is the subject of this report. In the Chemical Energy Storage (CES) scheme, a large quantity of thermal energy is stored as reactive chemicals formed through an endothermic chemical reaction. This stored energy can be released upon demand by reversing the process in an exothermic chemical reaction which simultaneously regenerates the starting material. In general, the storage or endothermic mode of a chemical energy storage process involves breaking chemical bonds and forming more energetic species which are stored. The energy is thus not stored in a chemical bond, but by the potential to form a chemical bond in an exothermic process.

The development of solar thermal electric conversion (STEC) power plants has been intrinsically tied to short-term (nominally 6 hours) energy storage. This design constraint results in an intermediate load power plant, i.e., energy is available when nature provides adequate insolation and not necessarily at the time of demand by the customer. The specification of short-term storage capacity in current STEC programs was determined on the basis of economic considerations using sensible and/or latent heat storage systems.

Because the reaction constituents of a chemical energy storage system are stored at a near-ambient temperature, energy can be stored for long periods of time. If the storage material is relatively inexpensive and the storage process efficient, significantly larger quantities of energy may be economically stored than with sensible and latent heat systems. The long-term storage capacity of chemical energy storage systems offers the prospect of solar thermal electric conversion (STEC) plants which can meet up to 100 percent of load requirements.* Such baseload, or autonomous STEC power plants, could conceivably supply a continuous output, 24 hours a day, 365 days a year. Heat storage can level the demand fluctuations during weekends and distribute unused energy from the weekend throughout the week. Moreover, chemical heat storage systems have opened up the possibility of leveling seasonal discrepancies between insolation and demand by running off the storage system on longer winter nights and on cludy days.

In view of its apparent advantages for solar applications, the concept of chemical energy storage has been examined in more or less detail by several previous workers (D1). For an introduction to the

---

*The STEC plants studied here are intended to be relatively large (100 MW$_e$) central power plants operated by a utility. The collector-receiver (or "front-end") portion of the STEC facility can be either a central-receiver (H1) type or a distributed collection (e.g., parabolic trough) type.

field of chemical energy storage, the reader is referred to papers by Prengle and Sun (P1), Wentworth and Chen (W1), and Schmidt (S1, S2).

While much work has been done on various individual reactions believed suitable for CES applications, Rocket Research Company (RRC) believed that a general survey of the chemical literature for promising chemical energy storage reactions was needed, and part of the present study was directed toward that end. Moreover, RRC believed that in addition to a study of the technical aspects of CES systems (suitable reactions, thermodynamic efficiencies, process design problems, etc.), an objective economic evaluation of CES, based on systems studies of STEC facilities with chemical energy storage systems, was needed. In the present study, particular attention has been paid to the potential economic benefits to STEC operation of long-term (e.g. seasonal) chemical energy storage.

In summary, the overall objective of the present study is the evaluation, on a total system basis, of the concept of chemical energy storage for STEC applications. Included in this overall objective are:

1. Determination of performance and cost requirements for chemical energy storage subsystems used in STEC power plants.

2. Examination of the technical and economic feasibility of extending STEC operation to baseload power generation by use of long-term chemical energy storage.

3. Identification of promising chemical reactions for such storage applications, and preliminary design and evaluation of storage subsystems based on these reactions.

1.1 PROGRAM DESCRIPTION

The program which produced the results described in this report was actually a combination of two different research contracts: NSF contract No. AER 75-22176, and Sandia Laboratories, Livermore (SLL) contract No. 18-2563.

The first part of the original NSF contract (Figure 1-1) involved selection of promising reactions, tabulation of thermodynamic and kinetic properties for these reactions, and division of the reactions selected into a low-temperature group (400 to 950 K) and a high-temperature group (950 to 1,500 K), according to the estimated operating temperature range of each reaction. Part 2 of the NSF effort involved more detailed study and evaluation of two promising reactions.

To examine the performance capabilities, size and cost of STEC facilities using long-term, chemical energy storage and to provide a more system-oriented basis for selecting the most promising reactions for further study, the add-on contract with Sandia Laboratories, Livermore (SLL 18-2563), was inserted between parts 1 and 2 of the original NSF effort. The add-on effort involved creation and use of a computer simulation of a STEC facility for systems studies of STEC plants with storage subsystems based on the reversible oxidation of SO_2. In addition, preliminary process designs of chemical energy storage subsystems based on other promising reactions were to be developed.

INTEGRATION OF "EXTENDED STORAGE" PROGRAM WITH NSF "CHEMICAL ENERGY STORAGE FOR SOLAR THERMAL ELECTRIC CONVERSION" PROGRAM

NSF PART 1

- REACTION SELECTION
- PROPERTIES TABULATION
- THERMODYNAMIC ANALYSIS

DOE
"EXTENDED STORAGE" PROGRAM

- COMPUTER SIMULATION OF STEC FACILITY
- SYSTEMS STUDIES OF STEC PLANTS (SO_2/SO_3 STORAGE)
- PRELIMINARY STORAGE PROCESS DESIGNS (OTHER REACTIONS)

NSF PART 2

- SELECTION OF TWO BEST REACTIONS
- EVALUATION
- RECOMMENDATIONS
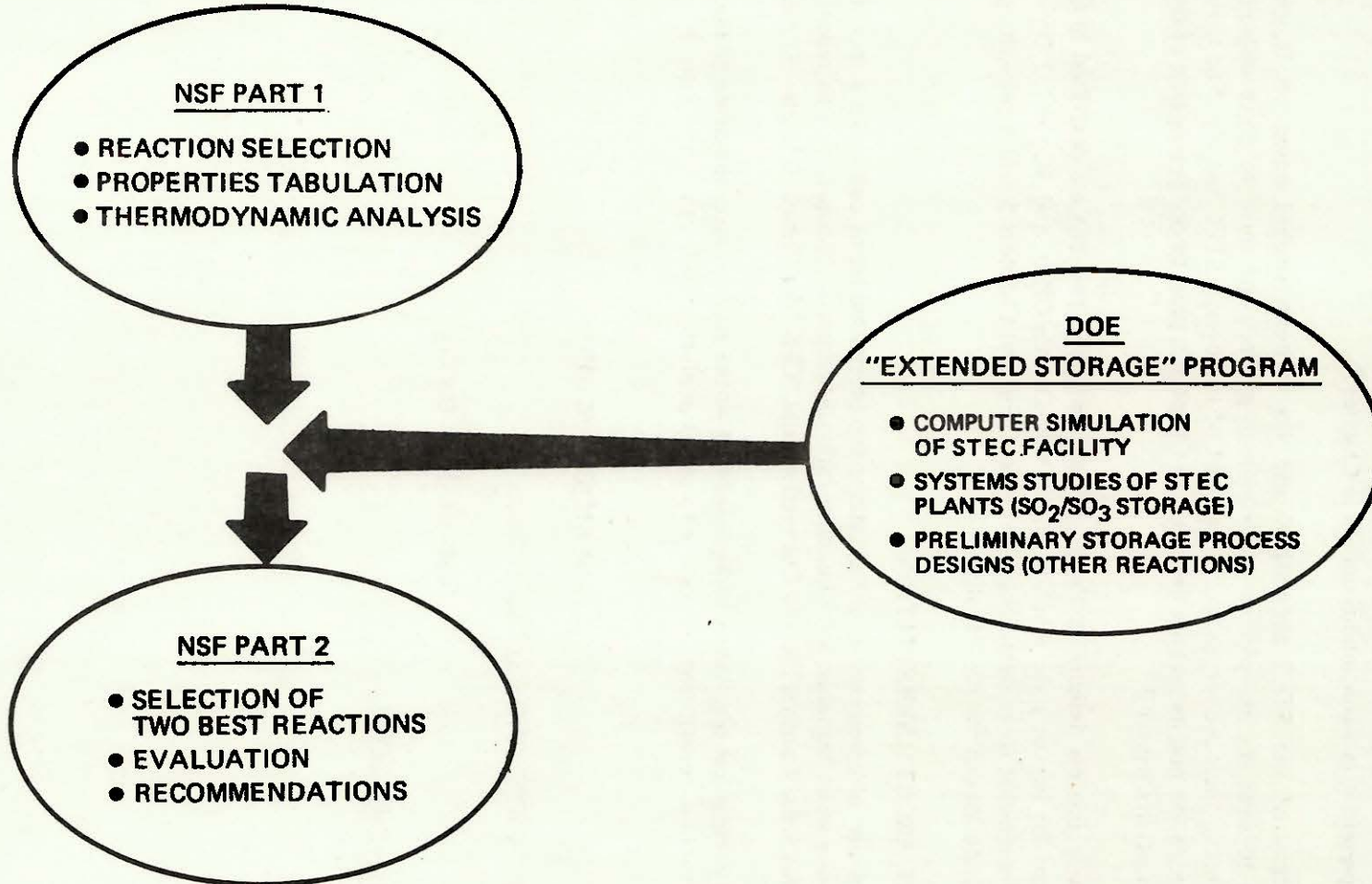
Starting with over 550 potential storage reactions, the candidate reactions were progressively screened to a list of twelve for design studies, and finally to two for further preliminary process designs. This screening process was in fact intermittent; it is convenient for reporting purposes, however, to present it as a continuous one, as in Chapter 3.

The description of the STEC simulation, and the systems studies based on it, provide an introduction to solar thermal electric conversion in general, and serve to place chemical energy storage systems in their proper perspective as part of the overall STEC facility. For these reasons, the STEC simulation and its uses are described in Chapter 2, prior to the description of the reaction screening process in Chapter 3.

The preliminary process designs for the nine final candidate reactions are described in Chapter 4. Process designs for two of these reactions ($CaO + H_2O = Ca(OH)_2$, and $SO_2 + 1/2\ O_2 = SO_3$) are described in somewhat more detail than the others. Finally, Chapters 5 and 6 present conclusions and recommendations of the present study.

1.2   A NOTE ABOUT ABBREVIATIONS

The judicious use of acronyms or abbreviations for often-used-terms can make a technical report such as this one more readable, and therefore more informative. Throughout this report, "STEC" will be used for Solar Thermal Electric Conversion, and "CES" for Chemical Energy Storage.

For simplicity, chemical reactions will be identified in the text by a combination of the minimum number of reaction constituents necessary to avoid confusion with other reactions. For example, the reaction.
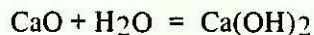
$$CaO + H_2O = Ca(OH)_2$$

will be noted as $CaO/Ca(OH)_2$, and the reaction

$$CaO + CO_2 = CaCO_3$$
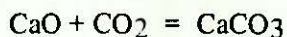
will be noted as $CaO/CaCO_3$.

CHAPTER 2

STEC SIMULATION AND SYSTEMS STUDIES

The very long storage times achievable with CES systems cause technical limitations to storage duration to become less important than economic limitations. With CES, it appears to be technically feasible to build a STEC plant with enough storage to satisfy a continuous demand. Is such an autonomous, or 100% solar plant, the most economical choice, or would a STEC facility with less storage (and thus satisfying less than 100 percent of the load from solar energy) produce electric power at a lower busbar energy cost? The systems studies described in this section were undertaken to answer this question.

As part of a general inquiry into the overall economics of STEC plants with long-term storage, the variation of the cost of STEC-produced electricity with location has been studied. The effect of insolation profiles from four disparate U. S. locations on STEC performance and cost has been examined in order to determine the relative value of long-term CES at these locations.

In addition to providing an overall look at the economics of long-term energy storage, these systems studies also helped establish the performance requirements for CES systems in STEC applications. Design requirements such as storage charging and discharging rates and storage capacity, determined with this system-oriented approach, ultimately lead to more realistic preliminary process designs of CES systems. Cost and efficiency estimates made from these designs are more realistic as well.

In order to examine the complex interplay between insolation, storage, and other STEC system components, computer simulation of a STEC facility was required. The model was sufficiently general as to allow variation of insolation and demand profiles, type of front-end design, and alternate energy cost (for hybrid analysis). The resolution necessary to accurately determine storage system performance requirements made hour-by-hour simulation necessary, and efficient data management for a simulated year of operation required use of a computer.

The work statement of the SLL add-on contract was written so that the STEC systems studies were performed before the development of preliminary process designs described in Chapter 4. The storage system model used in the computer simulation work was, therefore, adapted from a computer model developed by RRC under an earlier contract (Reference G1) for a CES system based on the reversible oxidation of sulfur dioxide (SO_2/SO_3). Although the results of systems studies based on only one energy storage reaction might seem of limited applicability, comparison of this early storage system model with later process designs based on other reactions, showed that the efficiency and cost of the earlier model was remarkably true to the later designs. The results of these systems studies are therefore believed to be applicable to CES in general.

2.1 APPROACH

For the purposes of computer simulation, the STEC facilities have been modeled as a collection of subsystems — collector field, receiver, turbogenerator, and energy storage (Figure 2-1). Each of

SOLAR THERMAL ELECTRIC CONVERSION PLANT MODEL
(WITH ALTERNATE ENERGY BACKUP)
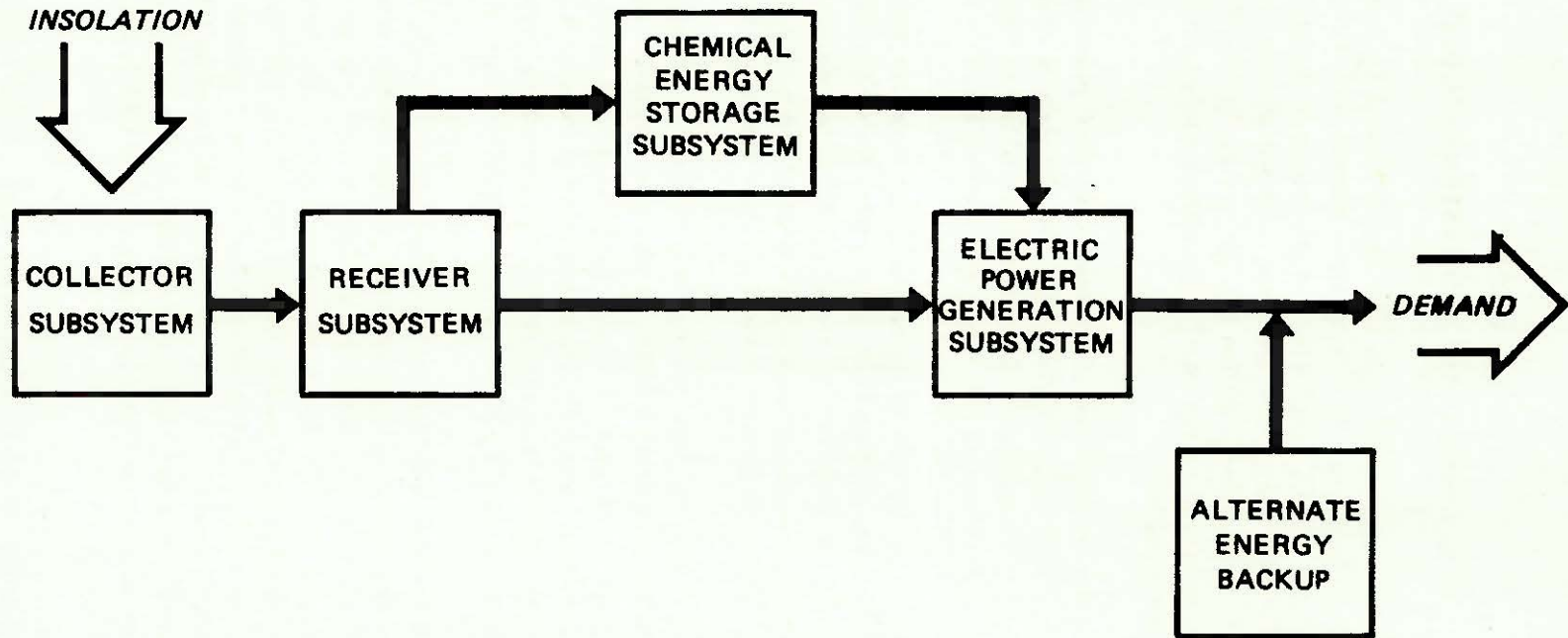
Figure 2-1

these subsystems is characterized by an operating thermal efficiency and a relation describing subsystem cost as a function of energy or power requirements. In general, the entire power production facility is modeled as a combination of a solar power plant and an alternate energy backup. This alternate energy backup can be an on-site combustion turbine or power purchased from a utility grid whenever necessary. The alternate energy supply option was removed for autonomous plant analyses.

The central feature of the simulation is an hour-by-hour energy balance on the entire STC facility, taken over the course of an entire year. From this energy balance and the hour-by-hour system performance map which results from it, the size, and thus cost, of each subsystem is computed.

The hourly energy balance is based on a sun-following dispatcher. That is, for each hour of the year, the electrical demand is compared with the available insolation. If the insolation, suitably reduced by subsystem inefficiencies, exceeds demand, the demand for that hour is completely fulfilled, and the excess energy charged to storage. If insolation falls short of demand, all energy from the receiver is routed through the turbogenerator to electrical output, and makeup energy is discharged from storage. If energy directly from the receiver plus that from storage is insufficient to meet the demand, the dispatcher, as a last resort, makes up the difference with the alternate energy backup. No transient operation of the receiver or turbogenerator is considered, and turnaround of the storage subsystem from the charge to the discharge mode is assumed to be feasible during the 1-hour time steps considered.

2.2 STEC SIMULATION INPUT SPECIFICATIONS

The following sections describe briefly the most important system characteristics (these are also the input specifications required by the two simulation codes STORAGE and CSTOPT).

2.2.1 STEC System Types

The original NSF contract was intended to study storage reactions which would be operational over different portions of a wide temperature range (400 to 1,300 K). The work statement required that the simulation be capable of modeling three types of STEC systems, each of them applicable over a portion of the 900 K temperature range. The three systems were chosen jointly by SLL and RRC to reflect differences in type as well as operating temperature. The systems, labeled A, B, and C, are described briefly below.

System A – A central receiver collection subsystem coupled with a steam Rankine power generation subsystem. Cost and performance of the receiver, collector, and turbogenerator subsystems are modeled after those designed by McDonnell-Douglas Astronautics Co. (References S3, E1, and M1). Receiver exit temperature, storage exit temperature, and turbine inlet temperature are assumed to be 783 K.

System B – A central receiver collection subsystem combined with an open-Brayton cycle power generation subsystem. Receiver exit temperature, storage exit temperature, and turbine inlet temperature are assumed to be 1,310 K. As in System A, cost and performance of the collector

subsystem are taken from McDonnell-Douglas design of collectors for the Barstow pilot plant. This collector field design was chosen for both systems A and B because, at about the time this simulation was being developed, that design was chosen over two other designs for actual production at Barstow. In addition, cosine corrections to the necessary insolation data were available for the McDonnell-Douglas collector field. The high-temperature receiver and turbo-generator cost and performance estimates were based on results of several current or recently completed receiver designs (References B1, B2, J1).

System C – A distributed collection system coupled with a central steam Rankine power generation subsystem. Receiver exit temperature, storage exit temperature, and turbine inlet temperature were assumed to be 588 K. The collectors are line focusing parabolic troughs with single axis tracking. Values for subsystem efficiencies and costs for distributed systems are difficult to find in the literature, and the values given below were gleaned from conversations with interested workers at the Jet Propulsion Laboratory and at Sandia Laboratories, Albuquerque. For the purposes of the present model, the collector and receiver subsystems of System C are considered as one, with an additional energy transport subsystem added to account for piping network energy losses.

Since the SO_2/SO_3 storage system operating temperature is most compatible with the System B model, the majority of systems studies described below were carried out using that STEC system. Some runs (not reported here) were performed with the intermediate temperature, System A model, with the questionable assumption that the SO_2/SO_3 input and output temperatures were compatible with the System A receiver and turbogenerator. No runs other than those necessary for debugging the code were made with the System C model because the SO_2/SO_3 storage subsystem operating temperatures were clearly not compatible with those of System C.

While the System A and C models were not used in the systems studies reported here, they were developed and included in the STEC simulation code as per the contract work statement, and are available for future use.

The model depicted in Figure 2-1 treats the solar and alternate energy systems as parallel sources of electric power. An interesting alternative, not treated here, might be to operate the receiver and a CES/fossil fuel backup system in series on hazy or cloudy days, so that the power cycle working fluid could be preheated by the receiver and boosted to nominal outlet temperatures by the CES exothermic reactor or by the backup system. Such an arrangement deserves further study.

2.2.2 Subsystem Efficiencies

Table 2-1 presents receiver and power generation subsystem efficiencies for all three STEC operating systems included in the STEC simulation. All component efficiencies, including those for the storage subsystem, are specified as program input, and are assumed to be constant, independent of hourly changes in power level or capacity. Storage system efficiency is discussed in section 2.2.7.

Table 2-1
SUBSYSTEM EFFICIENCIES USED IN STEC SIMULATION

STEC System	Subsystem Efficiency	
	Receiver, η_R	Power Generation, η_p
A	0.89	0.39
B	0.91	0.47
C	0.61	0.24

2.2.3 Subsystem Costs

The STEC simulation codes are written so that STEC plant nameplate output (in MW_e) is an input parameter. The size of each subsystem is determined by the hour-by-hour energy balance for the particular case of interest, and the subsystem costs are determined from the subsystem sizes. "Size" actually means power rating in the cases of the collector, receiver, and power generation subsystems. In general, a maximum charging rate, maximum discharging rate, and maximum storage capacity are calculated by the energy balance to completely characterize the chemical energy storage subsystem.

Collector and receiver subsystem costs are considered to be linear functions of the yearly maximum STEC input power required. The receiver is always sized to handle the maximum collector field output. The program code could easily have been modified to reduce the maximum receiver power rating in order to study the effects of receiver "clipping" on total system cost (section 2.4.1.1).

Both collector and receiver unit costs have units of $/m^2$*, and are input parameters. Current estimates of eventual prices of mass-produced heliostats for central-receiver STEC facilities range from $60/m^2$ to $120/m^2$ in 1978 dollars. All of the systems studies described in this report, have used System A and System B heliostat unit costs of $90/m^2$. System A receiver unit cost, used in this study, was $40/m^2$ (References S3, P2), while that for System B was $50/m^2$ (References B1, B2).

Cost estimates for distributed systems combine costs of collector, receiver, and piping subsystems into one lump sum. Based on the manufacture of 10^5 m^2 of collector area per year, several manufacturers have estimated collection system costs of from $129 to $215/m^2$ (Reference P3). About 20 percent of these prices are charged to tracking controls, supports, and piping. For reasons similar to those given for Systems A and B, collection system costs were treated as a parameter of

---

*Square meter of collector area.

the System C model. As more detailed cost estimates become available, the piping costs of the collection system may be considered separately and their dependence on collector field size accounted for in the System C model. No systems studies were carried out with the System C model, so specific values for subsystem unit costs are not given.

Costs C_p of the electric power generation subsystems were assumed to be exponential functions of the turbogenerator nameplate capacity P, in megawatts electric. The functional forms are given below, and are nearly linear.

System A:

$$C_p = 2.3 \times 10^7 (P/100)^{0.96} [=] dollars$$

System B:

$$C_p = 2.6 \times 10^7 (P/100)^{0.96}$$

System C:

$$C_p = 3.5 \times 10^7 (P/100)^{0.96}$$

The turbogenerator sizing calculation accounts for the generating capacity necessary to supply the parasitic power requirements of the storage subsystem. At present, the model assumes that electrical power is provided by the turbomachinery to the storage system, although in the future the model may be amended so that some combination of electrical and shaft work is provided instead. If $(Pd)_i$ and $(Pp)_i$ represent the average grid electrical demand and the average storage parasitic power demand for hour i, then:

$$(Pt)_i = (Pd)_i + (Pp)_i$$

represents the total average power output which the turbogenerator must provide during that hour. The value of $(Pd)_i$ is determined in the system sizing subroutine from the demand/load model, while that of $(Pp)_i$ is determined by the system sizing subroutine from the storage charge (or discharge) rate. The nameplate turbogenerator capacity is determined by the plant sizing subroutine as the yearly maximum of $(Pt)_i$.

Results of the systems studies indicate that in most cases of interest, the storage charging rate greatly exceeds the discharge rate. In many cases, the parasitic power requirements of the SO_2/SO_3 storage system were much greater than the nameplate capacity of the STEC plant, and the turbogenerator nameplate capacity can be up to five times the yearly maximum of Pd.

Such oversizing of the turbomachinery to meet the parasitic power demands of the yearly maximum storage charging rate means that at other times during the year, particularly when the STEC facility is running completely off of storage, the turbomachinery will operate at considerably less than its design capacity. No correction for reduced turbogenerator efficiency has been included

in the STEC simulation. Such corrections, if applied, might reduce power conversion efficiencies to 80 percent of their maximum values (References G2, B3). This disadvantage could be mitigated somewhat by operating several smaller turbines in parallel and adjusting the number operating at any time.

2.2.4 Location

In order to examine the potential benefits of long-term chemical energy storage to autonomous STEC operation at locations with less than ideal insolation profiles, insolation and electrical load demand data were obtained for four disparate U.S. locations. Although these locations were dictated in part by availability of suitable data, they were also chosen to reflect markedly different matches between insolation and demand profiles. Hourly insolation and electrical demand data were obtained for the following locations:

Location NC	Madison, Wisconsin
Location SE	Miami, Florida
Location SW	Albuquerque, New Mexico
Location NE	New York, New York

Locations were coded as indicated to make reference to them less cumbersome. Although insolation and demand data were obtained for all four locations, systems studies were performed primarily for locations NC and SE. Due to the difference in their latitudes, seasonal variation in insolation between the two locations is substantial. Moreover, the radically different climates cause the mismatch between insolation and demand to differ greatly between the two locations. Location SW represents the most attractive "solar" location for which suitable hourly insolation and demand data were available. Some studies were carried out for location SW as a "best case" for comparison purposes. Location NE was included as a "worst case" for comparison purposes only; very few runs were carried out for this location, and none are reported here.

2.2.5 Insolation Data

Hourly direct-normal insolation data for the year 1960 for the four chosen locations, were acquired from Sandia Laboratories, Livermore, and incorporated into programs STORAGE and CSTOPT. These data were derived from measured total-horizontal insolation data during a joint effort by Sandia Laboratories, Albuquerque, and the Aerospace Corporation (Reference R1), and are available on tape, without the cosine corrections described below, from the National Climatic Center, Asheville, North Carolina (Reference N1).

In order to minimize use of computer time, the insolation data for all locations has been stored with hourly collector field corrections for Systems A and B included. These corrections were obtained for the McDonnell-Douglas collector field configurations of System A and System B from Sandia Laboratories, Livermore, and are the result of calculations by their ray-trace program MIRVAL (Reference L1). Program MIRVAL is based on a Monte Carlo ray-trace technique, and accounts for

attenuation between the heliostats and the receiver, including hourly azimuth-elevation corrections. It does not account for sun-earth attentuation or receiver reflection and re-emission.[†]

In addition to the insolation data with cosine corrections included, RRC also obtained "raw" or uncorrected, hourly insolation data for the four locations of interest. In order that the accuracy of the System C model approach that of the other two, hourly cosine corrections were derived for a field of north-south oriented, parabolic collectors, and, together with reflectivity, absorptivity, convection and blocking losses, can be applied by STORAGE to the uncorrected direct-normal insolation data for each location.

The orientation and operation of the parabolic collector model is shown schematically in Figure 2-2, along with definitions of the angles of interest. The axis of each collector is oriented in a north-south direction, and tilted (toward the south at all U. S. locations) at an angle degree, from the horizontal, roughly equivalent to its latitude. The collectors follow the sun by rotation of the reflector about the axis of the receiver tube. The cosine correction, cosine a, is expressed as a function of the solar azimuth and elevation, which in turn are expressed as functions of the time at the longitude of the collector field.

The resulting cosine corrections are shown in Figures 2-3 and 2-4 for locations SE (latitude 25.7°N) and NC (latitude 43°N). The hourly variations shown in Figure 2-3 are decidedly uninteresting, being nearly constant throughout each of the days shown. Even the daily variation over the course of a year is not very great, as shown in Figure 2-4, and with proper tilting of the collectors, the difference between the corrections for location NC and SE is slight.

Several variations in orientation (such as east-west alignment of the focal axes) and tracking of the parabolic collectors were examined, but none displayed the consistently high cosine efficiencies of the N-S, tilted arrangement.

Early test runs and systems studies with program STORAGE were conducted before the derived, direct-normal insolation data described above became available. These early systems studies, and therefore a paper which was based on them (I1), were based on hourly, direct-normal insolation data which were constructed for the four locations by a combination of theoretical and experimental results. In order to help clarify the differences between insolation profiles used in that paper and the studies described below, the procedure used to calculate these data is described briefly as follows:

1. Calculate solar radiation on a horizontal surface outside the earth's atmosphere on an hourly basis.

2. Calculate the total (direct and diffuse) solar radiation on a horizontal surface at the latitude of the site of interest (Reference A1).

3. Using 1. and 2., compute the direct normal solar radiation on an hourly basis using the technique of Boes (Reference B4).

[†] Average effects of receiver reflection and re-emission are included in the constant receiver efficiencies of Table 2-1.

COSINE CORRECTION TO DIRECT NORMAL INSOLATION OF A
NORTH-SOUTH ORIENTED PARABOLIC-CYLINDRICAL COLLECTOR

RECEIVER TUBE
(FOCAL AXIS)

+Z

-Y
(N)

θ

NORMAL TO
COLLECTOR

a

SOLAR BEAM

PARABOLIC
CYLINDRICAL
COLLECTOR

-X
(W)

+X
(E)

β

+Y
(S)

ϕ

a IS ANGLE INCIDENCE, SOLAR BEAM
     TO NORMAL TO COLLECTOR

θ TILT ANGLE OF FOCAL AXIS TO
     HORIZONTAL

ϕ SOLAR AZIMUTH

β SOLAR ELEVATION

COSINE CORRECTION = $\cos a$
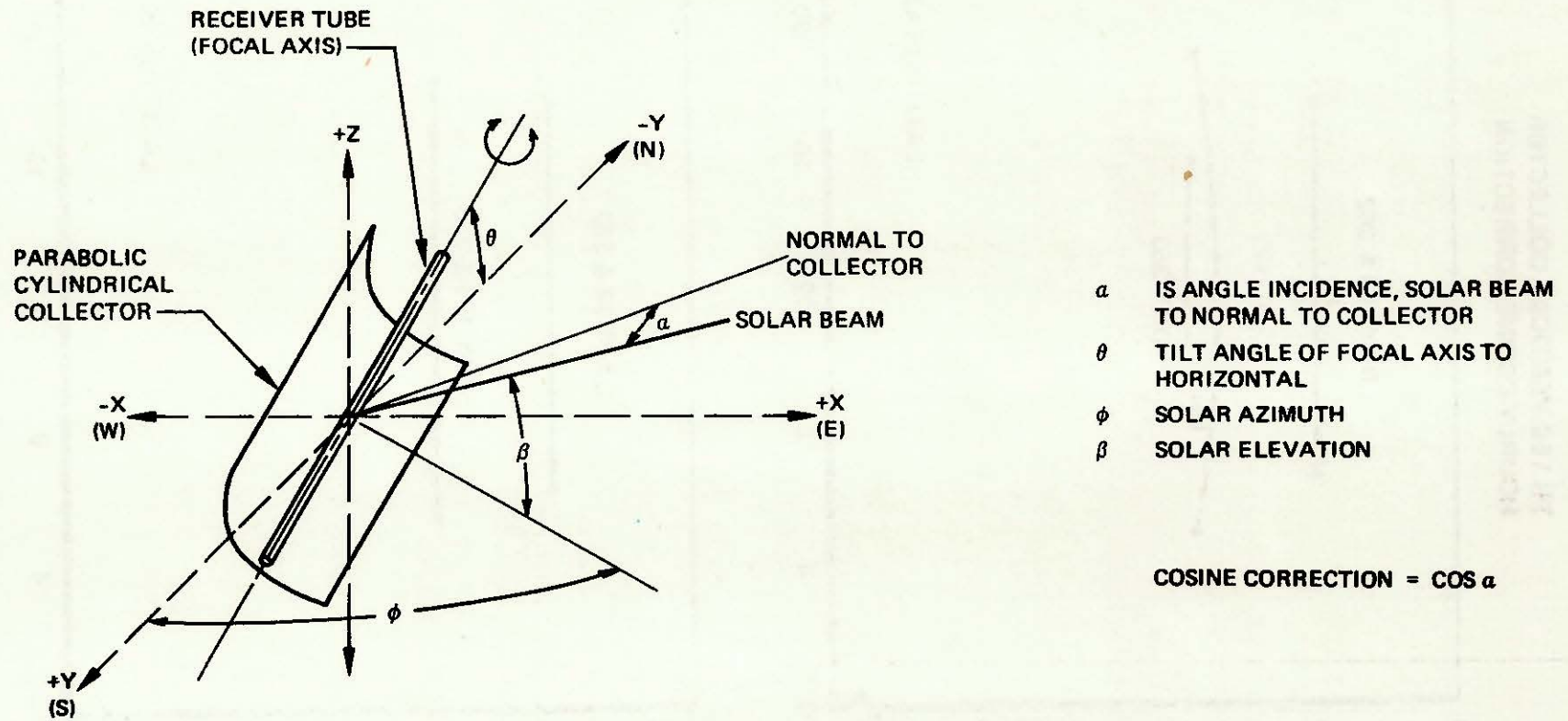
Figure 2-2

TILTED VERTICAL COLLECTOR
HOURLY COSINE CORRECTION
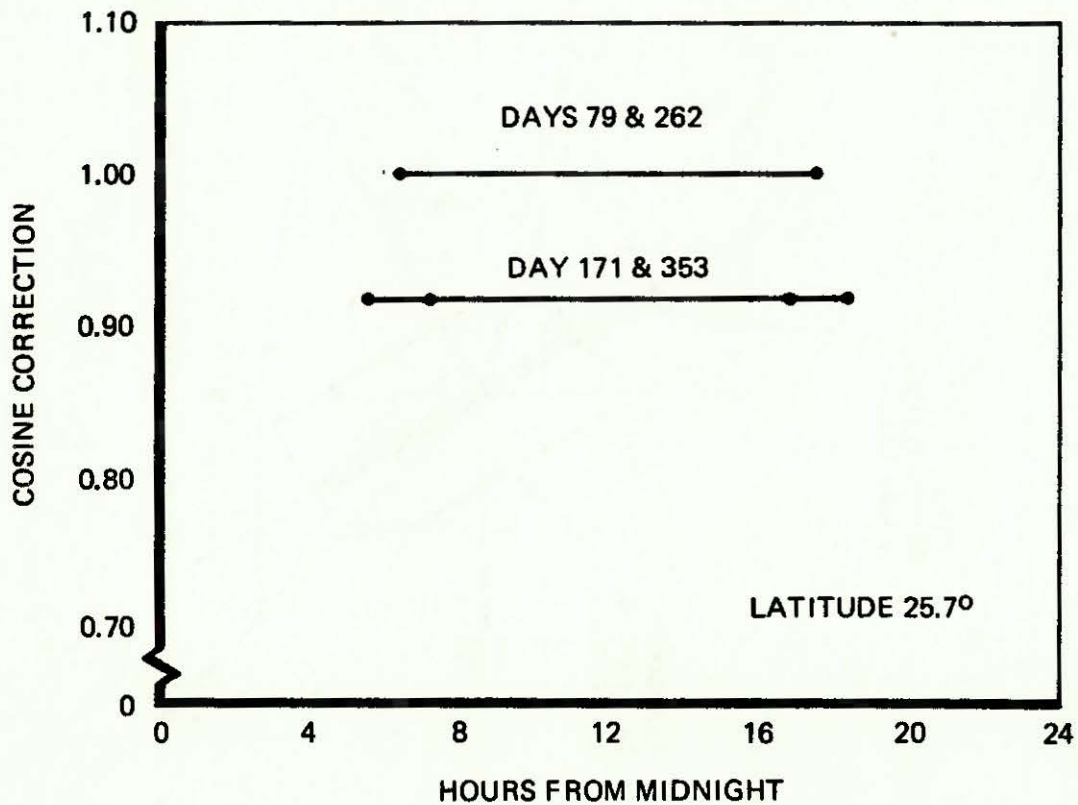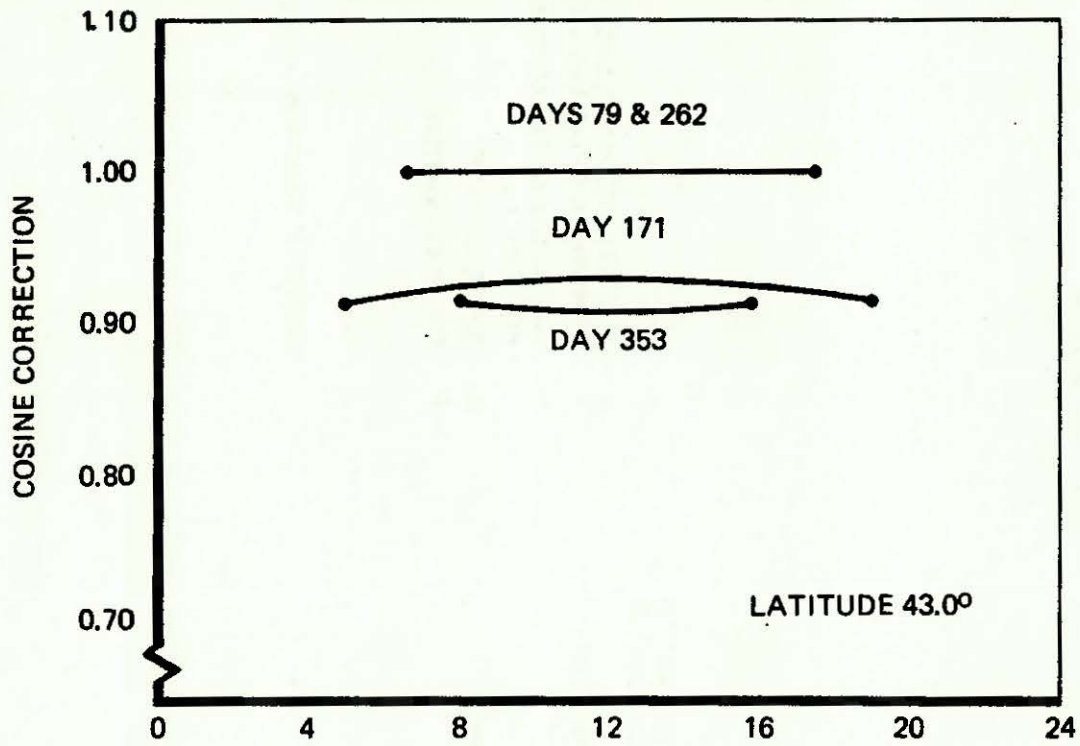
Figure 2-3

Figure 2-4

DAILY MEAN COSINE CORRECTION OF PARABOLIC
CYLINDRICAL COLLECTOR ROTATING ABOUT FOCAL AXIS

LOCATION SE (LAT = 25.7°)
TILTED 25.8° FROM HORIZ

LOCATION NC (LAT = 43.0°)
TILTED 41.8° FROM HORIZ

DAILY MEAN COSINE CORRECTION

DAY OF YEAR
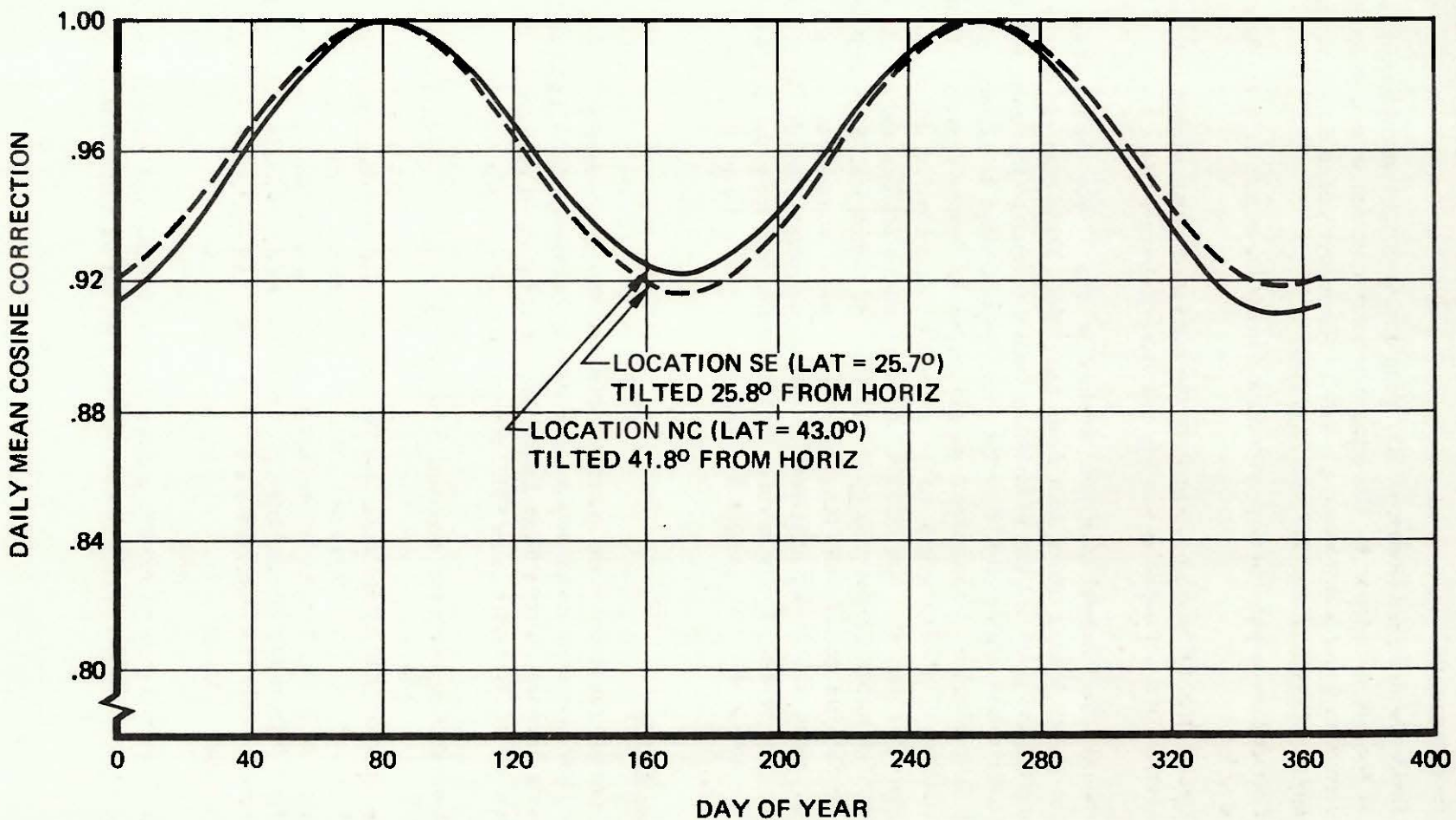
4. Integrate the computed hourly direct normal radiation and determine daily mean totals for each month.

5. Divide the measured (Reference B5) mean direct-normal insolation value for each month at the site of interest by the integrated value obtained in step 4. to obtain a mean correction factor which would account for attenuation due to clouds, dust, etc. Establish any seasonal effect upon the correction factor.

6. Correct the computed hourly direct normal insolation of step 3. by the factor obtained in step 5.

7. Deduct the diffuse component from the computed direct normal radiation, since this component is not usable by focusing collectors (Reference B4).

The final hourly direct normal insolation obtained in step 7. was the insolation input to the hour-by-hour energy balance and system sizing calculation. These data are ideal in at least one respect, for while the yearly integral of insolation used was equal to that measured, the effects of cloudiness were spread continuously over the year. In an attempt to examine the effect of bad weather on the performance and storage requirements of solar thermal conversion facilities, periods of solar occultation of arbitrary length and frequency were superposed on this insolation data. Early systems studies (11) were thus run with the "ideal" insolation profiles, and ones in which twelve 3-day "storms" occurred, commencing on the 15th day of each month. Such arbitrary choices of insolation profiles are useful only for indicating trends in component size and capital cost requirements. More reliable determination of such requirements, specific to a given location, required the more realistic hourly direct-normal insolation data from the SLL/Aerospace work. Except where noted, all results presented in this report were obtained with the SLL/Aerospace insolation data.

2.2.6 Demand Data

One of the primary purposes for the systems studies described here was to examine the economics of smoothing the seasonal mismatch between insolation and demand in STEC applications with long term or seasonal chemical energy storage. Early in the present study, it was believed that CES would make autonomous or 100 percent solar STEC power plants economically attractive.

As the systems studies proceeded, however, it became clear that the economics of autonomous STEC plants were not favorable, and that this fact could be satisfactorily established by systems studies of autonomous and hybrid plants with continuous, constant demand profiles (e.g. 100 MWe output, 24 hours/day, 365 days/year). Moreover, electrical demand profiles may change significantly in the 20 or 30 years before large-scale solar thermal conversion is first expected to become commercially usable. In the interest of time and money, therefore, use of nonconstant electrical demand profiles for systems work was abandoned. All results reported here are for STEC plants with constant output.

The local grid requirements of electric utilities at each location described in section 2.5 were obtained, however, as hourly tabulations of demand load for an entire year on computer cards

punched in the standard format of the Edison Electric Institute (Reference U1). These demand data were organized and stored on magnetic tape accessible by programs STORAGE and CSTOPT, as per contract requirements, and are available for future use with these programs.

2.2.7 CES Subsystem Model

The energy storage subsystem model used in the present systems studies was based on the reversible oxidation of sulfur trioxide: $SO_2 + 1/2 O_2 = SO_3$. The cost and performance parameters used were extracted from a substantially modified version of the SO_2/SO_3 energy storage system design developed by RRC under a previous contract (Reference G1). Neither the original design (called CESTOR) nor the modifications will be discussed at any length here. For a detailed discussion of an SO_2/SO_3 CES system, the reader is referred to section 4.2; while the SO_2/SO_3 storage system described there differs in many respects from the earlier design used in the systems studies, the salient features are the same.

The modifications to the original CESTOR design had two important results:

1. The round-trip efficiency* (thermal-to-thermal), η_{RT}, of the modified system fell to 0.40. Round-trip efficiencies of the original design ranged as high as 0.77. The decrease was due primarily to more realistic design of heat exchangers for recuperation of sensible and latent heats of reaction products.

2. The unit cost estimate ($/kg O_2 stored) for high-pressure oxygen storage vessels increased nearly fourfold over that of the original design. Reasons for this increase are discussed in section 4.2.3.

Table 2-2 presents pertinent cost and performance parameters for the SO_2/SO_3 energy storage subsystem model used in the systems analysis portion of this work.

Table 2-2
PERFORMANCE AND COST PARAMETERS USED TO CHARACTERIZE SO_2/SO_3 ENERGY STORAGE SUBSYSTEM FOR SYSTEMS STUDIES

Charging efficiency, η_c	0.57
Discharging efficiency, η_d	0.70
Round-trip efficiency, η_{RT}	0.40
Storage input temperature	1,089 K
Storage output temperature	1,089 K
Power-related unit cost	0.5×10^5 $/MW$_t$*
Energy-related unit cost	6,730 $/MW$_t^\dagger$-hr

*Based on MW_t (thermal) sent to storage

†Based on MW_t leaving storage

---

*See section 4.1.2 for discussion of CES system efficiencies.

Programs STORAGE and CSTOPT were written to accept storage charging efficiencies as thermal-to-thermal values. The efficiency of all energy conversions which occur before thermal energy is input to the storage system, or after thermal energy is released from the storage system, are taken into account by the efficiencies of other STEC subsystems. For the systems studies discussed here, the storage exit temperature and the receiver exit temperature are equal, so that the turbogenerator efficiency for energy from either source is the same. As will be discussed in section 4.3.2, optimum storage system input and output temperatures may not be equal for other candidate storage reactions. For study of such reactions with program STORAGE, storage output efficiencies must be altered (in all cases studied to date, they must be lowered) to account for the difference in availability between energy from storage and energy used directly from the receiver. Such corrections can easily be inserted when needed.

The preliminary process designs in Chapter 4, and the SO_2/SO_3 design used for the systems studies were characterized by a single power-related unit cost. Use of the single power-related cost parameter is based on the assumption that all process equipment of economic consequence is used in both the charging and discharging modes (this is indeed the case for the SO_2/SO_3 storage system design used in the systems studies reported below), and that the yearly maximum charging or discharging rate, therefore, determines the size and cost of such equipment. Results reported below support this assumption; in most cases of interest, storage charging rate far exceeded the discharging rate, so that a power-related cost estimate based on only the charging rate was adequate. The more detailed cost estimates based on the $CaO/Ca(OH)_2$ and SO_2/SO_3 storage system designs (sections 4.2.3 and 4.3.3) include both charging and discharging power-related costs. The reader will note that in both cases, the charging power-related unit costs far exceeded the discharging power-related costs.

2.2.8 Cost Estimation

All cost accounting in program STORAGE and program CSTOPT is carried out in 1978 dollars. After the cost of each STEC subsystem is calculated, these costs are added together to give the total capital equipment cost estimate, C_1. The busbar energy cost (BBEC) for the hybrid STEC plant, sketched in Figure 2-1, is then calculated according to:

$$BBEC = \frac{C_1 \cdot i \cdot f}{e_s} + ae_a + m \tag{2-1}$$

where:*

i	=	factor for interest during construction ($i = 1.3$ used in this work)
f	=	fixed charge rate ($f = 0.15$)
m	=	operation and maintenance cost ($m = \$0.006/kWh$)
e_s	=	total electricity output of solar portion of STEC plant [=] kWh
a	=	alternate energy unit cost [=] \$/kWh (1978 dollars)
e_a	=	total alternate energy required [=] kWh.

---

*The form of Equation 2-1 and the parametric values are patterned in part after the economic analysis used in SLL program BUCKS (B6).

The value of e_s and e_a calculated by STORAGE would in general be given by,

$$e_s = \sum_{i=1}^{n} d_{i_s} \quad \text{and} \quad e_a = \sum_{i=1}^{n} d_i - d_{i_s}$$

where:

    n =   number of hours of interest (8,760 for non-leap year, assuming no down time, planned or unplanned)

    d_i =   demand for hour i

    d_{i_s} =   output of solar portion of STEC plant in hour i

As explained in section 2.2.6, however, all studies reported here used a constant, continuous demand profile (100 MWe) for the entire STEC plant (solar plus alternate), so that e_s could actually be given by:

$$e_s = 8.760 \times 10^8 \, (s) \tag{2-2}$$

where s represents the fraction of the total demand which is met by the solar portion of the hybrid STEC plant. With e_s as in equation (2-2), e_a is given by,

$$e_a = 1 - s$$

For the studies reported here, then, the BBEC was calculated as follows:

$$BBEC = 2.2 \times 10^{-10} \frac{C_1}{s} + a(1 - s) + 0.006 \tag{2-3}$$

Large-scale solar electric power generation is not likely within the next 20 years or so, and while it is safe to assume that the cost of energy generated by conventional means will increase during that time, it is difficult to say by how much. Levelized (D2) alternate energy costs have, therefore, been set arbitrarily for the optimization studies described below at 0.100, 0.200, 0.300, 0.400 \$/kWh in 1978 dollars. Table 2-3 presents alternate energy escalation rates which produce these values. Consider the example of a levelized alternate energy cost of \$0.100/kWh. Taking the present cost of alternate electrical energy as \$0.030/kWh, and the other assumptions as shown in Table 2-3, an alternate energy escalation rate of 7.0 percent/year, through the year 2030, would result in a levelized alternate energy cost of \$0.100/kWh in the year 2000 (1978 dollars).

2.3 STEC SIMULATION CODE

At the level of detail of the STEC simulation presented here, the most important and useful independent variables are the storage capacity, Q, and the collector or heliostat area, A. The dependent variable of interest for economic evaluation is the busbar energy cost, BBEC The systems

Table 2-3
LEVELIZED ALTERNATE ELECTRIC ENERGY COSTS

(1978 Alternate Energy Costs $0.030/KWH)

Levelized Alternate Energy Cost ($/KWH)	Alternate Energy Cost Escalation Rate (Percent/Year)
0.100	7.0
0.200	9.1
0.300	10.3
0.400	11.1

All Costs in 1978 Dollars

General inflation rate	5%/year
Discount rate	8%
Plant startup date	2000
Plant economic life	30 years

studies reported here, then, were primarily concerned with finding the particular storage capacity and collector area which minimized the BBEC for a given case (plant type, location, etc.). This is true for both autonomous and hybrid STEC plants.

The conceptual division of STEC plants into autonomous and hybrid types provides a convenient approach to discussion of program STORAGE. The conditions for autonomous STEC operation provide a convenient starting point for the discussion, so that the simulation of 100 percent solar operation will be discussed first. The logic of program STORAGE is described briefly in section 2.3.2. Finally, incorporation of program STORAGE into an automatic optimization program, CSTOPT, is discussed in section 2.3.3.

2.3.1 Autonomous Solar Power Generation

For a given insolation profile, demand profile, and plant specification, there exists a minimum, or critical, collector area, A*, such that

$$\sum_{year} d_i = \sum_{year} i_j$$

where i_j and d_i are insolation and demand, respectively, for hour i. Insolation and demand are, of course, adjusted for system efficiencies so that they are on the same basis. For collector areas greater than or equal to A*, it is possible for a STEC plant, with the necessary storage capacity, to satisfy 100 percent of the demand load. Even with collector areas $\geqslant$A*, a STEC facility with less

than the necessary storage capacity may not be capable of stand-alone operation. STEC facilities with collector areas less than A* cannot satisfy 100 percent of the demand load, regardless of their storage size.

The relative position of the critical area, A*, is shown schematically in Figure 2-6. Associated with the critical area, A*, is a critical storage capacity Q*, and together they define the critical point. At all collector areas to the left of A*, it is theoretically impossible to meet 100 percent of the demand from solar energy, regardless of the storage capacity available, and hybrid operation is mandatory.

At all collector areas to the right of A*, it is possible to meet 100 percent of the demand from solar energy, if enough storage is available. The curve in Figure 2-6 represents schematically (for any A) the minimum storage capacity required to maximize the solar fraction at a given collector area. Points above the curve represent STEC plants with too much storage for their collector area. Points below the curve describe STEC plants which, due to storage limitations, can provide less than the maximum solar fraction which their collectors would allow. Points to the right of A*, but below the curve, can therefore not meet 100 percent of the demand from solar energy due to storage limitations, even though they have enough collector area to do so. Autonomous solutions, then, are confined to the region to the right of A* and on or above the curve. Although the program is capable of it, the present analysis does not consider solutions with greater than the minimum storage necessary to fully utilize the available collectors (i.e., all of the region above the curve), so the autonomous solutions are actually confined to points on the curve to the right of the critical point.

From an economic point of view, the general problem addressed by the systems studies described here is an optimization problem in two-space: to find the point in the A-Q plane at which the BBEC is a minimum. Within this general problem, the particular problem of finding the optimum autonomous solution is addressed.

2.3.2 Program STORAGE

From the point of view of the previous paragraph, program STORAGE may be generally described as a code which calculates the BBEC for a given storage capacity and collector area. It is also the purpose of this work to study STEC system, and particularly storage subsystem, performance, and design requirements over a wide range of solar fraction. The output of program STORAGE, therefore, contains considerably more than just the BBEC. Table 2-4 presents a list of important input specifications for STORAGE, while Table 2-5 tabulates important program output.

Figure 2-5 is a schematic representation of the program STORAGE flow sheet. The program first reads the input data, including those listed in Table 2-4, and uses this information to assemble the correct case to be run. The correct hourly insolation data are called from a tape file and read into an array within the program.

For each case, the first run through the energy balance and system sizing calculation is to determine the critical point for that case. Coordinates of subsequent A-Q points to be studied are normalized to the critical values, and run through a different version of the hour-by-hour energy balance (FSTR).

Table 2-4
IMPORTANT INPUT SPECIFICATIONS FOR PROGRAM STORAGE

1) System type (A, B, C)   Section 2.2.1

2) Location (NC, SE, SW, NE)   Section 2.2.4

3) Energy storage subsystem parameters   Section 2.2.7
   (η_c, η_d, unit costs)

4) Utilization conditions   Section 2.3.2

   a) Area fraction, f_a
   b) Storage fraction, f_s

5) Plant nameplate power rating   (e.g. 100 MW_e)

6) Alternate energy cost ($/kWh)   Section 2.2.8

7) Collector unit cost ($/m^2)   Section 2.2.3

8) Receiver unit cost ($/m^2)   Section 2.2.3

Table 2-5
SELECTED OUTPUT OF PROGRAM STORAGE

1) Busbar energy cost   Section 2.2.8

2) Cost breakdown

   a)   Front end and power generation subsystems

   b)   Storage subsystem major equipment costs

3) Size breakdown

4) System performance map (month-by-month)

   a)   Demand (MW_e-hr)

   b)   Solar input (MW_t-hr)

   c)   Fraction of solar input direct to grid

   d)   Fraction of electric output direct from collectors

   e)   Energy in storage at end of month

5) Maximum storage charge and discharge rates

6) Solar fraction

7) Maximum turbogenerator output

SCHEMATIC OF PROGRAM STORAGE

```
                        ┌─────────┐
                        │  START  │
                        └────┬────┘
                             │
                      ┌──────┴──────┐
                      │ READ INPUT  │◄──────────────┐
                      │    DATA     │               │
                      └──────┬──────┘               │
                             │                      │
                      ┌──────┴──────┐               │
                      │  ASSEMBLE   │               │
                      │   CORRECT   │               │
                      │ STEC MODEL &│               │
                      │  INSOLATION │               │
                      │    DATA     │               │
                      └──────┬──────┘               │
                             │                      │
                        ╱────┴────╲      NO         │
                       ╱ CRITICAL  ╲──────────┐     │
                       ╲  CASE?    ╱          │     │
                        ╲────┬────╱           │     │
                             │ YES            │     │
```

HOUR-BY-HOUR
ENERGY BALANCE

```
  ┌──────────┐                    ┌──────────┐
  │  ASSUME  │                    │  ASSUME  │
  │COLLECTOR │                    │ MAXIMUM  │◄──┐
  │   AREA   │                    │ STORAGE  │   │
  └────┬─────┘                    │ CAPACITY │   │
       │                          └────┬─────┘   │
  ┌────┴─────┐                         │         │
  │  ASSUME  │                         │         │
  │ INITIAL  │                         │         │
  │ STORAGE  │                         │         │
  │INVENTORY │                         │         │
  └────┬─────┘                         │         │
       │                               │         │
  ┌ ─ ─┼─ ─ ─ ─ ─ ─ ─ ─ ─ ─ ─ ─ ─ ─ ─ ┼ ─ ─ ┐   │
     ┌─┴──────┐                   ┌────┴───┐     │
  │  │ DESTOR │                   │ FRSTOR │ │   │
     └─┬──────┘                   └────┬───┘     │
  └ ─ ─┼─ ─ ─ ─ ─ ─ ─ ─ ─ ─ ─ ─ ─ ─ ─ ┼ ─ ─ ┘   │
       │                               │         │
   ╱───┴───╲    NO               ╱─────┴──╲  NO  │
  ╱ STEADY  ╲───────┐           ╱  STEADY  ╲─────┘
  ╲ STATE? ╱        │           ╲  STATE? ╱
   ╲───┬───╱        │            ╲────┬───╱
       │ YES        │                 │ YES
       │      ┌─────┴──────┐          │
       └─────►│  SIZE & COST│◄────────┘
              │     OF      │
              │ SUBSYSTEMS  │
              └──────┬──────┘
                     │
              ┌──────┴──────┐
              │   OUTPUT    │
              │    COST     │
              │  BREAKDOWN  │
              │ PERFORMANCE │
              │     MAP     │
              └──────┬──────┘
                     │
                ╱────┴────╲    YES
               ╱   MORE    ╲────────────┐
               ╲  CASES?   ╱            │
                ╲────┬────╱             │
                     │                  │
                ┌────┴────┐
                │   END   │
                └─────────┘
```
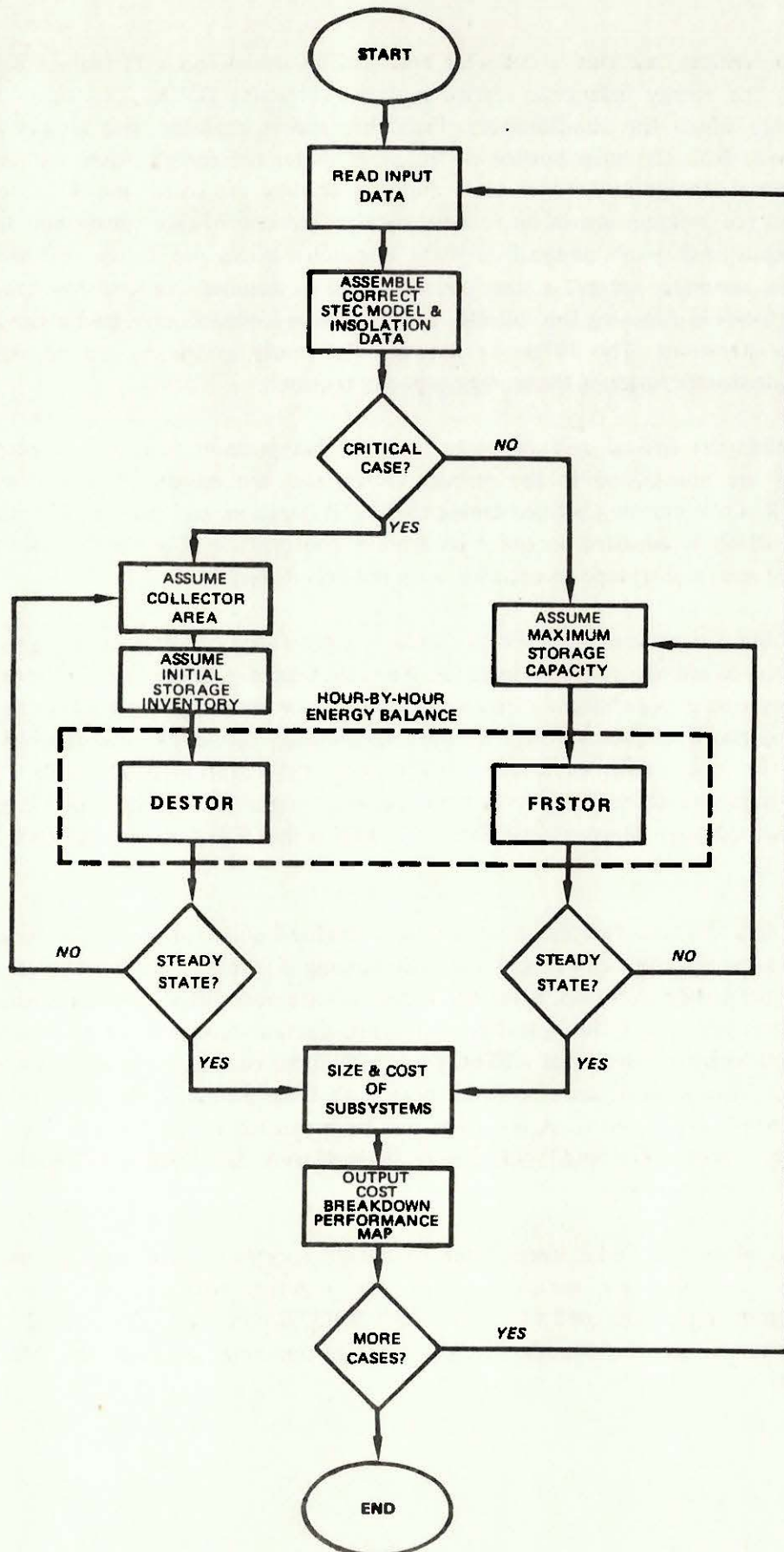
On the first, or critical case run, a collector area and an initial (hour 1) storage inventory are assumed before the energy balance is carried out by subroutine DSTR. This subroutine always stores any energy which the sun-following dispatcher makes available, and always attempts to satisfy the demand from the solar portion of the plant. After the energy balance is complete, the year-end and initial storage inventories are compared. If they are equal, the STEC system is at steady state, and the program moves on to estimate size and cost of each subsystem, and print the critical case output; if they are unequal, or if the dispatcher could not satisfy 100 percent of the demand without alternate energy, a new collector area is assumed and another energy balance carried out. With care in choosing the collector area recursion formula, convergence can be achieved in two or three iterations. The difference between the yearly maximum and minimum storage inventories, or the storage range, is the storage capacity required.

If cases other than the critical case are to be run, the independent variables collector area and storage capacity are normalized to the critical values, and the energy balance carried out by subroutine FSTR. Collector area is fixed during the FSTR iteration, and maximum storage capacity is the variable which is adjusted in order to achieve convergence. The convergence criterion is equality of initial and final storage inventories, as in the DSTR iteration.

As explained above for normalized collector areas less than unity, autonomous operation is not possible, regardless of storage capacity available. For normalized collector areas greater than unity, autonomous operation is possible for storage capacities on or above the curve CD in Figure 2-6. If, for a particular normalized collector area, a normalized storage capacity greater than on curve BCD is specified in the input, both subroutines FSTR and DSTR automatically reduce the storage capacity to the value which would fall on the curve (the maximum useful storage capacity). The primary difference between subroutines DSTR and FSTR is that FSTR allows less than 100 percent solar operation.

Input to FSTR includes four factors, representing normalized collector area (f_a), storage capacity (f_s), and the maximum storage charging (f_c) and discharging (f_d) rates. The first two are normalized to the values at the critical solution, while the latter two are normalized to the maximum charging or discharging rates possible at the f_a and f_s of interest. Certain choices of these factors will place limits on the four variables, such that a STEC plant with those constraints could not operate solely from solar input. The hybrid cases reported here have been primarily intended to explore the dependence of BBEC on f_a and f_s. A few cases will be presented which focus on limiting storage charging rates, or "storage clipping." No cases of interest were found for which limits on storage discharging rates were important.

In hybrid cases, subroutine FSTR keeps track of energy shortfall which must be made up with alternate energy. The alternate energy requirements, together with the alternate energy cost specified as program input, are used to calculate the BBEC according to Equation 2-3. This same equation is, of course, used to determine the BBEC, in autonomous cases with the solar fraction, s, set equal to unity.

SCHEMATIC OF RELATIONSHIP BETWEEN STORAGE CAPACITY AND COLLECTOR AREA

Solar involvement has been maximized. Pure solar designs must lie to the right of the critical collector area and above the minimum storage size for pure solar applications.
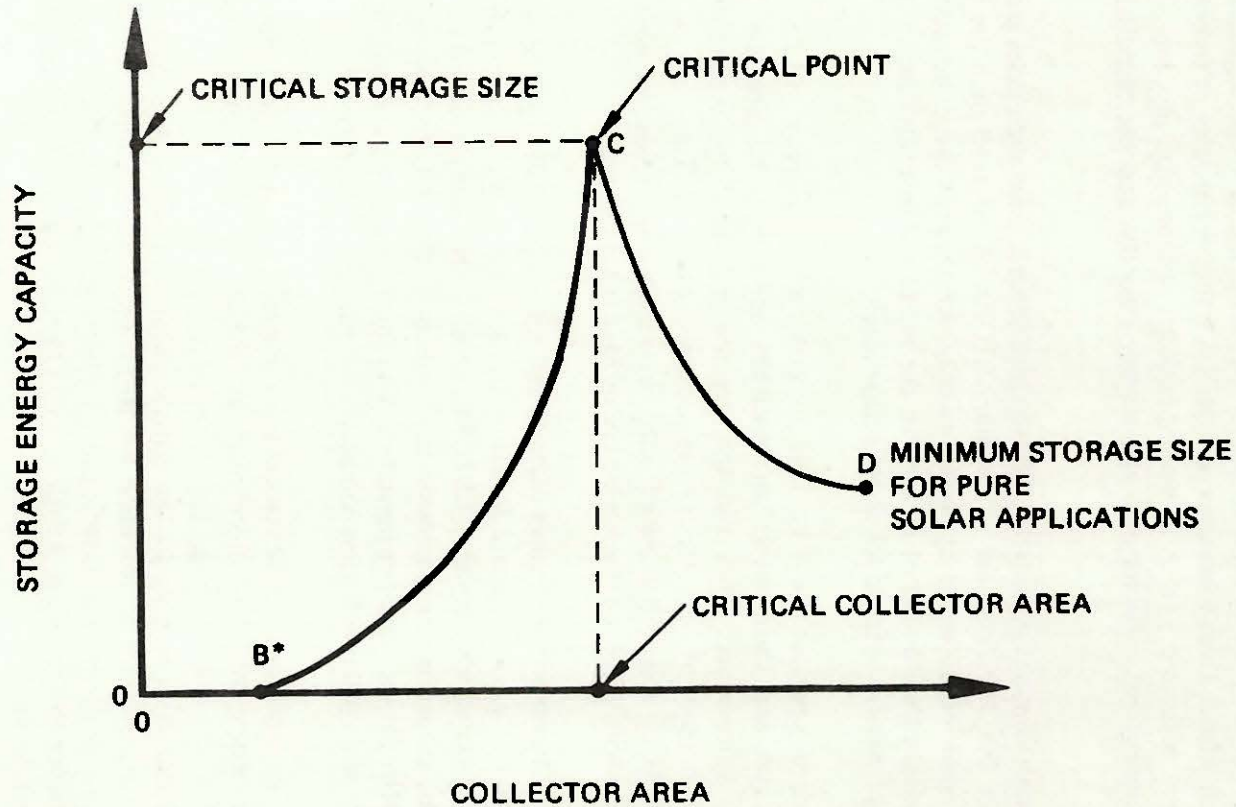
*THE POINT B REPRESENTS THE MINIMUM COLLECTOR AREA FOR WHICH THE PLANT NAMEPLATE OUTPUT CAN STILL BE PROVIDED FROM DIRECT SOLAR ENERGY, AT NOON ON THE BEST SOLAR DAY OF THE YEAR. "SOLAR MULTIPLES" ARE COMMONLY DEFINED IN TERMS OF THIS AREA, WHICH IS GIVEN A SOLAR MULTIPLE EQUAL TO 1.0.

A typical output listing from program STORAGE is reproduced in Figure 2-7. The particular case is for a STEC system B at location SE. The listing includes the critical case and an additional autonomous case for $f_a = 1.23$, $f_s = 0.30$.

2.3.3   Program CSTOPT

The optimum STEC facility, in all studies discussed here, is the one which produces electricity at the lowest levelized BBEC. It was noted in section 2.3.1 that for studies of hybrid STEC systems, the general problem addressed here is a two-dimensional optimization problem. The independent variables are the normalized collector area and storage capacity, and the objective function is the levelized BBEC.

Optimization for autonomous cases is relatively straightforward, since such cases are confined to the curve BC in Figure 2-6. Judicious use of program STORAGE to determine the BBEC at various points along this curve produces an optimum quickly. Removal of the constraint of 100 percent solar operation changes the domain of interest to the entire region below and including the curve BCD, and makes optimization very much more complicated.

While an experienced operator may be able to make good "guesses" as to the sequence of conditions to be run and thus obtain an optimum solution using program STORAGE, the sometimes lengthy turn-around times and the iterative nature of the procedure make a coded optimizer, with a minimum of operator involvement, advantageous. Therefore, a modified version of program STORAGE was incorporated into an existing optimization code, called SIMIN (Reference J2), obtained from the program library of Sandia Laboratories.

Subroutine SIMIN is based on the simplex method and finds a minimum (within covergence criteria specified by the user) of a real objective function. Both SIMIN and parts of STORAGE have been made subroutines of a master subroutine, CSTOPT, which carries out the executive tasks of reading input specifications, preparing the appropriate version of STORAGE for use by SIMIN, turning control over to SIMIN for the actual optimization, and finally obtaining and printing a performance map of the STEC facility at the optimum conditions determined by SIMIN.

Program CSTOPT is represented schematically in Figure 2-8. After the input specifications, including alternate energy cost, have been read and the correct STEC model and insolation data have been assembled, the critical design case is found and the independent variables f_a and f_s are defined by normalizing with respect to the critical point. Control is then turned over to SIMIN which directs subroutine FSTR to calculate the BBEC for selected points (f_a, f_s) until a suitable optimum solution has been found. Printed output includes a program STORAGE performance map and cost breakdown for the optimum solution, and a brief listing of the cases tried by SIMIN in its quest for the optimum one.

In adapting program STORAGE for inclusion as a subroutine in CSTOPT, considerable editing (removal of unneeded input and output statements, etc.) of the program in general, and streamlining of the critical hour-by-hour energy balance in particular were accomplished. A typical

SYSTEM SE (SOUTHEAST)   LATITUDE= 25.7

100 MW ELECTRICAL BASELOAD

COLLECTOR FIELD AREA=   4274766 SQ M = 1.65 SQ MI
INITIAL STORAGE=   3963 MW-HR, THERMAL
(STORAGE IN THERMAL ENERGY PRIOR TO STORAGE SYSTEM)

EFFICIENCIES   COLLECTOR   1.0000   RECEIVER   .8920   TRANSPORT   1.0000
                POWER GEN   .4700   TO STORAGE .5715   FROM STORAGE .7000

DATE	DEMAND MW-HR, EL	SOLAR INPUT MW-HR, TH	STORAGE, IN MW-HR, TH	STORAGE, OUT MW-HR, TH	RATIO, IN/OUT STORAGE	STORAGE, TOTAL MW-HR, TH
1/31	74400.0	444850.0	341745.0	258059.4	1.3243	87648.9
2/29	69600.0	336020.4	248562.2	242262.5	1.0260	93948.6
3/31	74400.0	411434.4	305112.3	240996.5	1.2660	158064.3
4/30	72000.0	365318.0	269007.3	240807.9	1.1171	186263.8
5/31	74400.0	409117.7	299379.0	231830.7	1.2914	253812.1
6/30	72000.0	268980.2	180901.1	235376.2	.7686	199336.9
7/31	74400.0	360967.2	254148.3	226130.3	1.1239	227354.9
8/31	74400.0	335800.7	237642.7	240985.6	.9861	224011.9
9/30	72000.0	228534.9	159022.5	270868.1	.5871	112166.3
10/31	74400.8	307488.7	218683.0	256720.3	.8518	74129.0
11/30	72000.0	314373.4	228994.4	254380.1	.9002	48743.3
12/31	74400.0	309608.3	226330.4	271110.4	.8348	3963.3

TOTAL SOLAR INPUT (MW-HR, THERMAL)   4092494

TOTAL DEMAND (MW-HR, ELEC)   =   878400

MAXIMUM IN STORAGE (MW-HR, THERMAL)   308557   (MW-HR, ELEC)   58016   (DATE)   5/26

MINIMUM IN STORAGE (MW-HR, THERMAL)   =0   (MW-HR, ELEC)   =0   (DATE)   1/ 1

RANGE IN STORAGE (MW-HR, THERMAL)   308557   (MW-HR, ELEC)   58016

CHANGE IN STORAGE (MW-HR, THERMAL)   0   (MW-HR, ELEC)   0

MAX RATE TO STORAGE (MW-HR/HR, THERMAL)   2554   MAX RATE FROM STORAGE (MW-HR/HR, THERMAL)   532

MAX TURBO-GEN POWER, CHARGE (MW, ELEC)   614.3   MAX TURBO-GEN POWER, DISCHARGE (MW, ELEC) 142.9

TOTAL FROM STORAGE (MW-HR, ELEC)   558341

DIRECT, SOLAR-TO-GRID (MW-HR, ELEC)   320059

STORAGE SUBSYSTEM COSTS (MEGADOLLARS)

RATE RELATED COSTS

REACTOR	52.877
HEAT EXCHANGERS	30.756
SEPARATOR COLUMN	27.960
VAPORIZER/CONDENSER	.811
COOLER	.363
REACTION PRODUCTS COMPRESSOR	20.093
OXYGEN COMPRESSOR	3.701
SO2 PUMPS	.148
SO3 PUMPS	.089
MIXER	.350
SUBTOTAL	137.150

CAPACITY RELATED COSTS

INITIAL SO3 INVENTORY	66.833
STORAGE VESSELS, O2	710.123
STORAGE VESSELS, SOX	53.431
SUBTOTAL	830.387

STORAGE SUBSYSTEM

TOTAL	967.538

Figure 2-7 (Continued)

SYSTEM SE (SOUTHEAST)   LATITUDE= 25.7

100 MW ELECTRICAL BASELOAD

COLLECTOR FIELD AREA=   5257963 SQ M = 2.03 SQ MI   (123.0 PCT)
INITIAL STORAGE=   66210 MW-HR, THERMAL
(STORAGE IN THERMAL ENERGY PRIOR TO STORAGE SYSTEM)

| EFFICIENCIES | COLLECTOR | 1.0000 | RECEIVER | .8920 | TRANSPORT | 1.0000 |
| | POWER GEN | .4700 | TO STORAGE | .5715 | FROM STORAGE | .7000 |

DATE	DEMAND	SOLAR INPUT	STOR, IN	STOR, OUT	RATIO IN/OUT	STOR, TOT	DEMAND SATISFIED	DELTA DEMAND	DEMAND HOURS NOT DELIVERED	STORAGE EXPELLED
	MW-HR,EL	MW-HR,TH	MW-HR,TH	MW-HR,TH		MW-HR,TH	MW-HR,EL	MW-HR,EL		MW-HR,TH
1/31	74400.0	547165.5	278551.1	257827.7	1.0837	87733.3	74400.0	.0	.0	154046.8
2/29	69600.0	413305.1	226958.5	239659.4	.9470	75032.4	69600.0	.0	.0	89500.3
3/31	74400.0	506064.3	249806.1	238720.6	1.0464	86117.8	74400.0	.0	.0	138805.6
4/30	72000.0	449341.1	228695.2	238178.8	.9602	76634.2	72000.0	.0	.0	114209.0
5/31	74400.0	503214.8	192054.6	228603.1	.8401	40085.7	74400.0	.0	.0	189967.7
6/30	72000.0	330845.4	234595.8	231653.6	1.0127	43028.0	72000.0	.0	.0	
7/31	74400.0	443989.7	231466.1	222621.1	1.0397	51872.9	74400.0	.0	.0	95334.4
8/31	74400.0	413034.9	265731.1	237646.4	1.1182	79957.6	74400.0	.0	.0	39468.6
9/30	72000.0	281098.0	204972.4	268527.8	.7633	16402.3	72000.0	.0	.0	.0
10/31	74400.0	375211.1	280608.1	253822.5	1.1055	43188.0	74400.0	.0	.0	.0
11/30	72000.0	365679.3	290203.3	251986.3	1.1517	81405.0	72000.0	.0	.0	2330.3
12/31	74400.0	360818.2	253516.3	268711.3	.9435	66209.9	74400.0	.0	.0	35373.6

TOTAL SOLAR INPUT (MW-HR, THERMAL)   5033767

TOTAL DEMAND (MW-HR, ELEC)   878400

TOTAL DEMAND DELIVERED (MW-HR, ELEC)   878400   (100.0 PCT)

TOTAL HOURS NOT DELIVERED (HRS)   0

STORAGE EXPELLED (MW-HR, THERMAL)   859036

MAXIMUM IN STORAGE (MW-HR, THERMAL)   92913   (MW-HR, ELEC)   17470   (DATE)   1/ 4

MINIMUM IN STORAGE (MW-HR, THERMAL)   0   (MW-HR, ELEC)   0   (DATE)   6/11

RANGE IN STORAGE (MW-HR, THERMAL)   92913   (MW-HR, ELEC)   17470   (30.1 PCT)

CHANGE IN STORAGE (MW-HR, THERMAL)   0   (MW-HR, ELEC)   0

MAX RATE TO STORAGE (MW-HR/HR, THERMAL)   3108   MAX RATE FROM STORAGE (MW-HR/HR, THERMAL)   532

MAX TURBO-GEN POWER, CHARGE (MW, ELEC)   726.0   MAX TURBO-GEN POWER, DISCHARGE (MW, ELEC)   142.9

TOTAL FROM STORAGE (MW-HR, ELEC)   552255

DIRECT, SOLAR-TO-GRID (MW-HR, ELEC)   326145

Figure 2-7 (Continued)

STORAGE SUBSYSTEM COSTS (MEGADOLLARS)

RATE RELATED COSTS

REACTOR	58.334
HEAT EXCHANGERS	37.431
SEPARATOR COLUMN	34.028
VAPORIZER/CONDENSER	.987
COOLER	.442
REACTION PRODUCTS COMPRESSOR	22.167
OXYGEN COMPRESSOR	4.083
SO2 PUMPS	.180
SO3 PUMPS	.109
MIXER	.425
SUBTOTAL	158.187

CAPACITY RELATED COSTS

INITIAL SO3 INVENTORY	20.125
STORAGE VESSELS, O2	213.833
STORAGE VESSELS, SO3	16.089
SUBTOTAL	250.047

STORAGE SUBSYSTEM

TOTAL	408.234

Figure 2-7 (Concluded)

SCHEMATIC OF PROGRAM CSTOPT

Flowchart:

START
↓
READ INPUT
↓
ASSEMBLE STEC MODEL & INSOLATION DATA
↓
CRITICAL DESIGN CASE SUBROUTINE DESTOR FROM PROGRAM STORAGE
↓
DEFINE SCALING FACTORS
↓
SIMIN — (fₐ, f_s →) SUBROUTINE FRSTOR FROM STORAGE; (BBEC); (→ LISTING OF ITERATIONS)
↓
SUBROUTINE FRSTOR FROM STORAGE → STANDARD OUTPUT (OPTIMUM SOLUTION ONLY) → MORE CASES? — YES → (back to READ INPUT) / NO → END
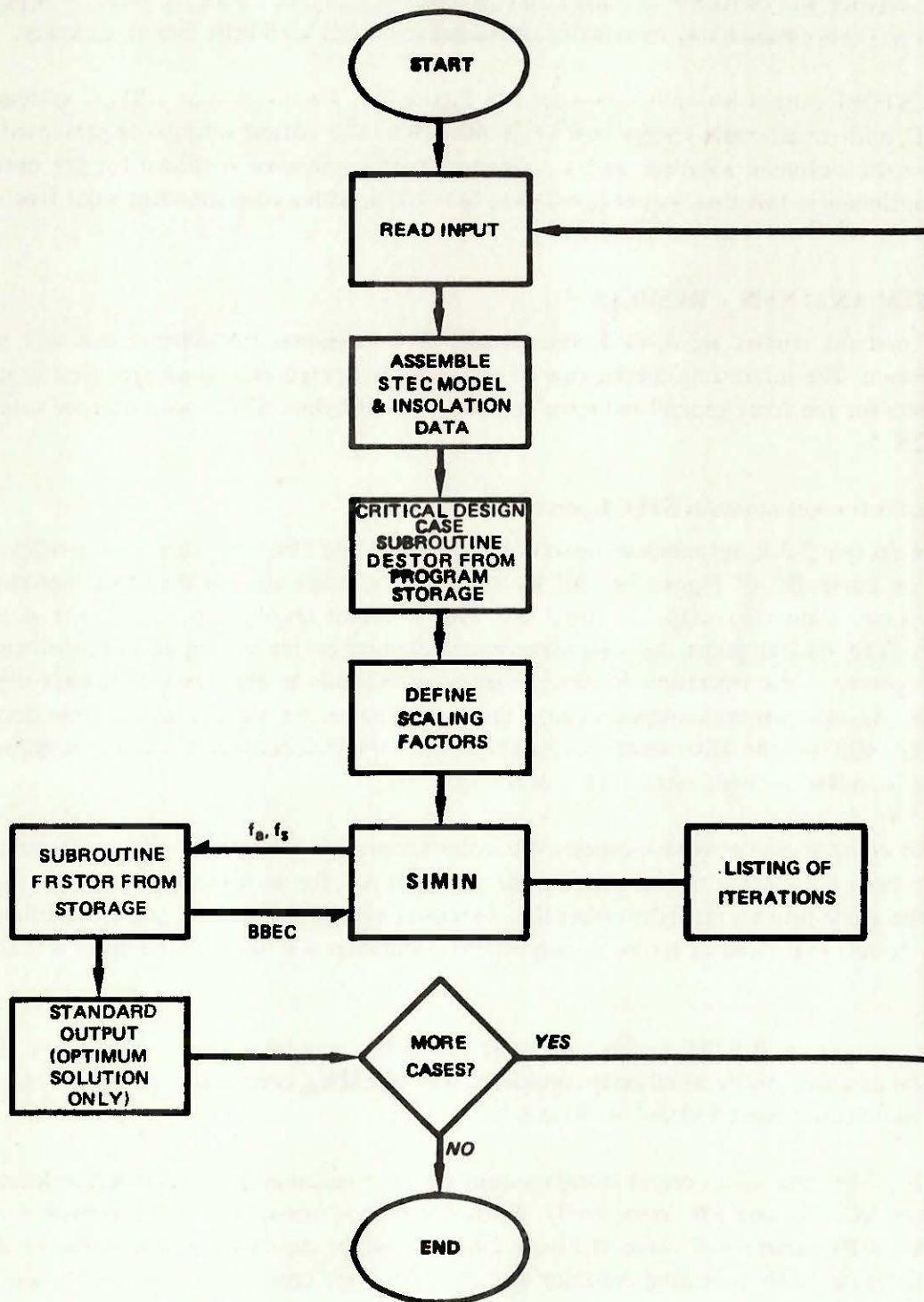
run of CSTOPT required 65 iterations (each one involving an evaluation of subroutine FRSTOR) before convergence was obtained, and used 30.6 seconds of cpu time on a CDC 6600. It is possible to shorten run times considerably by relaxing convergence criteria with little loss of accuracy.

A typical CSTOPT output listing is reproduced in Figure 2-9, for the case of a STEC system B at location NC, with an alternate energy cost of $0.400/kWh. The critical solution is presented first, followed by the optimum solution, and a subsystem cost breakdown is shown for the optimum case. The optimum in this case was at $f_a = 0.498$, $f_s = 0.016$, with a corresponding solar fraction of 0.566.

2.4 SYSTEM ANALYSIS – RESULTS

Results of systems studies are divided conceptually into categories for autonomous and hybrid STEC operation. The interesting special case of autonomous operation is considered first in section 2.4.1. Results for the more general and more complex case of hybrid STEC operation are presented in section 2.4.2.

2.4.1 Results for Autonomous STEC Operation

As noted in section 2.3.1, autonomous operation is confined to STEC configurations corresponding to points on curve BC of Figure 2-6. All locations and systems studied displayed autonomous operation curves similar in shape to curve BC, with different absolute values for the A and Q coordinates. The critical point, by definition corresponding to the minimum collector area for which 100 percent solar operation is possible, also corresponds to the greatest storage capacity requirement. As collector area increases above the critical value, the storage requirement decreases continuously until it eventually reaches a constant minimum which corresponds to the length of the longest solar occultation (night, storm, etc.) of the year.

As an aid to comparison between locations, the collector area coordinates of the results presented below have been normalized to the critical collector area, A^*, for each location. Storage capacity has also been made into an intensive rather than extensive variable by quoting storage requirements in hours*. Results expressed in terms of such intensive variables will be independent of STEC plant size.

Only results for system B STEC facilities are presented below, and those only for locations SE, NC, and SW. The demand profile in all cases considered was 100 MW$_e$, continuous. Heliostat costs were $900/m^2, and receiver costs $50/m^2 in all cases.

Figures 2-10, 2-11, and 2-12 present storage requirements as functions of normalized collector area for locations NC, SE, and SW, respectively. Critical collector areas, A^*, are also given for each location. As in the generalized curve of Figure 2-6, the storage capacity required for autonomous operation decreases with increasing collector area. Note that the critical collector area to which the

---

*One hour of storage time is the equivalent amount of stored energy which, upon discharge from storage, could produce the nameplate capacity of the plant for one hour.

SYSTEM NC (NORTH CENTRAL) LATITUDE= 43.0

100 MW ELECTRICAL BASELOAD

COLLECTOR FIELD AREA= 4807286 SQ M = 1.86 SQ MI
INITIAL STORAGE= 340743 MW-HR, THERMAL
(STORAGE IN THERMAL ENERGY PRIOR TO STORAGE SYSTEM)

| EFFICIENCIES | COLLECTOR 1.0000 | RECEIVER .8920 | TRANSPORT 1.0000 |
| | POWER GEN .4700 | TO STORAGE .5715 | FROM STORAGE .7000 |

DATE	DEMAND MW-HR, EL	SOLAR INPUT MW-HR, TH	STORAGE, IN MW-HR, TH	STORAGE, OUT MW-HR, TH	RATIO, IN/OUT STORAGE	STORAGE, TOTAL MW-HR, TH
1/31	74400.0	137153.2	98229.0	335423.6	.2929	103548.2
2/28	67200.0	73818A.3	175257.3	264401.5	.6628	14404.0
3/31	74400.0	426817.5	322810.6	250936.7	1.2864	86277.9
4/30	72000.0	386523.1	294409.9	267023.6	1.1175	117664.2
5/31	74400.0	376252.9	289060.7	279317.5	1.0349	127407.4
6/30	72000.0	435055.3	329783.2	237233.7	1.3901	219956.9
7/31	74400.0	600297.8	463501.4	215807.2	2.1478	467651.1
8/31	74400.0	496312.2	378819.9	235988.8	1.6052	610482.2
9/30	72000.0	400325.4	309360.4	263621.1	1.1735	656221.5
10/31	74400.0	345900.2	263255.8	282491.5	.9319	636985.9
11/30	72000.0	182532.6	132883.6	308101.3	.4313	461768.1
12/31	74400.0	246312.0	183062.8	304088.1	.6020	340742.8

TOTAL SOLAR INPUT (MW-HR, THERMAL) 4271668

TOTAL DEMAND (MW-HR, ELEC) 876000

MAXIMUM IN STORAGE (MW-HR, THERMAL) 729304 (MW-HR, ELEC) 137126 (DATE) 10/12

MINIMUM IN STORAGE (MW-HR, THERMAL) -0 (MW-HR, ELEC) -0 (DATE) 2/27

RANGE IN STORAGE (MW-HR, THERMAL) 729304 (MW-HR, ELEC) 137126

CHANGE IN STORAGE (MW-HR, THERMAL) 0 (MW-HR, ELEC) 0

MAX RATE TO STORAGE (MW-HR/HR, THERMAL) 2877 MAX RATE FROM STORAGE (MW-HR/HR, THERMAL) 532

MAX TURBO-GEN POWER, CHARGE (MW, ELEC) 679.4 MAX TURBO-GEN POWER, DISCHARGE (MW, ELEC) 142.9

TOTAL FROM STORAGE (MW-HR, ELEC) 610030

DIRECT, SOLAR-TO-GRID (MW-HR, ELEC) 265970

SYSTEM NC (NORTH CENTRAL) LATITUDE= 43.0

100 MW ELECTRICAL BASELOAD

COLLECTOR FIELD AREA=   2393917 SQ M =   1.00 SQ MI   (49.8 PCT)
INITIAL STORAGE=   0 MW-HR. THERMAL
(STORAGE IN THERMAL ENERGY PRIOR TO STORAGE SYSTEM)

EFFICIENCIES	COLLECTOR	1.0000	RECEIVER	.8920	TRANSPORT	1.0000
	POWER GEN	.4700	TO STORAGE	.5715	FROM STORAGE	.7000

DATE	DEMAND MW-HR.EL	SOLAR INPUT MW-HR.TH	STOR. IN MW-HR.TH	STOR. OUT MW-HR.TH	RATIO IN/OUT	STOR. TOT MW-HR.TH	DEMAND SATISFIED MW-HR.EL	DELTA DEMAND MW-HR.EL	DEMAND HOURS NOT DELIVERED	STORAGE EXPELLED MW-HR.TH
1/31	74400.0	199.1	39672.5	39672.5	1.0000	.0	17447.0	-56953.0	569.5	.0
2/28	67200.0	11611.3	72887.8	72844.3	1.0006	43.5	29165.8	-38034.2	380.3	.0
3/31	74400.0	21545.2	136340.2	136383.7	.9997	.0	50670.9	-23729.1	237.3	.0
4/30	72000.0	17479.6	127703.7	127703.7	1.0000	.0	43941.2	-28058.8	280.8	1583.9
5/31	74400.0	16365.2	109146.2	108718.5	1.0039	427.7	40620.0	-33780.0	337.8	15050.8
6/30	72000.0	21647.5	137656.4	135036.4	1.0194	3048.0	49975.9	-22024.1	220.2	3282.4
7/31	74400.0	24934.4	179650.2	179650.2	1.0051	3963.0	65256.0	-9144.0	91.4	19110.8
8/31	74400.0	24152.0	161740.6	160643.5	1.0068	5060.1	57802.7	-16597.3	166.0	.0
9/30	72000.0	19352.8	132444.2	137504.3	.9632	.0	47181.9	-24818.1	248.2	.0
10/31	74400.0	17250.3	111304.5	111304.5	1.0000	.0	40829.0	-33571.0	339.7	.0
11/30	72000.0	9897.0	54712.8	54712.8	1.0000	.0	22680.0	-49320.0	493.2	.0
12/31	74400.0	12657.7	75050.2	75050.2	1.0000	.0	30260.6	-44139.4	441.4	.0

TOTAL SOLAR INPUT (MW-HR. THERMAL)   2127192

TOTAL DEMAND (MW-HR, ELEC)   876000

TOTAL DEMAND DELIVERED (MW-HR, ELEC)   495831   (56.6 PCT)

TOTAL HOURS NOT DELIVERED (HRS)   3802

STORAGE EXPELLED (MW-HR, THERMAL)   39028

MAXIMUM IN STORAGE (MW-HR, THERMAL)   12020   (MW-HR, ELEC)   2260   (DATE)   4/28

MINIMUM IN STORAGE (MW-HR, THERMAL)   0   (MW-HR, ELEC)   0   (DATE)   1/ 1

RANGE IN STORAGE (MW-HR, THERMAL)   12020   (MW-HR, ELEC)   2260   (1.8 PCT)

CHANGE IN STORAGE (MW-HR, THERMAL)   -0   (MW-HR, ELEC)   -0

MAX RATE TO STORAGE (MW-HR/HR, THERMAL)   1326   MAX RATE FROM STORAGE (MW-HR/HR, THERMAL)   532

MAX TURBO-GEN POWER, CHARGE (MW, ELEC)   367.0   MAX TURBO-GEN POWER, DISCHARGE (MW, ELEC)   142.9

TOTAL FROM STORAGE (MW-HR, ELEC)   251806

DIRECT, SOLAR-TO-GRID (MW-HR, ELEC)   244025

Figure 2-9 (Continued)

STORAGE SUBSYSTEM COSTS (MEGADOLLARS)

RATE RELATED COSTS

REACTOR	38.100
HEAT EXCHANGERS	15.968
SEPARATOR COLUMN	14.516
VAPORIZER/CONDENSER	.421
COOLER	.189
REACTION PRODUCTS COMPRESSOR	14.478
OXYGEN COMPRESSOR	2.667
SO2 PUMPS	.077
SO3 PUMPS	.046
MIXER	.181
SUBTOTAL	86.644

CAPACITY RELATED COSTS

INITIAL SO3 INVENTORY	2.603
STORAGE VESSELS, O2	27.663
STORAGE VESSELS, SO2	2.081
SUBTOTAL	32.348

STORAGE SUBSYSTEM

TOTAL	118.992

SUBSYSTEM COSTS (MEGADOLLARS)

COLLECTOR	215.453
RECEIVER	119.696
MASTER CONTROL	3.351
TURBO-GENERATOR	135.886
ENERGY STORAGE	118.992
SYSTEM TOTAL	593.378

FOR AN ALTERNATE ENERGY COST OF	400.0 MIL/KW-HR
AND AN UTILIZATION FACTOR OF	.5660
THE MINIMUM BUSBAR ELECTRIC COST IS	332.1 MIL/KW-HR

Figure 2-9 (Concluded)

STORAGE REQUIREMENTS AND ENERGY DISCARD, LOCATION NC
AUTONOMOUS SOLAR THERMAL ELECTRIC POWER PLANT
SYSTEM B

$A^* = 4.81 \text{ km}^2$

STORAGE CAPACITY (HOURS)

FRACTION OF COLLECTED ENERGY DISCARDED

NORMALIZED COLLECTOR AREA, $f_a = A/A^*$

Figure 2-10
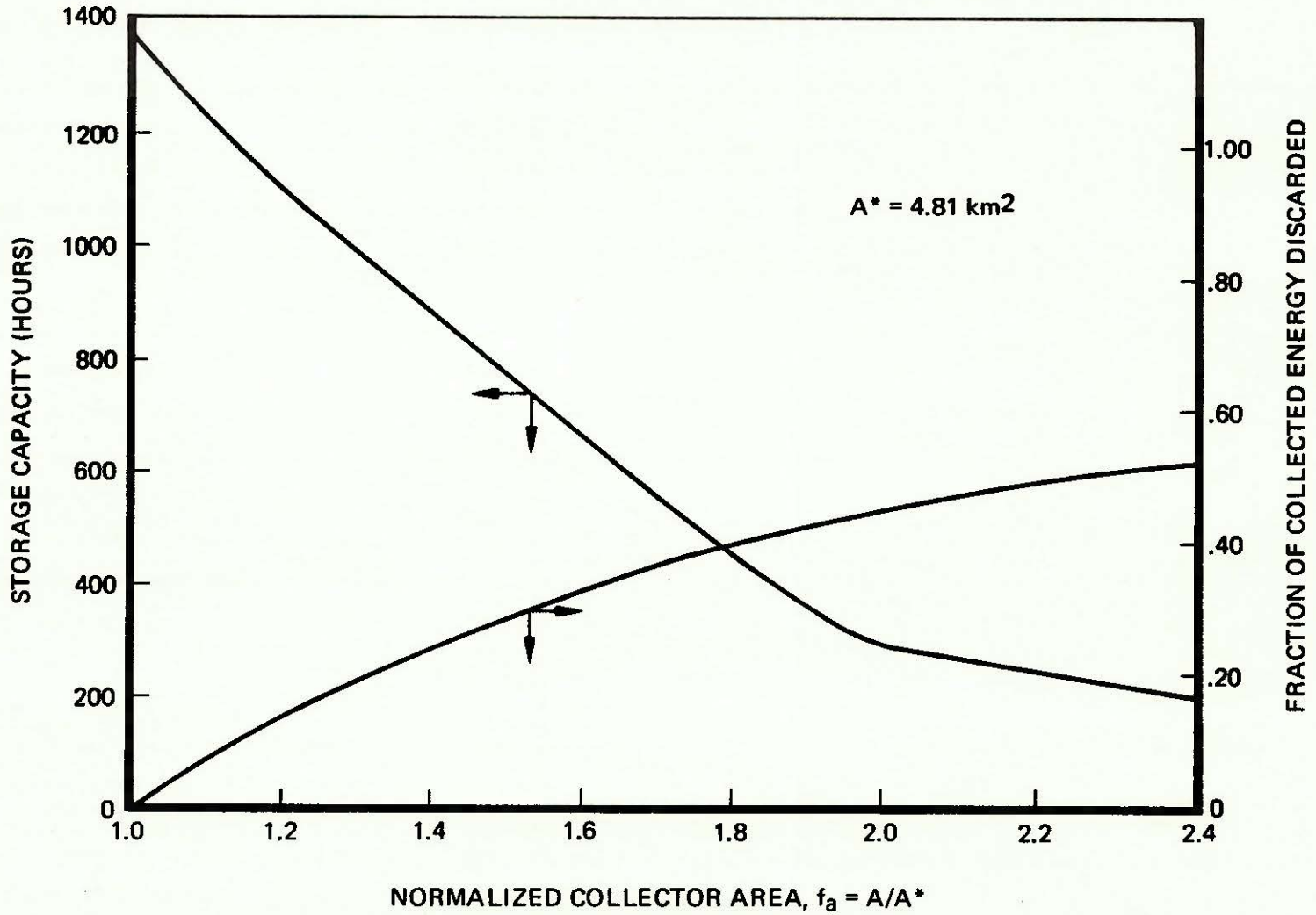
STORAGE REQUIREMENTS AND ENERGY DISCARD, LOCATION SE
AUTONOMOUS SOLAR THERMAL ELECTRIC POWER PLANT
SYSTEM B

$A^* = 4.28 \text{ km}^2$

NORMALIZED COLLECTOR AREA, $f_a = A/A^*$

Figure 2-11
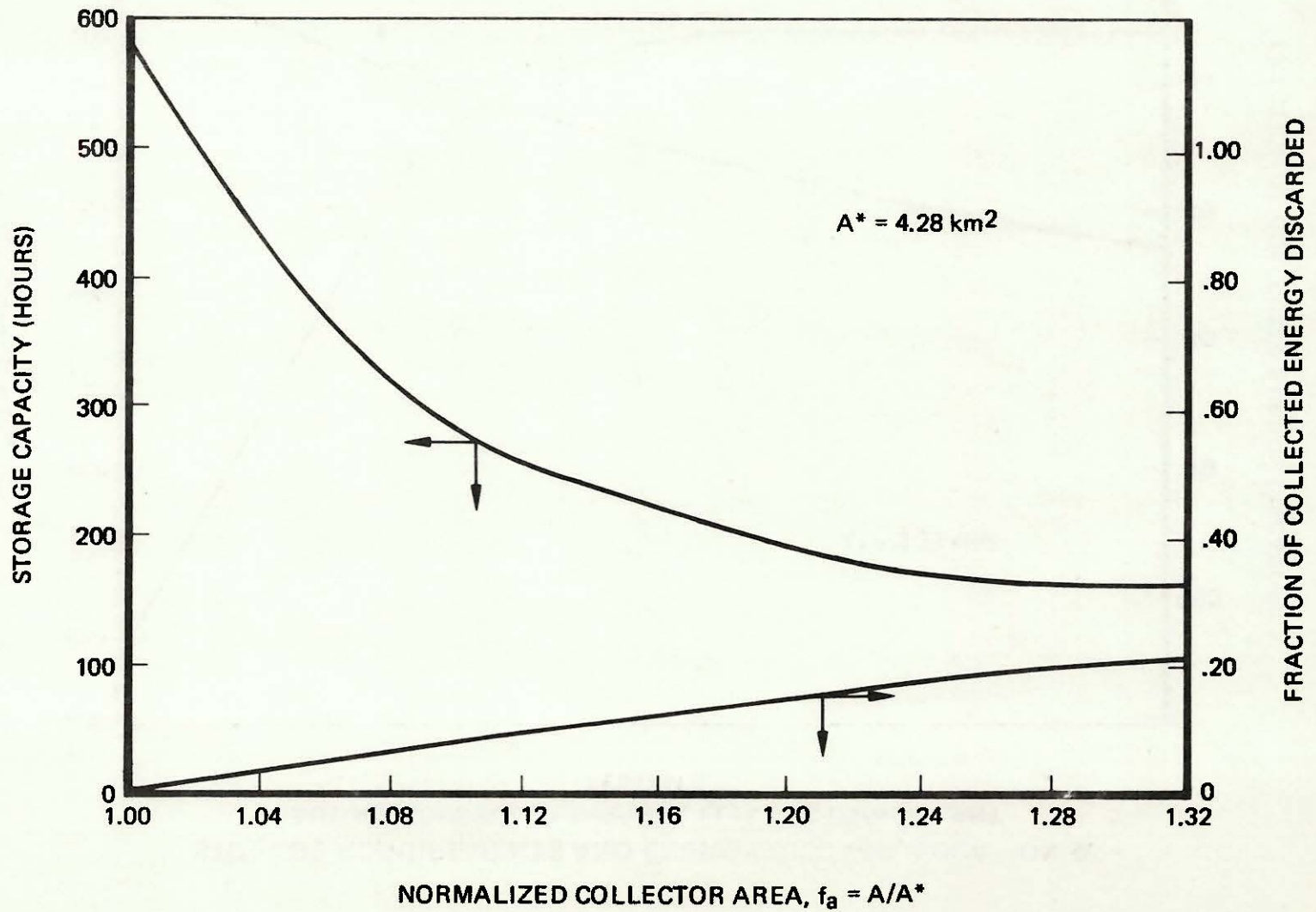
STORAGE REQUIREMENTS AND ENERGY DISCARD, LOCATION SW
AUTONOMOUS SOLAR THERMAL ELECTRIC POWER PLANT
SYSTEM B

$A^* = 2.36 \text{ km}^2$

NORMALIZED COLLECTOR AREA, $f_a = A/A^*$

STORAGE CAPACITY (HOURS)

FRACTION OF COLLECTED ENERGY DISCARDED
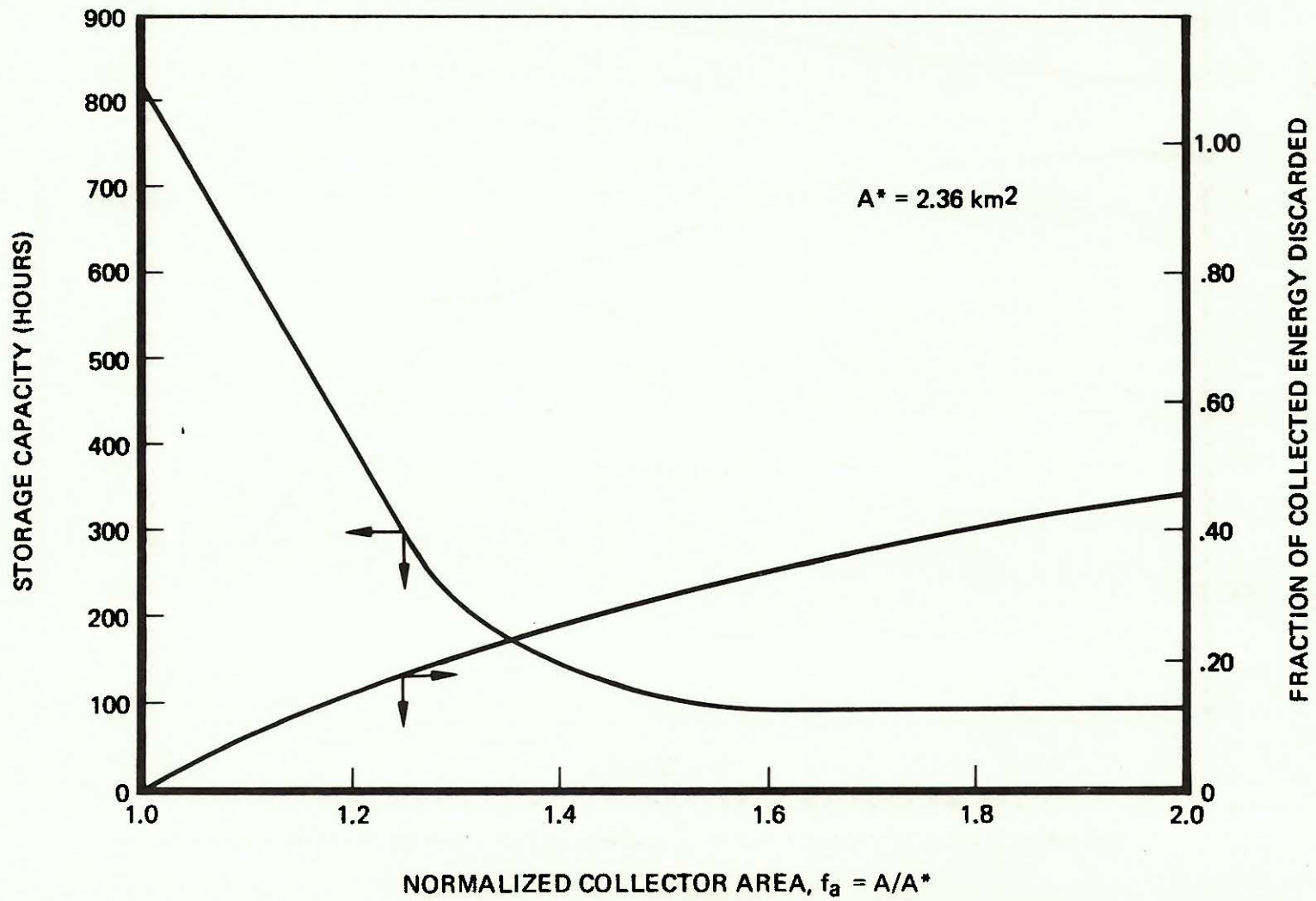
location SW curve is normalized is approximately half that of either location NC or SE, indicating that total yearly insolation at SW is significantly greater than that at the other two locations.

The similarity between the critical areas at locations NC and SE, reflecting the similarity in total yearly insolation at these locations, is surprising in view of the significant difference in their latitudes. Storage requirements at location NC, however, are considerably greater than those at location SE for all values of normalized area, indicating the more even distribution of insolation over the year at location SE. Storage requirements at location SW are intermediate between those at the two extreme latitudes. Critical collector area appears to be primarily dependent on total yearly insolation, while storage requirements appear to be more sensitive to the texture of that insolation.

The minimum storage capacities required for autonomous operation at locations NC and SE are, at approximately 200 hours, considerably greater than that at location SW. Minimum storage requirements at all three locations are much greater than the length of the longest night, indicating that their lengths are due to extended storms. This difference in the length of the longest period of solar occultation again reflects the relatively good weather at location SW.

In all of the cases considered above, as collector area increases above A* and storage requirements decrease, the storage subsystem capacity does not have to be large enough to store all the energy that the heliostats and receiver can collect. Thus it is possible (indeed economically beneficial) at certain times of the year to discard energy which could be collected because the storage subsystem is full. The fraction of the total energy collected over the course of the year, which could be discarded, is significant at areas of interest, as shown in Figures 2-10 through 2-12. Although this energy could be rejected by simply turning an appropriate number of heliostats away from their focus on the receiver, it could also be collected and used immediately (e.g. for "total energy" applications) or stored in some other storate subsystem, providing an energy credit for the total facility and possibly further increasing storage size. No such use of excess energy collected, or of reject process heat from the chemical storage subsystem, was included in the present analysis.

Undersizing of the receiver or "receiver clipping" at normalized collector areas greater than unity was not considered in the present analysis. The receiver was always sized to handle the maximum yearly output of the collector field, even though some energy was being discarded. Some cost saving would be achieved by appropriate undersizing of the receiver in such circumstances (References 13, 14, 15).

The dependent variable of interest for economic optimization is the BBEC. One might expect that as the collector area increases above the critical value and the storage requirements decrease, the trade-off in capital cost requirements between the two subsystems would produce a minimum in the BBEC. This is indeed the case as shown in Figures 2-13 through 2-15, in which busbar energy costs are plotted as a function of normalized collector area for 100 percent solar operation.

An autonomous STEC facility with area A = A* represents a very poor design solution because storage requirements (~1,380 hours in the case of location NC) and resulting storage costs are

BUSBAR ENERGY COST AT LOCATION NC
AUTONOMOUS SOLAR THERMAL ELECTRIC POWER PLANT
SYSTEM B

Figure 2-13

BBEC ($/kW-hr, 1978 DOLLARS)

$A^* = 4.81$ km^2

30-YEAR PLANT ECONOMIC LIFE
STARTUP IN YEAR 2000

NORMALIZED COLLECTOR AREA, $f_a = A/A^*$

Figure 2-14
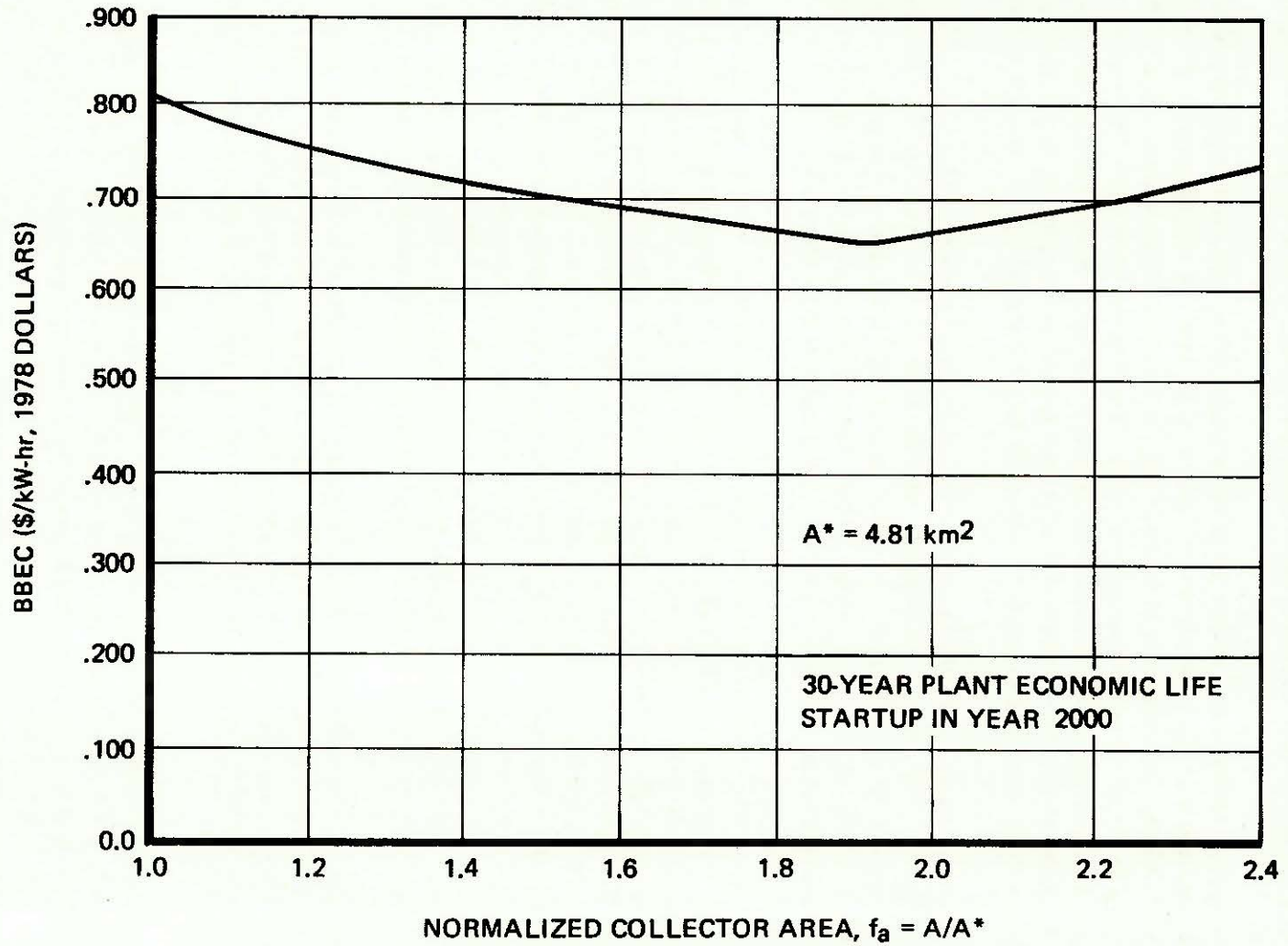
BUSBAR ENERGY COST AT LOCATION SE
AUTONOMOUS SOLAR THERMAL ELECTRIC POWER PLANT
SYSTEM B

30-YEAR PLANT ECONOMIC LIFE
STARTUP IN YEAR 2000

Y-axis: BBEC ($/kW-hr, 1978 DOLLARS)

X-axis: NORMALIZED COLLECTOR AREA, $f_a = A/A^*$
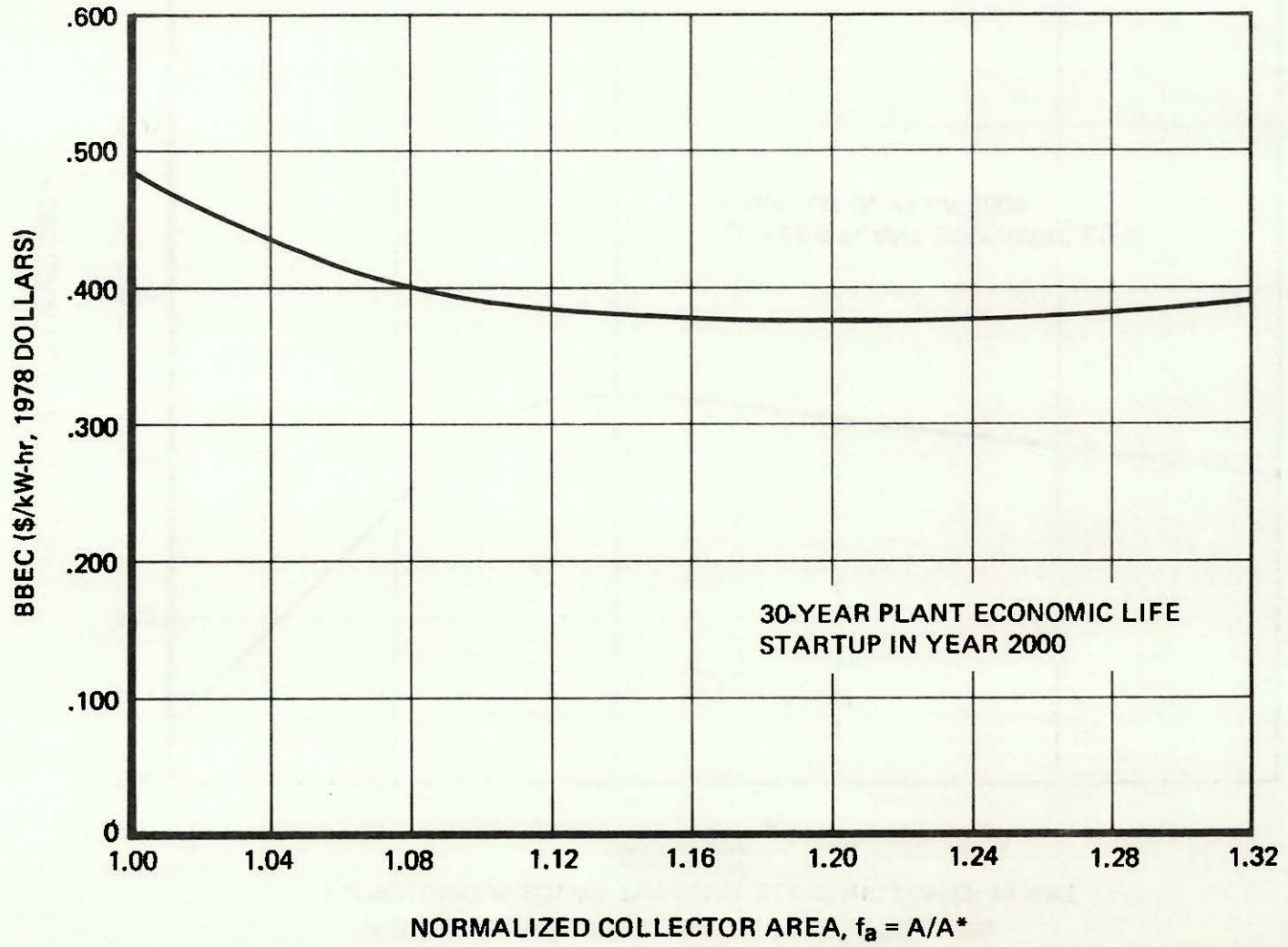
BUSBAR ENERGY COST AT LOCATION SW
AUTONOMOUS SOLAR THERMAL ELECTRIC POWER PLANT
SYSTEM B

30-YEAR PLANT ECONOMIC LIFE
STARTUP IN YEAR 2000

BBEC ($/kW-hr, 1978 DOLLARS)

NORMALIZED COLLECTOR AREA, $f_a = A/A^*$
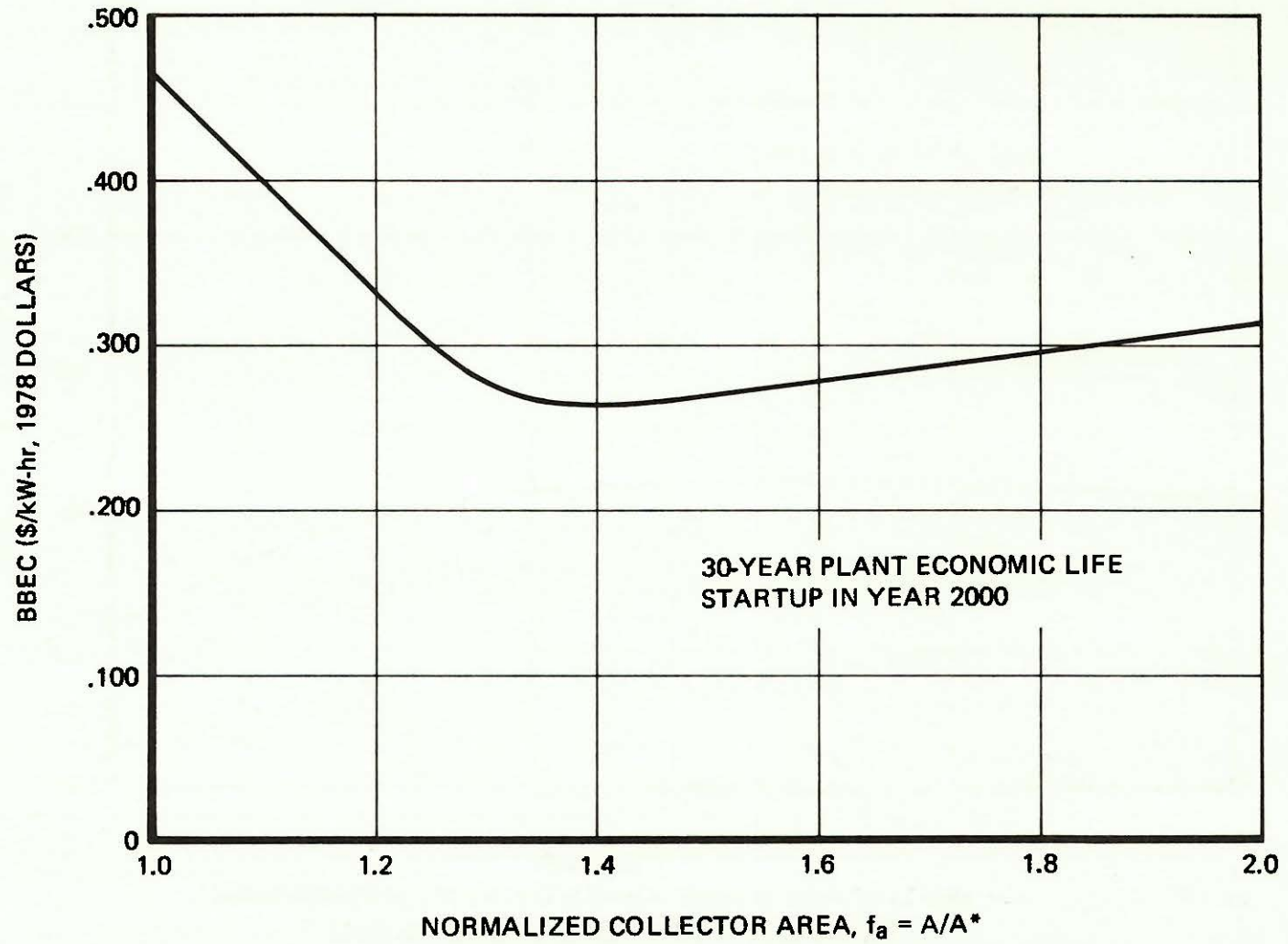
extremely high for the ($SO_3/SO_2/O_2$) system. These high storage costs are reflected in the relatively high BBEC at $A = A^*$. As area is increased beyond A^*, the BBEC decreases until it goes through a broad minimum in the vicinity of the minimum storage requirements. Further increase in the collector area simply adds heliostat costs to the total costs with no further reduction in storage requirements, so that the BBEC increases linearly.

Table 2-6 presents important characteristics of STEC plants operating at the minima of Figures 2-13 through 2-15. Normalized optimum values of the collector area and storage capacity are shown in parentheses.

2.4.1.1 Storage "Clipping"

The results discussed in section 2.4.1 were subject to the assumption that the maximum storage charging rate, and thus the storage power related equipment costs, are limited only by the yearly maximum, storage-dedicated output of the heliostat field. These charge rates, even at the optimum solutions are quite large, ranging from 2,157 MW_t at the SW optimum to 5,535 MW_t at the NC optimum.

The sun-following dispatcher used to obtain the results shown in Figures 2-13 through 2-15 has the following priorities for use of energy from the receiver during daylight hours.

1. Satisfy demand
2. Charge energy to storage
3. Discard energy if storage is full.

This dispatcher always charges energy to storage, when such energy is available, at the maximum rate possible, and energy discard occurs only when storage is full.

At collector areas greater than the critical area, a more economical dispatching scheme allows discard of energy even when storage is *not* full. A schematic comparison of the two types of dispatcher discussed above is presented in Figure 2-16. In the improved scheme, the rate-related storage components are sized to handle some charging rate less than the maximum available from the collector field. The lowest maximum charging rate for which pure-solar operation is possible varies with collector area and storage capacity, and a trial-and-error procedure was required to find it.

A "clipping" option was added (section 2.3.2) to program STORAGE, whereby a ceiling on the storage charging rate may be arbitrarily specified as a program input (f_c). This ceiling is specified as some fraction of the yearly maximum charge rate possible at the collector area and storage capacity of interest. This ceiling can then be progressively lowered in successive computer runs until a minimum is reached, below which pure-solar operation is no longer possible, as shown in Figure 2-17. This plot is made for a single collector area, that corresponding to the minimum in the BBEC curve of Figure 2-15; the origin of this curve corresponds to that minimum*. Figure 2-17 shows that

---

*Similar studies at collector areas slightly greater and slightly less than the one used here predicted higher BBEC at all storage charging rates.

Table 2-6
OPTIMUM SOLUTIONS FOR AUTONOMOUS STEC POWER PLANTS
NO STORAGE CLIPPING

System B, 100 MW$_e$ Continuous Demand

Location	Heliostat* Area (km^2)	Storage* Capacity (hrs)	BBEC[†] $/kWh	Capital Equipment Cost Breakdown (%)			
				Heliostats & Receiver	Turb-Gen	Storage	
						Power	Energy
Madison (NC)	9.1 (1.90)	337 (0.25)	0.653	53	17	10	20
Miami (SE)	5.2 (1.22)	178 (0.31)	0.376	53	18	11	18
Albuquerque (SW)	3.4 (1.42)	133 (0.16)	0.263	48	20	13	19

*In parenthesis — Normalized with respect to critical values

[†] 1978 Dollars

2-40

SCHEMATIC OF RELATIONSHIP BETWEEN STORAGE CAPACITY AND COLLECTOR AREA

Solar involvement has been maximized. Pure solar designs must lie to the right of the critical collector area and above the minimum storage size for pure solar applications.
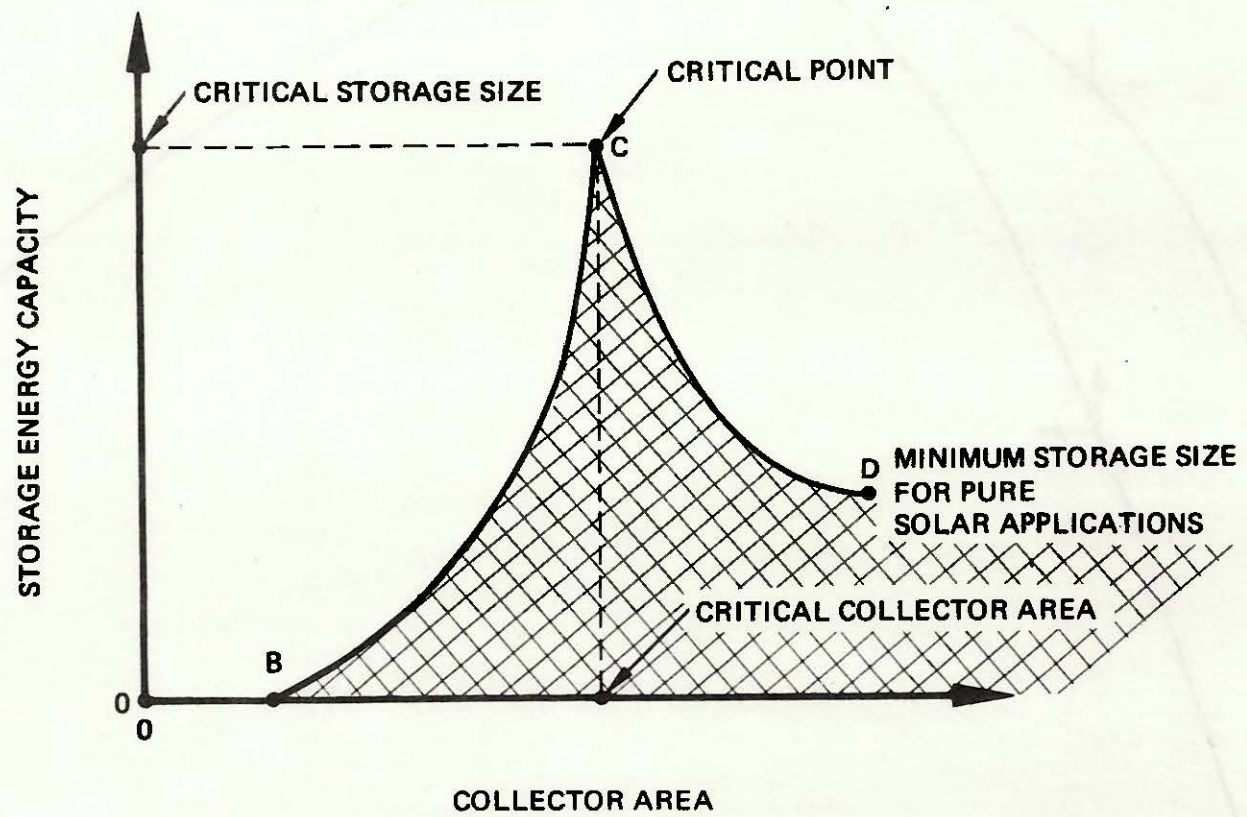
RESULTS OF CHARGING RATE OPTIMIZATION
LOCATION SW, f_a = 1.43
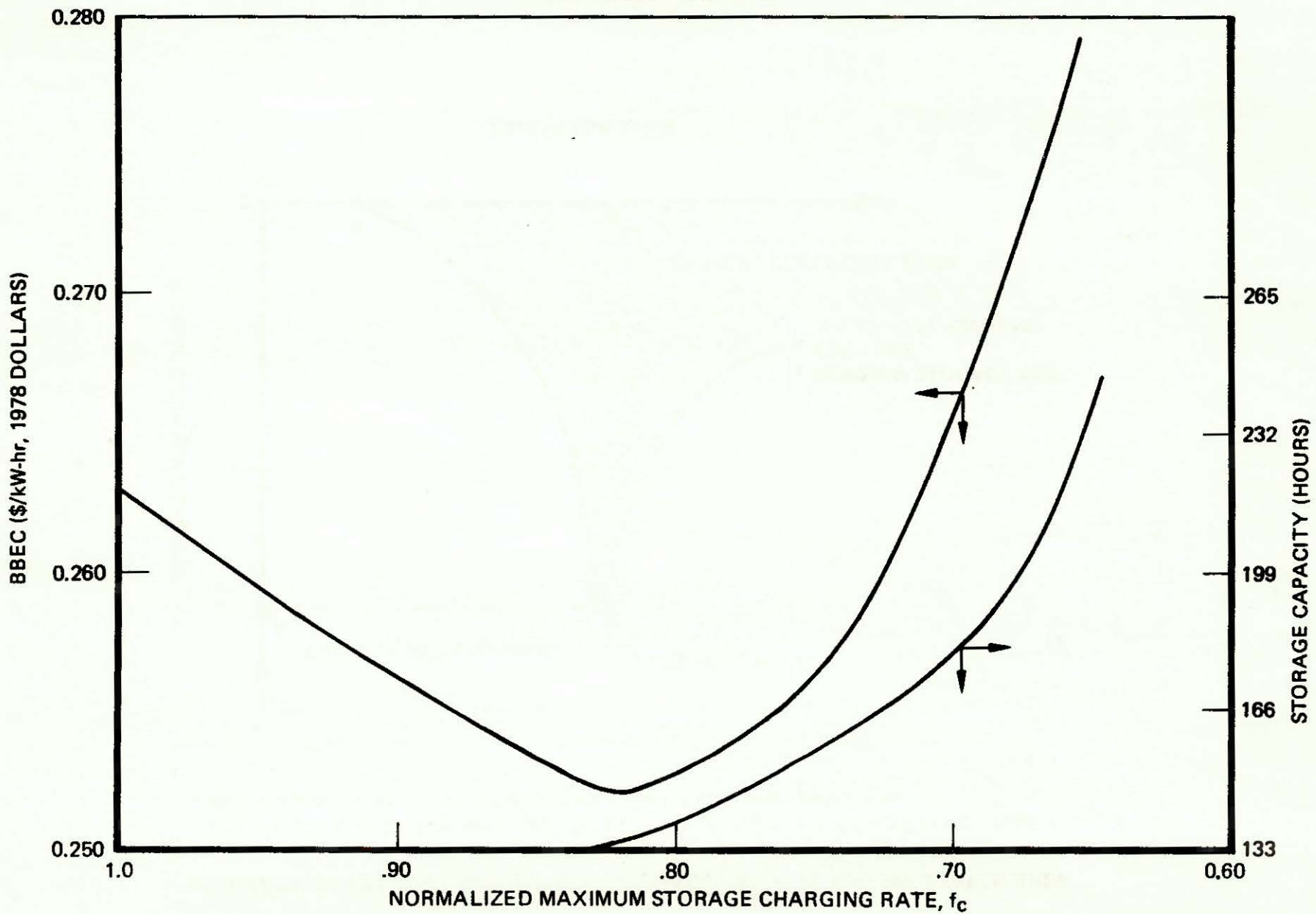
Figure 2-17

at location SW, pure solar operation is possible with maximum storage charging rates down to 65 percent of that at the origin, with the storage capacity increasing as the charging rate decreases. Decreases in the maximum storage charging rate result in decreased storage power-related costs (section 2.2.7), and the trade-off between storage rate and power-related costs produces a minimum in BBEC at 1,770 MW_t, 82 percent of that at the origin. Similar considerations at locations SE and NC result in reductions in maximum charging rate to 62 percent and 70 percent of the nonclipping values.

The small effect of storage clipping on overall STEC configuration is seen by comparing Tables 2-6 and 2-7. Clipping reduced optimum busbar energy costs an average of 5 percent; collector areas were unchanged, and storage capacities increased slightly. In the clipped cases, power-related costs accounted for a slightly smaller fraction of total storage subsystem cost than in the unclipped cases.

The optimum solutions described in Table 2-7 agree well with intuition; of the three, Albuquerque is the most attractive location for autonomous STEC plants, followed by locations SE and NC. Heliostat area, storage capacity, and maximum charging rate are all greatest at location NC, intermediate at location SE, and least at location SW; the BBEC reflects this ordering, with that at location NC being more than twice that at location SW.

It is interesting to note that in spite of the differences in texture and amount of insolation at the three locations, the relative cost of the various subsystems are very similar, with the capital equipment cost breakdown at locations NC and SE being identical. The receiver and heliostat costs account for at least half of the total capital equipment cost at all locations, emphasizing the importance of the unit costs of these items to the final value of the BBEC. The choice of these unit costs for this study was somewhat arbitrary (section 2.2.3), and the combination of less expensive designs and the benefits of mass production could lower them significantly.

The values of BBEC in Table 2-7 are, therefore, more valuable for their indication of the relative, rather than absolute, cost of autonomous solar power production at the three locations.

2.4.1.2 Charge to Discharge Ratio – Autonomous Cases

Even with some charge-rate clipping, the maximum charging rate for autonomous operation is very high at all three locations. For a 100 MW_e continuous plant output, the maximum storage discharge rate (which occurs whenever the plant runs solely off of storage) is 212 MW_t at the storage exit. Comparison of the value with those in Table 2-7 indicate that the maximum storage charging rate is eight (location SW) to eighteen (location NC) times the maximum storage discharge rate. All storage system capital equipment which is used in both the charging and discharging mode (reactors, etc.) must clearly be sized to accommodate the maximum charging rate in all autonomous cases.

In the SO_2/SO_3 storage subsystem design used in these studies, almost all rate-related process equipment is used in both the charging and discharging modes. The assumption that a single power-related cost parameter was sufficient for these studies (section 2.2.7) appears to be valid.

Table 2-7
OPTIMUM SOLUTIONS FOR AUTONOMOUS STEC POWER PLANTS
WITH STORAGE CLIPPING

System B, 100 MW$_e$ Continuous Demand

Location	Heliostat* Area (km^2)	Storage* Capacity (hrs)	BBEC[†] ($/kWh)	Maximum Charging Rate** (MW$_t$)	Capital Equipment Cost Breakdown (%)			
					Heliostats & Receiver	Turb-Gen	Storage	
							Power	Energy
Madison (NC)	9.2 (1.92)	362 (0.27)	0.616	3,874 (0.70)	55	14	8	23
Miami (SE)	5.2 (1.22)	200 (0.35)	0.350	1,908 (0.62)	55	14	8	23
Albuquerque (SW)	3.4 (1.42)	134 (0.16)	0.252	1,769 (0.82)	50	18	11	21

*In parenthesis – Normalized with respect to critical values

**In parenthesis – Normalized with respect to maximum receiver input power.

[†] 1978 Dollars

It is worth noting here that in the rare circumstance that the maximum storage discharge rate exceeds the maximum charging rate, program STORAGE sizes the power-related equipment to handle the maximum discharge power.

2.4.2 Results for Hybrid STEC Operation

Removal of the constraint for autonomous operation admits the possibility of solar-fossil, hybrid power generation facilities. In such a facility, the solar portion of the plant would provide less than 100 percent of the demand load, with the difference being made up by the alternate energy source.

The most economical solar-alternate mix will be determined by the relative cost of energy from the two sources, which rates will depend on (among other parameters) the location (and thus the insolation profile) and the system type being considered. Removal of the constraint for autonomous operation also admits the possibility of collector areas less than A*. Moreover, for a given collector area, the storage capacity may be less than that required to store all the energy collected but not sent directly to the turbogenerator. Thus, as in the stand-alone cases with areas greater than A*, it may be most economical, at certain times of the year, to discard energy which could be collected by the heliostats, because storage is full.

The design task, as described above, thus becomes an optimization problem with the objective function being the BBEC, independent variables being the collector area and the storage capacity, and the domain of interest being the crosshatched area in Figure 2-16. Alternate energy costs were set arbitrarily for the optimization studies described below (Table 2-3) at 0.100, 0.200, 0.300, 0.400 $/kWh in 1978 dollars.

Figures 2-18 and 2-19 give some idea of the behavior of the BBEC surface corresponding to the A-Q domain. The shape of the lines of constant cost are adapted from earlier "hand" optimized cases*, run before program CSTOPT was developed (Reference 11). The curves shown in these figures are actually constructed from a series of optima for the range of collector areas shown. For example, consider the curve for an alternate energy cost of $0.400 kWh in Figure 2-18. Each point on that curve represents the minimum of the BBEC vs. *storage time* curve for that collector area. The global minimum for the $0.400 kWh case occurs at $f_a = 0.77$, while that for the $0.300 kWh case occurs at $f_a = 0.55$.

The 100 percent solar curve, discussed in the preceding section is also shown in Figure 2-18, beginning at the critical collector area (normalized value of 1.0). The lines of constant cost in Figure 2-18 (plus some additional ones for higher alternate energy costs are plotted as a function of storage capacity in Figure 2-19. Lines of constant solar fraction are superimposed.

The constant BBEC curves in Figures 2-18 and 2-19 indicate the effect which alternate energy cost has on the optimum solution. As alternate energy becomes more expensive, the optimum solution calls for larger collector areas, larger storage capacities, and generally larger solar fraction. In the extreme case of infinite alternate energy cost, the optimum choice is an autonomous STEC plant, located at the minimum of the 100 percent solar curve.

---

*NOTE: These cases were run with estimated insolation data (section 2.2.5). These curves, therefore, do not correspond to the more recent results (Table 2-8) obtained using the more reliable SOLMET data.

OPTIMUM BBEC AS FUNCTION OF NORMALIZED COLLECTOR AREA
HYBRID STEC PLANT AT LOCATION NC
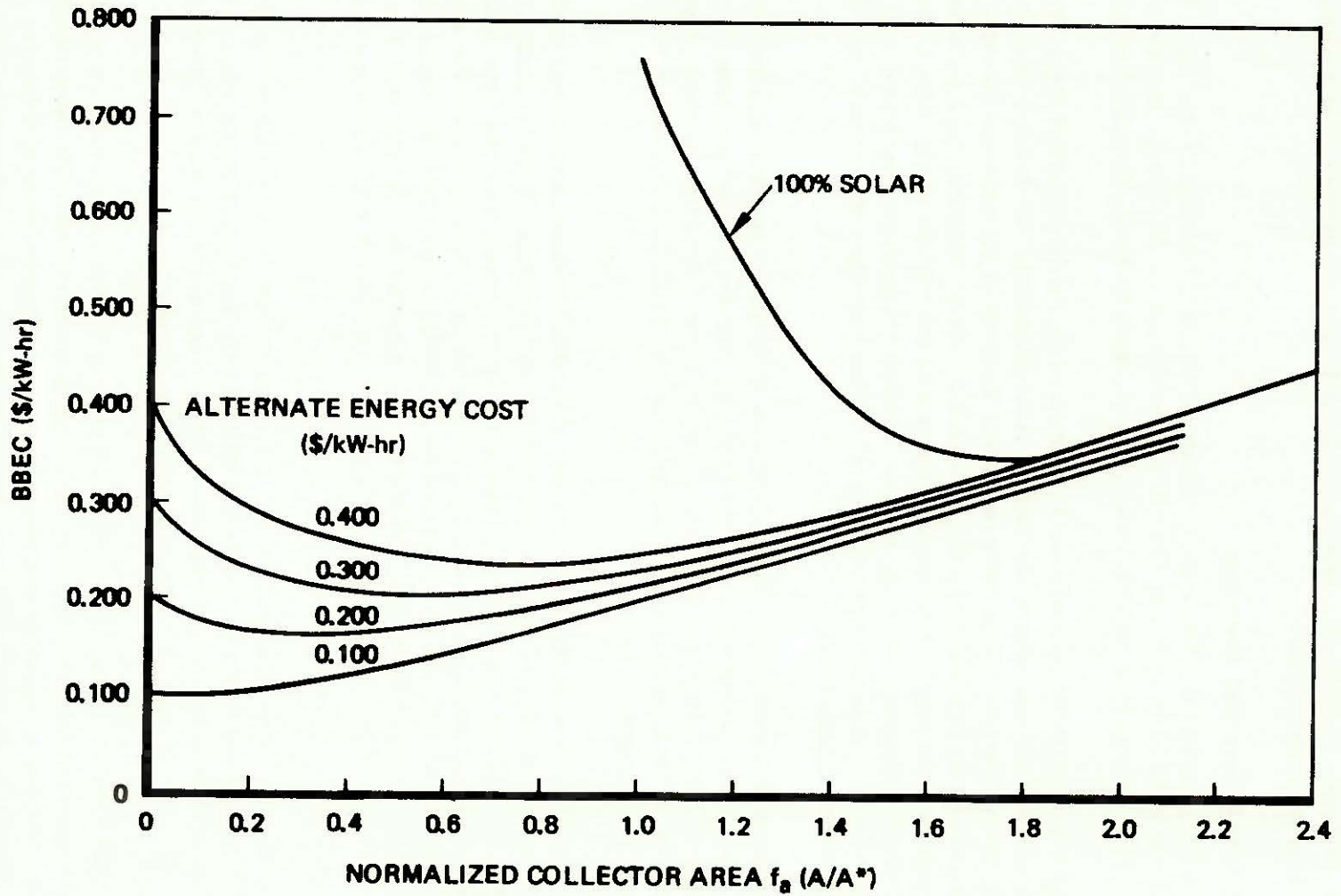
NOTE: THESE RESULTS CORRESPOND TO THE ESTIMATED INSOLATION DATA DESCRIBED IN SECTION 2.2.5
AND ARE GIVEN HERE FOR ILLUSTRATIVE PURPOSES ONLY. SEE TEXT FOR EXPLANATION.

Figure 2-18

Figure 2-19

OPTIMUM BBEC AS FUNCTION OF STORAGE CAPACITY
HYBRID STEC PLANT AT LOCATION NC

CURVE	ALTERNATE ENERGY COST ($/kW-hr, 1978 DOLLARS)
a	0.300
b	0.400
c	0.500
d	0.600
e	0.800

STORAGE CAPACITY (HOURS)

NOTE: THESE RESULTS CORRESPOND TO THE ESTIMATED INSOLATION DATA DESCRIBED IN SECTION 2.2.5, AND ARE GIVEN HERE FOR ILLUSTRATIVE PURPOSES ONLY. SEE TEXT FOR EXPLANATION.

Table 2-8 presents optimum solutions obtained with program CSTOPT for an alternate energy cost of $0.400/kWh. As in the autonomous cases, STEC system B is used, and the demand is a continuous 100 MW_e. Optimum solutions for alternate energy costs of 0.100, 0.200, and 0.300 $/kWh had extremely low solar fractions, indicating that the optimizer chose primarily to buy alternate energy rather than build a sizeable solar portion of the plant, i.e. at these alternate energy costs, for the subsystem unit costs used in this study, the STEC system modeled here would not be economically competitive. Due to time constraints, hybrid operation at location SW was not studied.

The general conclusion to be drawn from the results in Table 2-8 is that location SE is the more favorable of the two for central solar applications. The optimizer chooses to provide 75 percent of the load from solar at SE, and only 57 percent at NC. In both cases, the optimum solutions required collector areas less than the critical value. The optimum BBEC at both locations was significantly less than the corresponding value for autonomous operation (Table 2-8), in spite of the fact that the alternate energy cost of $0.400/kWh was quite high.

Perhaps the most surprising result of these hybrid studies (especially in the case of location SE) was that such high solar fractions could be achieved with less than 30 hours of storage. The hybrid STEC systems are apparently not very sensitive to the occasional extended storm or cloudy period. Such extended occultations occur relatively infrequently, while nighttime occultation occurs 365 times a year. Overnight storage requirements thus exert far more influence on the optimum storage time. Since the system is not constrained to a 100 percent solar solution, the most economical solution is to increase storage only slightly and purchase alternate energy to satisfy demand during a long cloudy period. Autonomous operation, on the other hand, requires storage capacities large enough to carry the system through the longest period of occultation of the year, and stand-alone plants are therefore more sensitive to changes in the insolation profile.

It appears then, that when the constraint of stand-alone operation is removed, storage times required for most economical operation (with plausible energy escalation rates) are much lower than had been previously believed. While many applications may require chemical storage subsystems primarily for the technical reason of the virtually limitless storage times which they allow, it appears that in most STEC applications the chemical storage subsystems must compete. on an economic basis, with the shorter term sensible and latent-heat storage subsystems.

2.4.2.1 Charge-to-Discharge Ratio – Hybrid Cases

The maximum storage charging rates in Table 2-8, while less than those in Table 2-7, are still quite large compared to the maximum discharging rates. As in the autonomous cases. the maximum discharging rate was 212 MW_t, measured at the storage exit. The ratios of charging to discharging rates, ranging from approximately six to eight, serve to validate the assumption that the charging rate is size determining for power-related storage components used in both modes.

Table 2-8
OPTIMUM SOLUTIONS FOR HYBRID STEC POWER PLANTS
ALTERNATE ENERGY COST = $0.400/Kw-hr

System B, 100 MW$_e$ Continuous Demand

Location	Heliostat* Area (km^2)	Storage* Capacity (hrs)	BBEC[†] ($/kWh)	Solar Fraction	Maximum Charging Rate (MW$_t$)	Capital Equipment Cost Breakdown (%)			
						Heliostats & Receiver	Turb-Gen	Storage	
								Power	Energy
Madison (NC)	2.4 (0.50)	22 (0.02)	0.332	0.57	1,326	56	23	15	6
Miami (SE)	3.2 (0.75)	29 (0.05)	0.298	0.75	1,746	58	22	14	6

*In parenthesis — Normalized with respect to critical values

[†] 1978 Dollars

2.5 CONCLUSIONS OF STEC SYSTEMS ANALYSIS

The most important conclusions drawn from the preceding results can be summarized as follows:

1. The autonomous solar thermal electric conversion plant which uses the (SO_3/SO_2) reaction for seasonal storage does not economically compete with a hybrid plant which has an alternate energy source available to it, based solely on BBEC. Supplying all of the demand with solar energy was found to be approximately 20 to 80 percent more expensive than supplying the demand partly from the sun and partly from alternate energy sources. This is due to the fact that it is cheaper to purchase backup energy, even at fairly high unit costs, than to build solar components which are used at full capacity only infrequently. A storage system with much lower energy-related unit cost would make such competition much closer.

2. Optimum storage requirements for autonomous STEC power plants which satisfy continuous baseloads are in the range of 100 to 400 hours.

3. Optimum storage requirements for hybrid STEC power plants which satisfy continuous baseloads are in the range of 20 to 30 hours, for a levelized alternate energy cost of $0.400/kWh.

4. In all autonomous and most hybrid cases of interest, the yearly maximum storage charging rates are greater than the maximum discharging rates, with the ratio of these quantities varying between approximately six for the best hybrid case and eighteen for the worst autonomous case. The maximum storage charging rate is, therefore, size determining for power-related storage process equipment used in both the endothermic and exothermic modes.

5. As could be expected under consistent assumptions for the Florida and Wisconsin simulations, the solar plant is more economically attractive in Florida. The Wisconsin system requires much more storage for both hybrid and autonomous operation that does the plant in Florida.

6. The concept of energy discard is important to the optimal design of any solar plant, hybrid or autonomous. The results presented herein underscore the desirability of oversizing or undersizing subsystems to obtain better utilization factors for the plant as a whole. This approach leads to lower busbar energy costs than designs which utilize all the energy collected. Use of discard energy and/or reject process heat from the storage subsystem, in a "total energy" application, may be an attractive option.

The first three of the above conclusions pertain to the overall economic feasibility of STEC plants with long-term storage, and to the importance of storage in any STEC facility. The latter three express the performance requirements and design constraints which a CES system must be designed to meet in STEC applications of interest here, and therefore provide valuable guidelines for the preliminary process designs to be described in Chapter 4.

The general applicability of these conclusions is of course limited by the many assumptions of efficiency and cost of various subsystems and components on which the model is based. Two key limitations of the systems studies described above bear mentioning:

1.   The use throughout the study of heliostat and receiver unit costs of $90/m^2 and $50/m^2 respectively.

2.   The use of only one storage subsystem model (SO_2/SO_3).

In view of the capital equipment cost breakdown of Tables 2-7 and 2-8, large increases or decreases in the front-end unit cost parameters would undoubtedly change the optimum busbar energy costs, collector areas, and storage capacities for both autonomous and hybrid STEC plants, and might substantially alter the solar/alternate mix of the optimum hybrid solutions. Similarly, a storage subsystem model based on a different reversible chemical reaction, with different charging and discharging efficiencies and different power and energy-related unit costs, might substantially alter the character of both the autonomous and hybrid solutions. For example, a $CaO/Ca(OH)_2$ storage subsystem model (section 4.3) with very low energy-related costs might cause the CSTOPT optimizer to choose a hybrid case solution with a substantially longer storage time than the 15 to 30 hours it chose for the SO_2/SO_3 cases.

The effect of variations in these and other key parameters, while important, are beyond the scope of the present work. For further parametric studies, the reader is referred to an excellent series of papers by J. J. Iannucci (References 12 – 15). The above limitations notwithstanding, these systems studies provide much insight into the overall economics of STEC systems and the cost and performance interplay between STEC subsystems, as well as valuable design criteria for energy storage subsystems in general and CES subsystems in particular.

CHAPTER 3
CHEMICAL REACTION SURVEY

The most important part of the original NSF contract was the screening of candidate chemical reactions for those which were promising for chemical energy storage applications. The ultimate goal of this screening process was the reduction of the candidate reactions to a manageable number of the most promising reactions for more careful examination and preliminary process design studies. The result of this process was that a list of over 550 candidate reactions was reduced to one containing twelve promising reactions for further study.

The reaction screening process can be divided conceptually and chronologically into an earlier evaluation based on physiochemical properties of reaction constituents, toxicity, flammability, etc., and a later one based more on equipment cost and engineering criteria. The earlier evaluation has been described in detail in previous interim reports for the NSF contract (Reference R2, R3), and is summarized in section 3.1, while the later evaluation, aimed primarily at reducing the remaining candidates to a manageable number for process design work, is described in section 3.2.

3.1 REACTION SELECTION AND EVALUATION

The ideal selection process would be one which would quickly consider all possible chemical interactions of all possible chemical compounds and would rank the resulting CES systems according to a set of pre-established selection criteria. It is obvious that the ideal was not attainable in this case, since all possible chemical compounds are not even known, but the number is certainly enormous. The number of possible chemical reactions would, of course, be larger. If we limit the chemical compounds to those which are "known", we still have a very large number, and to consider all the possible interactions is beyond the capacity of modern computers.

If a further limitation is imposed by requiring thermodynamic and physical property data to be available for any compound to be considered (which is a reasonable requirement for this program), the number of compounds may be reduced to a more manageable level.

It is still theoretically possible, however, to write a large number of chemical equations representing various combinations of these compounds. A chemist, by applying practical chemical knowledge, could quickly evaluate and discard many of these reactions. For example, when considering various reactions of calcium oxide, a chemist would immediately discard the thermal decomposition reaction $2\ CaO = 2\ Ca + O_2$ as impractical because calcium oxide is a refractory oxide and a very high temperature would be required. The reversible reaction with water, however, is well known to be energetic and is carried out on a large scale industrially. Other reactions which are not as well known may be found described in the literature, or the reaction products may be predicted by thermodynamics if sufficient data is available.

It became apparent early in the program that a completely thorough search for energy storage reactions could not be conducted in the allotted time. It was believed, however, that a systematic approach to the search was essential in order to avoid overlooking potentially useful reactions.

The method used to search for and select potential chemical energy storage reactions is depicted schematically in Figure 3-1. Starting with the periodic table of elements, it is logical to eliminate certain elements from consideration due to their high cost, or because they are highly toxic or not available in the quantities needed. Elements eliminated for these reasons are listed in Table 3-1.

An upper limit on unit cost of reaction constituents of $100/lb caused very expensive elements to be eliminated from consideration. This upper limit resulted from the assumption that the storage media themselves should not account for more than approximately 25 percent of the total STEC capital investment (Reference R2). Criteria for elimination of certain elements due to limited availability are closely linked with those for cost, and were based on preliminary estimates of the storage material required for the most likely STEC plant sizes.

After the elements in Table 3-1 were eliminated, the remaining elements were each considered individually and chemical compounds of each element with the other elements were listed. For example, compounds of hydrogen with lithium, boron, carbon, etc., were listed. Then compounds of lithium with boron, carbon, nitrogen, etc., were listed. First, binary compounds (with two different elements) were listed, then ternary compounds. In this way a list of approximately 750 compounds was generated.

Methane and ethane and their alkanol derivatives are the only organic compounds which were retained, since most organic reactions of larger molecules tend to be nonstoichiometric. Very few species of organic matter are capable of undergoing only one reaction under a given set of experimental conditions; side reactions almost invariably occur. The hydrogenation of benzene to cyclohexane and ethylene to ethane were also considered, however, since these reactions have been suggested for energy storage applications.

Chemical reactions were then listed using the selected elements and compounds. Approximately 550 reactions were generated, and for each reaction an attempt was made to calculate the heat of reaction (ΔH_R) at 298 K, and the Gibbs energy change (ΔG) at 298, 800, and 1,200 K. For many reactions, this was not possible because of lack of thermal data for one or more of the compounds involved.* A first-round selection of reactions was made based on the following criteria:

1. Reaction appears to be reversible
2. $\Delta H_{298\,K} \geq 110\,kcal/mole$
3. $|\Delta G|_{298\,K}$ or $|\Delta G|_{800\,K}$ or $|\Delta G|_{1,200\,K} \leq 10\,kcal/mole$

---

*It was assumed for these calculations that all solid phases in a given reaction were immiscible, since phase diagrams, entropies, and enthalpies of mixing were not available for many of the reactions with solid constituents. A more rigorous treatment, taking into account miscibility of solid constituents, might change the relative ranking of systems involving solids.

Figure 3-1
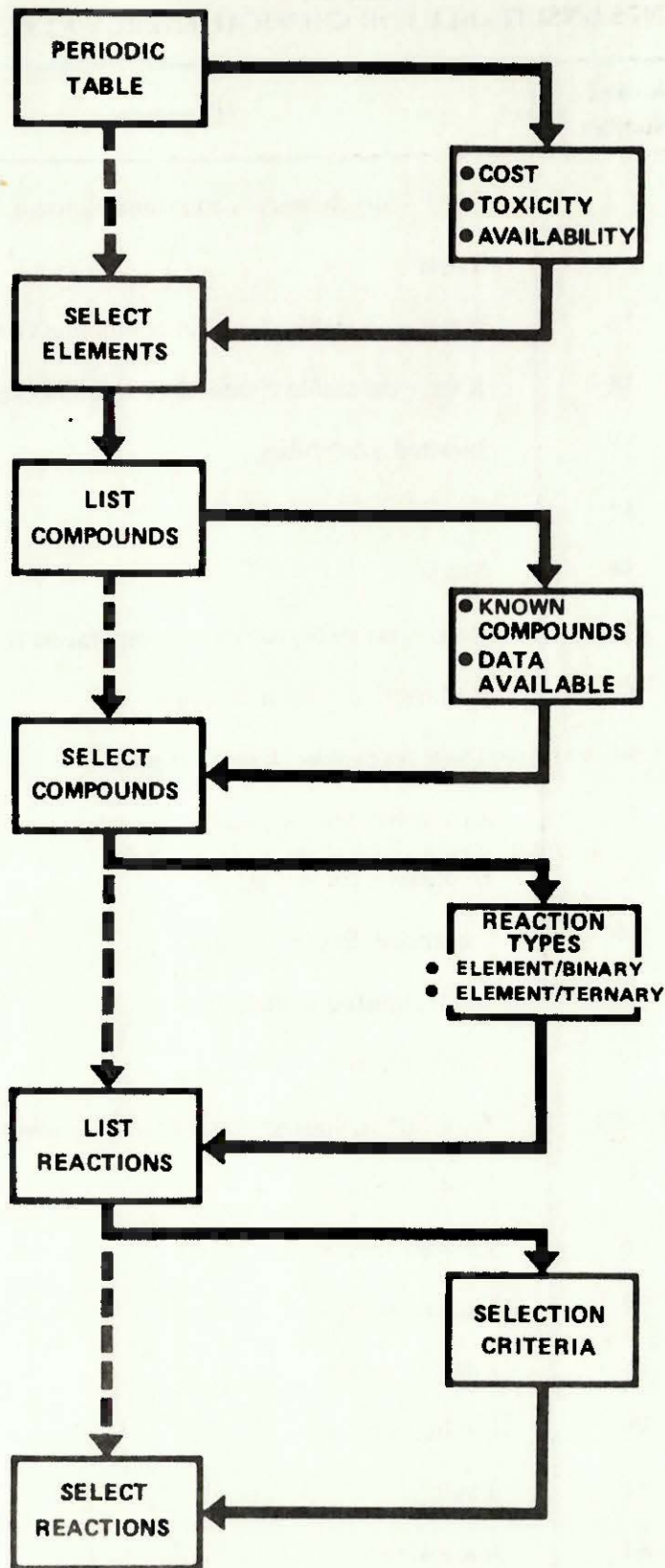
Table 3-1
ELEMENTS UNSUITABLE FOR CHEMICAL ENERGY REACTIONS

Element	Atomic Number	Comment
Helium	2	Inert — no chemical compounds known
Beryllium	4	Toxic
Neon	10	Rare — no stable chemical compounds known
Argon	18	Rare — no stable chemical compounds known
Scandium	21	Limited availability
Arsenic	33	Toxic
Selenium	34	Toxic
Krypton	36	Rare — no stable (at room temperature) compounds known
Technetium	43	Radioactive — limited supply
Ruthenium	44	Toxic, expensive, limited supply
Rhodium	45	Expensive, limited supply
Palladium	46	Expensive, limited supply
Indium	49	Expensive, limited supply
Antimony	51	Toxic, limited availability
Tellurium	52	Toxic, limited availability
Elements	59–71	Rare earths, limited supply, cerium representative of chemistry
Rhenium	75	Limited supply
Osmium	76	Limited supply
Iridium	77	Limited supply
Platinum	78	Limited supply
Gold	79	Limited supply
Thallium	81	Toxic
Elements	≥84	Radioactive

For each of the 85 reactions which passed these tests, an approximate equilibrium temperature, or "turning" temperature was calculated from:

$$T^* = \frac{\Delta H}{\Delta S}$$

where ΔH and ΔS are the standard enthalpy and entropy of reaction. According to these temperatures, the reactions were divided nominally into 49 "low" temperature reactions (400 K < T^* < 900 K) and 36 "high" temperature reactions (900 K < T^* < 1,500 K). This screening process is depicted schematically in Figure 3-2. The temperature range 400 to 1,500 K was chosen to include, with a comfortable margin for safety, the entire range of output temperatures of receivers likely to be used in STEC applications. Reactions with approximate equilibrium temperatures below 400 K or above 1,500 K were eliminated as being outside the scope of the current program even though they might otherwise appear to be excellent CES reactions.

The 85 reactions were then rated by four persons according to a simple rating scheme shown in Table 3-2. The four ratings for each reaction were then averaged, and the reactions were ranked 1 through 85 according to their composite numerical rating, as shown in Table 3-3. It was found that nearly all of the reactions could logically be classified into 14 categories based on the reaction or chemical type. These categories are listed in Table 3-4, and the reactions are listed by category in Table 3-5.

The field of 85 reactions was narrowed to 24 by selecting the most highly rated reactions from each of the 14 categories, while also including several reactions which were known to be under investigation by other workers for energy storage applications. These 24 reactions are listed in Table 3-6, along with estimates of their endothermic and exothermic reaction temperatures.

It should be noted that the selection of the temperatures in Table 3-5 was somewhat arbitrary, and was intended only to give a general idea of which STEC system type the reaction might best be suited for. The endothermic and exothermic temperatures for the solid/gas noncatalytic reactions such as the $Ca(OH)_2$ decomposition were those at which the solid would be in equilibrium with the gaseous reactant at partial pressures of 0.1 and 1.0 bar, respectively. For other reactions, the temperatures corresponded to equilibrium conversions of 90 and 10 percent at a total pressure of 1.0 bar, and for a few reactions (e.g. ammonium hydrogen sulfate decomposition) the temperatures listed were those used or recommended by other investigators.

Generation of any but the simplest of process designs for all 24 of the reactions in Table 3-6 was beyond the scope of this study. Rocket Research Company and the contract monitor, agreed, therefore, that the number of reactions be reduced to approximately 12 for the preliminary process design studies.

A few of the reactions in Table 3-6 were rejected due to lack of data, extreme toxicity, etc. The most important criteria used in this final selection process were storage cost and efficiency estimates based on very simple storage subsystem process flow sheets for 21 of the 24 candidate reactions. An

REACTION SELECTION PROCESS

PERIODIC TABLE

↓

49 ELEMENTS

↓

APPROXIMATELY 750 COMPOUNDS

↓

APPROXIMATELY 555 REACTIONS

REACTION APPEARS TO BE REVERSIBLE
$\Delta H \geqslant 110$ KCAL/KG

$|\Delta G|_{298^oK}$ OR $|\Delta G|_{800^oK} \leqslant 10$ KCAL/MOLE

$400^oK < \dfrac{\Delta H^o}{\Delta S^o} < 900^oK$

$|\Delta G|_{1,200^oK} \leqslant 10$ KCAL/MOLE

$900^oK < \dfrac{\Delta H^o}{\Delta S^o} < 1,500^oK$

49 REACTIONS   +   **36 REACTIONS = 85 TOTAL REACTIONS**
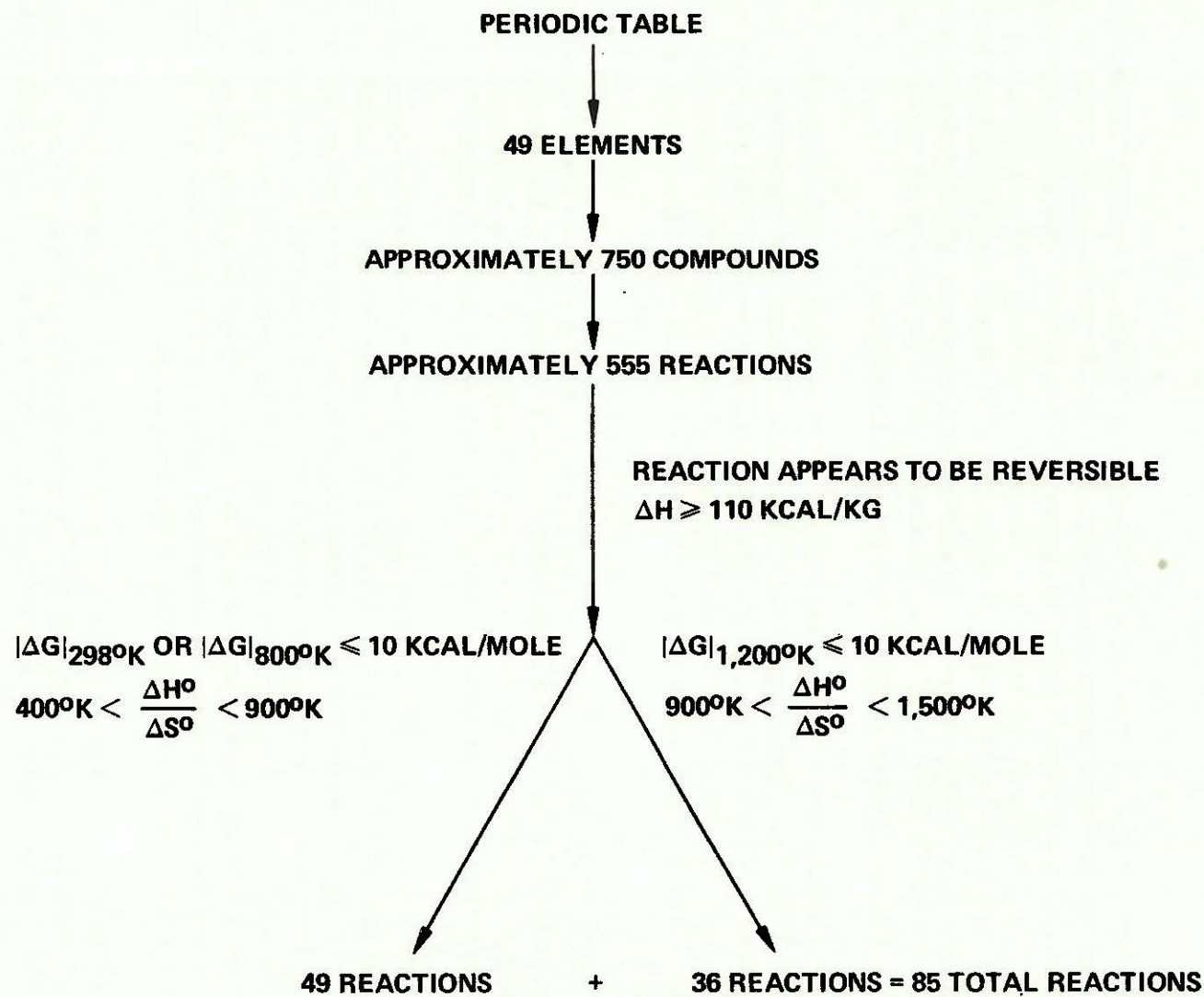
Figure 3-2

Table 3-2

**CHEMICAL ENERGY STORAGE REACTION
RATING METHOD**

No.	Criteria	Rating
1	Energy storage density	$\dfrac{Btu/ft^3}{1,000}$
2	Materials cost	$\dfrac{\$/M\ Btu}{100}$
3	Reversibility (side reactions)	1 = Reversible to 5 = Not reversible
4	Toxicity	1 = Not toxic to 5 = Very toxic
5	Corrosivity	1 = Not corrosive to 5 = Very corrosive
6	Storage pressure	1 = Atmosphere pressure 3 = Liquefied gas 5 = Compressed gas
7	Product separation	1 = Easy to 5 = Difficult
8	Handling complexity	1 = No solids 3 = 1 solid 5 = 2 or more solids

Rating = Criteria No. 1/ Σ criteria
2-8

Table 3-3
REACTIONS RANKED BY FOUR EVALUATORS

Rank	Rating	Reaction	Rank	Rating	Reaction
1	9.010	$CaO + H_2O = Ca(OH)_2$	44	0.978	$NH_3 + HI = NH_4I$
2	8.357	$Li_2O + SO_3 = Li_2SO_4$	45	0.940	$CH_4 + 2Li_2C_2 = 4LiH + 5C$
3	7.474	$K_2O + 3\,2\,O_2\ (AIR) = 2KO_2$	46	0.932	$K_2O + 3\,2\,O_2 = 2KO_2$
4	6.467	$MgO + H_2O = Mg(OH)_2$	47	0.906	$Li_2C_2 + H_2 = 2LiH + 2C$
5	5.157	$SrO + CO_2 = SrCO_3$	48	0.894	$CuO + H_2O = Cu(OH)_2$
6	5.234	$CaO + CO_2 = CaCO_3$	49	0.870	$2CaCO_3 + 4NO_2 = Ca(NO_2)_2 + Ca(NO_3)_2 + 2CO_2$
7	5.275	$ZnO + SO_3 = ZnSO_4$	50	0.856	$2CO = C + CO_2$
8	5.126	$2NH_3 + H_2O + SO_3 = (NH_4)_2SO_4$	51	0.767	$H_2 + 2Na = 2NaH$
9	4.930	$NH_3 + H_2O + SO_3 = NH_4HSO_4$	52	0.723	$CS_2 + 4H_2 = CH_4 + 2H_2S$
10	4.610	$NiO + SO_3 = NiSO_4$	53	0.699	$Li + 1\,2\,H_2 = LiH$
11	4.379	$Na_2O + 2NO_2 + 1\,2\,O_2 = 2NaNO_3$	54	0.675	$2NO + SO_2 = N_2O + SO_3$
12	4.299	$H_2O + SO_3 = H_2SO_4$	55	0.631	$C_6H_6 + 3H_2 = C_6H_{12}$
13	4.234	$CuO + SO_3 = CuSO_4$	56	0.591	$H_2 + CO = C + H_2O$
14	3.887	$Li_2O + CO_2 = Li_2CO_3$	57	0.550	$CO + Cl_2 = COCl_2$
15	3.596	$NH_3 + HCl = NH_4Cl$	58	0.547	$Na_2O + 3\,2\,O_2 = 2NaO_2$
16	3.474	$CS_2 = C + 2S$	59	0.526	$Mg + H_2 = MgH_2$
17	2.956	$NH_3 + HBr = NH_4Br$	60	0.500	$4HCl + O_2 = 2H_2O + 2Cl_2$
18	3.332	$Li_2O + 2NO_2 = LiNO_3 + LiNO_2$	61	0.504	$Li_2CO_3 + 2NO_2 = LiNO_2 + LiNO_3 + CO_2$
19	3.322	$BaO + 2NO_2 + 1\,2\,O_2 = Ba(NO_3)_2$	62	0.502	$CdO + CO_2 = CdCO_3$
20	3.321	$MgO + CO_2 = MgCO_3$	63	0.476	$CO + 3H_2 = CH_4 + H_2O$
21	3.132	$NH_3 + HF = NH_4F$	64	0.481	$FeO + CO_2 = FeCO_3$
22	2.837	$2NaOH + 2NO_2 = NaNO_2 + NaNO_3 + H_2O$	65	0.471	$3NO = N_2O + NO_2$
23	2.817	$CaO + 2NO_2 + 1\,2\,O_2 = Ca(NO_3)_2$	66	0.402	$2NH_3 + 6K = N_2 + 6KH$
24	2.816	$2NH_3 + H_2SO_4 = (NH_4)_2SO_4$	67	0.379	$C + 2H_2 = CH_4$
25	2.503	$2Ca(OH)_2 + 4NO_2 = Ca(NO_3)_2 + Ca(NO_2)_2 + 2H_2O$	68	0.376	$2H_2 + CO_2 = C + 2H_2O$
26	2.286	$MgCl_2 + NH_3 = MgCl_2 \cdot NH_3$	69	0.368	$CH_4 + 4Na = C + 4NaH$
27	2.262	$MnO + CO_2 = MnCO_3$	70	0.358	$SiH_4 + Mg = Si + MgH_2$
28	2.033	$NH_3 + H_3PO_4 = NH_4H_2PO_4$	71	0.339	$2NO + O_2 = 2NO_2$
29	2.006	$NaF + HF = NaHF_2$	72	0.339	$CO + H_2O = CO_2 + H_2$
30	1.905	$KF + HF = KHF_2$	73	0.309	$CO + 2H_2 = CH_3OH$
31	1.585	$2NH_3 + 6Na = N_2 + 6NaH$	74	0.300	$CH_4 + 4K = C + 4KH$
32	1.601	$2NO_2 + 3SO_2 = N_2O + 3\,SO_3$	75	0.288	$H_2 + 2K = 2KH$
33	1.572	$Na_2S + CO_2 + H_2O = H_2S + Na_2CO_3$	76	0.287	$Cs_2O + SO_3 = Cs_2SO_4$
34	1.451	$CS_2 + H_2S = CH_4 + 4S$	77	0.256	$Ti + H_2 = TiH_2$
35	1.331	$FeCl_2 \cdot NH_3 + NH_3 = FeCl_2 \cdot 2NH_3$	78	0.244	$N_2 + 3H_2 = 2NH_3$
36	1.235	$2LiOH + 2NO_2 = LiNO_2 + LiNO_3 + H_2O$	79	0.186	$2NO + Cl_2 = 2NOCl$
37	1.162	$SO_2 + 1\,2\,O_2 = SO_3$	80	0.180	$VCl_2 + 1\,2\,Cl_2 = VCl_3$
38	1.140	$KF + BF_3 = KBF_4$	81	0.167	$CaC_2 + 4H_2 = 2CH_4 + Ca$
39	1.086	$Na_2CO_3 + 2NO_2 = NaNO_2 + NaNO_3 + CO_2$	82	0.077	$2Li_3N + 3H_2 = N_2 + 6LiH$
40	1.067	$C + 2Cl_2 = CCl_4$	83	0.058	$N_2 + 3F_2 = 2NF_3$
41	1.070	$4HF + SiO_2 = SiF_4 + 2H_2O$	84	0.019	$IF_5 + F_2 = IF_7$
42	1.020	$ZnO + CO_2 = ZnCO_3$	85	0.013	$SiH_4 + 4Na = 4NaH$
43	0.990	$Ca + H_2 = CaH_2$			

Table 3-4
CHEMICAL ENERGY STORAGE REACTION CATEGORIES

- Metal oxides/hydroxides
- Metal sulfates
- Peroxides/superoxides
- Carbonates
- Ammonia reactions
- NO_2 reaction with oxides, hydroxides, carbonates
- Carbon disulfide
- Fluorine/fluorides
- Sulfur trioxide
- Chlorine/chlorides
- Hydrides
- Organic reactions
- Nitrogen oxides
- Miscellaneous

Table 3-5
POTENTIAL CHEMICAL ENERGY STORAGE REACTIONS
ARRANGED BY REACTION TYPE

Group or Classification	Rating (Rank)	Reactions	T_{equil} °K	Group or Classification	Rating (Rank)	Reactions	T_{equil} °K
1.0 Metal hydroxides	1	$CaO_{(S)} + H_{2(G)} = Ca(OH)_{2(S)}$	720	5.0 Ammonia	8	$2NH_{3(G)} + H_2O_{(G)} + SO_{3(G)} = (NH_4)_2SO_{4(S)}$	740
	4	$MgO_{(S)} + H_2O_{(G)} = Mg(OH)_{2(S)}$	535		9	$NH_{3(G)} + H_2O_{(G)} + SO_{3(G)} = NH_4HSO_{4(S)}$	740
	48	$CuO_{(S)} + H_2O_{(G)} = Cu(OH)_{2(S)}$			23	$2NH_{3(G)} + H_2SO^{4(L)} = (NH_4)_2SO_{4(S)}$	850
2.0 Metal sulfates	2	$Li_2O_{(S)} + SO_{3(G)} = Li_2SO_{4(S)}$	⩾1,100		15	$NH_{3(G)} + HCl_{(G)} = NH_4Cl_{(S)}$	620
	7	$ZnO_{(S)} + SO_{3(G)} = ZnSO_{4(S)}$	1,340		17	$NH_{3(G)} + HBr_{(G)} = NH_4Br_{(S)}$	680
	10	$NiO_{(S)} + SO_{3(G)} = NiSO_{4(S)}$	1,160		21	$NH_{3(G)} + HF_{(G)} = NH_4F_{(S)}$	517
	14	$CuO_{(S)} + SO_{3(G)} = CuSO_{4(S)}$	1,180		44	$NH_{3(G)} + HI_{(G)} = NH_4I_{(S)}$	640
	76	$Cs_2O_{(S)} + SO_{3(G)} = Cs_2SO_{4(S)}$			26	$MgCl_{2(S)} + NH_{3(G)} = MgCl_2 \cdot NH_{3(S)}$	572–644
3.0 Peroxides superoxides	3	$K_2O_{(S)} + 3/2O_2 \text{(Air)} = 2KO_2$	573–1,073		35	$FeCl_2 \cdot NH_{3(S)} + NH_{3(G)} = FeCl_2 \cdot 2NH_{3(S)}$	500–550
	46	$K_2O_{(S)} + 3/2O_2 = 2KO_2$	573–1,073		28	$NH_{3(G)} + H_3PO_{4(S)} = NH_4H_2PO_4$	926
	57	$Na_2O_{(S)} + 3/2O_2 = 2NaO_2$	710		31	$2NH_{3(G)} + 6Na_{(S)} = N_{2(G)} + 6NaH_{(S)}$	940
4.0 Carbonates	5	$SrO_{(S)} + CO_{2(G)} = SrCO_{3(S)}$	1,372		66	$2NH_{3(G)} + 6K_{(S)} = N_{2(G)} + 6KH_{(S)}$	910
	6	$CaO_{(S)} + CO_{2(G)} = CaCO_{3(S)}$	1,108		78	$N_{2(G)} + 3H_{2(G)} = 2NH_{3(G)}$	460
	13	$Li_2O_{(S)} + CO_{2(G)} = Li_2CO_{3(S)}$	1,390	6.0 NO_2 with oxides, hydroxides, carbonates	11	$Na_2O_{(S)} + 2NO_{2(G)} + 1/2O_2 = 2NaNO_3$	1,486
	20	$MgO_{(S)} + CO_{2(G)} = MgCO_{3(S)}$	670		18	$Li_2O_{(S)} + 2NO_{2(G)} = LiNO_2 + LiNO_3$	1,089
	27	$MnO_{(S)} + CO_{2(G)} = MnCO_{3(S)}$	620		19	$BaO_{(S)} + 2NO_{2(G)} + 1/2O_{2(G)} = Ba(NO_3)_{2(S)}$	1,233
	42	$ZnO_{(S)} + CO_{2(G)} = ZnCO_{3(S)}$	405		22	$2NaOH_{(S)} + 2NO_{2(G)} = NaNO_{2(S)} + NaNO_{3(S)} + H_2O_{(G)}$	1,212
	62	$CdO_{(S)} + CO_{2(G)} = CdCO_{3(S)}$	610		24	$CaO_{(S)} + 2NO_{2(G)} + 1/2O_2 = Ca(NO_3)_2$	740
					25	$2Ca(OH)_2 + 4NO_2 = Ca(NO_3)_{2(S)} + Ca(NO_2)_{2(S)}$	868
					36	$2LiOH + 2NO_2 = LiNO_2 + LiNO_3 + H_2O$	1,120
					39	$Na_2CO_3 + 2NO_2 = NaNO_2 + NaNO_3 + CO_2$	624
					49	$2CaCO_3 + 4NO_2 = Ca(NO_2)_2 + Ca(NO_3)_2 + CO_2$	

Table 3-5 (Concluded)
POTENTIAL CHEMICAL ENERGY STORAGE REACTIONS
ARRANGED BY REACTION TYPE

Group or Classification	Rating (Rank)	Reactions	T_{equil} $^\circ$K	Group or Classification	Rating (Rank)	Reactions	T_{equil} $^\circ$K
7.0 Carbon disulfide	16	$CS_{2(G)} = C_{(S)} + 2S_{(S)}$	700	11.0 Hydrides	43	$Ca_{(S)} + H_{2(G)} = CaH_{2(S)}$	1,450
	34	$CS_{2(G)} + H_2S = CH_{4(G)} + 4S_{(S)}$	450		45	$CH_{4(G)} + 2Li_2C_{2(S)} = 4LiH_{(S)} + 5C_{(S)}$	870
	52	$CS_{2(G)} + 4H_{2(G)} = CH_{4(G)} + 2H_2S_{(G)}$	1,450		47	$H_{2(G)} + Li_2C_{2(S)} = 2LiH_{(S)} + 2C_{(S)}$	885
8.0 Fluorine — fluorides	29	$HF_{(G)} + NaF_{(S)} = NaHF_{2(S)}$	486		51	$H_{2(G)} + 2Na_{(S)} = 2NaH_{(S)}$	735
	30	$HF_{(G)} + KF_{(S)} = KHF_{2(S)}$	685		53	$H_{2(G)} + 2Li_{(S)} = 2LiH_{(S)}$	1,220
	38	$KF_{(S)} + BF_{3(G)} = KBF_{4(S)}$	978 (845 KP)		59	$H_{2(G)} + Mg_{(S)} = MgH_{2(S)}$	575
	41	$4HF_{(G)} + SiO_2 = SiF_{4(G)} + 2H_2O_{(G)}$	940		69	$CH_{4(G)} + 4Na_{(S)} = C_{(S)} + 4NaH_{(S)}$	670
	83	$N_{2(G)} + F_{2(G)} = 2NF_{3(G)}$	945		70	$SiH_{4(G)} + 2Mg_{(S)} = Si_{(S)} + 2MgH_{2(S)}$	980
9.0 SO₃	32	$3SO_{2(G)} + 2NO_{2(G)} = N_2O_{(G)} + 3SO_{3(G)}$	1,200	12.0 Organics, CH₄, CO, and CO₂	50	$2CO_{(G)} = C_{(S)} + CO_{2(G)}$	980
	37	$SO_{2(G)} + 1/2O_{2(G)} = SO_{3(G)}$	1,055		55	$C_6H_{6(G)} + 3H_{2(G)} = C_6H_{12(G)}$	600
	54	$SO_{2(G)} + 2NO_{(G)} = N_2O_{(G)} + SO_{3(G)}$	1,025			$C_2H_{4(G)} + H_{2(G)} = C_2H_{6(G)}$	840–1,200
10.0 Chlorine — chlorides	40	$C_{(S)} + 2Cl_{2(G)} = CCl_{4(L)}$	675		56	$H_{2(G)} + CO_{(G)} = C_{(S)} + H_2O_{(G)}$	980
	58	$CO_{(G)} + Cl_{2(G)} = COCl_{2(G)}$	800		63	$3H_{2(G)} + CO_{(G)} = CH_4 + H_2O$	960
	60	$4HCl_{(G)} + O_{2(G)} = 2H_2O_{(G)} + 2Cl_{2(G)}$	890		67	$2H2_{(G)} + C_{(S)} = CH_{4(G)}$	930
	79	$2NO_{(G)} + Cl_{2(G)} = 2NOCl_{(S)}$	640		68	$2H2_{(G)} + CO_{2(G)} = C_{(S)} + 2H_2O_{(G)}$	980
	80	$VCl_{2(S)} + 1/2Cl_{2(G)} = VCl_{3(G)}$	1,295		72	$CO_{(G)} + H_2O_{(G)} = CO_{2(G)} + H_{2(G)}$	980
					73	$CO_{(G)} + 2H_{2(G)} = CH_3OH_{(G)}$	415
				13.0 NO, NO₂	65	$3NO_{(G)} = N_2O_{(G)} + NO_{2(G)}$	900
					71	$2NO_{(G)} + O_{2(G)} = 2NO_{2(G)}$	780
				14.0 Miscellaneous	33	$Na_2S_{(S)} + CO_{2(G)} + H_2O_{(G)} = H_2S_{(G)} + Na_2CO_{3(S)}$	921

Table 3-6
REACTIONS RANKED IN ORDER OF
DECREASING ENDOTHERMIC REACTION TEMPERATURE

Reaction	TEndothermic $^{\circ}K$	TExothermic $^{\circ}K$
$Ca + H_2 = CaH_2$	1,350	1,150
$K_2O_2 + O_2 = 2KO_2$	1,300	900
$K_2O_2 + O_2(AIR) = 2KO_2$	1,300	750
$C_2H_4 + H_2 = C_2H_6$	1,200	1,000
$NH_3 + H_2O + SO_3 = NH_4HSO_4$	1,200	700
$ZnO + SO_3 = ZnSO_4$	1,175	1,060
$CaO + CO_2 = CaCO_3$	1,125	1,000
$2SO_2 + O_2 = 2SO_3$	1,100	800
$CO + 3H_2 = CH_4 + H_2O$	1,100	700
$4HCl + O_2 = 2H_2O + 2Cl_2$	900	700
$CaO + H_2O = Ca(OH)_2$	800	675
$CS_2 = C + 2S$	800	600
$C + 2Cl_2 = CCl_4$	750	550
$HF + KF = KHF_2$	725	600
$MgO + CO_2 = MgCO_3$	700	600
$2Na + H_2 = 2NaH$	700	600
$MgCl_2 + NH_3 = MgCl_2 \cdot NH_3$	640	540
$N_2 + 3H_2 = 2NH_3$	600	800
$C_6H_6 + 3H_2 = C_6H_{12}$	590	670
$MgO + H_2O = Mg(OH)_2$	550	450
$FeCl_2 \cdot NH_3 + NH_3 = FeCl_2 \cdot 2NH_3$	550	450
$Li_2O + SO_3 = Li_2SO_4$	*	*
$Na_2O + 2NO_2 + 1/2O_2 = 2NaNO_3$	*	*
$NH_3 + HCl = NH_4Cl$	*	*

*Not established

example of such a process flow sheet is shown in Figure 3-3. Comparison of Figure 3-3 with Figures 4-3 and 4-4 should give the reader an idea of the very basic nature of these early flow sheets. Details of the design procedure and of individual designs are discussed in a previous report (Reference R4). Important simplifying assumptions used for these flow sheets included:

1. All solid/gas noncatalytic reactors were batch type

2. Each CES subsystem was assumed to be interfaced with a solar power plant with a nominal output of 10 MW_e, and a 24 hour storage capacity. The charge-to-discharge ratio was assumed to be low enough that the storage discharge rate determined the size of the rate related process equipment*

3. Separation processes were assumed to be 100 percent efficient and separation work, W, was estimated by:

$$W = -RT\sum_i n_i \ln X_i$$

   where i denotes various components to be separated.

4. All thermal energy above 350 K was recoverable for use in other parts of the process if needed. All energy below 350 K was discarded

5. Reactions proceeded to equilibrium. Endothermic and exothermic reactions were assumed to take place at the temperatures indicated in Table 3-6.

6. Heat of condensation or fusion of reactants (e.g. H_2O in $CaO/Ca(OH)_2$ system) were assumed to be useful and credited to the system for efficiency calculations. Similarly, heat required to vaporize or melt such reactants was assumed to be available and not charged against the system.

7. Permanent gases were assumed to be stored at 150 bar pressure and 298 K.

8. The total cost of process equipment was estimated by listing the major equipment units, establishing a cost for each unit, and adding 10 percent of the total cost to cover miscellaneous items. The cost of equipment items was usually obtained from Guthrie (Reference G3) for the size determined by the plant capacity. In a few instances, other sources of cost information were used; but, whatever the source, the costs were escalated to 1978 values by use of the Marshall and Swift (M&S) Equipment Cost Index as published in *Chemical Engineering*. Costs of reactants were obtained from the Chemical Marketing Reporter.

The thermal-to-thermal efficiencies and cost estimates derived from these simplified flow sheets were used only for comparison of the 24 candidate reactions; in view of the simplifying assumptions on which the designs were based, the absolute values of the efficiency and cost estimates cannot be

---

*As a result of the systems studies described in Chapter 2, this constraint was relaxed for the process design studies performed later.

SIMPLIFIED SCHEMATIC OF CHEMICAL ENERGY SYSTEM
USING METAL OXIDE/HYDROXIDES
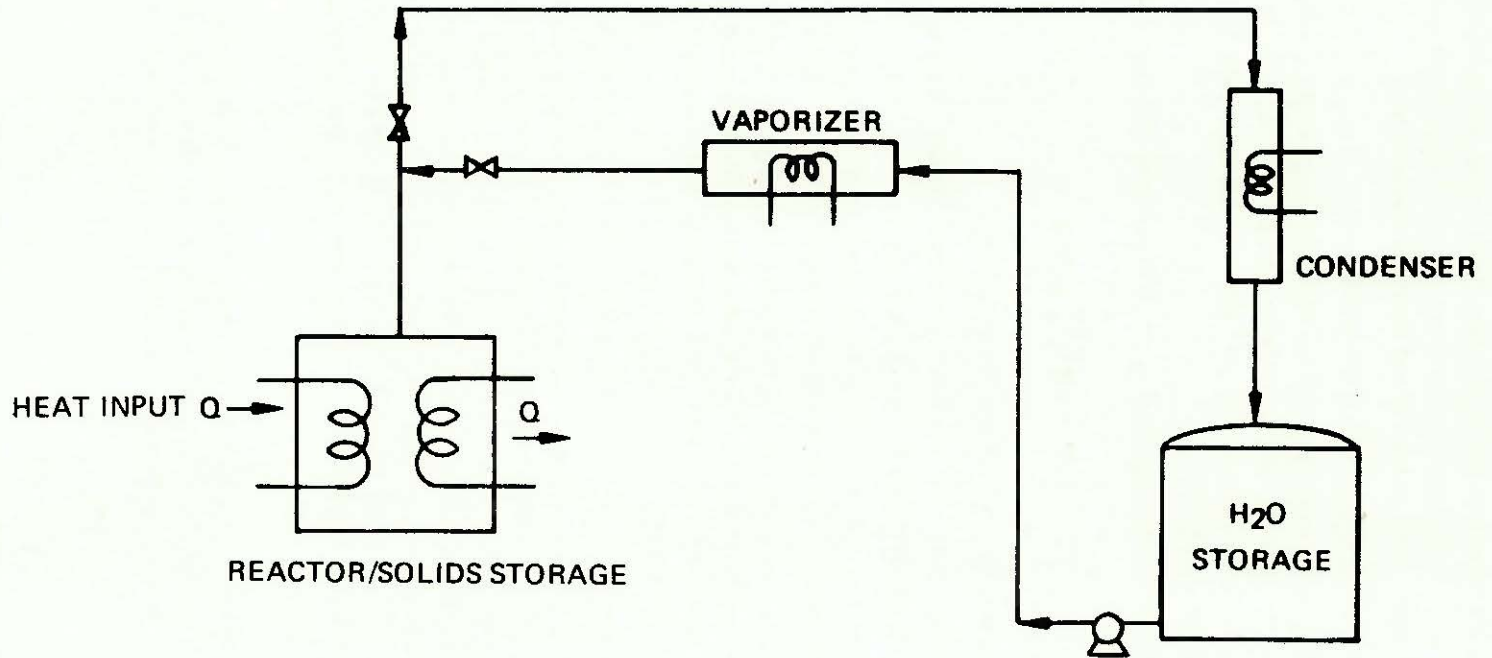
expected to be realistic. The storage subsystem efficiencies and the energy and power related unit costs* in Table 3-7 are, therefore, normalized to those for the $CaO/Ca(OH)_2$** system.

The reactions chosen from those in Table 3-7 for further preliminary design studies are listed in Table 3-8. In addition to capital costs, several other criteria were used to select the reactions in this table, including reversibility, data availability, corrosivity and toxicity. While only one reaction was eliminated on the basis of data availability alone, and only one on the basis of corrosivity alone, these criteria were used in conjunction with the capital cost estimates in decisions for which these estimates would not have been sufficient by themselves. Brief discussions of each reaction eliminated from Table 3-7 are presented below.

Several reactions were eliminated without recourse to cost considerations, simply on the basis of technical difficulties with the reaction and/or data availability. These include:

$$2Na_2O + 4NO_2 + O_2 = 4 NaNO_3$$
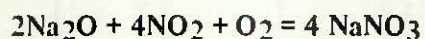
This reaction is irreversible. In the endothermic mode, the thermal decomposition of the sodium nitrate would produce large amounts of elemental nitrogen. The reaction is thus not a candidate for energy storage applications.

$$NH_3 + HCl = NH_4 Cl$$
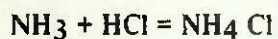
No method is at present known for the physical separation of the endothermic reaction products. The reaction of NH_3 and HCl does not require a catalyst and occurs readily at storage temperatures, so they cannot be stored together. The only known separation method (chemical decomposition of the ammonia into nitrogen and hydrogen with subsequent storage of the gases) places very heavy efficiency and cost penalties on the system so as to make it economically unattractive.

$$Li_2O + SO_3 = Li_2 SO_3$$
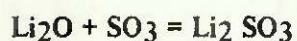
There are major uncertainties concerning this reaction which the small amount of data in the literature is unable to resolve. The actual decomposition process for $Li_2 SO_3$ is unknown, as is even the melting point of Li_2O. Due to these uncertainties, a storage system based on this reaction is not considered technically feasible at this time.

$$HF + KF = KHF_2$$
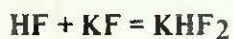
Although its relative capital cost ranking made this reaction appear promising, the extreme corrosivity of the reactants (especially HF) make a storage system based on this reaction unattractive. Severe handling and materials problems are associated with HF. Indeed, the requirements for special construction materials made the equipment capital cost estimations uncertain, so that actual capital cost requirements could well be higher than estimated. In addition, no references could be found in the literature for this reaction, so that design data are apparently nonexistent.

---

*Power-related costs include all capital items where size is dependent on processing rate such as reactors, pipes, and valves. Energy costs include all storage vessel and chemical inventory costs. Solid/gas, noncatalytic batch reactors were included in power-related costs.

**This choice was not intended to show favoritism. It was made simply because the $Ca(OH)_2$ system ranked at or near the top of each list.

Table 3-7
CANDIDATE CHEMICAL REACTIONS RANKED IN ORDER OF
DECREASING THERMAL EFFICIENCY

Reaction	Relative[†] Thermal Efficiency	Relative[†] Power Related Unit Cost	Relative[†] Energy Related Unit Cost
$CaO + H_2O = Ca(OH)_2$	1.00	1.0	1.0
$CS_2 = C + 2S$	0.99	1.2	5.2
$MgO + H_2O = Mg(OH)_2$	0.96	1.0	2.4
$HF + KF = KHF_2$	0.93	3.6	29.1
$ZnO + SO_3 = ZnSO_4$	0.93	1.2	7.7
$K_2O_2 + O_2 (air) = 2KO_2$	0.87	8.3	12.1
$CaO + CO_2 = CaCO_3$	0.84	3.0	15.8
$Ca + H_2 = CaH_2$	0.77	10.5	76.2
$NH_3 + H_2O + SO_3 = NH_4HSO_4$	0.75	0.8	5.6
$MgO + CO_2 = MgCO_3$	0.72	4.2	28.8
$MgCl_2 + NH_3 = MgCl_2 \cdot NH_3$	0.72	2.1	12.9
$FeCl_2 \cdot NH_3 + NH_3 = FeCl_2 \cdot 2NH_3$	0.62	2.7	29.0
$2Na + H_2 = 2NaH$	0.63	16.5	105.0
$C_6H_6 + 3H_2 = C_6H_{12}$	0.62	11.2	87.4
$K_2O_2 + O_2 = 2KO_2$	0.59	10.3	144.4
$C_2H_4 + H_2 = C_2H_6$	0.52	7.5	148.0
$2SO_2 + O_2 = 2SO_3$	0.47	4.2	75.3
$C + 2Cl_2 = C Cl_4$	0.42	4.7	37.2
$4 HCl + O_2 = 2H_2O + 2Cl_2$	0.38	10.8	287.0
$CO + 3H_2 = CH_4 + H_2O$	0.32	14.7	342.0
$N_2 + 3H_2 = 2NH_3$	0.16	74.7	530.0
$Li_2O + SO_3 = Li_2SO_4$	*	*	*
$Na_2O + 2NO_2 + 1/2 O_2 = NaNO_3$	*	*	*
$NH_3 + HCl = NH_4 Cl$	*	*	*

*Not established

†Normalized to the $CaO/Ca(OH)_2$ system

Table 3-8
CHEMICAL REACTIONS CHOSEN FOR PRELIMINARY
PROCESS DESIGN STUDY

1) $NH_3 + SO_3 + H_2O = NH_4 HSO_4$

2) $CaO + H_2O = Ca(OH)_2$

3) $MgO + H_2O = Mg(OH)_2$

4) $ZnO + SO_3 = ZnSO_4$

5) $CS_2 = C + 2S$

6) $MgCl_2 + NH_3 = MgCl_2 \cdot NH_3$

7) $CaO + CO_2 = CaCO_3$

8) $MgO + CO_2 = MgCO_3$

9) $2SO_2 + O_2 = 2SO_3$

10) $FeCl_2 \cdot NH_3 = FeCl_2 \cdot 2NH_3$

11) $C_2H_4 + H_2 = C_2H_6$

12) $C_6H_6 + 3H_2 = C_6H_{12}$

$C + 2Cl_2 = CCl_4$
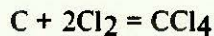
This reaction was rejected primarily for lack of data. No information on the feasibility of this reaction could be found in the literature. Results from the systems studies described in Chapter 2, indicate that storage subsystems based on the SO_2/SO_3 reaction are probably only marginally cost-effective in seasonal storage applications. It seemed appropriate, therefore, in choosing reactions for further study, to give considerable weight to those with estimated capacity and/or rate-related costs lower than those of the SO_2/SO_3 system. An additional seven reactions were eliminated at least in part due to such higher capacity and/or rate-related capital cost estimates. Only two of these, the ammonia and methanation/reformation reactions, were eliminated solely on the basis of cost. The rest were deemed unlikely candidates, at present, for energy storage applications due to a combination of high capital cost requirements and lack of published technical data. These reactions include:

$N_2 + 3H_2 = 2NH_3$
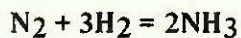
A storage subsystem based on the synthesis/decomposition of ammonia would suffer from extremely high rate and capacity related costs. Both the rate and capacity related costs are driven up by the low round-trip efficiency (estimated to be 27 percent) of such a storage system. The rate-related costs are driven up still further by the cost of the high pressure (300 atm) exothermic reactor, and the capacity related costs are higher due to the expensive, high-pressure vessels required

for N_2 and H_2 storage. These high pressure gas storage costs could be reduced considerably if existing underground caverns or salt domes could be used, but such site specific storage systems, however attractive, are beyond the scope of this study.

$CO + 3H_2 = H_2O + CH_4$
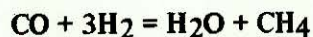
While this reaction has been proposed and is being studied for use in chemical heat pipe applications, the low round-trip efficiency together with high pressure storage requirements for methane and hydrogen cause this system to have capacity related costs too high for energy storage applications.

$Ca + H_2 = CaH_2$
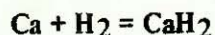
Although estimated energy-related costs are approximately equal to those for the closed SO_2/SO_3 system, rate-related costs are more than twice as high. At reaction temperatures, calcium is a liquid, and no information could be found in the literature on the interaction of hydrogen and liquid calcium.

$2Na + H_2 = 2NaH$
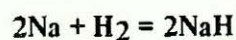
Both power-related and energy-related unit costs for this reaction are higher than those for the SO_2/SO_3 reaction. Liquid sodium is very corrosive, and equipment designed to transport, react, and store it would be expensive. Moreover, storage of large quantities of elemental sodium would present safety problems due to its reactivity with water.

$4HCl + O_2 = 2H_2O + 2Cl_2$
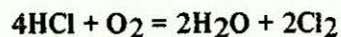
The estimated thermal efficiency of a storage subsystem based on this reaction is low, and the energy-related unit cost is prohibitive. In spite of the fact that the oxidation of hydrogen chloride by oxygen to produce chlorine was once used commercially (known as the Deacon process), no kinetic information was found in a preliminary search.

$K_2O_2 + O_2 = 2KO_2$; $K_2O_2 + O_2$ (air) $= 2KO_2$

Due to O_2 storage requirements, the capacity related costs of the closed cycle reaction are extremely high. While the capacity-related cost requirements of the open-cycle reaction are considerably lower, both systems have been eliminated for the present due to a lack of information. No literature references were found for this reaction.

While most of the 12 reactions selected for further study showed clear cost and performance advantages, three were included in spite of cost and/or technical problems. Both the benzene/ cyclohexane and the ethylene/ethane reactions were at best only moderate performers on the cost scale, and indeed the capacity-related costs for the latter reaction were higher than all but five other reactions (all eliminated) on the list. Both reactions, however, are apparently well studied and characterized, and were chosen as representative organic reactions for inclusion in a group of otherwise completely inorganic reactions. In addition, the benzene/cyclohexane reaction is receiving study elsewhere for possible energy storage applications, and should, therefore, be included for

comparison with the other reactions. Most organic reactions are subject to by-product formation, a potentially vexing problem in view of the large number of reaction cycles required in solar energy storage applications. The extent of by-product formation in these reactions is unknown at present, but could in the future prove one or both of these reactions to be unfeasible for RCR energy storage.

The ammonium hydrogen sulfate reaction ranked at or near the top of the list for both rate-related and capacity-related capital cost requirements, and therefore appeared to be an ideal candidate for energy storage applications. A potentially severe drawback to this reaction, however, is the dissociation of a large fraction of the SO_3 at reaction temperatures. The capital cost estimates in Table 3-1 did not reflect the considerably more complicated system which would be necessary to account for this SO_3 dissociation, since the extent of this problem is at present unknown. The cost estimates for a workable RCR storage subsystem based on this reaction could be much higher. This reaction is presently being studied for energy storage applications (Reference P1) at the University of Houston, and it is hoped that a clearer definition of the NH_4HSO_4 reaction sequence as well as cost estimates for a viable storage subsystem will result from this study.

Finally, it should be noted that the ranking of reaction in this study was based primarily on storage capability. Many of the reactions which are not useful for energy storage because of low storage densities may still be useful for energy transmission in chemical heat pipes.

CHAPTER 4

PRELIMINARY PROCESS DESIGNS FOR CHEMICAL ENERGY STORAGE SYSTEMS

Preliminary process designs are presented in this section for most of the reactions listed in Table 3-8. The objectives of the process design work described here include:

1. Evaluation of cost and performance of energy storage subsystems based on the most promising reactions identified in Chapter 3.

2. Identification of important technical problems, advantages, and trade-offs of chemical energy storage processes, including those which are specific to particular reactions and those which apply to a larger group of reactions or to CES processes in general.

After discussions in section 4.1 of the approach to the design work and of the major assumptions or ground rules on which the designs are based, the individual designs are discussed in sections 4.2 through 4.4. The preliminary process designs of the SO_2/SO_3 and $CaO/Ca(OH)_2$ reactions are presented in considerably more detail than those of the other candidate reactions. These two reactions were chosen for extended discussion in part because, overall, they are the two most likely reactions for the CES applications considered in this study; in addition, these two reactions are representative of the two basically different types or groups into which the nine reaction candidates can be divided (section 4.1). Much of the discussion of the SO_2/SO_3 and $CaO/Ca(OH)_2$ designs, then, applies to the other reactions in their respective groups. The discussions in sections 4.2 and 4.3 then serve to describe these two particular reactions, as well as to introduce and discuss the common problems of the other preliminary process designs in their respective groups. Finally, important cost and performance results from all the designs are tabulated (Table 4-24) for comparison among the reactions.

4.1 APPROACH

Table 4-1 presents a summary of the disposition of the reactions originally considered for design studies. Preliminary process designs and cost estimates for nine storage subsystems were developed, with the cost and efficiency estimate for the NH_4HSO_4 system pending publication of the results of workers at the Solar Energy Laboratory of the University of Houston. The $MgO/Mg(OH)_2$ system was eliminated on the basis of poor exothermic reaction kinetics observed by other workers (References B7, E2), as was the ammoniated ferrous chloride system (References J3, M2). The mono-ammoniated $MgCl_2$ system was eliminated due to the occurrence of irreversible side reactions in the endothermic mode, the products of which are apparently highly corrosive (Reference M2, p. IV-6). In place of the mono-ammoniated $MgCl_2$ system, the di-ammoniated $MgCl_2$ system was inserted. While undesirable side reactions apparently occur for this reaction as well, the problem is less severe.

---

*Several reactions in that table were either discarded or replaced, as discussed in section 4.1.

Table 4-1

CHEMICAL REACTIONS
CHOSEN FOR PRELIMINARY PROCESS DESIGN STUDIES

$CaO + H_2O = Ca(OH)_2$
$CaO + CO_2 = CaCO_3$
$MgO + CO_2 = M_gCO_3$
$ZnO + SO_3 = ZnSO_4$ } Solid-gas noncatalytic
$CS_2 = C + 2S$
$*MgCl_2 \cdot NH_3 + NH_3 = MgCl_2 \cdot 2NH_3$

} Preliminary process designs complete

$2SO_2 + O_2 = 2SO_3$
$C_2H_4 + H_2 = C_2H_6$ } Solid-gas catalytic
$C_6H_6 + 3H_2 = C_6H_{12}$

$NH_3 + SO_3 + H_2O = NH_4 HSO_4$ Design pending results of other workers

$MgO + H_2O = Mg(OH)_2$
$FeCl_2 \cdot NH_3 + NH_3 = FeCl_2 \cdot 2NH_3$ } Discarded based on experimental results of other workers
$MgCl_2 + NH_3 = MgCl_2 \cdot NH_3$

*Substituted for discarded mono-ammoniate of $MgCl_2$

Each of the nine remaining reactions fall into one of two basic reaction types:

1. Solid-gas, noncatalytic, in which one or more of the reaction constituents is a solid (e.g. CaO, $Ca(OH)_2$), while the remaining constituents are gaseous at reaction temperatures

2. Solid-gas, catalytic, in which all reaction constituents are gaseous at reaction temperatures, but a solid catalyst (or at lease a solid catalyst support) is required for the reactions to proceed efficiently and selectively.

The reactor designs for the catalytic reactions in group 2., while of course complicated by many technical considerations, are fairly standard. Reactants are generally passed through a packed catalyst bed at the appropriate temperature and pressure, where the reaction takes place. Products leaving the reactor are cooled, separated, and recycled or stored as needed. Catalyst poisoning, degeneration, or coking may cause the catalyst activity to decrease to such an extent that replacement or regeneration is necessary. With the notable exception of petroleum cracking catalysts, most catalysts are chosen so that continuous regeneration or replacement is unnecessary; packed catalyst beds are regenerated in place or replaced during periods of scheduled downtime. For the three catalytic reactions considered here, it is assumed that catalyst regeneration, if necessary, is required seldom enough to allow packed bed reactor designs.

The solid/gas reactions in group 1., apparently promising based on the thermodynamic analyses and simple design criteria used so far, present a challenging reactor design problem, one for which there is not much precedent in the literature. It is fair to say that no completely satisfactory reactor design was found for these reactions, although an apparently workable, moving bed design was developed. The particulars of the design problem and the proposed solutions will be discussed in section 4.3.2 for the $CaO/Ca(OH)_2$ system. As mentioned above, the fundamental aspects of the proposed moving-bed reactor design apply equally well to the other solid/gas, noncatalytic reactions, and the preliminary process designs for those reactions are based on similar reactor designs.

4.1.1 Capital Cost Estimates

Funding and time constraints limited the process designs to the level of detail which lead to capital cost estimates of the type that Peters and Timmerhaus call "study estimates" (Reference P4). Only major items of process equipment were considered in the process designs, and the total plant capital cost was estimated from these major items using the factored cost estimation technique of Guthrie (Reference G3). A 15 percent contingency was added to the total capital cost estimate, and all capital costs were converted to 1978 dollars with the M&S plant cost index.

Capital cost estimates for each process are divided into power-related and energy-related unit costs. The energy-related cost includes all the costs of all storage vessels and the reactant costs, and the power-related cost accounts for all other process equipment. The energy-related unit costs were calculated by dividing the total energy-related capital cost by the total storage capacity, in MW_t-hr at the storage system outlet, for which the processes were designed. The power-related unit costs were calculated by dividing the total power-related capital cost by the maximum charging rate, in MW_t at the storage system inlet, for which the processes were designed.

While the power and energy-related unit costs described above do provide a means of comparing the candidate reactions, it is important to note that care must be exercised in using them to compare storage-related costs to the costs of other STEC components, or to compare CES costs to those of other types of storage. These unit costs are presented in the form in which they would be specified as input to programs STORAGE and CSTOPT (sections 2.3.2 and 2.3.3); calculation of total storage subsystem cost from them requires information about charging rates and storage capacities which must ultimately be based on assumptions of plant location, demand profile, type of operation (hybrid or autonomous), alternate energy cost, etc.

4.1.2 Storage Efficiencies: Definition

Many different definitions of the efficiency of CES subsystems have been proposed and are presently in use. One is as good as another, provided each is clearly defined. Overall storage subsystem efficiency is characterized in the present study by the round-trip efficiency, μ_{RT}. This overall thermal-to-thermal efficiency is the useful energy output from storage per unit of energy input to storage, and does not take into account differences in temperature (and thus in availability) between storage input and output. Such differences in availability are accounted for in program

STORAGE by changes in the power-cycle efficiency for energy from storage. This should be kept in mind when comparing round-trip efficiencies of CES subsystems with greatly differing output temperatures.

For the purposes of process design work, it is useful to write the storage round-trip efficiency as the product of a charging efficiency, η_c and a discharging efficiency, η_d. These charging and discharging efficiencies are defined as follows:

$$\eta_c \equiv \frac{e_c}{\Sigma q_c + \Sigma w_c}$$

$$\eta_d \equiv \frac{\Sigma q_d}{e_c},$$

where:

e_c	=	potential energy stored as enthalpy of reaction
Σq_c	=	sum of heat inputs to charging process
Σq_d	=	sum of energy outputs to power cycle(s)
Σw_c	=	sum of thermal equivalents of mechanical work inputs to charging cycle.

From the above definitions,

$$\eta_{RT} = \eta_c \cdot \eta_d = \frac{\Sigma q_d}{\Sigma q_c + \Sigma w_c}$$

The term Σq_d implies more than one storage output to a power cycle, and has been written that way for generality. All of the CES subsystems considered in the following sections, however, have only one power-generating output.

Although mechanical work in the discharge mode does not appear explicitly in the expression for the discharge efficiency, it is implicit in that expression, for,

$$\Sigma q_d = e_c - \Sigma q_r - \Sigma w_d,$$

where:

Σq_r	=	sum of reject process heat from discharging cycle
Σw_d	=	sum of thermal equivalents of mechanical work inputs to discharging cycle.

4.1.3 Important CES Process Design Assumptions

Any process design work, even the preliminary design work described here, is a series of design decisions based on the experience and judgment of the designer. So it is impossible to list all the

design criteria used in the process designs described in the sections to follow. The more important ones have been summarized below. Some have been mentioned previously, but bear repeating.

1. The only source of process heat in the charging mode was the receiver. No lower grade process heat was assumed to be available from other STEC subsystems or from outside the STEC plant.

2. The only source of process heat in the discharging mode was the exothermic chemical reaction itself. As in 1., no lower grade process heat was available from other sources.

3. No energy credit was taken for storage system reject heat, even though it might be useful to some other process, or in some "total energy" application.

4. All shaft work required by the storage subsystem was supplied by electric motors; the electricity to run these motors was produced at the efficiency of the STEC turbogenerator for the appropriate storage operating mode. Thus, electricity to supply charging mode shaft work was produced by the turbogenerator with energy directly from the receiver, while electricity for discharge parasitic power was produced by the turbogenerator at an efficiency associated with the storage subsystem discharge temperature.

5. Endothermic and exothermic reactions were assumed to take place at their approximately optimum temperatures. No attempt was made to force the storage subsystem design to produce energy from storage at the same temperature as the storage input, if the efficiency or cost penalties to do so were prohibitive.

6. Process equipment was designed to be used in both the charging and discharging modes whenever possible.

7. All the CES processes were designed to handle a 2,500 MW_t maximum charging rate, defined at storage input, and a maximum discharging rate which was the thermal equivalent of 100 MW_e, at the appropriate turbogenerator efficiency.

8. All the CES processes were designed to provide 2.5 x 10^4 MW_e-hr* storage capacity.

9. Cooling water was assumed to be available to all processes in any quantity needed, and at no charge, at 305 K.

10. All capital cost estimates were developed using the factored cost estimation technique of Guthrie (Reference G3), except where more reliable or more current information was available. All costs were converted to 1978 dollars using the M&S equipment cost index, and chemical costs were obtained from the Chemical Marketing Reporter or vendor quotes.

It is worth noting here that the size of process equipment in CES subsystems designed to meet the requirements of 7. and 8. above was usually extremely large, so large in fact that multiple components (e.g. multiple heat exchangers or compressors) in parallel, all of the largest size available, were often required. The economy of scale was, therefore, used to full advantage for most

---

* 250 hours of storage at 100 MW_e continuous STEC output when running solely on energy from storage.

capital items. After the maximum sizes had been exceeded for most components and multiple units in parallel were required, the total capital cost became a linear function of plant size. All of the process designs discussed below required equipment sizes large enough that the total capital cost was in this linear region.

The merits of some of the above assumptions will be discussed where appropriate as part of the process descriptions which follow.

CES STORAGE SUBSYSTEMS – PRELIMINARY PROCESS DESIGNS

4.2 SO_2/SO_3 ENERGY STORAGE SUBSYSTEM

4.2.1 Flowsheets

Figures 4-1 and 4-2 present schematic flow diagrams for the preliminary process design of the SO_2/SO_3 energy storage subsystem. Tables 4-2 and 4-3 are keys to the two flowsheets, presenting tabulated information on important process variables at various points noted on the flowsheets. Flow rates are given as moles per mole of reactor feed in both tables. It should be noted that the molar flow rate in the reactor feed streams are different in the endothermic and exothermic modes, so the flow rates in Table 4-2 and 4-3 are not referenced to the same basis. Brief discussions of the flowsheets follows.

Endothermic Mode

Liquid SO_3 is taken from storage at 2 bar, is compressed, preheated in HE1, mixed with liquid SO_3 recycle from the distillation column, and partially vaporized in HE2. Vaporization is completed in HE3 with heat from the power cycle working fluid stream, the temperature of the combined vapor streams is raised to 771 K in the recuperator (HE4) and the SO_3 feed stream then enters the reactor. The reactor consists of a series of ten packed catalyst beds separated by 9 interbed heat exchangers. The design is taken with few changes from an earlier SO_2/SO_3 reactor design by RRC (Reference G1). The reader is referred to reference G1 for details of the reactor design. Reactor pressure is between 1.7 and 2.0 bar. The reactant stream and the receiver output stream pass through the reactor train in countercurrent flow, with the receiver stream giving up heat to the reactant stream for enthalpy of reaction and some sensible heating. Reaction proceeds to 90 percent of the equilibrium conversion.* After cooling in the recuperator, the products stream, containing SO_3, SO_2, and O_2, is cooled for compression by the intermediate heat transfer stream and cooling water in HE5 and HE6. The products stream is successively compressed and cooled by three compressors in order to remove most of the sulfur oxides by condensation. The noncondensible O_2, containing some SO_2, is sent to storage at 40 bar. The condensed sulfur oxide streams are fed to a standard (approximately 20 theoretical stages) distillation column, where the SO_2 and SO_3

---

*It was assumed that a suitable high-temperature catalyst can be developed which can operate at the very high temperatures of this storage system and catalyze both the endothermic and exothermic reactions. Efforts to develop such a catalyst are in progress at RRC (S7).

SO₂/SO₃ ENERGY STORAGE SUBSYSTEM
ENDOTHERMIC MODE
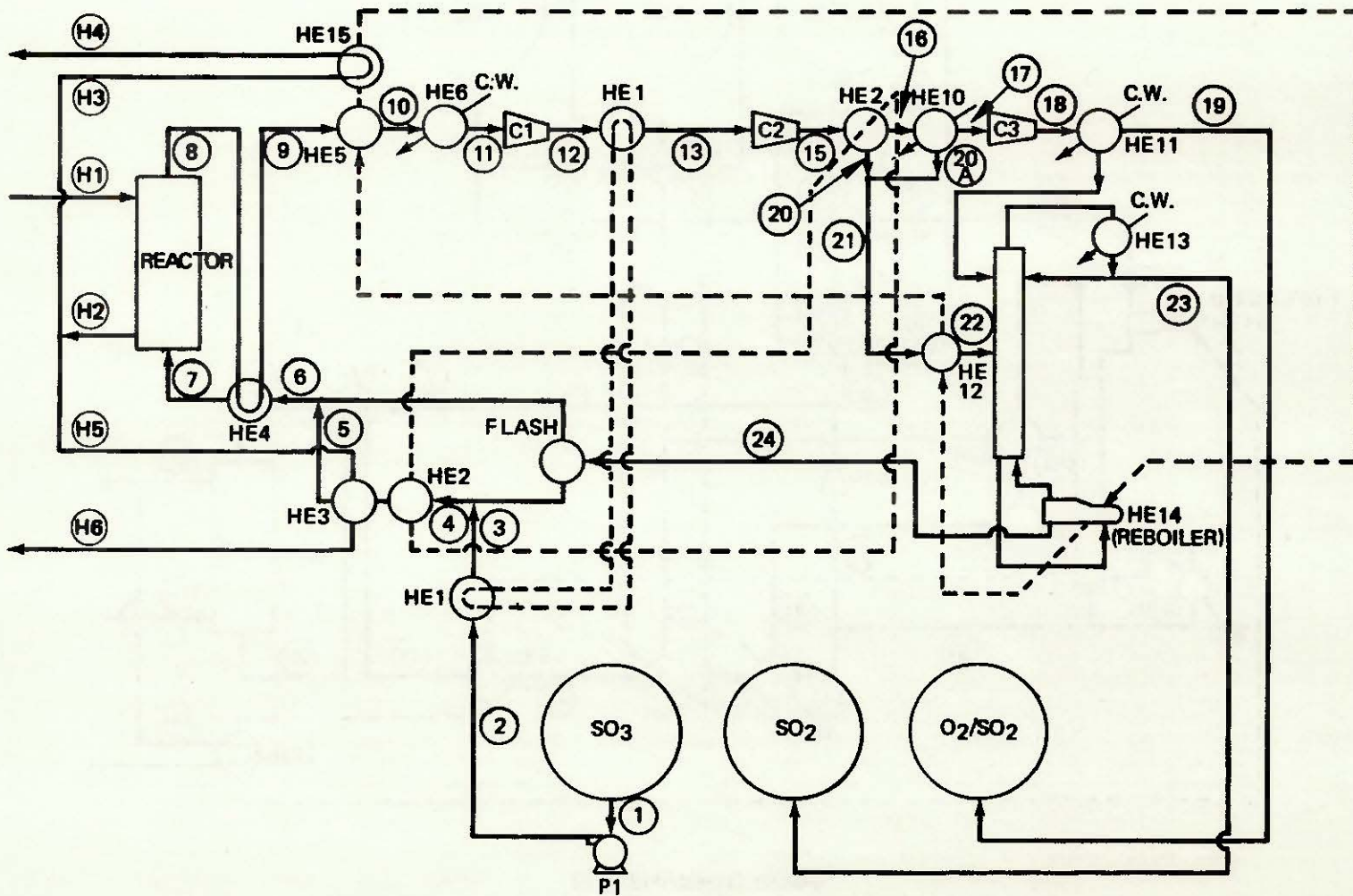
SO2/SO3 ENERGY STORAGE SUBSYSTEM
EXOTHERMIC MODE

Figure 4-2
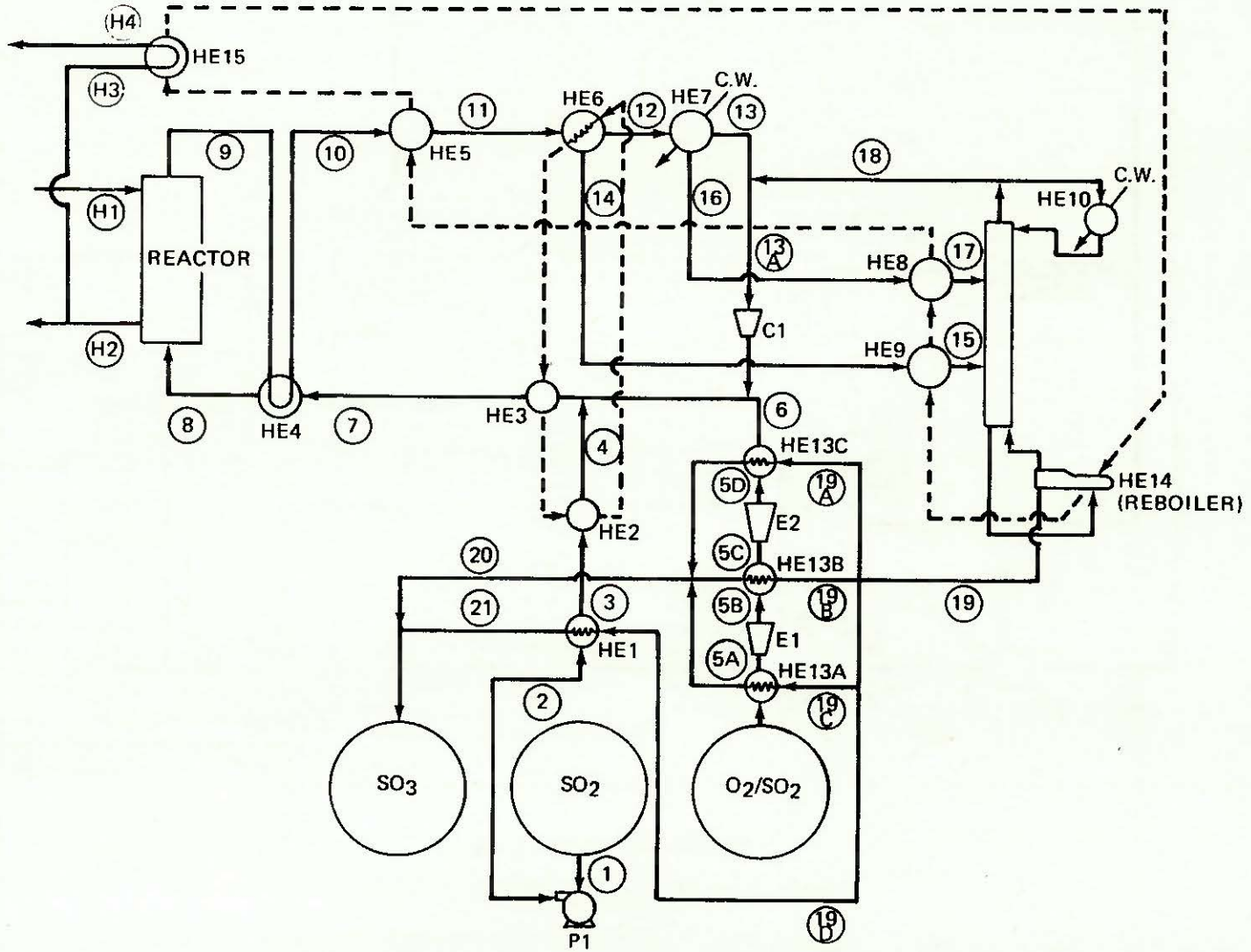
Table 4-2
SO₂/SO₃ ENERGY STORAGE SYSTEM
KEY TO PROCESS FLOW SHEET FOR ENDOTHERMIC MODE

Stream	Flow Rate (Moles/Mole Reactor Feed)	Temp (K)	Pressure (bar)	State	Composition (Mole Fraction)		
					SO_3	SO_2	O_2
1	0.595	298	1.0	ℓ	0.99	0.01	—
2	0.595	298	2.0		0.99	0.01	—
3	0.595	332	2.0		0.99	0.01	—
4	0.924	332	2.0		0.99	0.01	—
5	0.924	332	2.0	ν	0.99	0.01	—
6	1.000	332	2.0		0.99	0.01	—
7	1.000	771	2.0		0.99	0.01	—
8	1.215	960	2.0		0.469	0.354	0.177
9	1.215	546	2.0		0.469	0.354	0.177
10	1.215	375	2.0		0.469	0.354	0.177
11	1.215	311	1.7		0.469	0.354	0.177
12	1.215	394	4.87		0.469	0.354	0.177
13	1.215	356	4.87		0.469	0.354	0.177
15	1.215	451	13.96		0.469	0.354	0.177
16	0.411	342	13.96		0.137	0.339	0.524
17	0.308	311	13.96		0.016	0.286	0.698
18	0.308	394	40.00		0.016	0.286	0.698
19	0.249	311	40.00		0.0014	0.133	0.865
20	0.805	342	13.96	ℓ	0.639	0.361	—
20A	0.102	311	13.96		0.50	0.50	—
21	0.907	~339	13.96		0.623	0.377	—
22	0.907	355	13.96		0.623	0.377	—
23	0.558	330	10.0		0.01	0.99	—
24	0.408	383	10.0		0.99	0.01	—
H1	11.20	1,093	36.2	ν	—	Air	—
H2	11.20	854	35.2		—	Air	—
H3	8.29	854	35.2		—	Air	—
H4	8.29	754	34.7		—	Air	—
H5	2.91	854	35.2		—	Air	—
H6	2.91	754	34.7		—	Air	—

Table 4-3
SO₂/SO₃ ENERGY STORAGE SUBSYSTEM
KEY TO PROCESS FLOW SHEET FOR EXOTHERMIC MODE

Stream	Flow Rate (Moles/Mole Reactor Feed)	Temp (K)	Pressure (bar)	State	Composition (Mole Fraction) SO₃	SO₂	O₂
1	0.495	298	10.0	ℓ	0.01	0.99	—
2	0.495	298	12.6		0.01	0.99	—
3	0.495	340	12.6		0.01	0.99	—
4	0.495	340	12.6	v	0.01	0.99	—
5	0.247	298	40.0		0.001	0.119	0.870
5A	0.247	373	40.0		0.001	0.119	0.870
5B	0.247	306	20.0		0.001	0.119	0.870
5C	0.247	373	20.0		0.001	0.119	0.870
5D	0.247	306	12.6		0.001	0.119	0.870
6	0.247	373	12.6		0.001	0.119	0.870
7	1.000	358	12.6		0.001	0.659	0.330
8	1.000	804	12.6		0.001	0.659	0.330
9	0.750	972	12.6		0.678	0.214	0.107
10	0.750	600	12.6		0.678	0.214	0.107
11	0.750	367	12.6		0.678	0.214	0.107
12	0.443	362	12.6		0.549	0.270	0.181
13	0.100	311	12.6		(0.055)	0.133	0.812
13A	0.250	326	10.0		0.01	0.66	0.33
14	0.307	362	12.6	ℓ	0.866	0.134	—
15	0.307	370	10.0		0.866	0.134	—
16	0.343	311	12.6		0.684	0.316	—
17	0.343	359	10.0		0.684	0.316	—
18	0.150	330	10.0	v	0.010	0.990	—
19	0.500	383	10.0	ℓ	0.99	0.01	—
19A	0.052	383	10.0		0.99	0.01	—
19B	0.052	383	10.0		0.99	0.01	—
19C	0.058	383	10.0		0.99	0.01	—
19D	0.338	383	10.0		0.99	0.01	—
20	0.162	351	10.0		0.99	0.01	—
21	0.338	351	10.0		0.99	0.01	—
H1	9.12	855	35.0	v	—	Air	—
H2	9.12	1,089	38.7		—	Air	—
H3	0.49	1,089	38.7		—	Air	—
H4	0.49	855	35.0		—	Air	—

fractions are separated. The condensed overhead product, predominantly SO_2 with some SO_3 is sent to storage at 10 bar, while the bottom product, primarily SO_3 with some SO_2, is sent to recycle. No attempt was made to estimate the effect of O_2 dissolved in the column feed stream on the distillation column performance. The degree of O_2 dissolution is unknown, and its presence was neglected.

Next to the reactor itself, the reboiler HE14 is the largest energy consumer in the charging mode, and heat input from the power cycle stream (after it leaves the reactor) is required to supplement the heat available from within the process. The use of very high temperature heat to satisfy the relatively low temperature requirements of HE14 and HE3 represents a major source of inefficiency in the present design. Such an arrangement was necessary due to assumption (1) of section 4.1.3.

Exothermic Mode

Liquid SO_2 is taken from storage at 10 bar, compressed to 12.6 bar, preheated and vaporized in HE1 and HE2, and mixed with the O_2 feed stream prior to further heating in HE3. The oxygen stream leaves storage at 40 bar, is expanded through two turboexpanders to 12.6 bar, and mixed with the SO_2/O_2 recycle stream before being mixed with the SO_2 feed stream. Heaters are placed before, between, and after the two O_2 turboexpanders to prevent SO_2 condensation during expansion and to reheat the O_2 stream after expansion from 40 bar. The feed stream is heated to 804 K in the recuperator (HE4) and fed to the reactor. The same reactor is used in both the endothermic and exothermic modes, except that the flow is reversed. The reacting stream flows countercurrent to the working fluid stream in the reactor, releasing energy through exothermic recombination of SO_2 and O_2 for power production and (through HE15) for part of the distillation column reboiler duty.

After cooling in HE4 and HE5, the reaction products stream, containing SO_2, SO_3, and O_2, is partially condensed in HE6, with the heat of condensation serving to preheat parts of the feed stream. The condensates from HE6 and HE7, both containing mixtures of SO_2 and SO_3, are fed to the distillation column for separation. The uncondensed overhead product of the column is combined with the noncondensible gas stream from HE7, recompressed, and recycled. The bottom product, rich in SO_3, is cooled in the O_2 expansion train heaters, reduced in pressure, and stored at approximately 2 bar.

As in the endothermic mode, the distillation column reboiler is a major consumer of relatively high temperature energy, and requires use of some of the reactor output to supplement energy available from recuperation. And as in the endothermic process flowsheet, energy at the reactor output temperature has been used in HE15. A more efficient design for both modes would use heat from one of the first few interbed heat exchangers in the reactor as input to HE15. This energy would be at a lower temperature than in the present design, but still adequate for the purpose, and less entropy would be created. The above improvements in the process design were not made because, in the interest of time, it was necessary to use the results of the earlier reactor design (Reference G1) with as few changes as possible. Use in other parts of the process of the heat from one or more of the interbed heat exchangers would change substantially the temperature and conversion in each of the catalyst beds, and a complete redesign of the reactor would be required.

4.2.2 SO_2/SO_3 Storage Subsystem Efficiency

Table 4-4 sketches the calculation of the charging, discharging, and round-trip efficiencies for the SO_2/SO_3 storage subsystem design just described. The compressor inputs are of course recorded as thermal equivalents of the mechanical work requirements.

The reader will note that the O_2 turboexpander outputs in the exothermic mode are hardly worth the capital investment required to obtain them. These outputs were calculated by assuming that all the O_2 expanded from 40 atm; in fact, as the O_2 storage vessels were emptied, the pressure drop through the turboexpanders would decrease, and their work output would be lower still. The turboexpanders have been included, therefore, for illustration, and it is unlikely they would be included in an actual CES system.

4.2.3 SO_2/SO_3 Storage Subsystem Capital Cost

Table 4-5 presents a capital cost breakdown for a SO_2/SO_3 CES subsystem designed for a 2,500 MW_t maximum charge rate, a 212 MW_t maximum discharge rate, and a 250-hour storage capacity. Although not patterned after any particular location, these parametric values are intended to be representative of the results for the 100 MW_e STEC facilities discussed in Chapter 2 (Tables 2-6 through 2-8).

The most important components which are intended to be used in both the endothermic and exothermic modes are the reactor, distillation column, and recuperator (HE4), and the distillation column condenser (HE13, endothermic mode designation). The endothermic mode charging requirements are size determining for these shared components, so they are listed under the endothermic mode costs. With these inclusions, over 99 percent of the power-related capital costs are attributable to the endothermic mode, and therefore are dependent on the maximum charging rate. Quotation of only one power-related cost, predominantly charging-power related, is therefore justified for the designs in section 4.4.

The cost of the O_2 storage vessels dominates the energy-related capital costs; indeed, it dominates the cost of the entire storage subsystem when 250 hours of storage are required. Special effort was, therefore, made to obtain a realistic cost estimate for these vessels. The numbers in parenthesis next to the O_2 storage vessel cost in Table 4-5 represent the lower and upper bounds in the range of vessel cost estimates. The cost estimate used ($1,144 x 10^6) is the average of the two extremes. The lower of the two extremes was based on actual vendor quotes for U. S. Steel seamless pressure vessels (2 m^3 volume, 167 bar maximum pressure), while the upper limit was based on field fabricated horizontal, cylindrical pressure vessels (78 m^3 volume, 40 bar maximum pressure) designed according to industry standards (P4, p476), and costing approximately $3/kg of steel used. Both estimates assumed carbon steel construction.

In comparing the different O_2 storage vessel costs, and, indeed, in considering all the costs in Table 4-5, the reader should keep in mind that for such a storage subsystem compatible with a 100 MW_e, autonomous STEC system, the quantities, sizes, and costs of process components are so enormous as to make their consideration academic. For instance, approximately 99,000 of the smaller, 2 m^3

Table 4-4
SO$_2$/SO$_3$ STORAGE SUBSYSTEM EFFICIENCY

<u>Endothermic mode</u>

Energy input requirements:

HE3	1.4 kcal/mole reactor feed
Reactor	13.3
HE15	4.1
C1, C2, C3	5.3
	24.1 kcal/mole reactor feed

Energy charged to storage: 9.8 kcal/mole reactor feed

Charging efficiency: $\eta_c = \dfrac{9.8}{24.1} = 0.41$

<u>Exothermic mode</u>

Energy input requirements:

Reactor	11.6 kcal/mole reactor feed
C1	~ 0.01
E1, E2	~ -0.01
	11.6 kcal/mole reactor feed

Energy transferred to power cycle: 9.3 kcal/mole reactor feed

Discharging efficiency: $\eta_d = \dfrac{9.3}{11.6} = 0.80$

<u>Round-trip efficiency:</u> $\eta_{RT} = \eta_c \cdot \eta_d = 0.33$

4-13

Table 4-5
SO_2/SO_3 STORAGE SUBSYSTEM COST BREAKDOWN

Maximum charge rate:	2,500 MW_t
Maximum discharge rate:	212 MW_t
Storage capacity:	250 hrs

Power-Related Equipment	Estimated Cost (10^6 $*$)	Relative Cost (%)
Endothermic Mode		
Reactor	53.6	21.5
Distillation column	26.8	10.7
HE1	5.2	2.1
HE2	24.4	9.8
HE3	6.9	2.8
HE4	47.3	18.9
HE5	2.6	1.0
HE6	3.0	1.2
HE10	5.3	2.1
HE11	2.4	1.0
HE12	1.7	0.7
HE13	12.4	5.0
HE14	4.4	1.8
HE15	2.4	1.0
C1	20.6	8.2
C2	24.1	9.6
C3	5.2	2.1
	248.3	99.5
Exothermic Mode		
HE1 – HE13C	1.4	0.5
	249.7	100.0
Energy-Related Equipment		
O_2 storage	1,144 (647–1640)	90.0
SO_2 storage	49	3.8
SO_3 storage	41	3.2
Chemical inventory	39	3.0
	1,273	100.0

Power related unit cost: $\dfrac{\$249.7 \times 10^6}{2,500 \text{ MW}_t} = \$1 \times 10^5/\text{MW}_t$

Energy related unit cost: $\dfrac{\$1,273 \times 10^6}{(250)(212) \text{ MW}_t\text{-hr}} = \$2.4 \times 10^4/\text{MW}_t\text{-hr}$

*1978 Dollars

storage vessels would be required for the plant under consideration, while the number of the larger, 78 m^3 vessels required would be 12,500! Larger, spherical storage vessels were considered but rejected because welding of the thicker vessel walls was too difficult and expensive. Clearly 99,000, or even 12,000 such vessels is out of the question, so if such a plant were built, the storage system would have to have a lower capacity than the 250 hours used here. For storage times of 20 hours or so, the cheaper seamless pressure vessels may well be more attractive, so that the energy-related unit cost would be cheaper than that shown in the table. Longer storage times would probably require larger, welded O_2 storage vessels, and the energy-related unit cost would increase.

Table 4-5 also presents the calculated unit costs: a power-related unit cost of $\$1 \times 10^5$ MW_t of maximum charging rate, and an energy-related unit cost of $\$2.4 \times 10^4/MW_t$-hr of storage capacity. Comparison of these unit costs with those of Table 2-2 reveals that the more detailed process design described in this section resulted in increased unit costs over those estimated from earlier designs. The round-trip efficiency of the present design also changed, decreasing to 0.33 from the earlier estimate of 0.40. The decrease in efficiency was due primarily to more realistic heat transfer assumptions and to the introduction of a more workable separation scheme in the present design. The increased unit costs of the present design were due in part to the decreased efficiency, but also to more realistic estimates of key component costs. This is especially true of the energy-related unit cost, which is nearly four times the earlier estimate. The increase is due almost entirely to more realistic (increased) O_2 storage vessel cost estimates.

4.2.4 Alternate SO_2/SO_3 Storage Subsystem Designs

Time and resources would not allow much optimization of the preliminary process designs developed under this contract, and the flowsheets presented in this and succeeding sections are not held to be optimum ones. Nevertheless, it is useful to pick out the biggest energy users in the above process design and try to design them differently or eliminate them in order to improve the process efficiency.

The biggest energy users in the above design are the distillation column reboiler and the SO_3 (endothermic mode) and SO_2 (exothermic mode) feed boilers. The size and energy requirements of these components are intrinsically dependent on the conversion within the reactor. At the conversions obtainable in the above design, recycle streams, and, therefore, separation of the sulfur oxides, are necessary in both modes. The heat input to the reboiler is large and is at the boiling point of SO_3, a relatively high temperature with respect to potential waste heat streams within the storage subsystem (but not with respect to heat potentially available from the adjacent power plant). In this case, efficiency of the distillation is very important, and the extra cost of more trays in the column to keep the reflux rates low is worth it. Fortunately, SO_2 and SO_3 have such different volatilities that their separation is relatively easy.

In the endothermic mode, additional relatively high-temperature energy is required to vaporize the purified SO_3 for recycle. Elimination of the distillation column in this mode would require that the SO_3 feed rate be increased, and with it the high quality heat input to HE2 and HE3. Moreover, storage of the partially converted SO_2/SO_3 stream without separation would cause the exothermic

mode reactor conversion to decrease drastically. These effects more than compensate for the potential energy savings from elimination of the distillation column in the endothermic mode.

In the exothermic mode, SO_3 from the distillation column bottoms does not have to be vaporized for recycle, and SO_2 from the column overhead is already vaporized, so the energy "costs" of recycle are less. It should be noted, however, that the overall efficiency of the distillation column in the exothermic mode is lower than in the endothermic mode because the feed composition is further away from being equimolar (Reference H2).

The above discussion indicates that it may be possible to increase the overall storage subsystem efficiency by increasing the conversion per reactor pass, and thus reducing recycle, in both modes. Some changes in conversion can be accomplished by changes in reactor pressure, but the equilibrium conversion is a rather weak function of pressure ($\alpha p^{1/2}$), and the drastic pressure changes required to achieve significant improvements in efficiency cost more (in capital investment, and operating headaches), than they are worth. In the endothermic mode, pressure must be reduced to increase the conversion (at constant temperature). There is not much range between the operating pressure of the present design and subatmospheric pressure where all the problems of vacuum operation obtain. In the exothermic mode, reactor pressure must be so high to achieve substantial improvement in conversion that increased vessel wall thicknesses, compressor costs and compressor power requirements become prohibitive.

Reaction temperature is a more effective means of controlling equilibrium conversion than is pressure. From a thermodynamic point-of-view, higher temperature favors dissociation*, while lower temperature favors the association reaction. Ideally then, for highest conversions the endothermic reactor should be operated at the highest temperature possible, and the exothermic reactor at the lowest. Of course, there may be kinetic limitations to this "ideal" arrangement, especially at the low exothermic temperature favored by equilibrium considerations only. Perhaps more importantly, the availability difference between a higher endothermic temperature and a lower exothermic temperature tends to offset the gains in storage system efficiency attributable to that difference.

The primary design for the SO_2/SO_3 storage system described above had identical endothermic and exothermic reaction temperatures primarily because substantially different receiver and storage output temperatures dictate different power cycles for energy direct from the receiver and energy from storage. This is especially true for the open-Brayton cycle specified here, since such cycles are not suitable for "derated" operation. The capital investment for a second, storage-dedicated turbogenerator would be substantial. In addition, the general ground rules for the present study were that the storage subsystem be a "black box" within the STEC system, as in Figure 2-1, which would accept and produce energy at the same temperature; no secondary power cycle for storage output was envisioned.

---

* This is true of all the reactions considered in this section, except the C/CS_2 reaction.

In order to determine the advantage, if any, of wider separation between endothermic and exothermic reactor temperatures, two alternate storage system design cases were examined. Both cases were designed for heat input from an advanced receiver at 1,310 K (the maximum considered for the entire program) and storage system output to a storage-dedicated power cycle (most likely a steam-Rankine cycle) at 680 K. Only charging and discharging efficiencies were examined; no cost estimates for the alternate cases were made.

Case 1 considered only the effect of the different storage input and output temperatures. Except for these different temperatures, the design was the same as above. Conversion-per-pass through the exothermic reactor was quite high at the lower storage output temperature, so the distillation was eliminated from the exothermic mode in Case 2. Reactants were passed through the reactor once, and after condensation (and attendant separation of noncondensible O_2) the sulfur oxide stream was sent directly to storage. Conversion in the reactor in both cases was assumed to be 90 percent of the equilibrium conversion. Table 4-6 presents key temperatures and pressures for the two alternate cases, while Table 4-7 presents efficiencies for the original design and the two alternate cases.

Table 4-6
ALTERNATE SO_2/SO_3 ENERGY STORAGE SUBSYSTEM DESIGNS

	Endothermic Mode	Exothermic Mode
Receiver output temperature	1,310 K	
Storage output temperature		735 K
Reactor input temperature	856 K	526 K
Reactor output temperature	1,154 K	745 K
Reaction Pressure	2 bar	12.6 bar

Table 4-7
RESULTS OF SO_2/SO_3 ALTERNATE DESIGN STUDIES

	η_c	η_d	η_{RT}	η_{RT} (corrected)
Original design	0.41	0.80	0.33	0.33
Alternate case 1	0.53	0.83	0.44	0.34
Alternate case 2	0.46	0.83	0.39	0.30

To facilitate comparison of the alternate design cases with the original design, the decreased availability of energy from storage in the alternate designs had to be accounted for. This was done by multiplying the alternate case round-trip efficiencies by the ratio of the Carnot efficiencies of two heat engines, one operating between 1,310 K and 298 K, and the other between 735 K and 298 K. The corrected values of η_{RT} are given in the last column of Table 4-7.

As expected, the increased conversion per reactor pass in the alternate cases caused an increase in both the charging and discharging efficiencies. The greater increase was in the charging efficiency because recycle of SO_3 in the endothermic mode requires more energy input than does recycle of SO_2 and O_2 in the exothermic mode. These increases in efficiency are only apparent, however, for when the availability correction is applied, the differences in η_{RT} of the three cases are quite small, and removal of the distillation column in the exothermic mode actually caused the round-trip efficiency to decrease slightly.

Elimination of the distillation column (from the Case 2 system) in the exothermic mode had a greater effect on the charging efficiency than on the discharging efficiency. In the exothermic mode, the energy savings from elimination of the reboiler duty is almost completely offset by the increased SO_2 preheating and vaporization required. Elimination of the distillation column in the exothermic mode caused the feed to the endothermic reactor to be lower in SO_3 mole fraction, so that conversion per pass, and thus charging efficiency, was lowered.

It should be noted here that the discharging efficiency in Case 1, above, was calculated using a rather optimistic distillation column design (approximately 5 percent efficiency). More pessimistic designs could put the discharge efficiency as low as 53 percent, and thus the round-trip efficiency as low as 28 percent. Deletion of the distillation column from the Case 1 design would then certainly be called for, but the round-trip efficiency of Case 2 would still be less than the baseline case. As noted above, conversion in the baseline exothermic mode is such that deletion of the column from the baseline exothermic design would decrease η_{RT}.

A key (conservative) assumption in the above test case designs was that of 90 percent of equilibrium conversion in both the endothermic and exothermic reactions; present industrial practice indicates that greater conversions may be possible, especially in the exothermic mode. Near complete conversion in the exothermic mode would increase the discharging efficiency of Case 2 to well above 90 percent.

4.2.5   Conclusions of SO_2/SO_3 Storage System Design Study

While the baseline design described in section 4.2.1 does not represent a completely optimized system, brief examination of the most promising design changes resulted in no significant improvements in system efficiency. Improvements in capital cost may result from these or similar design changes, but it appears that within the constraints outlined in section 4.1.3, significant improvements in round-trip efficiency are unlikely.

As far as improved efficiency is concerned, the key constraint is that which limits integration of the storage system with heat sources and sinks other than the (solar) receiver, the highest temperature input to the turbomachinery, and necessary cooling water streams. Under this constraint, the most efficient designs will generally be those which accept heat from the receiver at the highest process temperatures possible, and reject heat to the atmosphere (cooling water, etc.) at the lowest process temperatures possible. Thus, great inefficiency (entropy production) occurs in HE15 and HE3 of the endothermic mode, and HE15 of the exothermic mode, in which the temperature differences between streams are very large.

Moreover, in the present design, great care has been taken to recuperate heat within the process at temperature differences which are as low as possible. The process design which resulted is somewhat more contorted than it might have been for a standard industrial design, and equipment costs (particularly heat exchangers) somewhat higher.

Significant improvements in the efficiency of chemical energy storage systems over those calculated above will require removal of the above input/output constraints, allowing heat sources and/or sinks which can be integrated with the storage system. Such sinks might make profitable use of storage system heat rejected at temperatures higher than minimum. For example:

1. Heat from condensing SO_2 in HE10 might supply an appropriately sized district heating system. The potential benefits both to the storage facility and the heating system might make operation of the distillation at higher pressure (and, thus, higher HE10 temperature) economical. Such a process design change would, to a greater or lesser extent, affect all other parts of the design, so that the process flowsheet and attendant specifications might look significantly different.

2. Another example — H_2O condensation in $CaO/Ca(OH)_2$ system presented in the next section — represents an extremely large energy credit. Such a potential energy use might make it attractive to compress the H_2O vapor in order to condense it at a higher, more useful temperature. Or, the condenser HE13 could simply be used as a preheater for the main heating unit (maybe boiler) of the heating system.

Heat sources other than the receiver would, of course, be useful within any of the CES systems. There are many uses for low-grade process heat within these storage systems: uses to which it is very inefficient to commit high-grade energy from the receiver.

1. For example, low-grade waste heat from another chemical plant might provide some or all of the reboiler duty, or SO_3 heat of vaporization in HE2 and HE3 (endothermic mode), or SO_2 heat of vaporization in HE3 in the exothermic mode, depending on the temperature of the source. These heat exchangers consume a large amount of low-grade heat.

2. Uses for such low-grade process heat in the $CaO/Ca(OH)_2$ system are probably confined to the preheating and vaporization of H_2O in the exothermic mode because of the requirements for direct contact heating of the solid reaction constituents. Nonetheless, elimination of part or all of the HE2 and HE3 duty in the exothermic mode would greatly increase the discharging efficiency.

3. Heat sources within the STEC facility itself, such as extraction streams from the turbines in the power plant, could provide low-grade process heat as well. Determining that optimum design for integration of turbine extraction streams with the CES storage subsystem would require involved systems analysis which is beyond the scope of this study. In addition to the large number of combinations of extraction streams and to the difficulties of formulating an objective function, such an analysis would be complicated greatly by the independently varying storage charge rate and direct power production rate.

Finally, a combination of a sensible or latent heat storage system with a chemical energy storage system may prove more efficient for intermediate and long-term storage applications than either one separately. From a systems point-of-view, the sensible system could provide short term, highly efficient storage, while the CES system could provide intermediate and long-term storage. Moreover, part of the sensible system could be used as a heat sink/source for the chemical energy storage system, thereby increasing the efficiency of the chemical part of the combination. Such hybrid storage systems definitely deserve further study.

The possibilities, briefly highlighted above, for integration of a CES system with other heat sources and sinks are obviously far too numerous to be considered in detail in this study. Nonetheless, an important conclusion of the present study is that such integration is imperative if CES is to be economically competitive with other types of energy storage.

4.3 CaO/Ca(OH)$_2$ ENERGY STORAGE SUBSYSTEM

The CaO/Ca(OH)$_2$ reaction is one of the six reactions in Table 4-1 identified as solid/gas, noncatalytic. The CaO/Ca(OH)$_2$ reaction has been chosen as representative of this class of reactions and by way of introduction to the reaction group, the process design for this reaction, in particular the reactor design, will be discussed in some detail in section 4.3.2. While temperatures, pressures, and efficiencies may vary among the storage systems based on the solid/gas, noncatalytic reactions, much of the discussion presented below for the CaO/Ca(OH)$_2$ system is pertinent to all of the reactions in this group.

4.3.1 Process Flowsheets

The presence of a solid reaction constituent in each solid/gas, noncatalytic case profoundly affects the reactor design and, thus, the entire process design. Before discussing the reactor design in detail however, it is helpful to become acquainted with the general process design. Brief discussions of the endothermic and exothermic process flowsheets are therefore presented below. The flowsheets are presented in Figures 4-3 and 4-4, with keys to the two flowsheets presented in Tables 4-8 and 4-9, respectively. Brief discussions of the flowsheets follow.

Endothermic Mode

The solids flow may be picked up with the solid Ca(OH)$_2$ (approximately 10 mole percent CaO) in storage at slightly above atmospheric pressure. After mechanical transportation to the Ca(OH)$_2$ feed

CaO/Ca(OH)$_2$ ENERGY STORAGE SYSTEM
ENDOTHERMIC MODE
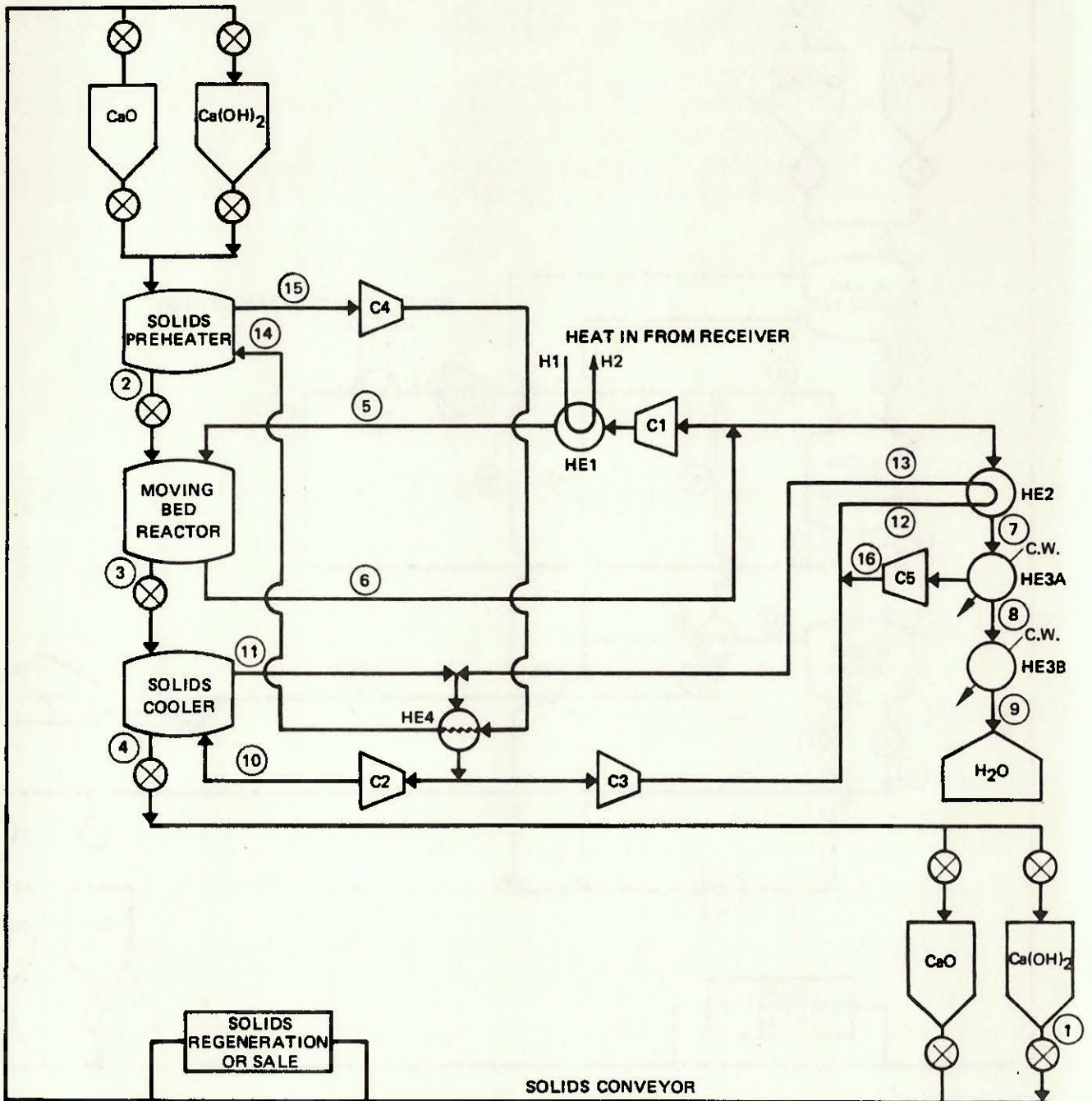
CaO/Ca(OH)$_2$ ENERGY STORAGE SYSTEM
EXOTHERMIC MODE
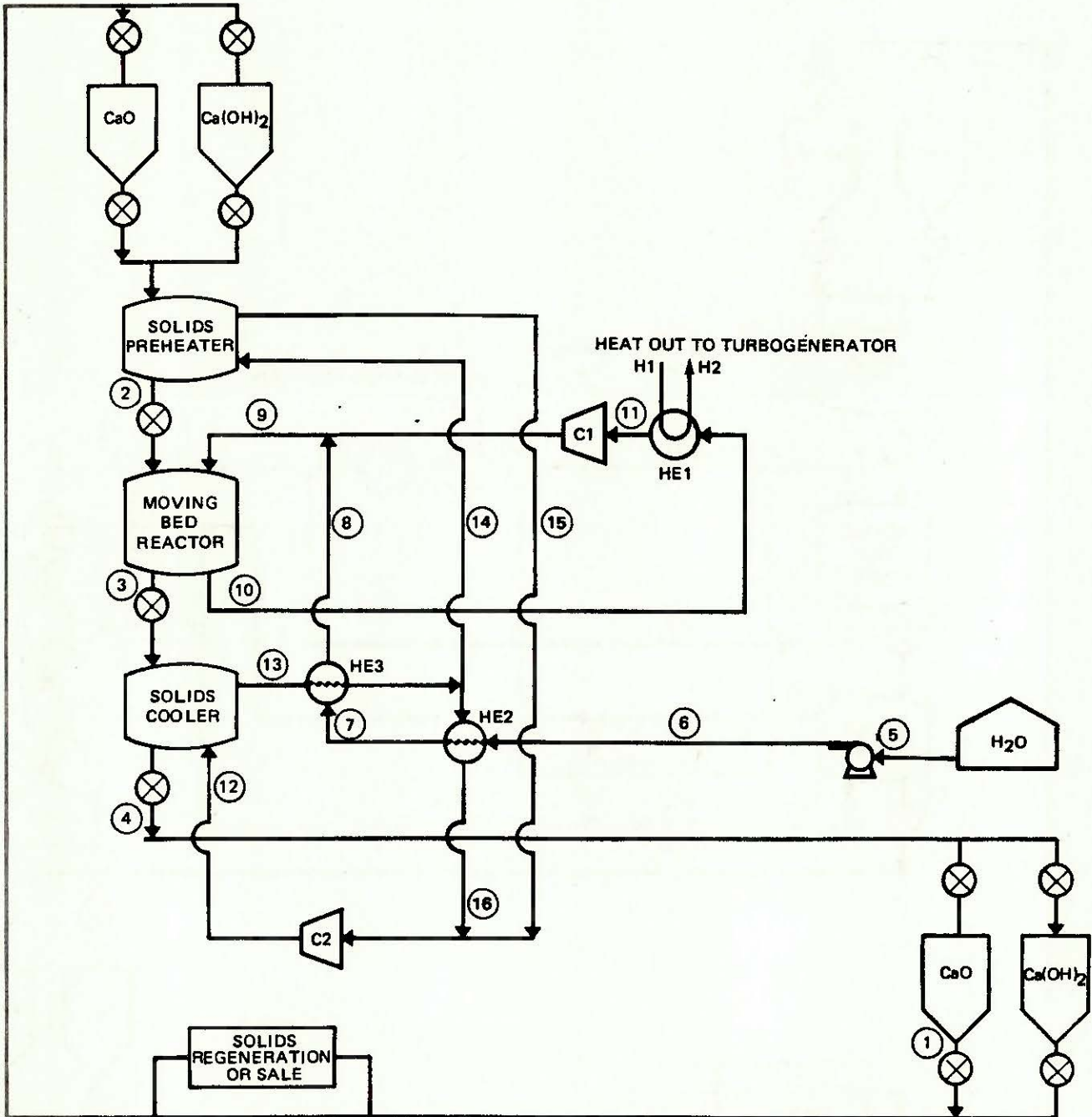
Table 4-8
CaO/Ca(OH)$_2$ ENERGY STORAGE SYSTEM
KEY TO ENDOTHERMIC MODE PROCESS FLOWSHEET

Stream	Flow Rate (Moles/Mole Solid Reactor Feed)	Temp. (K)	Pressure (bar)	Composition (mole fraction)			
				Solid Phase		Fluid Phase	
				Ca(OH)$_2$	CaO	H$_2$O	N$_2$
1	1.00 (s)	298	1.1	0.9	0.1	1.0	Trace
2	1.00 (s)	725	2.0	0.9	0.1	1.0	Trace
3	1.00 (s)	833	1.8	0.1	0.9	1.0	Trace
4	1.00 (s)	400	1.9	0.1	0.9	Trace	1.0
5	5.82 (v)	1,210	2.0	—	—	1.0	Trace
6	6.62 (v)	833	1.8	—	—	1.0	Trace
7	0.80 (v)	398	1.8	—	—	1.0	Trace
8	0.80 (l)	398	1.8	—	—	1.0	—
9	0.80 (l)	311	1.8	—	—	1.0	—
10	1.85 (v)	389	2.0	—	—	Trace	1.0
11	1.85 (v)	823	1.8	—	—	Trace	1.0
12	0.97 (v)	389	2.0	—	—	Trace	1.0
13	0.97 (v)	823	1.8	—	—	Trace	1.0
14	2.35 (v)	813	2.0	—	—	1.0	Trace
15	2.35 (v)	320	1.8	—	—	1.0	Trace
16	—	398	1.8	—	—	Trace	1.0
H1	7.41 (v)	1,310	36.2	—	—	—	Air
H2	7.41 (v)	994	34.6	—	—	—	Air

Table 4-9
CaO/Ca(OH)$_2$ ENERGY STORAGE SYSTEM
KEY TO EXOTHERMIC MODE PROCESS FLOWSHEET

Stream	Flow Rate (Moles/Mole Solid Reactor Feed)	Temp. (K)	Pressure (bar)	Composition (mole fraction)			
				Solid Phase		Fluid Phase	
				Ca(OH)$_2$	CaO	H$_2$O	N$_2$
1	1.00 (s)	298	1.1	0.10	0.90	Trace	1.0
2	1.00 (s)	670	8.5	0.10	0.90	1.0	Trace
3	1.00 (s)	970	18.0	0.90	0.10	1.0	Trace
4	1.00 (s)	410	1.1	0.90	0.10	1.0	Trace
5	0.80 (l)	298	1.0	—	—	1.0	—
6	0.80 (l)	298	20.5	—	—	1.0	—
7	0.80 (l)	486	20.2	—	—	1.0	—
8	0.80 (v)	613	20.0	—	—	1.0	—
9	4.27 (v)	613	20.0	—	—	1.0	Trace
10	3.47 (v)	970	19.0	—	—	1.0	Trace
11	3.47 (v)	600	18.0	—	—	1.0	Trace
12	2.50 (v)	331	10.5	—	—	1.0	Trace
13	2.50 (v)	960	9.5	—	—	1.0	Trace
14	1.60 (v)	680	8.5	—	—	1.0	Trace
15	1.60 (v)	320	8.0	—	—	1.0	Trace
16	0.90 (v)	320	8.0	—	—	1.0	Trace
H1	1.02 (l)	600	164.0	—	—	1.0	—
H2	1.02 (v)	970	164.0	—	—	1.0	—

hopper, the Ca(OH)$_2$ feed is heated in the solids preheater by direct contact with a water vapor, intermediate heat transfer loop. This intermediate steam loop is heated by indirect contact with cooling solids leaving the reactor. The Ca(OH)$_2$ passes through rotary airlock feeders to the moving bed reactor train (section 4.3.2), where it is dehydrated, with the heat of reaction coming from sensible heat of a cooling pure H$_2$O carrier gas stream. Contact between the reacting solids and the carrier-gas stream is direct, and the pressure within the reactor is approximately 2 bar. The hot CaO (approximately 10 mole percent Ca(OH)$_2$ leaving the reactor train is cooled by direct contact with a nitrogen* (or possibly argon) stream at approximately 1.9 bar, and sent to storage bins at slightly above atmospheric pressure. Part of the carrier gas stream leaving the reactor is cooled, condensed, and sent to storage. The remainder of the carrier gas stream is compressed, reheated in HE1 with energy from the receiver, and sent back to the moving bed reactors.

Nitrogen leaving the solids cooler is combined with a similar nitrogen stream leaving the H$_2$O cooler, HE2, and passed through HE4 where it heats by indirect contact the water vapor stream from the solids preheater. Small amounts of N$_2$ which manage to leak across the airlock feeders into the H$_2$O carrier gas loop are recovered as noncondensibles from the H$_2$O condenser, HE3A, and returned to the N$_2$ loop.

Exothermic Mode

The solids flow may be picked up starting with the solid CaO (approximately 10-mole percent Ca(OH)$_2$) in storage. After mechanical transportation to the feed hopper, the CaO is fed to the solids preheater, where it is heated with water vapor which has been directly contacted with cooling Ca(OH)$_2$ in the solids cooler. The CaO passes through airlock feeders to the moving bed reactor train (same as in endothermic mode) where it is hydrated by the pure steam gas stream at approximately 20 bar. The hot Ca(OH)$_2$ which leaves the reactor is cooled by direct contact with steam at approximately 10 bar and sent to storage at slightly above atmospheric pressure.

Water from storage is pressurized, preheated in HE2, vaporized in HE3, and mixed with the steam recycle stream for feed to the reactor. Upon leaving the reactor, excess or carrier steam, now at 970 K discharges energy to the turbomachinery in HE1, and is recompressed before mixing with the steam feed stream.

4.3.2   CaO/Ca(OH)$_2$ Storage Subsystem Efficiency

Table 4-10 sketches the calculation of the charging, discharging, and round-trip efficiencies for the CaO/Ca(OH)$_2$ storage subsystem described above. Values of energy are given in units of kcal per mole of *solid* reactor feed; as in the SO$_2$/SO$_3$ design, the endothermic and exothermic values are normalized to different reactor feed rates.

Unlike the baseline SO$_2$/SO$_3$ CES process design, the CaO/Ca(OH)$_2$ system input and output temperatures are different. The storage system accepts energy from the receiver at 1,310 K, but sends energy to the turbogenerator at only 870 K. The round-trip efficiency of 0.35, calculated

---

*Inert gas is used instead of air in order to avoid possible formation of calcium carbonate.

Table 4-10
CaO/Ca(OH)$_2$ STORAGE SUBSYSTEM EFFICIENCY

Endothermic Mode

Energy input requirements:

HE1	18.4	kcal/mole solid reactor feed
C1	8.4	
C2	1.1	
C3	0.6	
C4	1.3	
	29.8	kcal/mole solid reactor feed

Energy charged to storage: 19.0 kcal/mole solid reactor feed

Charging efficiency: $\eta_c = \dfrac{19.0}{29.8} = 0.64$

Exothermic Mode

Energy input requirements:

Reactor	18.9	kcal/mole solid reactor feed
C1	1.3	
C2	1.3	
	21.5	kcal/mole solid reactor feed

Energy transferred to power cycle: 11.8

Discharging efficiency: $\eta_d = \dfrac{11.8}{21.5} = 0.55$

Round-trip efficiency: $\eta_{RT} = \eta_c \cdot \eta_d = 0.35$

Efficiency correction factor: 0.85

Corrected round-trip efficiency: 0.30

without regard to availability loss through storage, has therefore been corrected by a factor which is the ratio of the Carnot efficiencies of heat engines operating between 870 K and 298 K, and between 1,310 K and 298 K, respectively. This corrected efficiency is presented to facilitate comparison with the SO_2/SO_3 efficiency and with those given in the remainder of this section. For studies of the $CaO/Ca(OH)_2$, or other, storage system using program STORAGE, the uncorrected efficiencies would be used to characterize the storage model.

4.3.3 CaO/Ca(OH)$_2$ Storage Subsystem Capital Cost

Table 4-11 presents a breakdown of the capital cost estimate for a $CaO/Ca(OH)_2$ subsystem designed to meet the same input/output rates and storage capacity as was the SO_2/SO_3 system broken down in paragraph 4.2.3.

The reactor, solids preheater, solids cooler, and HE1 were assumed to be usable in both the endothermic and exothermic modes. Since the charging rate requirements are size determining for these shared components, the components are listed under endothermic mode costs. As in the case of the SO_2/SO_3 cost breakdown, almost all of the power-related capital costs (over 97 percent) were attributable to the endothermic mode, and the quotation of only one power-related unit cost is sufficient.

The largest capital cost items in the $CaO/Ca(OH)_2$ design were a direct result of the need to move large amounts of gas for heat transfer purposes. The main compressor, C1 and heat exchanger HE1 in the endothermic mode, accounted for more than a third of the total power-related capital costs. Still greater, was the cost of the N_2/steam heat exchanger, HE4, which alone accounted for nearly 40 percent of the power-related costs. This heat exchanger was so large and costly because of its very large duty and because of the relatively low overall heat transfer coefficient associated with gas/gas, indirect heat transfer.

The three capital cost items described above stand as testimony to the major liability of the solid/gas noncatalytic reactions in energy storage applications: the difficulty of transferring heat into and out of the solid reactants, compounded by the inefficiency of gas/gas heat exchange.

4.3.4 Process Choices for Solid/Gas, Noncatalytic Reactions

The presence of a solid reactant in each of the six reactions in the first group of Table 4-1 presents an interesting reactor design problem. The development of the reactor design proposed here can best be summarized by three design questions:

1. Should the process be continuous or batch with respect to the solid reactant?
2. Should convection within the reactor be forced or free?
3. Should heat transfer to and from the reacting solids be direct or indirect?

The answers to these questions helped determine the reactor design for the solid/gas, noncatalytic reactions, and the choices for the specific case of the $CaO/Ca(OH)_2$ reaction are discussed briefly below.

Table 4-11

CaO/Ca(OH)$_2$ STORAGE SUBSYSTEM COST BREAKDOWN

Maximum charge rate: 2,500 MW$_t$
Maximum discharge rate: 256 MW$_t$
Storage capacity: 250 hours

Power Related Equipment Endothermic Mode	Estimated Cost (10^6 $*$)	Relative Cost (%)
Reactor	4.5	0.9
Solids preheater and cooler	4.4	0.8
HE1	37.2	7.1
HE2	61.7	11.9
HE3A	9.2	1.8
HE3B	2.6	0.5
HE4	194.0	37.4
C1	140.0	27.0
C2	20.3	3.9
C3	10.0	1.8
C4	20.1	3.9
Solids transport system	1.9	0.4
Feed hoppers	0.1	–
	506.0	97.4
Exothermic Mode		
HE1	4.6	0.9
HE2	0.6	0.1
HE3	0.5	0.1
C1	3.5	0.7
C2	4.1	0.8
	13.3	2.6
	519.3	100.0
Energy Related Equipment		
H$_2$O storage	3.8	5.8
Solids storage	49.5	75.5
Chemical inventory	12.3	18.7
	65.6	100.0

Power related unit cost: $\dfrac{\$519.3 \times 10^6}{2,500 \text{ MW}_t} = \$2.0 \times 10^5/\text{MW}_t$

Energy related unit cost: $\dfrac{\$65.6 \times 10^6}{(250 \times 256) \text{ MW}_t\text{-hr}} = \$1.0 \times 10^5/\text{MW}_t\text{-hr}$

* 1978 dollars

1. Batch or continuous? Choice: continuous.

   A batch process in this case is one in which the solid reactant is stored and reacted in the same vessel (as shown schematically in Figure 3-3). Continuous processing involves transportation of the solids from storage to a separate vessel for reaction, followed by transportation of reacted solids back to storage. The volume of the reactor/storage vessel in a batch system then varies directly with the storage capacity; doubling the capacity of the energy storage subsystem from, say, 10 to 20 hours will cause the required reactor volume to double. In the case of continuous processing, the reactor volume is independent* of storage capacity and depends on the maximum charging (or discharging) rate. The high temperatures and (in the exothermic mode) higher pressures required for reaction cause the reactor to be a more costly component than the solids storage vessels, so that minimization of reactor size is economically desirable.

   The contract under which this study was chartered required design of CES subsystems with capacities ranging from 6 hours to that which would give a STEC facility autonomous, or baseload capability. It may be that batch systems would be more economical than continuous ones for storage systems at the lower end of this range. It is easily shown, however, that batch reactor/storage vessels become prohibitively large for storage facilities with intermediate and long storage times, so that continuous systems are the clear choice for the one design type which is workable over the entire range of storage capacities required.

   In addition to capital cost advantages, continuous processes offer the advantage of continuous regeneration or replacement of the solid reactants, should this be necessary. Batch processes, on the other hand, must be shut down to change the solids charge. Continuous reactors also offer the design and operating convenience of a global reaction rate which is essentially constant, whereas the global reaction rate varies with the state of charge in batch reactors.

   In view of their significant advantages, as outlined above, the storage subsystems based on all of the solid gas, noncatalytic reactions considered here were designed with continuous reactors.

2. Free or forced convection? Choice: forced convection.

   In a "passive" reactor design, the only driving force causing convection of the gaseous phase in the solids bed would be pressure drops within the bed caused by evolution or consumption of the gaseous reactant (again, see Figure 3-3). Forced convection, driven by compressors, of the gas phase through the solids bed results in very much better heat and mass transfer coefficients within the bed. Preliminary analysis indicated that the improved heat and mass transfer rates were worth the higher power consumption and

---

*This is true only for the simple design argument presented here. It should be noted, however, that the results of Chapter 2 indicate that, for a given solar fraction, the storage capacity and maximum charging rate are not independent: an increase in the storage capacity will generally require a corresponding increase in the maximum charging rate.

added capital costs of the necessary compressors. Indeed, the poor heat and mass transfer coefficients in passive systems would make such systems completely unworkable in view of the high storage charging rates required in STEC systems (section 2.4.1).

3. Direct or indirect heat transfer? Choice: direct heat transfer.

Systems with these two types of heat transfer are represented schematically in Figure 4-5 (both cases shown have forced convection). "Indirect" heat transfer involves transfer of heat across a tube wall between a fluid stream and the solids bed, and mass transfer occurs between the solids and a second gas stream. In "direct" designs, the heat-carrying gas stream is in direct, intimate contact with the solids bed, and heat is transferred into the gas stream in separate heat exchangers. For batch systems or continuous systems with slowly moving solids beds (i.e. nonfluidized), the overall heat transfer coefficients will be highest with direct heat transfer. Moreover, in indirect cases (again, nonfluidized), the tube diameters necessary to give adequate heat transfer coefficients between the tube wall and the solids, are so small as to make maintenance difficult. In batch reactors, agglomeration, sintering, or other degeneration of solid particles might make solids replacement necessary. Such replacement would be very difficult and time consuming with the small tube sizes mentioned above. Continuous reactors with indirect heat transfer, requiring movement of solids downward through the small tube, would present near insurmountable design problems.

The primary disadvantage of direct contact heat transfer is the higher fluid recycle rates it requires. This problem will be discussed in more detail in section 4.3.5. In spite of this disadvantage, and in view of the objections to fluidized bed designs discussed below, direct heat transfer designs have been chosen for all the solid/gas, noncatalytic reactions considered here.

Figure 4-6 presents a simplified summary of the storage process design options considered for the solid/gas, noncatalytic designs. The one reactor type not mentioned until now, the fluidized bed, is shown at right. Fluidized bed reactors offer several tempting advantages. Due to agitation of the solids bed, the heat transfer coefficients between the tube walls and the solids are quite high. Moreover, fluidized bed reactors are easily designed for continous processing. Finally, compressor power requirements of a fluidized bed system were estimated to be considerably lower than those for a moving bed type system.

Fluidized bed systems have one disadvantage which precluded their use in the present design study, however. The solids agitation which results in such high bed heat transfer coefficients would most probably cause unacceptable solids breakup and formation of fines. Such degradation, if appreciable, would render a reaction essentially irreversible from an operational point of view. The repeated temperature cycling between extreme limits, as well as the density changes associated with repeated reaction cycles, would undoubtedly cause some solids breakup in any reactor design. Indeed, some workers have observed such solids degradation in bench-scale studies (Reference B7, p. 211). Although the true extent of such degradation problems is unknown, it was decided that the potential advantages of fluidized bed reactors did not outweigh the potentially crippling disadvantages. A brief discussion of an alternate $CaO/Ca(OH)_2$ energy storage subsystem based on a fluidized bed reactor is presented in section 4.3.12.

SCHEMATIC COMPARISON OF DIRECT AND INDIRECT HEAT TRANSFER

Figure 4-5

HEAT IN OR OUT

FLUID
STORAGE

DIRECT HEAT TRANSFER

HEAT IN
OR OUT

FLUID
STORAGE
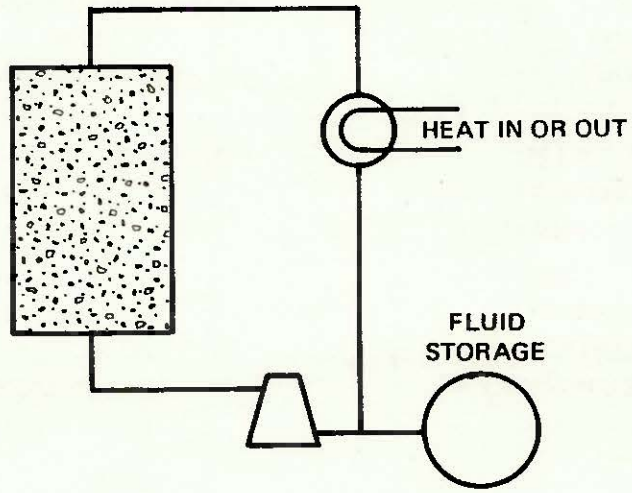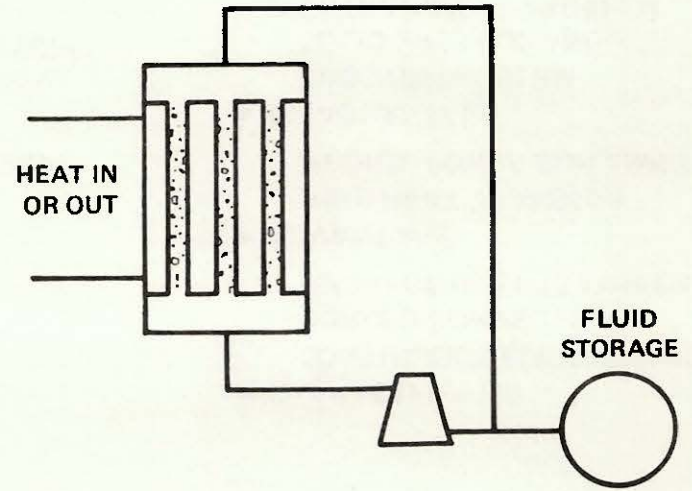
INDIRECT HEAT TRANSFER

SUMMARY OF STORAGE PROCESS DESIGN OPTIONS
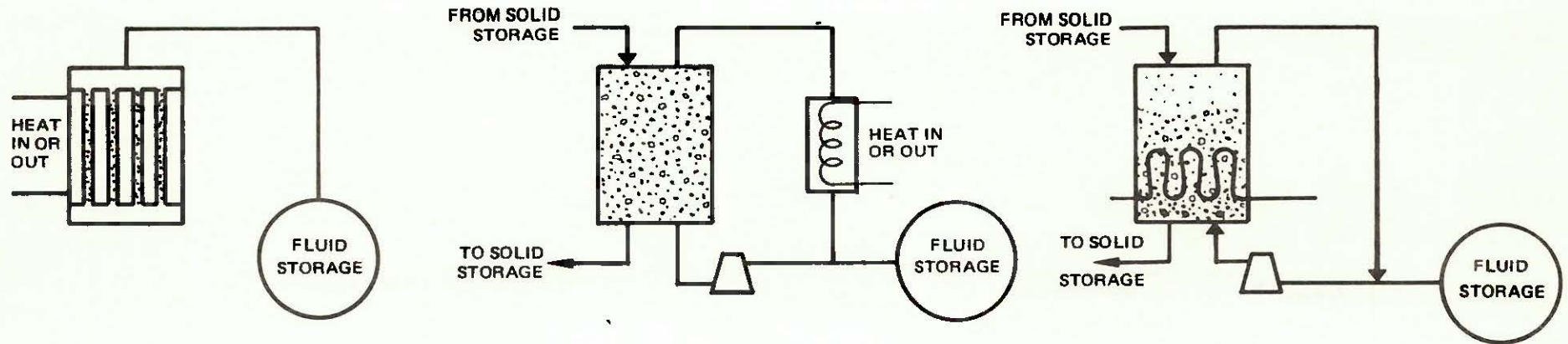
- CHARACTERISTIC –
  BATCH
  FREE CONVECTION
  INDIRECT HEAT TRANSFER

- ADVANTAGE –
  SIMPLE DESIGN
  LOW POWER CONSUMPTION

- DISADVANTAGE –
  MAINTENANCE PROBLEM
  LOW HEAT TRANSFER
  SIZE DEPENDENT ON STORAGE
  CAPACITY

- CHARACTERISTIC –
  MOVING BED
  FORCED CONVECTION
  DIRECT HEAT TRANSFER

- ADVANTAGE –
  LOW MAINTENANCE
  RELATIVELY SIMPLE DESIGN

- DISADVANTAGE
  HIGH POWER CONSUMPTION
  DUE TO HIGH FLUID RECYCLE
  RATE

- CHARACTERISTIC –
  CONTINUOUS FLUIDIZED BED
  FORCED CONVECTION
  INDIRECT HEAT TRANSFER

- ADVANTAGE –
  HIGH HEAT TRANSFER
  MEDIUM POWER CONSUMPTION

- DISADVANTAGE
  EROSION PROBLEM
  SOLID BREAKUP AND
  ENTRAINMENT PROBLEM
  COMPLICATED DESIGN

Figure 4-6

4.3.5   Reactor Design

The reactor design chosen for the solid/gas, noncatalytic reactions is represented by the middle schematic in Figure 4-6. The designs are continuous (moving bed), and there is direct heat transfer between the reacting solids and the carrier gas, which is forced through the solids bed and a primary heat exchanger by compression. The reactor design chosen to minimize the pressure drop through the reactor, while keeping solids residence time reasonable, is a moving bed type with radial flow in the gas phase (Figure 4-7). To further reduce pressure drop, the reactor was divided into several parts, through which the solids flows in series and the gas phase flows in parallel (Figure 4-8). Preliminary analysis of the $CaO/Ca(OH)_2$ system indicated that four modules in the reactor train resulted in an acceptable pressure drop. Rotary airlock feeders between the modules were included to minimize mixing of parallel gas streams between beds.

Kinetic data on the $CaO/Ca(OH)_2$ reaction were the best of any of the noncatalytic reactions. Nonetheless, these data did not apply for the temperatures, compositions, and pressures of interest. The rate equation used for the decomposition reaction was obtained by extrapolation of the data in reference M3.

Indications are that $Ca(OH)_2$ decomposition may best be described by the "shrinking-core" model (Reference S4). Theoretical presentations of this model are generally simplified to the case of an irreversible reaction, although the case for a reversible reaction has been worked out (Reference S5). According to the model, the decomposition reaction would take place at the surface of the unreacted core of $Ca(OH)_2$. As reaction proceeded, water vapor concentration (and thus pressure) would build up near this surface, and H_2O vapor would diffuse down the concentration gradient outward through the porous product CaO to the particle boundary.

Lack of appropriate intrinsic reaction rate data and of the value of the effective diffusivity of H_2O vapor in the CaO product layer prevented effective use of the shrinking core model, and the following simplifying assumptions were made in order to estimate the endothermic reaction solids residence time.

1. Chemical reaction is rate controlling (i.e., intra- and inter-particle heat and mass transfer limitations were assumed to be negligible).

2. The solid phase passes through the reactor in plug flow (i.e., residence time is the same for all solid particles).

3. Concentration of H_2O vapor is constant throughout the reactor.

Under these assumptions, the estimated solids residence time for the $Ca(OH)_2$ decomposition reaction is 2.2 minutes; estimates of reactor size and cost for that system were made using double this value, or 4.4 minutes. Solid particles were assumed to be uniform in size with 0.64 cm diameter. The reactor trains are envisioned to be 2.43 m in diameter, with a total bed height (four reactors in series) of 9.14 m. A total of 25 such reactor trains would be required for a storage system capable of a 2,500 MW_t maximum charging rate, typical of a 100 MW_e, autonomous STEC plant at location SE. Total module height, with solids preheater, solids cooler, and four moving bed

SCHEMATIC OF RADIAL-FLOW, MOVING BED REACTOR DESIGN
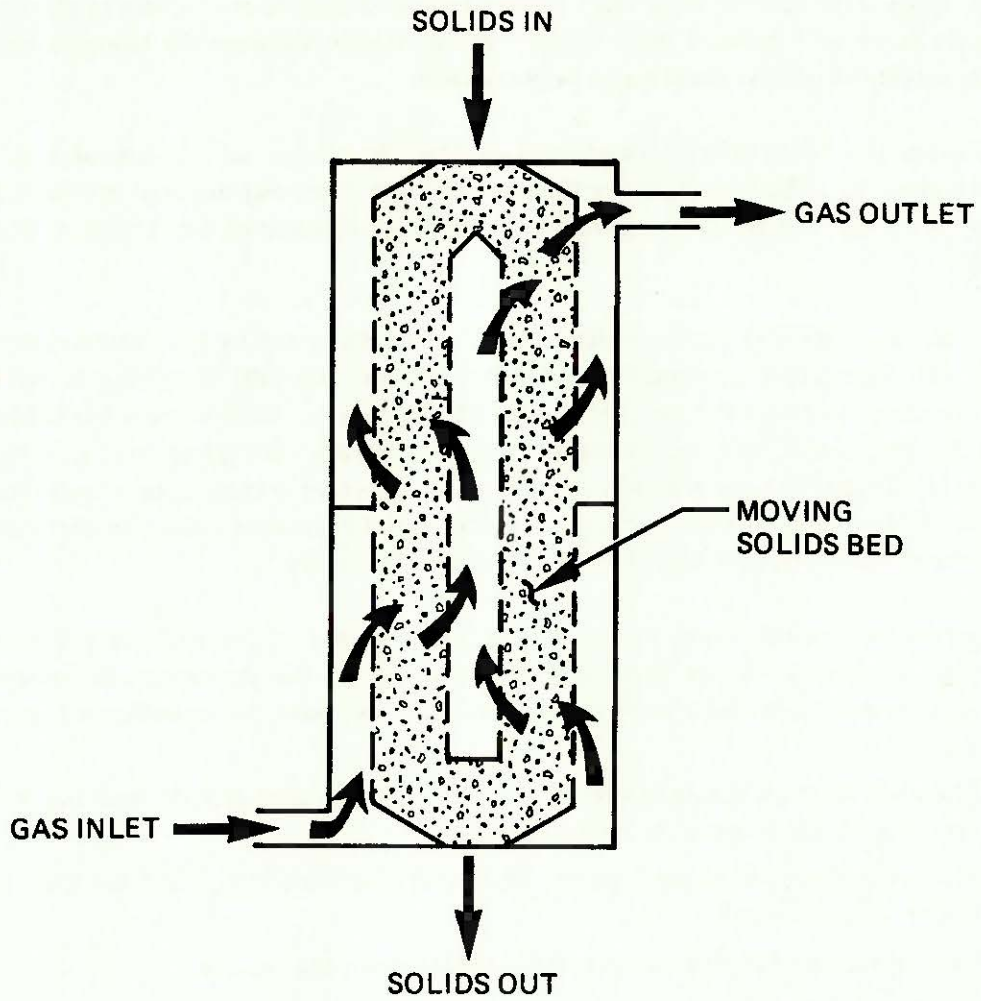
after "Gas Purification", Kohl and Riesenfeld, p. 448

ISOLATED SCHEMATIC
OF MOVING BED REACTOR TRAIN

SOLIDS INPUT

GAS
INPUT STREAM

MOVING BED
REACTORS

GAS
EXIT STREAM

SOLIDS
OUTPUT
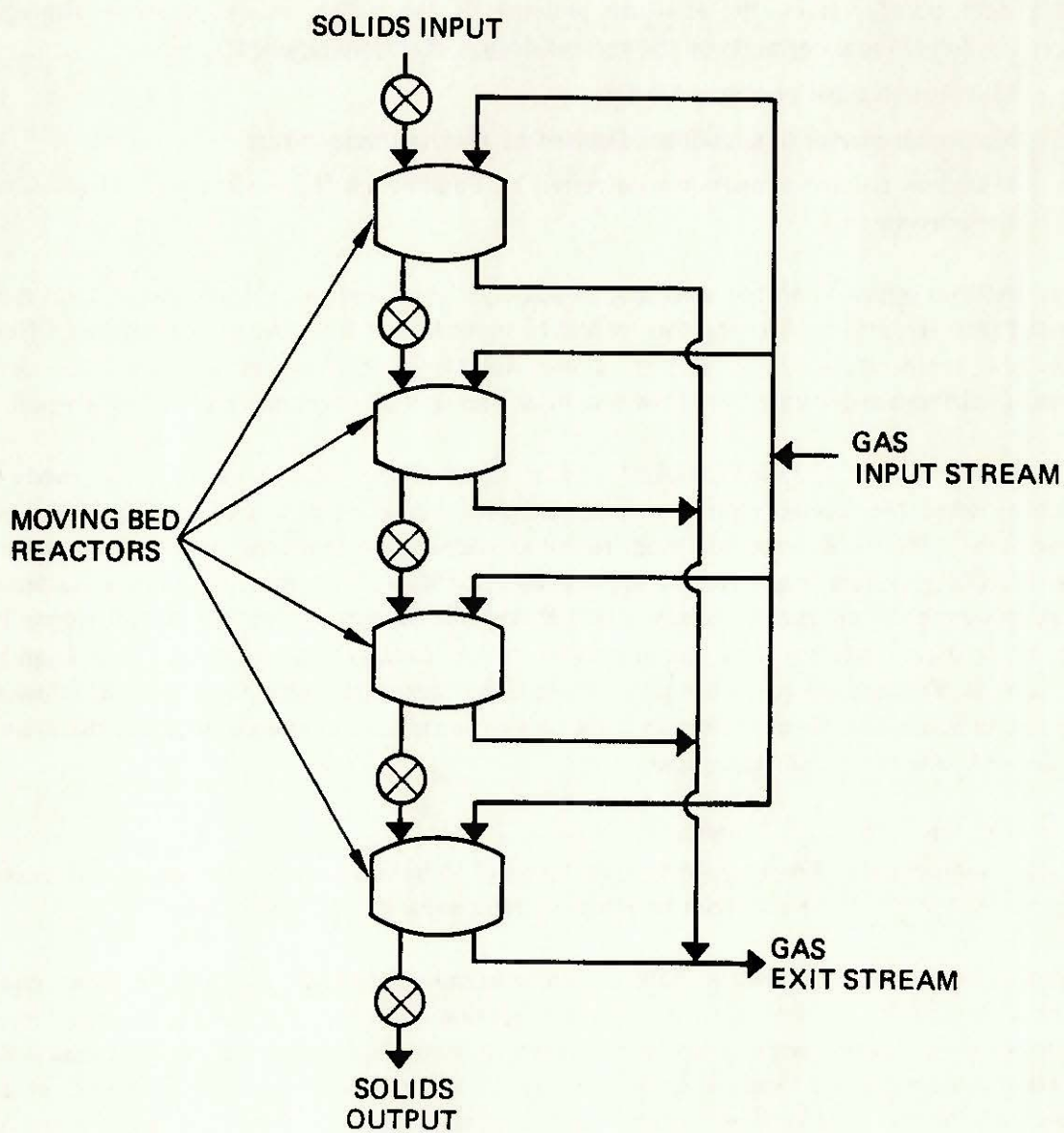
reactors, would be approximately 22 m. Rough calculations indicate that gas velocity in the reactor is sufficient to make external heat transfer resistance negligible.

In the present study, absolute pressure in the endothermic mode was kept less than one-half the equilibrium vapor pressure of the $Ca(OH)_2$ throughout the moving bed reactors to facilitate dissociation. Figure 4-9 indicates the very strong dependence of the equilibrium vapor pressure of $Ca(OH)_2$ on temperature. Primarily to avoid contamination of the system, but also to assure workable heat transfer rates, the absolute pressure of the system was kept above atmospheric pressure. The following constraints on the reactor design, therefore, applied:

1. Minimum reactor pressure: 1.0 bar

2. Maximum reactor temperature: dictated by receiver temperature

3. Minimum reactor temperature: dictated by equilibrium thermodynamics of reaction and the pressure in 1.

These restrictions apply to all the solid gas, noncatalyst reactions studied here. Since heat must be transferred into the moving bed reactors by loss of sensible heat from the carrier gas, the difference between the temperatures in 2. and 3. above determines the carrier gas flow rate. As this temperature difference decreases, the flow rate must increase, all other parameters being equal.

In the particular case of the $CaO/Ca(OH)_2$ system, early designs used an endothermic mode input temperature from the receiver similar to that used in the baseline design of the SO_2/SO_3 system, approximately 1,100 K. From equilibrium thermodynamics, the minimum reactor temperature for the $CaO/Ca(OH)_2$ system was therefore approximately 800 K. Therefore, the carrier gas temperature had to vary between approximately 1,000 K and 850 K; such a small temperature drop in the reactor dictated an extremely large carrier gas flow rate in order to transfer enough heat from HE10 to the reactor. Pressure drops in the reactor and HE1 were extremely large for such flow rates, causing the efficiency to be quite low and the cost of the main compressor (C1) and the main heat exchanger (HE1) to be prohibitively large.

Of the constraints 1. through 3. above, the only one which it is possible or convenient to change is the receiver temperature. The receiver temperature had to be increased to the maximum considered in the present study, 1,310 K, in order to achieve a reasonable charging efficiency.

The same reactors are to be used in both the endothermic and exothermic modes. Since charging rates are expected to be much greater than discharging rates (section 2.4.1), the reactors were sized for the endothermic mode. Even if the exothermic reaction rate is found to be much slower than anticipated, requiring longer residence times, the excess reactor capacity available should be adequate. All of the moving bed reactors were designed for the exothermic reaction pressures, although the great majority are needed only in the endothermic mode.

As in the endothermic process, reactor design is governed by a set of three constraints:

1. Maximum reactor pressure: 20 bar

CALCULATED VAPOR PRESSURE OF CaO/Ca(OH)$_2$ SYSTEM

PRESSURE (bar) vs 1000/T (K^{-1})
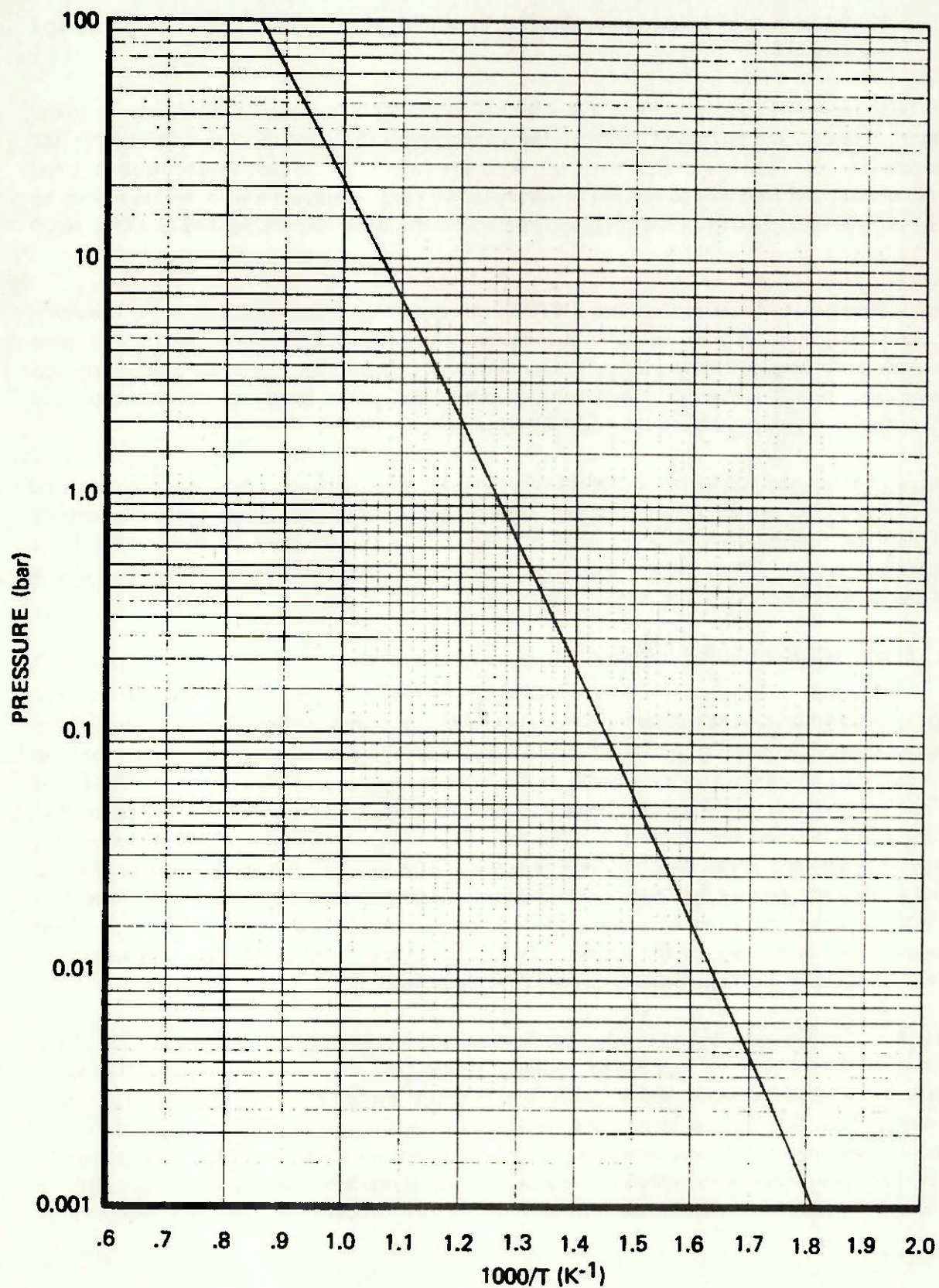
2. Minimum reactor temperature: dictated by power generation cycle

3. Maximum reactor temperature: dictated by equilibrium thermodynamics of reaction and pressure in 1.

Again, these restrictions apply to all of the solid/gas, noncatalytic reactions studied here. As in the endothermic mode, the difference between the temperatures in 2. and 3. above determines the carrier gas flow rate. The upper limit on the reactor pressure of 20 bar was chosen to limit vessel shell thicknesses and thus cost to reasonable values and to keep compression work within reason. In addition, it was desired to keep the pressure drop across the rotary airlock feeders at or below 20 bar.

Storage system output temperatures near 1,310 K were out of the question (Figure 4-9). Moreover, early exothermic mode designs with output temperatures similar to those in the SO_2/SO_3 system had very low discharging efficiencies and extremely high capital costs due to the high carrier gas flow rates required. Therefore, the baseline $CaO/Ca(OH)_2$ system was designed to produce chemical energy suitable for input to a standard steam-Rankine power cycle.

As discussed in section 4.2.4 for the SO_2/SO_3 system, the great difference between the input and output temperatures would require different power cycles for energy direct from the receiver (1,310 K) and energy from storage (870 K). Such must be the case, however, because a $CaO/Ca(OH)_2$ energy storage system with equal input and output temperatures would be far too costly and inefficient.

4.3.6   Solids Preheater and Solids Cooler

Most of the chemical reactions considered in the final group of twelve are best suited for energy storage systems with input temperatures at or above the input temperature of conventional steam turbogenerators. The sensible and latent heat necessary to raise reactants to these reaction temperatures are in most cases comparable to the enthalpy of reaction, and recuperation of heat from cooling products is therefore a must for efficient operation. Liquid phase reactants and products would be ideal for efficient recuperation since heat exchange between liquid streams is relatively efficient and cheap. Less desirable is the case in which one or both of the reactant and product streams are gaseous over part of the temperature range between ambient temperatures and that of the reaction; heat transfer coefficients are lower, recuperation is less efficient, and heat exchangers more costly. Six of the reactions in Table 4-1 have solid constituents, however, and recuperation for these reactions presents special design problems.

Indirect heat transfer into and out of the solids stream is necessary for the same reason as in the reactor train. In the case of heating or cooling of solids which are primarily $Ca(OH)_2$ (solids preheater in endothermic mode, solids cooler in exothermic mode) water vapor is the best choice for a carrier fluid. Nitrogen has been chosen as the carrier gas for cooling solids (primarily CaO) in the endothermic mode in order to avoid untimely hydration of the CaO. The use of different carrier gases in the solids preheater and solids cooler makes an additional heat exchanger necessary (HE4 in endothermic mode). In addition to the airlock feeders between reactors and recuperation

equipment, precautions have been taken to minimize mixing of water and nitrogen carrier gases; pressure in the solids cooler has been kept slightly higher than in the reactor to assure that what small amount of crossflow occurs is into the reactor carrier stream where separation of the gases is easier.

Water vapor is used as a carrier gas in both the solids preheater and cooler in the exothermic mode. It is believed that the temperatures in the solids preheater are low enough (hence the reaction rate slow enough) that no significant hydration will take place. Better reaction rate data and some pilot plant work may be necessary before this design decision can be confirmed.

4.3.7 Noncondensible Carrier Gas

Early designs used nitrogen as a carrier gas in the endothermic mode. The nitrogen reduced the partial pressure of the reaction product water and, therefore, made possible operation at higher total pressure, with more efficient heat transfer. Separation of the water from the N_2 stream proved to be inefficient, however, due to high compression work, and the capital cost requirements for compressors and recuperative heat exchangers were prohibitive.

4.3.8 Solids Transport

The same concerns about solids degradation which weighed against fluidized bed reactors led to rejection of a pneumatic transport system. Transporation of solids to and from storage would have to be carried out by mechanical conveyors and elevators.

4.3.9 Solids Regeneration

Some degradation of solid material is bound to occur as a result of a combination of abrasion, severe temperature changes, and many reaction cycles. Fines would be generated by such degradation, and cyclone separators (not shown in flowsheets) would of course be required at various points throughout the process. Should solids degradation be such that a significant solids makeup stream is required, significant incentive may exist to develop a process for regenerating the solids to particle sizes usable in the reactor train. The nature of this process is unknown at present (some work has been done on pelletizing or agglomerating $Mg(OH)_2$ with inorganic binders, Reference B7), as is the degree of degradation which would make it necessary. The process has, therefore, been represented as a "black-box" on the flowsheet, and was not considered in the efficiency or cost estimate for the $CaO/Ca(OH)_2$ system.

4.3.10 Mass Flow Into and Out of Storage Subsystems — "Open" CES Systems

An alternative to regeneration of degraded solid particles would be to trade commercially in CaO or $Ca(OH)_2$. For example, unusable CaO could be sold to some commercial user for whose purposes the "degraded" oxide was adequate, and suitable $Ca(OH)_2$ bought as makeup (or vice versa). The details of such trade are beyond the scope of this study, and no accounting for it has been made in efficiency or cost estimates.

The possibility of such trade with chemical processes outside the STEC storage system will exist for any storage reaction with one or more constituents, not necessarily solids, for which there is large enough commercial trade. The attractiveness of such trade will depend on an overall economic analysis of the storage process and other regeneration schemes. Nonetheless, consideration of such trade provides important perspective in which to view chemical energy storage. Throughout this study, the chemical energy storage systems have been viewed as closed with respect to mass transfer; only heat and mechanical work can be exchanged with outside processes, and then in a very restricted manner. In a broader sense, chemical energy storage systems can be categorized with respect to the relative sizes of input/output streams and holdup, i.e. in terms of residence time. At one extreme is a completely closed-loop storage system (infinite residence time), while at the other is a solar powered chemical process plant with only such residence time as is necessary for the proper functioning of the process. For all but the most remote locations for a STEC facility, the optimum chemical energy storage system will probably fall somewhere between these two extremes. In such a system, a solar powered chemical process which produced a useful and valuable product would also serve as an energy storage system for a (most probably hybrid) solar power generation plant. Economic evaluation of such a process would be complex, as would comparison with the more easily evaluated extremes mentioned above. Nonetheless, such an "open" energy storage process may prove to be the most economical application of reversible chemical reactions to energy storage in STEC plants.

4.3.11 System Reversibility

Changeover between charging and discharging modes could be accomplished continuously in the $CaO/Ca(OH)_2$ system described above, with a portion of the reactor dedicated to each mode during the changing period. In the event that a rapid changeover of the entire reactor from one mode to the other were required, it could be accomplished readily by changing the pressure of the carrier gas stream, thereby reversing the reaction of the hot solid phase already in the reactor.

4.3.12 Alternate $CaO/Ca(OH)_2$ Storage System Designs

In section 4.3.4, the potential advantages of fluidized-bed reactors in the $CaO/Ca(OH)_2$ system were discussed, as well as the primary reason for rejection of that reactor type. Solids degradation and breakup may well render the reaction irreversible, and such degradation would likely be aggravated to an unacceptable degree by fluidized-bed processing. Nonetheless, the attraction of reduced compression work requirements and significantly better heat transfer characteristics warranted a brief examination of a $CaO/Ca(OH)_2$ storage system based on fluidized-bed reaction. At the outset, the important assumption must be made that contrary to the above discussion, solids degradation will not occur to any appreciable extent, and that any size CaO or $Ca(OH)_2$ particles are available. The design study of the fluidized-bed system was necessarily brief, but of sufficient depth to reveal the major benefits and drawbacks of such a system.

Preliminary design calculations indicate that the compressor (or blower) work requirements of the fluidized bed systems would be considerably lower than those of the moving-bed systems. Compressor work reductions would, of course, be greatest for endothermic operation, where

evolving water vapor would aid in fluidizing the reacting solids. Conversely, water vapor is consumed in exothermic operation, and compression work requirements would be greater than would be required to fluidize a similar bed of nonreacting solids.

The use of solid particulates small enough to fluidize in the reactor would lead to some design constraints for both the reactor and associated heat transfer equipment. In the endothermic mode, evolving water vapor would cause the degree of fluidization (or, more precisely, the gas flow rate) to increase with height in the bed. Thus, a bed barely fluidized at the bottom might approach entrained-bed operation at the top. Careful design with the possible use of exit streams at intermediate heights within the bed would be required to avoid serious entrainment problems in the endothermic mode. Some forced convection would be needed to fluidize the lower parts of the reactor bed, even in the endothermic mode, and those studies which have claimed that such beds will "fluidize themselves" are not realistic.

Use of small solid particles for reactor fluidization effectively precludes use of moving bed designs for solids preheating and cooling, since pressure drop through such beds would be quite high. Fluidized bed heat exchangers would be required for recuperative heat transfer between solid products and reactants.

Moving-bed designs offer the attractive advantage of near counter-current contacting of the solids and the heating (or cooling) gas stream in the solids preheater or cooler. Fluidized beds, on the other hand, operate under conditions approaching complete backmixing, and the temperatures achievable with one each fluidized-bed, solids preheater and cooler are not nearly so high as is possible with moving-bed designs.

Since heating of reactants to reaction temperatures requires a significant amount of heat relative to the enthalpy of reaction (especially for high temperature reactions), efficient heat transfer between incoming reactants and hot reaction products is absolutely necessary. Such regeneration might require two series of cascading fluidized-bed heat exchangers — one for the unreacted solids and one for the reacted solids. Each "mini-bed" in a series would operate at a different temperature, so that solids temperatures could be raised or lowered in a series of step changes. There would, of course, be an optimum number of such mini-beds for each series, determined by capital cost vs. efficiency considerations, but the scope of this rough study would not allow much design optimization.

The expense and/or difficulty of fluidized-bed recuperation may result in an overall decrease in storage system efficiency. In short, use of fluidized-bed technology in these storage systems appear to offer mixed blessings. Further study of the technical and economic advantages/disadvantages of fluidized-bed storage system designs is recommended.

4.4 PROCESS DESIGNS OF REMAINING CHEMICAL REACTIONS

Schematics of the process designs of storage systems based on the remaining seven reactions of Table 4-1 are presented in the following sections. It was noted earlier that much of the discussions of the SO_2/SO_3 and $CaO/Ca(OH)_2$ energy storage subsystems applies to the catalytic and

noncatalytic reaction groups, respectively (Table 4-1). The discussions of the storage subsystems based on the remaining seven reactions are, therefore, somewhat abbreviated; important design temperatures or pressures are tabulated, remarkable features of the various processes are noted, and some comparison of the systems are given. However, detailed tabulation of flow conditions throughout the processes are not included.

The reactor designs in the five solid/gas, noncatalytic processes are all based on the moving-bed design discussed at some length in section 4.3.5. The reactor designs in the ethane/ethylene and benzene/cyclohexane processes are similar to the SO_2/SO_3 reactor design: a series of packed catalyst beds separated by interbed heat exchangers.

4.4.1 The $CaO/CaCO_3$ and $MgO/MgCO_3$ Energy Storage Subsystems

Process flowsheets for the endothermic and exothermic modes of the $CaO/CaCO_3$ storage design are presented in Figures 4-10 and 4-11, respectively, while similar flowsheets for the $MgO/MgCO_3$ designs are presented in Figures 4-12 and 4-13. These designs use moving-bed reactors similar to that in the $CaO/Ca(OH)_2$ storage system design, and, therefore, resemble the $CaO/Ca(OH)_2$ design in most of its important features (the primary difference being the extremely high storage pressure required for the CO_2).

Important design specifications for the two storage systems are presented in Table 4-12, and efficiency and unit cost estimates based on the above designs are presented in Table 4-13.

The results in Table 4-13 indicate important differences between the two storage systems. The higher charging efficiency of the $MgO/MgCO_3$ system is due primarily to its lower operating temperature. For a given compression ratio, the work of compression will vary directly with absolute temperature, so that parasitic power requirements for the compressor will cause the efficiency of a process (charging or discharging) to decrease with increasing temperature. With pressure drops and CO_2 circulation rates through the reactor — HE1 loops roughly equal in the two carbonate designs, the higher temperature $CaO/CaCO_3$ system, thus, has the lower charging efficiency.

Energy-related capital costs of the $MgO/MgCO_3$ system are nearly twice those of the $CaO/CaCO_3$ system. This difference in costs is due almost entirely to the lower enthalpy of reaction of the $MgO/MgCO_3$ reaction. The standard enthalpy of reaction of the $CaO/CaCO_3$ system, 42.8 kcal/mole, is approximately 1.5 times greater than that of the $MgO/MgCO_3$ system at 28.9 kcal/mole. With the discharge efficiencies of the two systems being nearly equal, then, approximately 1.5 times as much CO_2 must be stored by the $MgO/MgCO_3$ system in order to discharge the same amount of energy as heat to the turbogenerators. High-pressure storage of CO_2 is by far the most costly energy-related capital expense in both carbonate systems, so that an additional increase in this expense is most certainly evident in the final accounting for energy-related costs. The remainder of the energy-related capital cost difference between the two systems is due to the much higher cost of solid phase chemical constituents for the magnesium-based system:

CaO/CaCO₃ ENERGY STORAGE SUBSYSTEM
PRELIMINARY PROCESS FLOW SHEET
ENDOTHERMIC MODE (CaCO₃ ⟶ CaO + CO₂)

Figure 4-10
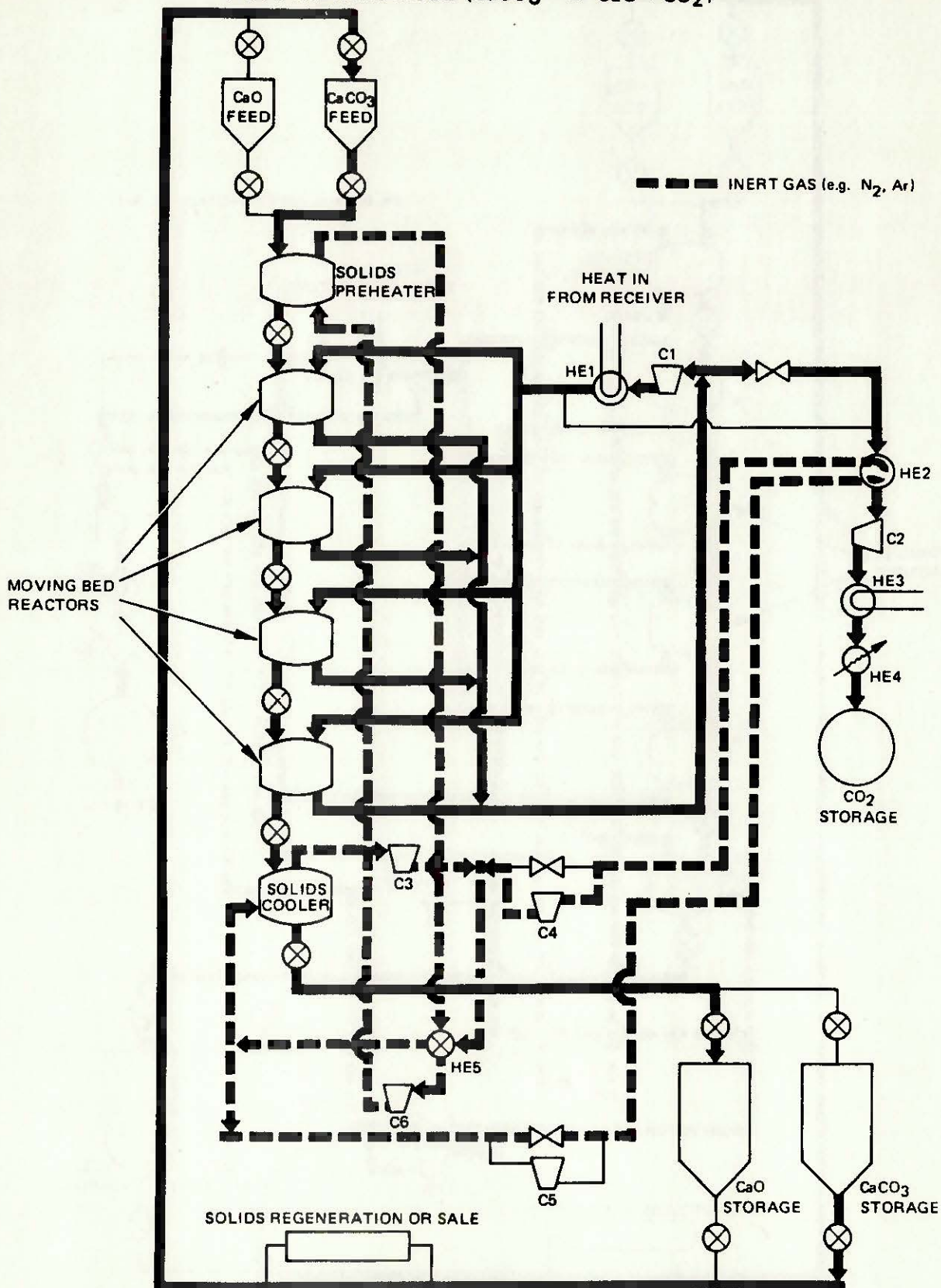
CaO/CaCO3 ENERGY STORAGE SUBSYSTEM
PRELIMINARY PROCESS FLOW SHEET
EXOTHERMIC MODE (CaO + CO₂ ⟶ CaCO₃)
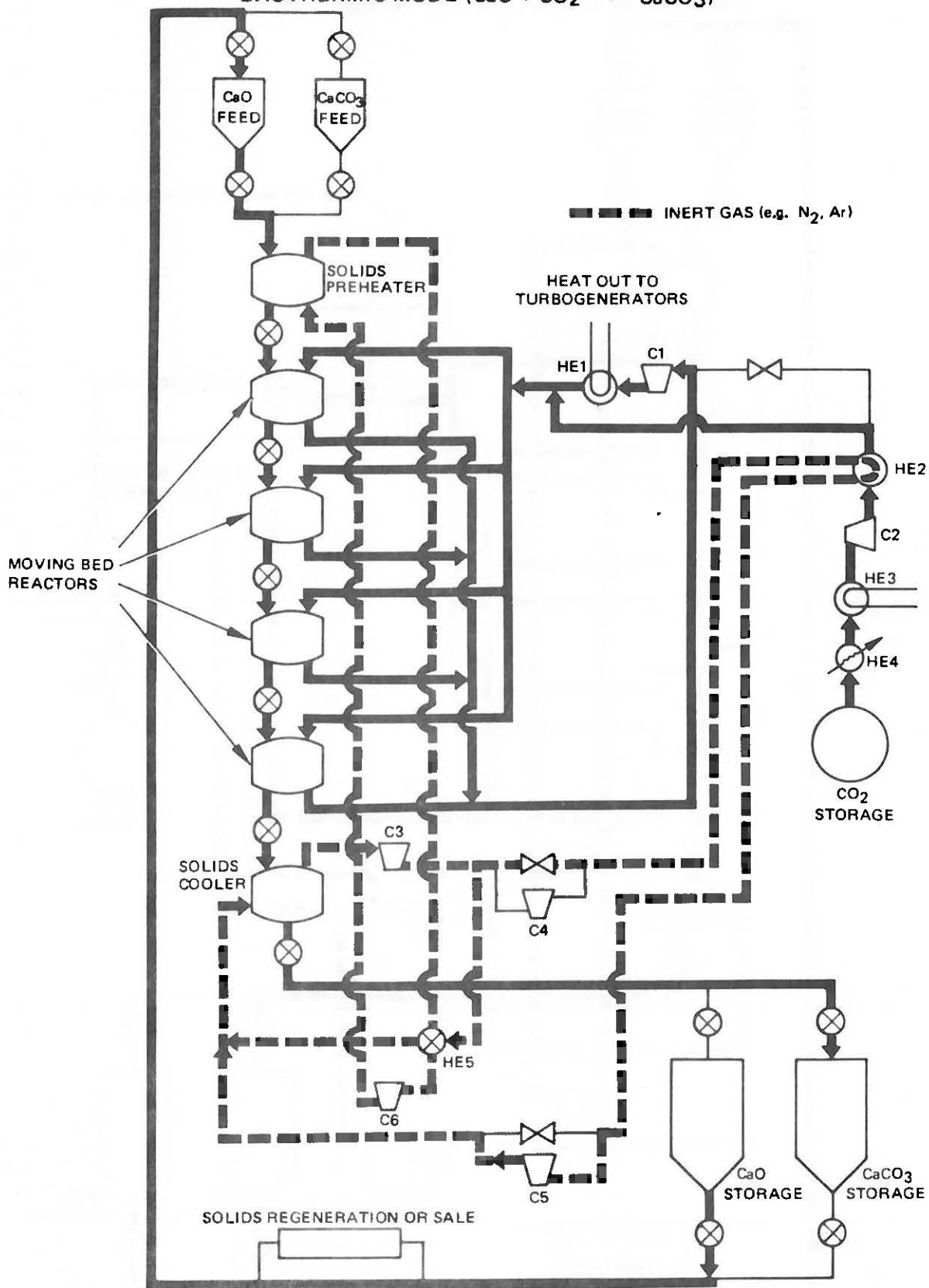
■ ■ ■ ■ INERT GAS (e.g. N₂, Ar)

CaO FEED

CaCO₃ FEED

SOLIDS PREHEATER

HEAT OUT TO TURBOGENERATORS

HE1

C1

HE2

C2

HE3

HE4

CO₂ STORAGE

MOVING BED REACTORS

C3

C4

SOLIDS COOLER

HE5

C6

C5

CaO STORAGE

CaCO₃ STORAGE

SOLIDS REGENERATION OR SALE

MgO/MgCO₃ ENERGY STORAGE SUBSYSTEM PRELIMINARY PROCESS FLOW SHEET ENDOTHERMIC MODE (MgCO₃ → MgO + CO₂)

MgO/MgCO$_3$ ENERGY STORAGE SUBSYSTEM
PRELIMINARY PROCESS FLOW SHEET
ENDOTHERMIC MODE (MgCO$_3 \rightarrow$ MgO + CO$_2$)

- - - INERT GAS (e.g. N$_2$, Ar)

MgO FEED

MgCO$_3$ FEED

SOLIDS PREHEATER

HEAT IN FROM RECEIVER

HE1 C1

HE2

C2

HE3

HE4

CO$_2$ STORAGE

MOVING BED REACTORS

SOLIDS COOLER

C3

C4

HE5

C6

C5

MgO STORAGE

MgCO$_3$ STORAGE

SOLIDS REGENERATION OR SALE

MECHANICAL CONVEYING SYSTEM

MgO/MgCO₃ ENERGY STORAGE SUBSYSTEM
PRELIMINARY PROCESS FLOW SHEET
EXOTHERMIC MODE (MgO + CO₂ ⟶ MgCO₃)

Figure 4-13. MgO/MgCO₃ Energy Storage Subsystem Preliminary Process Flow Sheet, Exothermic Mode
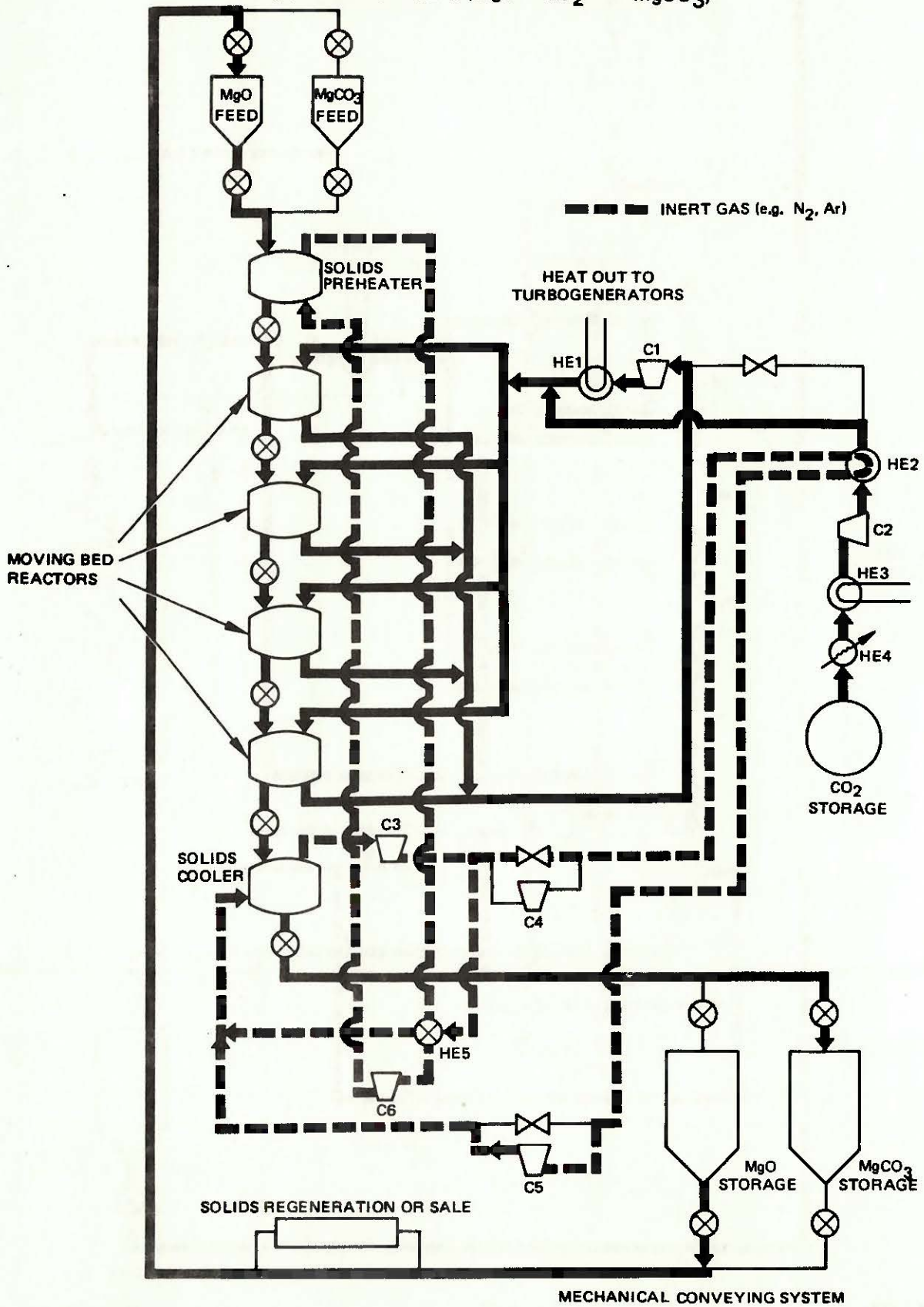
Table 4-12
DESIGN PARAMETERS FOR ALKALINE EARTH-CARBONATE SYSTEMS

	$CaO/CaCO_3$	$MgO/MgCO_3$
Temperature from receiver	1,310 K	930 K
Average endothermic reaction temperature	1,192 K	805 K
Average endothermic reaction pressure	0.85 bar	0.9 bar
Temperature to turbogenerator	1,310 K	588 K
Average exothermic reaction temperature	1,337 K	610 K
Average exothermic reaction pressure	20 bar	20 bar
CO_2 storage pressure	60 bar	60 bar

Table 4-13
RESULTS OF DESIGN STUDIES OF ALKALINE-EARTH CARBONATE SYSTEMS

	$CaO/CaCO_3$	$MgO/MgCO_3$
Charging efficiency	0.31	0.48
Discharging efficiency	0.88	0.83
Round-trip efficiency	0.27	0.40
Power-related capital cost	$1.0 \times 10^5/MW_t$	$9.8 \times 10^5/MW_t$
Energy-related capital cost	$4.7 \times 10^3/MW_t$-hr	$9.7 \times 10^3/MW_t$-hr

━ ━

CaO ($0.015/lb, $0.034/kg) $CaCO_3$ ($0.0095/lb, $0.021/kg)
MgO ($0.51/lb, $1.12/kg) $MgCO_3$ ($0.22/lb, $0.48/kg)*

The power-related costs of the $MgO/MgCO_3$ system are nearly 10 times higher than those of the $CaO/CaCO_3$ system, due primarily to the much greater reactor costs of the former.

The reactor in the $CaO/CaCO_3$ system accounts for ~0.6 percent of the power-related capital costs, with the largest capital requirements being for C1 and HE1. The $MgO/MgCO_3$ reactor, on the other hand, accounts for ~89 percent of the power-related costs of that system. Data concerning the

---

*Chemical Marketing Reporter, 213 (21), May 22, 1978

dissociation reaction kinetics of the $MgO/MgCO_3$ system is sketchy and the scope of the present effort did not allow an exhaustive literature search. Extrapolation of available kinetic data (Reference B8) into the temperature range of interest resulted in estimated solids residence times of ~500 hours! It would appear, then, that even at the relatively high endothermic reaction temperature used in the present design, the dissociation reaction rate is prohibitively slow. While faster reaction rates (hence shorter residence times) may be possible, such improvements cannot be justified on the basis of data at hand, and reaction kinetics must remain a serious drawback to a storage system based on the $MgO/MgCO_3$ reaction.

4.4.2 The $ZnO/ZnSO_4$ Energy Storage Subsystem

The preliminary process design of a storage system based on the above reaction is presented in Figures 4-14 and 4-15. Important design specifications for this system are presented in Table 4-14, and results of the preliminary design study are presented in Table 4-15.

Table 4-14
DESIGN PARAMETERS FOR THE $ZnO/ZnSO_4$
ENERGY STORAGE SUBSYSTEM

Temperature from receiver	1,310 K
Average endothermic reaction temperature	1,176 K
Average endothermic reaction pressure	0.85 bar
Temperature to turbogenerator	1,310 K
Average exothermic reaction temperature	1,360 K
Average exothermic reaction pressure	34 bar
SO_3 storage pressure	1.6 bar

Table 4-15
RESULTS OF DESIGN STUDIES OF THE $ZnO/ZnSO_4$
ENERGY STORAGE SUBSYSTEM

Charging efficiency	0.39
Discharging efficiency	0.75
Round-trip efficiency	0.30
Power-related capital cost	$1.4 \times 10^5/MW_t$
Energy-related capital cost	$3.3 \times 10^3/MW_t$-hr

ZnO/ZnSO$_4$ ENERGY STORAGE SUBSYSTEM
PRELIMINARY PROCESS FLOW SHEET
ENDOTHERMIC MODE (ZnSO$_4$ $\longrightarrow$ ZnO + SO$_3$)
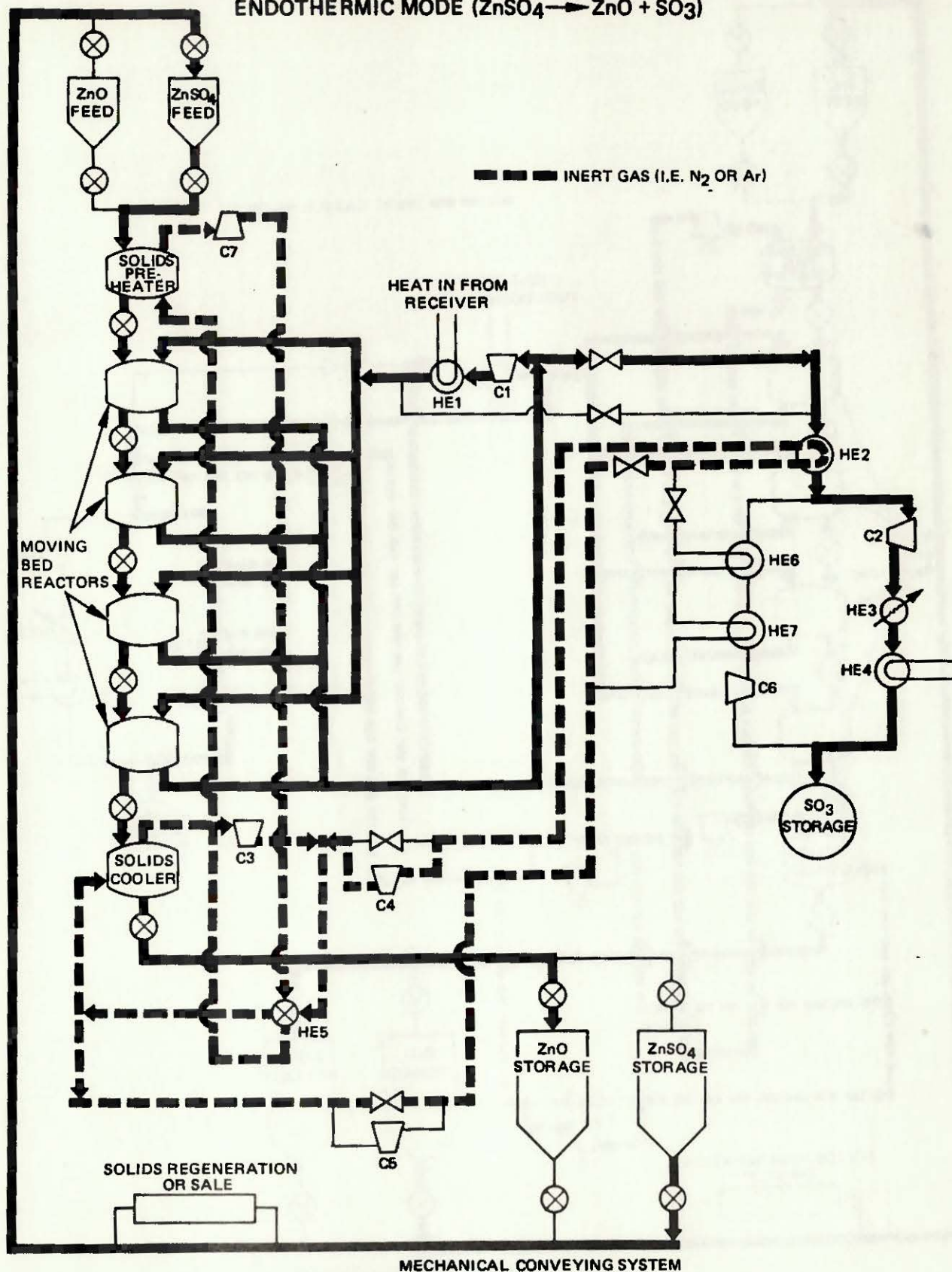
ZnO/ZnSO₄ ENERGY STORAGE SUBSYSTEM
PRELIMINARY PROCESS FLOW SHEET
EXOTHERMIC MODE (ZnO + SO₃ ⟶ ZnSO₄)

INERT GAS (I.E. N₂ OR Ar)

ZnO FEED

ZnSO₄ FEED

SOLIDS PRE-HEATER

C7

HEAT OUT TO TURBOGENERATOR

MOVING BED REACTORS

HE1

C1

HE2

C2

HE6

HE3

HE7

HE4

C6

SO₃ STORAGE

SOLIDS COOLER

C3

C4

HE5

ZnO STORAGE

ZnSO₄ STORAGE

SOLIDS REGENERATION OR SALE

C5

MECHANICAL CONVEYING SYSTEM
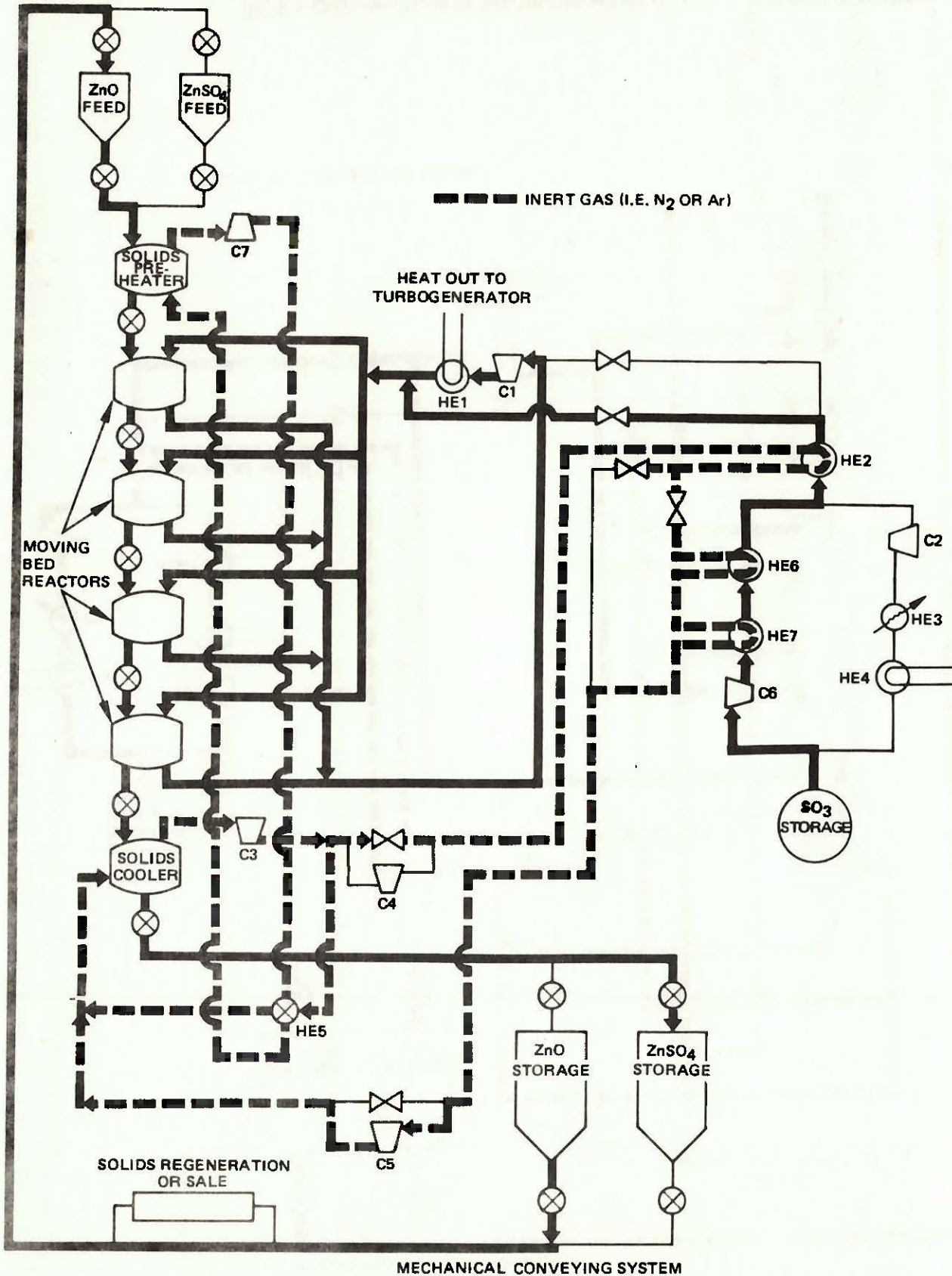
The charging efficiency of the $ZnO/ZnSO_4$ system is higher than that of the $CaO/CaCO_3$ system (which has similar endothermic temperature and molar enthalpy of reaction) because the molar heat capacity of SO_3 (19.2 cal/g-mole K) is significantly higher than that of CO_2 (13.2 cal/g-mole K). Less SO_3 must be recirculated per mole of $ZnSO_4$ dissociated, so parasitic compression losses are lower and charging efficiency higher. In addition, considerably greater compression work is required to bring the CO_2 to its storage pressure of 60 bar than to compress SO_3 for storage, a fact which lowers the $CaO/CaCO_3$ charging efficiency still further relative to that of the $ZnO/ZnSO_4$ system.

The discharging efficiency of the $ZnO/ZnSO_4$ system is lower than that of the $CaO/CaCO_3$ system due to the much greater compression work which must be exerted to compress the SO_3 from its storage pressure (1.6 bar) to the exothermic mode operating pressure (20 bar). This compression requires 16 kcal/mole reacted in the ZnO/Zn SO_4 system, and only 5 kcal/mole reacted in the $CaO/CaCO_3$ system.

The major power-related cost items are the compressor C1 (56%), the reactor train (12%), and the main heat exchanger HE1 (10%). Due to the corrosivity of $ZnSO_4$, and its decomposition products 304 stainless steel cladding was specified on all solids handling equipment.

Kinetics information on the $ZnO/ZnSO_4$ reaction is next to nonexistent, and the data that was available (Reference P5) was for lower temperatures than are called for in the present design. When a curve fitted to these data was extrapolated to temperatures of interest, the predicted solids residence times were unrealistically short. In view of the heat an mass transfer limitations which would undoubtedly be important in such a reactor, it was decided to make a more conservative estimate of the solids residence time ($\sim$70 min) times that for the case based solely on extrapolated reaction kinetics) for reactor design purposes. Use of this increased residence time did not greatly affect the power-related capital cost estimate, however, bringing the reactor-train cost to only 12 percent of the total.

Two potential problems of CES systems based on the $ZnO/ZnSO_4$ reaction should be mentioned: the volatility of zinc oxide and partial decomposition of SO_3 to SO_2 and O_2 during the $ZnSO_4$ pyrolysis. Of all the metal oxides encountered in the group of twelve reactions considered here, ZnO is the most volatile; some of it may sublime in the range of 1,176 K and deposit on cooler surfaces in other parts of the system. When roasting zinc ores containing $ZnSO_4$, almost all of the sulfur comes off as SO_2 rather than SO_3. This may be caused by contaminants in the ore which catalyze the SO_3 decomposition. The $ZnSO_4$ used in CES systems would have to be free of such contaminants. If SO_3 decomposition did occur, a separate (and costly) loop would be required to separate, collect and reconnect the SO_2 to SO_3.

4.4.3 The C/CS_2 Energy Storage Subsystem

The preliminary process design for the C/CS_2 storage subsystem is presented in Figures 4-16 and 4-17. Important design specifications for the system are presented in Table 4-16, and efficiency and cost estimates based on the above designs are presented in Table 4-17.

C/S/CS$_2$ ENERGY STORAGE SUBSYSTEM
PRELIMINARY PROCESS FLOWSHEET
ENDOTHERMIC MODE (C+2S → CS$_2$)

HEAT IN
FROM RECEIVER

C1

C.W.

HE5

HE4

HE3

HE2

CS$_2$
STORAGE

HE1

REACTOR

HE9

HE8

HE7

HE6

S
STORAGE

C
STORAGE

HE10

HE12

HE11

SULFUR
MELTING
POT

INTERMEDIATE HEAT
TRANSFER LOOP

Figure 4-16
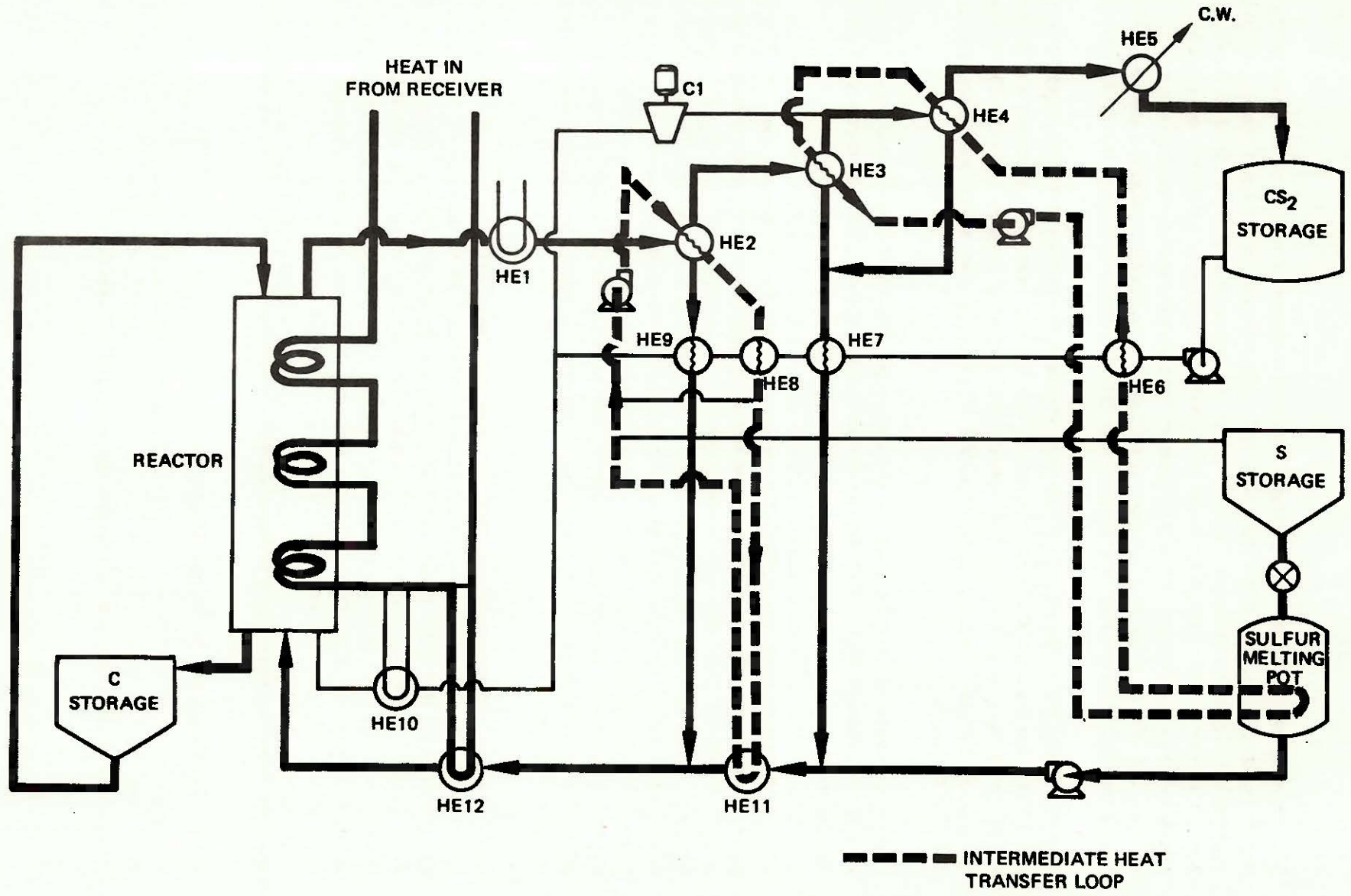
C/S/CS₂ ENERGY STORAGE SUBSYSTEM
PRELIMINARY PROCESS FLOWSHEET
EXOTHERMIC MODE (CS₂ → C+2S)
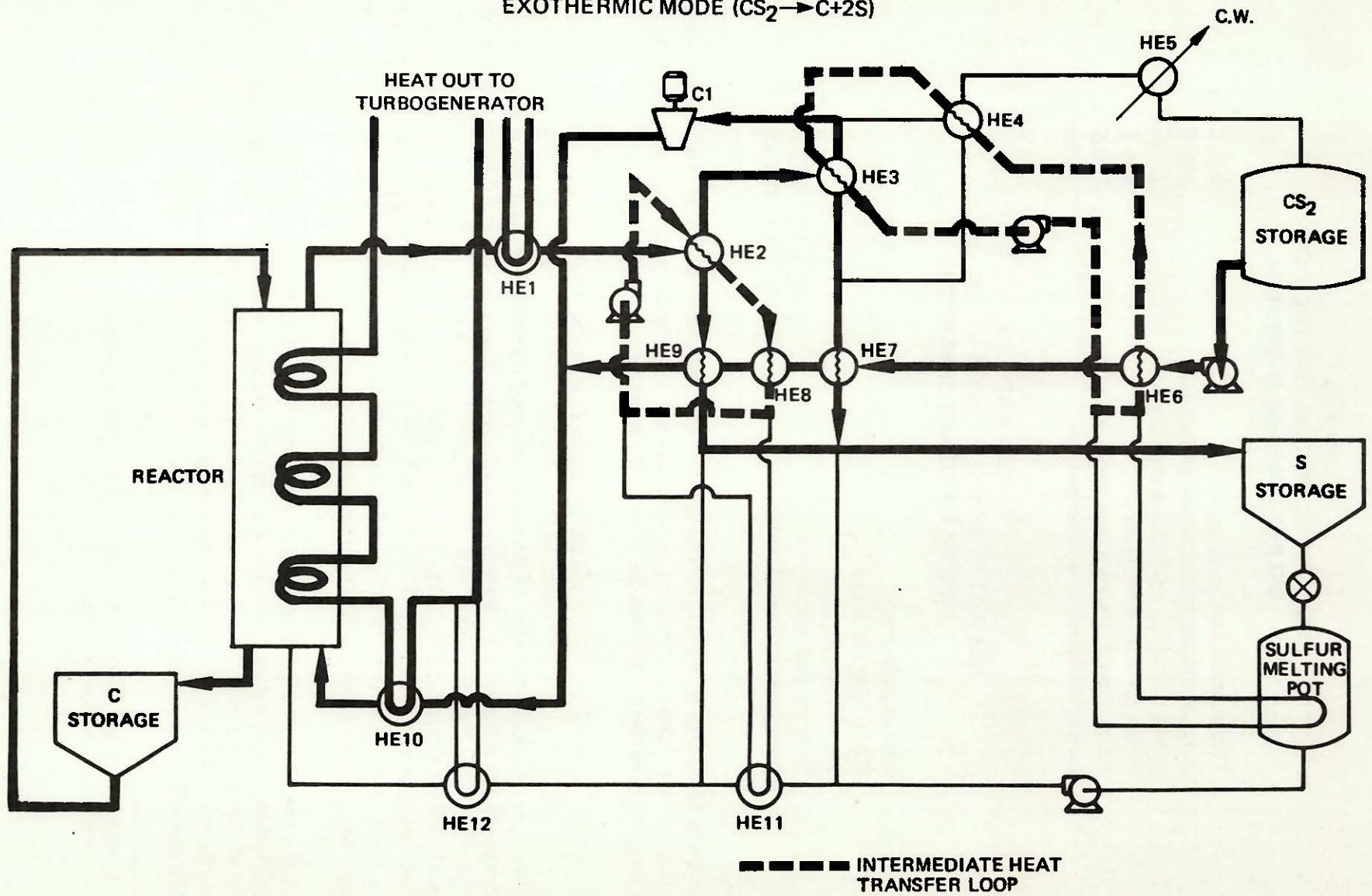
Table 4-16
DESIGN PARAMETERS FOR THE C/CS$_2$
ENERGY STORAGE SUBSYSTEM

Temperature from receiver	920 K
Average endothermic reaction temperature	800 K
Average endothermic reaction pressure	1.7 bar
Temperature to turbogenerator	690 K
Average exothermic reaction temperature	720 K
Average exothermic reaction pressure	2.3 bar

Table 4-17
RESULTS OF DESIGN STUDIES OF THE C/CS$_2$
ENERGY STORAGE SUBSYSTEM

Charging efficiency	0.78
Discharging efficiency	0.80
Round-trip efficiency	0.62
Power-related capital cost	$0.5 x 10^5/MW$_t$
Energy-related capital cost	$0.5 x 10^3/MW$_t$-hr

The thermodynamics of the CS$_2$/C/S reaction deserve some comment here. The standard enthalpy of formation of liquid CS$_2$ is given as 21.4 kcal/mole (Reference S6), based on a sulfur reference state of the S$_8$ allotrope. The reaction then must proceed as

$$1/4\ S_8 \rightleftharpoons 2S + C \rightleftharpoons CS_2\ *$$
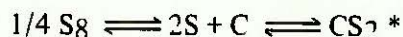
In fact, the standard enthalpy of formation of monatomic sulfur from S$_8$ is *greater* than the enthalpy of formation of CS$_2$ from S$_8$. The actual synthesis of CS$_2$ from C and S, then, is slightly exothermic. The large heat input to the reaction from solid sulfur in the stable S$_8$ allotrope is to dissociate the S$_8$ into S (or S$_2$). The formation of CS$_2$ can thus be thought of as a way of keeping the monatomic or diatomic sulfur from returning to the S$_8$ form on cooling. Moreover, most of the heat input to the reaction will occur as the sulfur liquid is vaporized and superheated to reaction temperature, rather than as the CS$_2$ synthesis reaction occurs.

Like the reactions considered in sections 4.4.1 and 4.4.2, the CS$_2$/C/S reaction is of the solid/gas type. Unlike those reactions, however, there is only one solid reactant, and reaction need take place only at the outer surface of the carbon particles. Intra-particle heat and mass transfer resistances may therefore be less of a problem than in the other solid gas reactions In addition, the great difference in boiling points between the gaseous components, carbon disulfide and sulfur make their

---

*These equations do not necessarily represent the actual reaction mechanism; they are used here only to illustrate the thermodynamic point being made.

separation relatively easy and inexpensive. Also, transfer of heat between hot product streams and cooler reactant streams requires relatively little gas-gas heat exchange, thereby minimizing the high capital costs and pressure drops associated with such operations.

There are major uncertainties, to be sure, associated with a proposed $CS_2/C/S$ storage subsystem, the primary one being the lack of kinetic data for the exothermic dissociation of CS_2 to carbon and sulfur. It is apparently not known whether this dissociation reaction occurs rapidly enough to be useful at the temperatures of interest here. Since the other aspects of the reaction offer the hope of an economical storage cycle, the preliminary process flowsheet and cost estimate presented above were constructed on the *assumption* that the dissociation kinetics will offer no insurmoutable technical or economic obstacles. This assumption may prove to be invalid; however, the attractive economics of the $CS_2/C/S$ cycle make such an assumption warranted for the preliminary study at hand.

Reactor design in both the endothermic and exothermic modes has been based on the assumption that reaction occurs at the surface of solid carbon particles contained in a packed or moving bed. Thus, in the endothermic mode, sulfur vapor enters the reactor, which is filled with hot carbon particles, reacts at the particle surface to form CS_2 and leaves the reactor as a mixture of S and CS_2. Conversely, in the exothermic mode, CS_2 enters the reactor, dissociates at the surface of the carbon particles to carbon, which remains on the particle, and sulfur which leaves the reactor along with unreacted CS_2. In both modes, it was assumed that reaction proceeded to 90% of the equilibrium conversion. In neither case was intra-particle diffusion a significant factor. The synthesis of CS_2 according to the above model is a well known process, and until about 1950 was the traditional industrial route. As stated above, the dissociation reaction has not been studied – both the mechanism and rate of this reaction have been assumed. Although the reactor is depicted as a counterflow, solid-gas reactor with intermediate heating and cooling stages, a more efficient design may use a quenching type reactor (Reference V1) into which "cold shots" of relatively cool (or relatively hot in the case of endothermic operation) reactant are injected at successive points along the reactor. Such a reaction scheme would allow efficient heating or cooling of a moving bed type reactor without the use of external heat exchangers. As in the $CaO/Ca(OH)_2$ reactor, direct-contact heat transfer is employed within the reactor bed itself.

It should not be forgotten that the entire C/CS_2 process design is based on a fundamental assumption about the kinetics of the CS_2 dissociation reaction. Without a doubt, validation of the process as an energy storage operation will require experimental study of the dissociation reaction as modeled.

4.4.4 The Di-Ammoniated $MgCl_2$ Energy Storage Subsystem

As stated earlier, it was originally the intent of this study to examined the feasibility of the following chemical reaction for storage applications:

$$MgCl_2 + NH_3 \rightleftharpoons MgCl_2 \cdot NH_3$$

Equilibrium thermodynamics (Reference R3, p. 102) indicates that the equilibrium vapor pressure of NH_3 for the mono-ammoniate is quite low in the range of temperature considered in this study. As in the case of the $CaO/Ca(OH)_2$ system, higher temperatures would produce equilibrium vapor pressures more conducive to storage system use, but it has been reported recently (Reference J3) that the mono-ammoniate system exhibited severe corrosion problems as well as apparent undesirable side reactions at these temperatures. In general, it is felt that much basic laboratory work remains to be done before this reaction can be considered seriously for storage applications at high temperature.

For the reasons discussed above, it was decided to carry out a preliminary process design for a storage system based on the di-ammoniate dissociation rather than the reaction originally planned. It was assumed for study purposes that no dissociation of mono-ammoniated $MgCl_2$ occurred anywhere in this process.

Process flowsheets for the endothermic and exothermic modes of the di-ammoniate design are presented in Figures 4-18 and 4-19. Important design specifications for the system are presented in Table 4-18, and efficiency and cost estimates based on the above designs are presented in Table 4-19.

The upper and lower bounds on power-related cost given above represent power-related equipment with and without stainless steel cladding where appropriate. Such cladding may or may not be necessary, depending on the outcome of further corrosion studies on this reaction.

The high energy related costs are due in part to the cost of the high pressure NH_3 storage tanks, and to the very high cost of purchasing the initial charge of $MgCl_2$.

4.4.5 The C_2H_4/C_2H_6 Energy Storage Subsystem

Figures 4-20 and 4-21 present preliminary process flowsheets for the endothermic and exothermic modes, respectively, of an energy storage subsystem based on the heading reaction. Important design specifications for this storage system are presented in Table 4-20, and performance and cost estimates based on the above designs are listed in Table 4-21.

For the present C_2H_4/C_2H_6 process design work, the simplifying assumption was made that a selective catalyst is available such that no side reactions occur in either the endothermic or exothermic modes. Both reactions will occur thermally without a catalyst. The endothermic reaction is widely used for manufacture of ethylene by noncatalytic pyrolysis; however, significant amounts of acetylene (Reference T1) and higher molecular weight compounds, such as propylene, are formed. Industrial ethane feed streams usually contain significant amounts of impurities, however, and the magnitude of the side-reaction problem with pure ethane feed streams is unknown. The exothermic reaction is catalyzed by nickel (M4) and cobalt x zeolite (Reference G4). Significant by-product formation in a CES system based on the C_2H_4/C_2H_6 reaction would cause complicated additional separation equipment to be required to remove these by-products. Such

AMMONIATED MgCl2 ENERGY STORAGE SUBSYSTEM
PRELIMINARY PROCESS FLOW SHEET
ENDOTHERMIC MODE ($MgCl_2 \cdot 2NH_3 \longrightarrow MgCl_2 \cdot NH_3 + NH_3$)
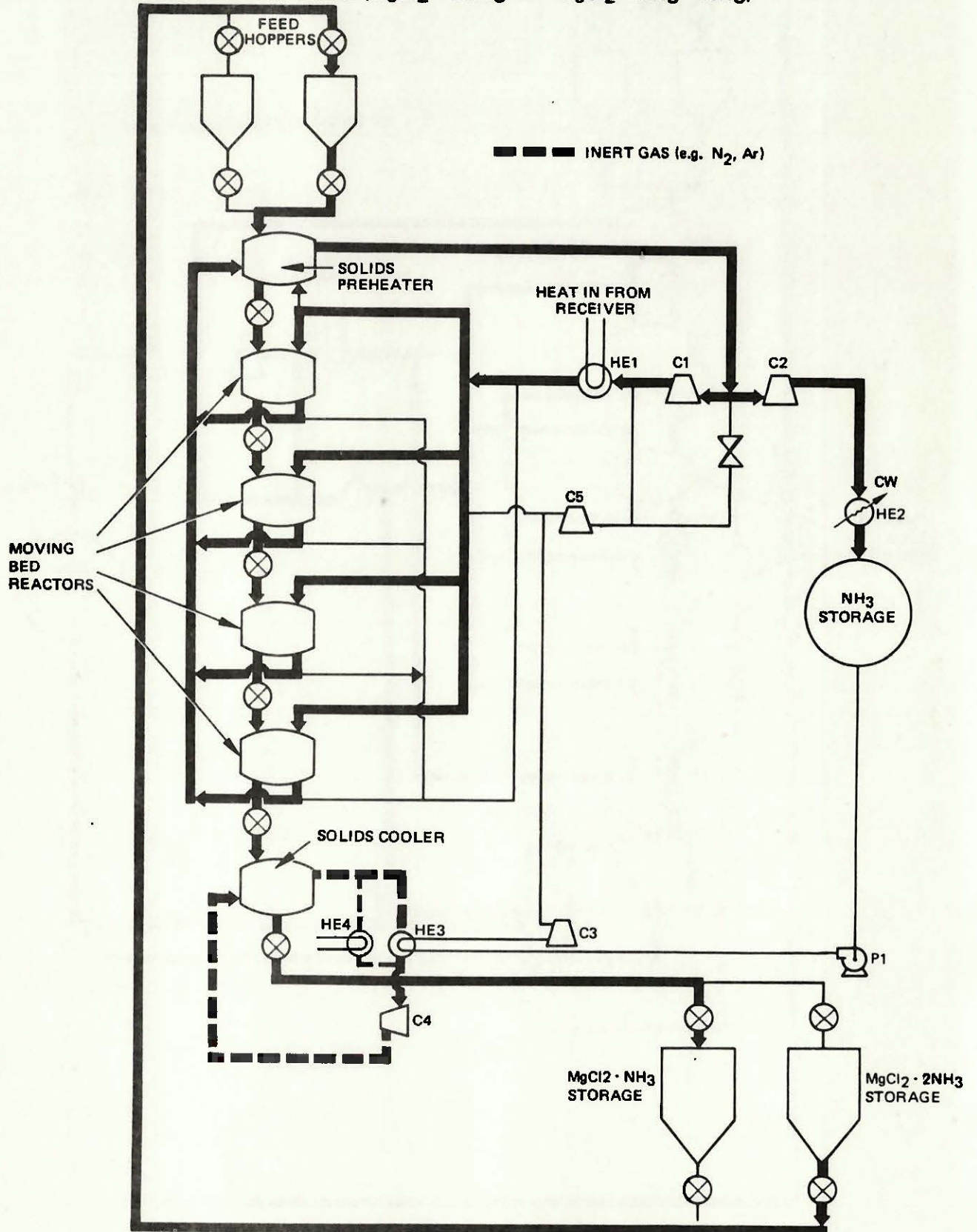
FEED HOPPERS

▬▬ ▬▬ ▬▬ INERT GAS (e.g. N_2, Ar)

SOLIDS PREHEATER

HEAT IN FROM RECEIVER

HE1   C1   C2

C5

CW
HE2

NH3 STORAGE

MOVING BED REACTORS

SOLIDS COOLER

HE4   HE3   C3

P1

C4

MgCl2 · NH3 STORAGE

MgCl2 · 2NH3 STORAGE

AMMONIATED MgCl₂ ENERGY STORAGE SUBSYSTEM
PRELIMINARY PROCESS FLOW SHEET
EXOTHERMIC MODE ($MgCl_2 \cdot NH_3 + NH_3 \longrightarrow MgCl_2 \cdot 2NH_3$)

FEED HOPPERS

INERT GAS (e.g. N₂, Ar)

SOLIDS PREHEATER

HEAT OUT TO TURBOGENERATOR

HE1 C1 C2

C5

CW
HE2

MOVING BED REACTORS

NH₃ STORAGE

SOLIDS COOLER

HE4 HE3 C3

P1

C4

MgCl₂ · NH₃ STORAGE

MgCl₂ · 2NH₃ STORAGE
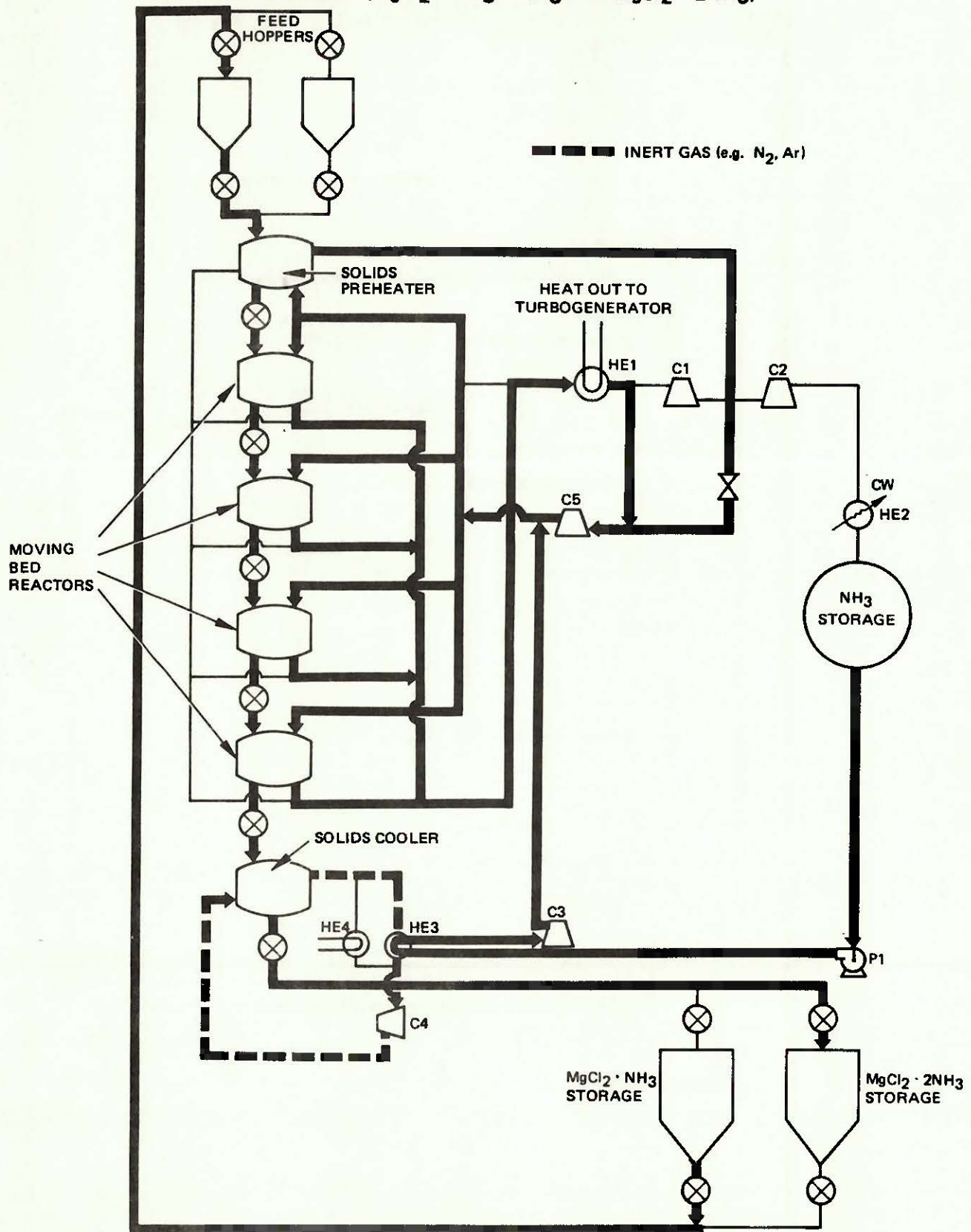
C_2H_4/C_2H_6 ENERGY STORAGE SUBSYSTEM
PRELIMINARY PROCESS FLOWSHEET
ENDOTHERMIC MODE ($C_2H_6 \longrightarrow C_2H_4 + H_2$)
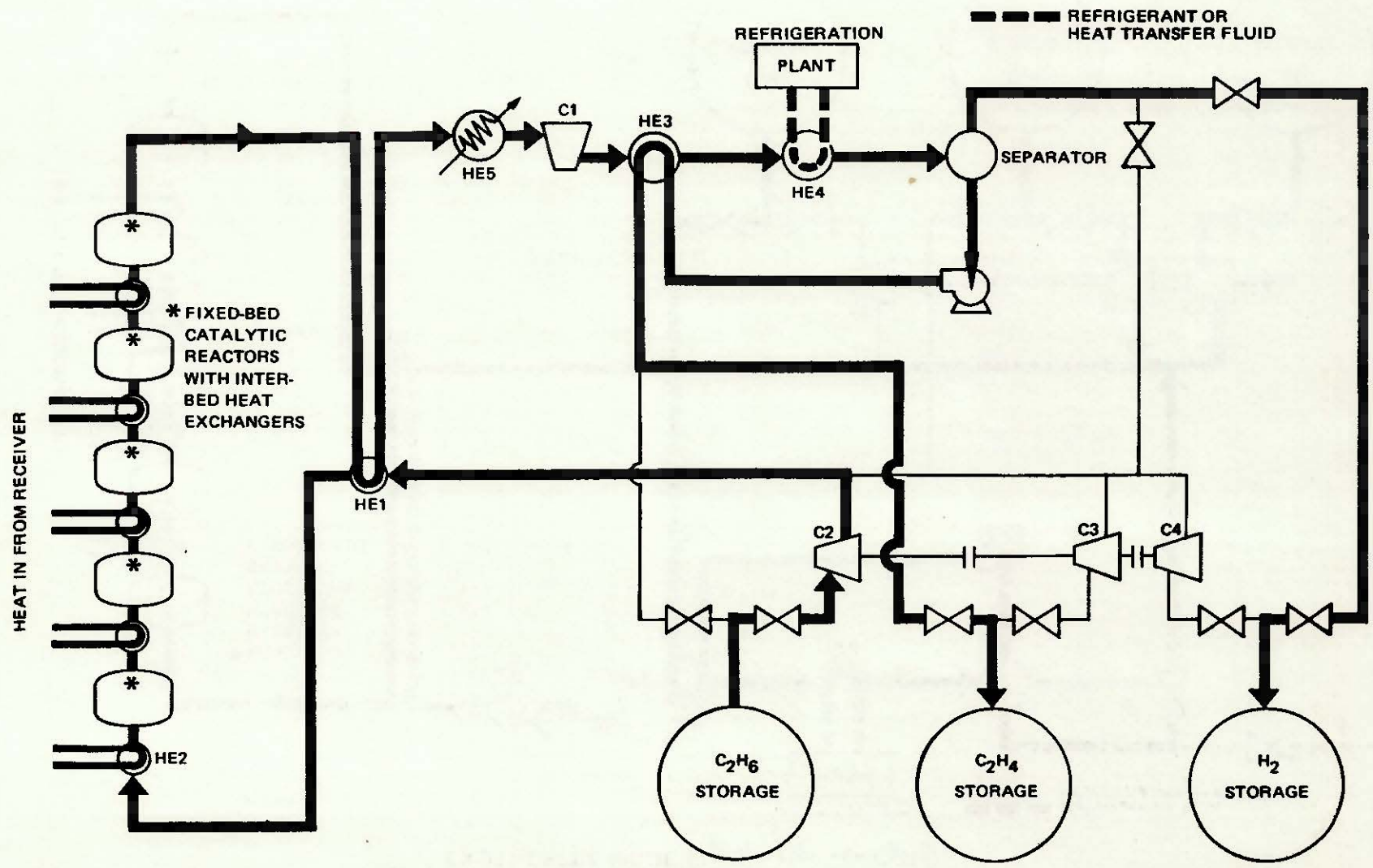
Figure 4-20

C2H4/C2H6 ENERGY STORAGE SUBSYSTEM
PRELIMINARY PROCESS FLOWSHEET
EXOTHERMIC MODE (C2H4 + H2 ⟶ C2H6)
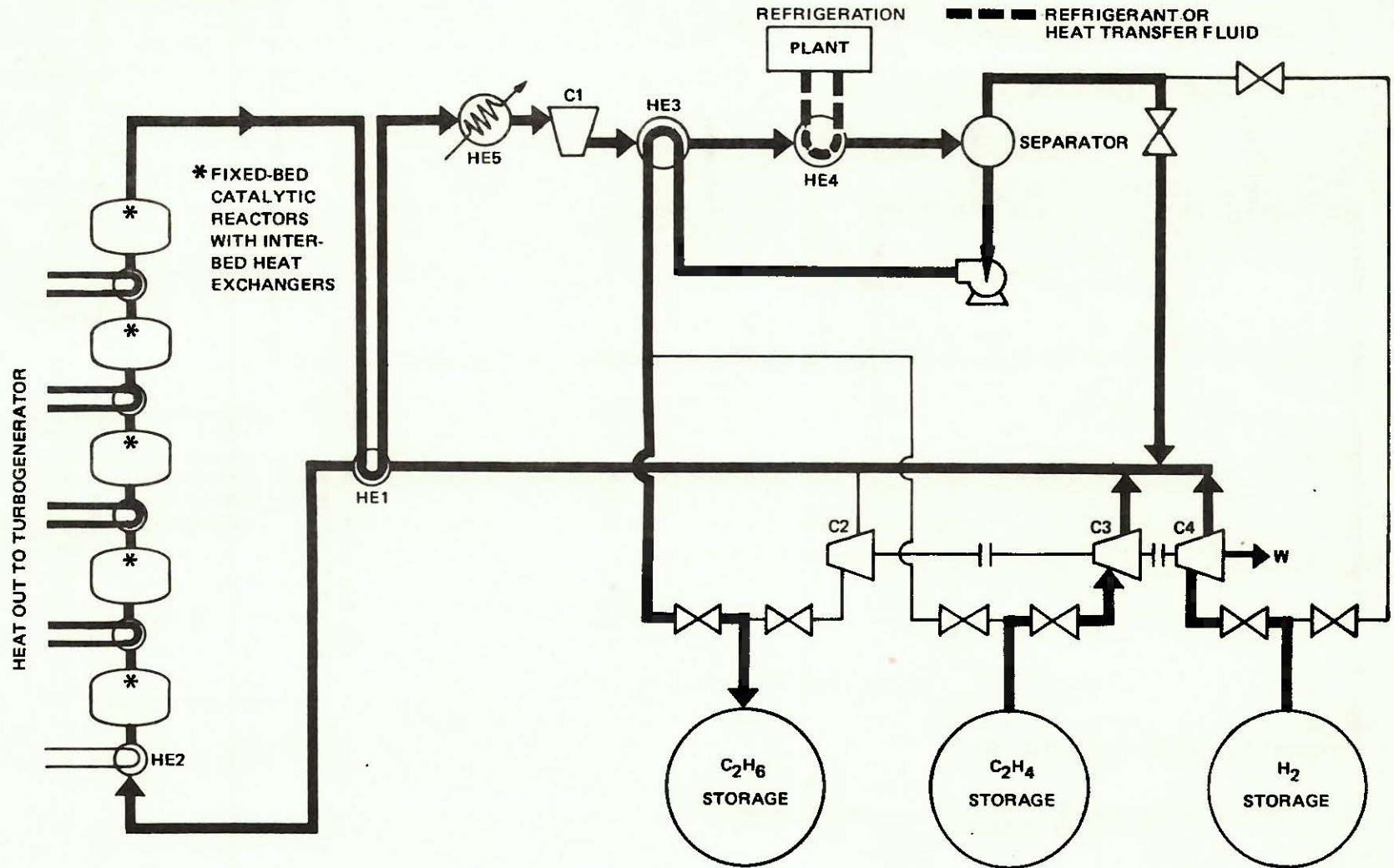
Table 4-18
DESIGN PARAMETERS FOR THE AMMONIATED $MgCl_2$ ENERGY STORAGE SUBSYSTEM

Temperature from receiver	783 K
Average endothermic reaction temperature	653 K
Average endothermic reaction pressure	1.5 bar
Temperature to turbogenerator	588 K
Average exothermic reaction temperature	598 K
Average exothermic reaction pressure	10 bar
Liquid NH_3 storage pressure	8.8 bar

Table 4-19
RESULTS OF DESIGN STUDIES OF THE AMMONIATED $MgCl_2$ ENERGY STORAGE SUBSYSTEM

Charging efficiency	0.43
Discharging efficiency	0.65
Round-trip efficiency	0.28
Power-related capital cost	$1.0 - 1.4 \times 10^5/MW_t$
Energy-related capital cost	$3.2 \times 10^3/MW_t\text{-hr}$

Table 4-20
DESIGN PARAMETERS FOR THE C_2H_4/C_2H_6 ENERGY STORAGE SUBSYSTEM

Temperature from receiver	1,310 K
Average endothermic reaction temperature	1,166 K
Average endothermic reaction pressure	1.1 bar
Temperature to turbogenerator	950 K
Average exothermic reaction temperature	990 K
Average exothermic reaction pressure	40 bar
H_2 storage pressure	177 bar

Table 4-21
RESULTS OF DESIGN STUDIES OF THE C_2H_4/C_2H_6 ENERGY STORAGE SUBSYSTEM

Charging efficiency	0.49
Discharging efficiency	0.78
Round-trip efficiency	0.38
Power-related capital cost	$1.0 \times 10^5/MW_t$
Energy-related capital cost	$12.4 \times 10^3/MW_t\text{-hr}$

equipment would undoubtedly decrease the round-trip efficiency of the CES system and add significantly to its cost. In addition, substantial make-up streams might be required to replace reactants lost by irreversible by-product formation.

Both the charging and discharging efficiencies of the C_2H_4/C_2H_6 storage system are less than those of the C_6H_6/C_6H_{12} system to be discussed below. This difference is due primarily to the greater difficulty of separation of reaction products in the C_2H_4/C_2H_6 system. The cause of this difficulty lies in part in the fact that the critical temperatures of ethylene ($T_c = 283$ K) and ethane ($T_c = 305$ K) are near or below the generally accepted minimum temperature of ordinary cooling water (294 K). Therefore, liquefaction of even a pure ethane stream requires refrigeration. In addition, the partial pressures of these gases are reduced for both the endothermic and exothermic modes by the presence of "noncondensable" hydrogen, with the result that the temperature necessary for separation of the hydrocarbon fractions by liquefaction is further reduced. This effect is particularly important in the endothermic mode, in which the reactor exit stream is 47 mole percent hydrogen.

For the present process design, a refrigeration plant was specified which provided cooling to 239 K, with a coefficient of performance of 2.6. Even with such low temperatures available, considerable compression of the reaction products stream was necessary to achieve the design value of 90 percent liquefaction of the hydrocarbon fractions. In the endothermic mode, compression of the reaction products stream to 177 bar was required, and the hydrogen (along with a small amount of hydrocarbon vapor) was stored at this pressure. While refrigeration was required for liquefaction in the exothermic mode, compression above the reaction pressure of 40 bar was not necessary.

The work required to drive the refrigeration plant, and the work required to compress the reaction products stream to accomplish liquefaction in the endothermic mode, were the most important causes of inefficiency in the storage process. While some of these parasitic work requirements could have been eliminated by simply compressing and storing the reaction product mixture without separation, it was deemed unwise to store a potentially detonable, stoichiometric mixture of hydrogen and ethylene at high pressure.

The reactors in Figures 4-20 and 4-21 are intended to be packed-bed, catalytic reactors with a catlayst which is active in both the endothermic and exothermic modes. For the purposes of performance and cost estimation, the reactors have been treated as a series of ten adiabatic, fixed-bed reactors with inter-bed heat exchangers (although the schematic illustration shows only five reactors in the train). An optimum design may require that the heat exchangers be within the catalyst beds, but the more straightforward cost and performance estimates used here are adequate for a preliminary process design.

As expected, energy-related capital costs are quite high for this reaction, with the greatest part of these costs due to the hydrogen storage vessels. The most expensive power-related component in the

present design is the reactor train, which accounts for approximately 50 percent of the power-related capital costs.*

4.4.6 The C_6H_6/C_6H_{12} Energy Storage Subsystem

The preliminary process design for a storage system based on the heading reaction is presented schematically in Figures 4-22 and 4-23. Important design specifications for this storage system are presented in Table 4-22, and performance and cost estimates based on the above design are presented in Table 4-23.

Table 4-22
DESIGN PARAMETERS FOR THE C_6H_6/C_6H_{12}
ENERGY STORAGE SUBSYSTEM

Temperature from receiver	588 K
Average endothermic reaction temperature	566 K
Average endothermic reaction pressure	1.1 bar
Temperature to turbogenerator	588 K
Average exothermic reaction temperature	610 K
Average exothermic reaction pressure	37 bar
H_2 storage pressure	68 bar

Table 4-23
RESULTS OF DESIGN STUDIES OF THE C_6H_6/C_6H_{12}
ENERGY STORAGE SUBSYSTEM

Charging efficiency	0.55
Discharging efficiency	0.88
Round-trip efficiency	0.48
Power-related capital cost	$0.8 \times 10^5/MW_t$
Energy-related capital cost	$11.1 \times 10^3/MW_t$

As in the ethane/ethylene design, it was assumed that no side reactions (e.g., formation of methylcyclopentane) occur to any appreciable extent. Differences in power and energy-related capital costs between the C_2H_4/C_2H_6 and C_6H_6/C_6H_{12} systems are primarily reflections of their different efficiencies.

---

*Catalyst costs are not included in the C_2H_4/C_2H_6 or $C_6/H_6/C_6H_{12}$ cost estimates discussed herein. This reactor cost includes and is dominated by the inter-bed heat exchanger costs. As in the case of the solid/gas, noncatalytic reactions, heat transfer between storage and the rest of the solar plant is a major capital cost item.

C_6H_6/C_6H_{12} ENERGY STORAGE SUBSYSTEM
PRELIMINARY PROCESS DESIGN
ENDOTHERMIC MODE ($C_6H_{12} \longrightarrow C_6H_6 + 3H_2$)
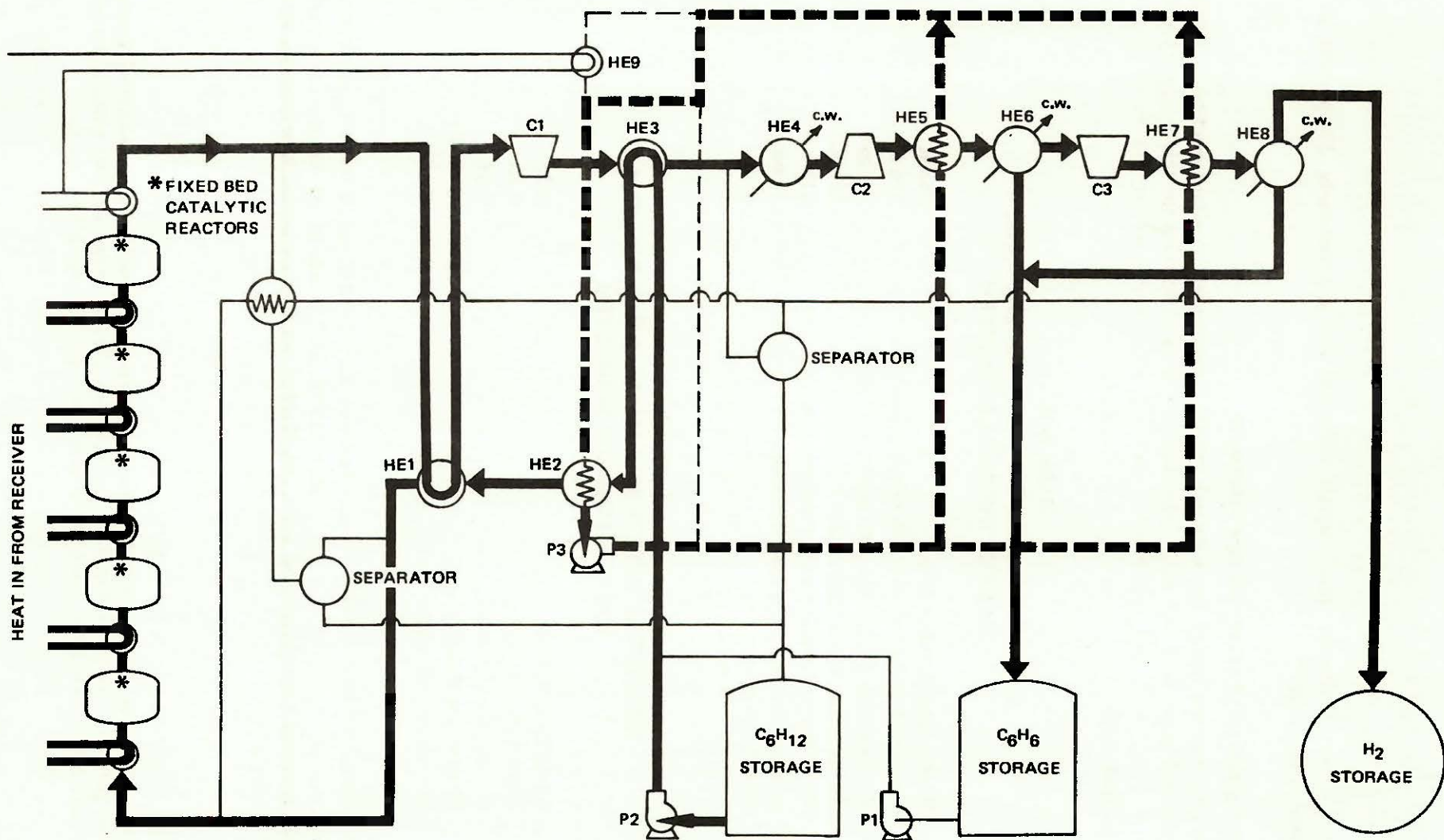
Figure 4-22

29017-42(1)

4-64

C_6H_6/C_6H_{12} ENERGY STORAGE SUBSYSTEM
PRELIMINARY PROCESS DESIGN
EXOTHERMIC MODE ($C_6H_6 + 3H_2 \longrightarrow C_6H_{12}$)
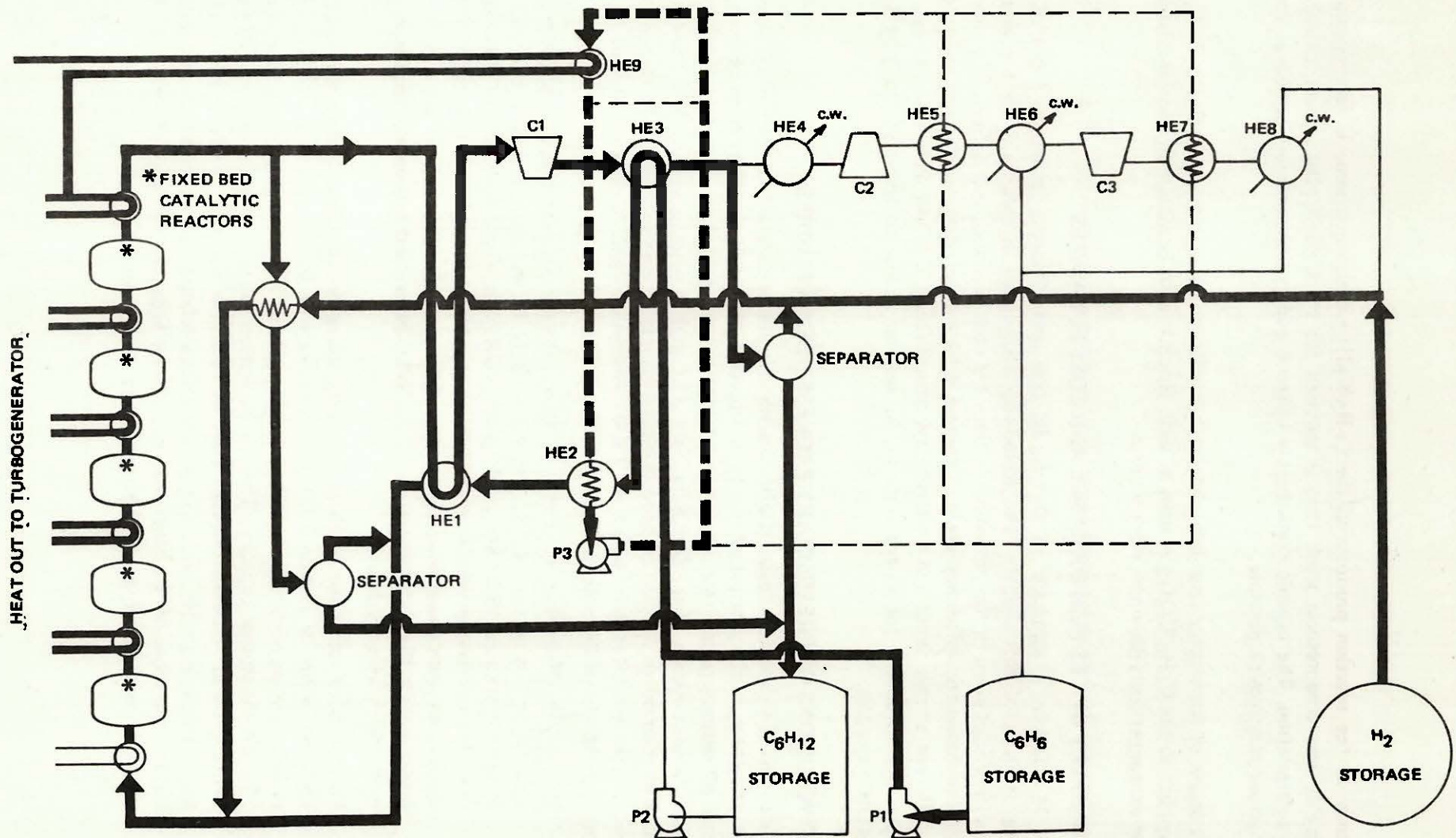
Separation of the reaction products in the C_6H_6/C_6H_{12} reaction scheme is accomplished with considerably less compression work than is required for the C_2H_4/C_2H_6 system, and does not require refrigeration. The organic constituents benzene and cyclohexane are stored as liquids at slightly above atmospheric pressure.

The discussion of the reactor cost and performance estimate discussed for the C_2H_4/C_2H_6 system above applies to the C_6H_6/C_6H_{12} system as well. Reactor costs dominate the power-related costs, and heat exchanger costs dominate reactor costs.

4.5 SUMMARY OF CES PERFORMANCE AND COST ESTIMATES

Table 4-24 contains a summary of the capital cost and efficiency estimates reported in the preceding sections of this chapter. The round-trip efficiencies in column 3 are the thermal-to-thermal efficiencies given in the preceding sections for each reaction, and defined in section 4.1.2. The values of round-trip efficiency given in column 4 have been corrected for availability changes due to different storage input and output temperatures (section 4.2.4). Power and energy-related unit costs were estimated for all reactions in the manner similar to those of the SO_2/SO_3 and $CaO/Ca(OH)_2$ systems.

4.6 CONCLUSIONS OF PRELIMINARY PROCESS DESIGN STUDIES

The conclusions of the process design studies described in this section are not easily tied together by narrative; therefore, in the interest of clarity and brevity, they will simply be listed. For expanded discussion of various points, the reader is referred to the preceding sections of this chapter, particularly the discussions of the SO_2/SO_3 and $CaO/Ca(OH)_2$ systems in sections 4.2 and 4.3. The reader is also referred to the list of process design assumptions in section 4.1.3. The conclusions presented below are ultimately based on these assumptions and, therefore, limited by them. Important conclusions of the process design studies include:

1. Round-trip efficiencies of chemical energy storage systems designed according to the assumptions of section 4.1.3, will most likely be less than 0.5, with the most likely candidate systems (SO_2/SO_3 and $CaO/Ca(OH)_2$) having efficiencies of approximately 0.35. Efforts to improve these efficiencies should concentrate on integration of the CES subsystems with other processes which could act as heat sources or sinks; such process might include the turbogenerators of the STEC plant itself, adjoining chemical processes, or district heating systems.

2. Power-related unit costs of chemical energy storage systems (again, designed according to the assumptions of section 4.1.3) will most likely be greater than $\$1 \times 10^5/MW_t$ charging capacity. Energy-related unit costs of such systems will most likely be greater than $\$1 \times 10^3/MW_t$-hr storage capacity. The one exception to these statements, the C/CS_2 system, is discussed in 7. below. Storage systems based on reactions involving noncondensible constituents (e.g., H_2, O_2, CO_2) have energy-related unit costs which are very much higher than those of the other reactions. These high costs are due, of course, to the high capital investment required for high pressure storage vessels.

CHAPTER 5
CONCLUSIONS

Conclusions of the systems studies and process design sections of this report, presented previously in sections 2.5 and 4.6, respectively, are repeated here for convenience and completeness.

Conclusions of STEC Systems Analysis

1. The autonomous solar thermal electric conversion plant which uses the SO_2/SO_3 reaction for seasonal storage does not economically compete with a hybrid plant which has an alternate energy source available to it, based solely on BBEC. Supplying all of the demand with solar energy was found to be 20 to 80 percent more expensive than supplying the demand partly from the sun and partly from alternate energy sources. This is due to the fact that it is cheaper to purchase backup energy, even at fairly high unit costs, than to build solar components which are used at full capacity only infrequently. A storage system with much lower energy-related unit cost would make such competition much closer.

2. Optimum storage requirements for autonomous STEC power plants which satisfy continuous baseloads are in the range of 100 to 400 hours.

3. Optimum storage requirements for hybrid STEC power plants which satisfy continuous baseloads are in the range of 20 to 30 hours, for a levelized alternate energy cost of $0.400/kWh.

4. In all autonomous and most hybrid cases of interest, the yearly maximum storage charging rates are greater than the maximum discharging rates, with the ratio of these quantities varying between approximately six for the best hybrid case and eighteen for the worst autonomous case. The maximum storage charging rate is, therefore, size determining for power-related storage process equipment used in both the endothermic and exothermic modes.

5. As could be expected under consistent assumptions for the Florida and Wisconsin simulations, the solar plant is more economically attractive in Florida. The Wisconsin system requires much more storage for both hybrid and autonomous operation that does the plant in Florida.

6. The concept of energy discard is important to the optimal design of any solar plant, hybrid or autonomous. The results presented herein underscore the desirability of oversizing or undersizing subsystems to obtain better utilization factors for the plant as a whole. This approach leads to lower busbar energy costs than designs which utilize all the energy collected. Use of discard energy and/or reject process heat from the storage subsystem, in a "total energy" application, may therefore be an attractive option.

The general applicability of these conclusions is of course limited by the many assumptions of efficiency and cost of various subsystems and components on which the model is based. Two key limitations of the systems studies described above bear mentioning:

1. The use throughout the study of heliostat and receiver unit costs of $90/m^2 and $50/m^2, respectively.

2. The use of only one storage subsystem model (SO_2/SO_3).

In view of the capital equipment cost breakdown of Tables 2-7 and 2-8, large increases or decreases in the front-end unit cost parameters would undoubtedly change the optimum busbar energy costs, collector areas, and storage capacities for both autonomous and hybrid STEC plants, and might substantially alter the solar/alternate mix of the optimum hybrid solutions. Similarly, a storage subsystem model based on a different reversible chemical reaction, with different charging and discharging efficiencies and different power and energy-related unit costs, might substantially alter the character of both the autonomous and hybrid solutions. For example, a $CaO/Ca(OH)_2$ storage subsystem model (section 4.3) with very low energy-related costs might cause the optimizer to choose a hybrid case solution with a substantially longer storage time than the 15 to 30 hours it chose for the SO_2/SO_3 cases.

Conclusions of Preliminary Process Design Studies

At the outset, the reader is referred to the list of process design assumptions in section 4.1.3. The conclusions presented below are ultimately based on these assumptions, and therefore limited by them.

1. Round-trip efficiencies of chemical energy storage systems designed according to the assumptions of section 4.1.3, will most likely be less than 0.5, with the most likely candidate systems (SO_2/SO_3 and $CaO/Ca(OH)_2$) having efficiencies of approximately 0.35. Efforts to improve these efficiencies should concentrate on integration of the CES subsystems with other processes which could act as heat sources or sinks: such processes might include the turbogenerators of the STEC plant itself, adjoining chemical processes, or district heating systems.

2. Power-related unit costs of chemical energy storage systems (again, designed according to the assumptions of section 4.1.3) will most likely be greater than $1 \times 10^5/MW_t$ charging capacity. Energy-related unit costs of such systems will most likely be greater than $1 \times 10^3/MW_t$-hr storage capacity. The one exception to these statements, the C/CS_2 system, is discussed in 7. below. Storage systems based on reactions involving noncondensible constituents (e.g. H_2, O_2, CO_2) have energy-related unit costs which are very much higher than those of the other reactions. These high costs are due, of course, to the high capital investment required for high pressure storage vessels.

3. A major design difficulty in all the energy storage systems studied was efficient heat transfer into and out of the reactor, and efficient heat transfer between reactant and product streams. This problem is severe in the systems which use solid reactants, and causes such systems to have very high gas circulation rates through the reactor, large and

expensive gas/gas heat exchangers for recuperation, and high compressor costs and compression work requirements.

4. The heat transfer problems, mentioned in 3., associated with solid/gas noncatalytic reactions result in an uncommon reactor design; the suggested reactor design for such reactions is a moving-bed type, with direct heat transfer, and radial flow in the gas phase.

5. For the reasons mentioned in 3., energy storage systems based on solid/gas noncatalytic reactions generally exhibit lower round-trip efficiencies than those based on the catalytic reactions considered.

6. Required storage input temperatures for all the process designs considered were higher than expected from the "turning" temperatures listed in Table 3-5, and in several cases, storage output temperatures required for most efficient storage system operation were substantially lower than the input temperatures. These temperature differences were due primarily to consideration of heat transfer limitations within the storage system. Earlier estimates of storage input and output temperatures were based solely on equilibrium thermodynamics. While all CES systems can be designed to discharge energy at the same temperature at which it was charged, such designs are in many cases far less efficient, far more costly, or both, than designs in which the output temperature is substantially lower than the input temperature.

7. The C/CS_2 system is apparently a promising one according to the preliminary process design, but it must be remembered that its design was based on several key assumptions. Any further study of the C/CS_2 reaction for energy storage applications should attempt first to verify or reject those assumptions. In all likelihood, reliable kinetic information, even if it indicates that the reaction will proceed as modeled here, will cause the estimated round-trip efficiency to decrease substantially, causing the unit costs to increase as well.

The CES system efficiencies of 0.20 to 0.50 which resulted from the process design studies described in Chapter 4 are well below earlier estimates based primarily on equilibrium thermodynamics; these estimates are also well below those for current designs of sensible heat storage subsystems. Moreover, the results of the systems studies of Chapter 2 indicate that optimum storage times (capacities) for the hybrid STEC plants are in the range (20 to 30 hours) in which sensible or latent heat storage systems may be technically competitive with the CES systems. It is not the purpose of the present research effort to compare, in detail, CES with other types of energy storage. However, it appears that from the point of view of efficiency or storage duration, CES offers no clear advantage over the sensible heat storage systems now under consideration for short-term storage in STEC applications. This conclusion must be qualified: it applies only to CES subsystems which interact with their environment in the limited sense described in section 4.1.3. Integration of CES systems with other processes such as adjoining chemical plants, district heating systems or the turbogenerator of the STEC plant itself may considerably improve the overall efficiency of the integrated system, and make CES a more attractive energy storage option. CES systems, of course, remain the only option for the very long storage times required of autonomous STEC plants.

CHAPTER 6
RECOMMENDATIONS FOR FURTHER WORK

While the overall results of this study may have removed some of the glitter from the concept of long-term CES which helped initiate it, the promise of using reversible chemical reactions for energy storage/transport has by no means been eliminated. Finances and time necessarily limited the scope of the present study, and it is hoped that the (sometimes arbitrary) constraints which limited the applicability of the preceding results and conclusions have been clearly and consistently stated in this report. Beyond these constraints, several areas of research beckon, and several of the more promising ones are listed below.

1. Examine the potential advantage of thermal integration of CES systems with other processes which act as heat sources or sinks. An immediate candidate for such integration is the STEC power cycle, especially if it is a steam-Rankine cycle: small vapor streams bled from the turbine at intermediate points might provide needed process heat for the storage subsystem. Other possibilities include sale of low grade, reject process heat to district heating systems or to other chemical processes.

2. Examine the potential advantage of mass flow between CES systems and other chemical processes. Potential "open" systems might span the range from solar fired chemical processes with very little energy storage capability to energy storage subsystems which exchange mass with their surroundings only to replenish some reactant which has been lost or rendered unusable.

3. Study experimentally the effects of reaction cycling and agitation on the physical integrity of solid reaction constituents, particularly CaO and $Ca(OH)_2$. The results of such studies would provide a better understanding of the extent of the solids – breakup problem (and of the need for solids regeneration or replacement) in storage subsystems based on solid/gas, noncatalytic reactions. The particle size, density, and resulting pore structure required for mechanical stability of the solid reactant particles, determined by such a study, would greatly affect the inter- and intra-particle heat and mass transfer limitations which would have to be considered in any detailed reactor design, moving-bed or otherwise. Information about the mechanical stability of various particle sizes and types would also prove indispensable in evaluating the feasibility of fluidized bed reactor designs.

4. Some further study of the C/CS_2 reaction is justified, specifically an experimental study of the kinetics of noncatalytic dissociation of CS_2.

5. An evaluation of the economic and technical feasibility of a storage-dedicated receiver, separate from the receiver dedicated to direct power production, is warranted. These two receivers would be mounted on the same tower, but would produce energy at the temperatures and pressures most suited for the particular subsystem to which they were dedicated. The need for such a storage-dedicated receiver is due to the very specific input temperature requirements of CES systems, and at least one justification for it lies in the very high, maximum storage charging rates required in all STEC applications considered in Chapter 2.

6.   The technical and economic feasibility of using reversible chemical reactions for energy transport within distributed STEC power plants should be examined. Such "chemical heat pipe" systems might or might not be coupled with a chemical energy storage subsystem. The approach to such a study should be similar to the present one, with equal emphasis on technical and economic considerations.

7.   Fairly detailed economic analysis, including systems studies like those described in Chapter 2. should be made an integral part of future studies designed to evaluate various alternative subsystem designs or technical innovations in STEC applications. The complex interplay between parts of STEC systems is not easily discerned, especially in view of the large variation in cost projections for various components, and can lead to unexpected results. The large number of important parameters in any acceptable system model makes modeling and analysis by computer an indispensable tool.

REFERENCES

A1 American Society of Heating, Refrigeration, and Air Conditioning Engineers, "ASHRAE Handbook of Fundamentals," Chapter 22 (1972)

B1 Black and Veatch Consulting Engineers, "Solar Thermal Conversion to Electricity Utilizing a Central Receiver, Open Cycle Gas Turbine," EPRI Report Number ER-387-SY, March 1977

B2 Boeing Engineering and Construction, "Closed-Cycle High Temperature Central Receiver Concept for Solar Electric Power," EPRI Report Number RP377-1, June 1976

B3 Brammert, K., Rurik, J., and Griepentrog, H., Trans. of ASME, (ASME Paper No. 74-GT-7), October 1974

B4 Boes, E. D., "Estimating the Direct Component of Solar Radiation," Sandia Laboratories Report SAND 75-0565, November 1975

B5 Boes, E. D., et. al., "Distribution of Direct and Total Solar Radiation Availabilities for the USA," Sandia Laboratories Report No. SAND 76-0411, August 1976

B6 Brune, J. M., "BUCKS – Economic Analysis Model of Solar Electric Power Plants," Sandia Laboratories Report SAND 77-8279, January 1978

B7 Bauerle, G., Chung, D., Ervin, G., Guan, J., and Springer, T., "Storage of Solar Energy by Inorganic Oxide/Hydroxides," presented at the Joint Conference 1976 of the American Section of the International Solar Energy Society and the Solar Energy Society of Canada, Inc., August 15th – 20th, 1976

B8 Britton, H. T. S., Gregg, S. J., and Winsor, G. W., "The Calcination of Dolomite," Trans. Faraday Soc., 48, 63 (1952)

C1 Chubb, T. A., "Analysis of Gas Dissociation Solar Thermal Power System," Solar Energy, 17, 129–136 (1975)

C2 Chubb, T. A., "Gas Dissociation Thermal Power System," U.S. Patent 3,972,183 (April 17, 1975/August 3, 1976)

D1 Daniels, F., Direct Use of the Sun's Energy, Yale University Press, New Haven (1964)

D2 Doane, J. W., et. al., "The Cost of Energy from Utility-Owned Solar Electric Systems," JPL Report No. 5040-29, June 1976

E1   Easton C. R., Raetz, J. E., Vant-Hull, L. L., "Collector Field Design for a Central Receiver Solar Thermal Power Plant," in Sharing the Sun! Solar Technology in the Seventies, Volume 5, p. 374 (1976)

E2   Ervin G. Jr., Chung, D. K., and Springer, T. H., "A Study of the Use of Inorganic Oxides for Solar Energy Storage for Heating and Cooling of Buildings," Final Report under NSF Grant AER74-09069-A01, Report No.: NSF/RANN/SE/GI-44126/FR/75/2, October 1975

G1   Gintz, J. R., "Technical and Economic Assessment of Phase Change and Thermochemical Advanced Thermal Energy Storage (TES) Systems," Final Report, Volume IV, Boeing Engineering and Construction, EPRI Report No. EM-256, December 1976

G2   General Electric Co., "Heat Rates for Fossil Reheat Cycles Using General Electric Steam Turbine Generators 150 kW and Larger," Publication No. GET-2050C, (1974)

G3   Guthrie, K. M., "Process Plant Estimating Evaluation and Control," Craftsman Book Company of America, Solana Beach, CA (1974)

G4   Gryaznova, Z. V. and Kolodieva, E. V., "Kinetics of Ethylene Hydrogenation on Cobalt X Zeolite," Dokl. Akad. Navk SSSR 1970, 190(6), 1383-6

H1   Hildebrandt, A. F. and Vant-Hull, L. L., "A Tower-Top Focus Solar Energy Collector," Mechanical Engineering, 96(9), 23 (1974)

H2   Hougen, O. A., Watson, K. M., and Ragatz, R. A., "Chemical Process Principles," Part II, 2nd Ed., John Wiley & Sons (New York), p. 982, (1959)

I1   Iannucci, J. J., Smith, R. D., and Swet, C. J., "Energy Storage Requirements for Autonomous and Hybrid Solar Thermal Electric Power Plants," presented at the International Solar Energy Congress, New Delhi, India, January 1978 (to be published in the Proceedings).

I2   Iannucci, J. J., "Goals of Chemical Energy Storage," Proceedings of Focus on Solar Technology: A Review of Advanced Solar Thermal Power Systems, Denver, November 1978

I3   Iannucci, J. J., "Systems Impact of Thermochemical Energy Storage for Solar Applications," Proceedings of Third Annual Storage Contractors' Information Exchange Meeting, Springfield, VA, December 5-6, 1978

I4   Iannucci, J. J., "The Value of Seasonal Storage of Solar Energy," Proceedings of the Applications Workshop on Thermal Storage Integrated into Solar Power Plants, February 1978

I5   Iannucci, J. J. and Eicker, P. J., "Central Solar/Fossil Hybrid Electrical Generation: Storage Impacts," Proceedings of the Annual Meeting of the American Section of the International Solar Energy Society, Denver, August 1978

J1 Jarvinian, P. O., "Solar Heated-Air Turbine Generating Systems," in Proc. 10th Intersoc. Energy Conv. Eng. Conf., University of Delaware (Aug. 17–22, 1975), Institute of Electrical and Electronics Engineers, Inc., New York (1975)

J2 Jefferson, T. H., "User's Guide to the Sandia Mathematical Program Library at Livermore," Sandia Report Number SAND77-8274 (October 1977)

J3 Jaeger, F. A., et. al., "Development of Ammoniated Salts Thermochemical Energy Storage Systems," Phase IB Final Report, May 1978. Report No. SAN/1229-1, May 1978

L1 Leary, P. L. and Hankins, J. D., "A User's Guide for MIRVAL – A Computer Code for Comparing Designs of Heliostat-Receiver Optics for Central Receiver Solar Power Plants," Sandia Laboratories Report No. SAND 77-8280, February 1979

M1 MacDonnell-Douglas, Inc., Semi-Annual Review, presented at the ERDA Solar Thermal Projects Semi-Annual Review Meeting, Seattle, Washington, August 23, 1977

M2 Martin-Marietta Corp., Topical Report: "Development of Ammoniated Salts Thermochemical Energy Storage Systems, Phase 1, Task 3, Salt Kinetics," Contract No. E(04-3)-1229, September 1976

M3 Mikhail, R. S., Brunauer, S., and Copeland, L. E., "Kinetics of the Thermal Decomposition of Calcium Hydroxide," J. Colloid Interface Sci, 21, 394-404 (1966)

M4 Matsuzaki, I., et al: "Kinetics of the Nickel-Catalyzed Hydrogenation of Ethylene and its Variation With Catalyst Poisoning," J. Res. Inst. Catal., Hokkaido Univ., 16(2), 543-54 (1968)

N1 National Oceanic and Atmospheric Administration, "Hourly Solar Radiation-Surface Meteorological Observations," Solmet Final Report, Volumes I and II (TD-9724), February 1979

P1 Prengle, H. W. and Sun, C. H., "Operational Chemical Storage Cycles for Utilization of Solar Energy to Produce Heat or Electric Power," Solar Energy 18, 561-7 (1976)

P2 Personal Communication with Members of Sandia Laboratories, Livermore, Systems Studies Division III

P3 Personal Communication with Jim Leonard, Sandia Laboratories, Albuquerque

P4 Peters, M. S. and Timmerhaus, K. D., "Plant Design and Economics for Chemical Engineers," 2nd edition, McGraw Hill, p. 97 (1968)

P5 Pechkovskii, V. V., Zvesdin, A. G., and Beresneva, T. I., "Kinetics of Thermal Decomposition of Magnesium, Zinc, Copper, and Cobalt Sulfates," Kinetica i Kataliz, 4 (13), 208 (1963)

R1   Randal, C. M. and Whitson, M. E., "Hourly Insolation and Meteorological Data Bases Including Improved Direct Insolation Estimate," Sandia Laboratories Report No. SAND 78-7047, December 1977

R2   Rocket Research Company, "Chemical Energy Storage for Solar-Thermal Conversion," Interim Report No. 1 (76-R-538), prepared for the National Science Foundation under Grant No. AER-75-22176

R3   Rocket Research Company, "Chemical Energy Storage for Solar-Thermal Conversion," Interim Report No. 2 (77-R-558), prepared for National Science Foundation under Grant No. AER-75-22176

R4   Rocket Research Company, "Reversible Chemical Reactions for Electrical Utility Energy Applications," Final Report, EPRI Contract TPS-76-658, April 1, 1977

S1   Schmidt, E. W., "Reversible Chemical Reactions for Heat Storage," German Society of Engineers (Verein Deutscher Ingienieure) Conference: "Rational Energy Utilization by Energy Storage," October 10–11, 1977, Stuttgart, West Germany, VDI Berichte, Vol. 288, p. 115–125

S2   Schmidt, E. W. and Lowe, P., "Thermochemical Energy Storage Systems," 11th Intersociety Energy Conversion Engineering Conference, Vol. I, p. 665–672, Paper 769116; A77-12738, (1976)

S3   Sandia Project Division 8132, "Recommendations for the Conceptual Design of the Barstow, California, Solar Central Receiver Pilot Plant — Executive Summary," Sandia Laboratories Report No. SAND 77-8035, October 1977

S4   Smith, J. M., "Chemical Engineering Kinetics," 2nd ed., McGraw Hill (New York) p. 576, 1970

S5   Shen, J. and Smith, J. M., Ind. Eng. Chem. Fund. Quart., 4, 293 (1965)

S6   Stull, D. R. and Prophet, H., "JANAF Thermochemical Tables," National Bureau of Standards, NSRDS-NBS 37, U. S. Government Printing Office (June 1971)

S7   Schmidt, E. W., "Development of a Long-Life, High-Temperature Catalyst for the SO_2/SO_3 Energy Storage System," RRC contract (in progress) with Sandia Laboratories, Livermore (No. SAN87-9119); Proceedings, Third DOE Storage Contractors Information Exchange Meeting, Arlington, VA (1978)

T1   Thomas, C. L., "Catalytic Processes and Proven Catalysts," Academic Press (New York) 1970, p. 42

V1   Vancini, C. A., "Synthesis of Ammonia," MacMillan Press, Ltd., London, p. 136 (1971)

W1   Wentworth, W. E. and Chen, E., "Simple Thermal Decomposition Reactions for Storage of Solar Thermal Energy," Solar Energy 18, 205-14 (1976)

J. Peerson
Argonne National Laboratory
Building D-362
Argonne, Illinois 60439

Canada Institute for STI
Library Serial ACO
National Res. Council
Ottawa, CANADA K1A0S2

Head Office
Central Mortgage and Housing Corp.
Ottawa KIA 097, CANADA
Attn: P. Favot
      J. Wadsworth

Erhard Modinger
In Den Backenlandern
7056 Weinstadt-Strumpfelbach
CHEMOWERK
WEST GERMANY

Dr. T. Rose
EIC Corporation
55 Chapel Street
Newton, Massachusetts 02158

Electric Power Research Institute
P. O. Box 10412
Palo Alto, California 94304
Attn: A. Fickett
      B. Mehta
      T. Schneider

General Electric
Corporate Research and Development
Schenectady, New York 1201
Attn: J. B. Comly
      J. W. Flock
      H. B. Vakil

Gilbert Associates, Inc.
P. O. Box 1498
Reading, Pennsylvania 19603
Attn: H. Chen
      J. Stewart

Jet Propulsion Laboratory
4800 Oak Grove Drive
Pasadena, California 91103
Attn: J. C. Becker
       C. England
       T. Fujita
       L. P. Leibowitz
       R. Manvi
       J. H. Schredder
       V. Truscello
       R. Turner

NASA-Lewis Research Center
Cleveland, Ohio 44101
Attn: J. Calogeras
       W. J. Masica

K. P. Ananth
Midwest Research Institute
425 Volker Boulevard

Rocket Research Company
York Center
Redmond, Washington 98052
Attn: D. Huxtable
       E. W. Schmidt
       R. D. Smith

Rockwell International
Energy Systems Group
8900 De Soto Avenue
Canoga Park, California 91304
Attn: J. K. Rosemary
       T. H. Springer

Solar Energy Research Institute
1536 Cole Boulevard
Golden, Colorado 80401
Attn: F. Baylin
       C. Benhan
       R. J. Copeland
       M. D. Cotton
       J. Finegold
       J. P. Thornton
       K. J. Touryan
       C. Wyman

C. J. Swet
Route 4, Box 258
Mt. Airy, Maryland 21771

J. H. Scott, 4700
G. E. Brandvold, 4710
V. L. Dugan, 4720
J. F. Banas, 4722
W. P. Schimmel, 4723
R. K. Traeger, 4740
H. M. Dodd, 4744
D. M. Haaland, 5823
T. B. Cook, 8000; Attn: W. J. Spencer, 8100
                        A. N. Blackwell, 8200
R. J. Gallagher, 8124
C. C. Hiller, 8124
B. F. Murphey, 8300
D. M. Schuster, 8310
W. R. Hoover, 8312
R. W. Mar, 8313
M. C. Nichols, 8313
B. E. Mills, 8315
L. A. West, 8315
R. L. Rinne, 8320
J. J. Iannucci, 8326
C. F. Melius, 8326
R. M. Green, 8353
R. E. Mitchell, 8354
L. Gutierrez, 8400
R. C. Wayne, 8450
T. D. Brumleve, 8451
P. J. Eicker, 8451
J. J. Bartel, 8452
J. D. Fish, 8452
A. C. Skinrood, 8452
T. T. Bramlette, 8453
R. W. Carling, 8453
L. G. Radosevich, 8453
C. T. Schafer, 8453
W. G. Wilson, 8453
Publications Division, 8265, for TIC (27)
Publications Division, 8265/Technical Library Processes and Systems Division, 3141
Technical Library Processes and Systems Division, 3141 (2)
Library and Security Classification Division, 8266-2 (3)